2018

To grow or survive: Plants modulate Brassinosteroid-regulated transcription factor BES1 during drought to balance growth and stress responses

Trevor Nolan
Iowa State University

To grow or survive: Plants modulate Brassinosteroid-regulated transcription factor BES1 during drought to balance growth and stress responses

by

Trevor M. Nolan

A dissertation submitted to the graduate faculty

in partial fulfillment of the requirements for the degree of

DOCTOR OF PHILOSOPHY

Major: Genetics

Program of Study Committee:

Yanhai Yin, Major Professor
Diane C. Bassham
Justin W. Walley
Bing Yang
Steven A. Whitham

The student author, whose presentation of the scholarship herein was approved by the program of study committee, is solely responsible for the content of this dissertation. The Graduate College will ensure this dissertation is globally accessible and will not permit alterations after a degree is conferred.

Iowa State University

Ames, IA

2018

DEDICATION

This dissertation is dedicated to my wife Breanna and our children Adyline and Hudson.

You have filled this journey with love, support and happiness.

TABLE OF CONTENTS

ACKNOWLEDGEMENTS vi

ABSTRACT viii

CHAPTER 1: GENERAL INTRODUCTION: CROSS-TALK OF BRASSINOSTEROID SIGNALING IN CONTROLLING GROWTH AND STRESS RESPONSES 1
- 1.1 Abstract 1
- 1.2 Introduction 2
  - 1.2.1 Overview of BR signaling 2
  - 1.2.2 BES1 and BZR1 function with other transcriptional regulators to promote growth 4
- 1.3 Crosstalk Between BR and Drought 8
  - 1.3.1 Antagonism between BR and ABA pathways 9
  - 1.3.2 BR-ABA crosstalk at BR receptor complexes 10
  - 1.3.3 BIN2 kinase regulates multiple aspects of BR-ABA crosstalk 11
  - 1.3.4 Inhibition of ABA signaling by BES1 and BZR1 13
  - 1.3.5 Interactions between the BR pathway and drought stress 15
  - 1.3.6 Reciprocal inhibition between BR and drought pathways mediated by BES1 and RD26 16
  - 1.3.7 Degradation of BES1 by selective autophagy during drought stress 19
- 1.4 Crosstalk Between BR and Plant Immunity 23
  - 1.4.1 Interactions between BR signaling and immunity at receptor complexes and the receptor-kinase substrates 23
  - 1.4.2 Interactions between BR signaling and immunity at transcription levels 28
  - 1.4.3 BR signaling and virus immunity 30
- 1.5 Summary and future directions 31
- 1.6 Acknowledgements 32
- 1.7 References 32
- 1.8 Figures 50
- 1.9 Dissertation Organization 54

CHAPTER 2: SELECTIVE AUTOPHAGY OF BES1 MEDIATED BY DSK2 BALANCES PLANT GROWTH AND SURVIVAL 57
- 2.1 Abstract 57
- 2.2 Introduction 58
- 2.3 Results 61
  - 2.3.1 BES1 is degraded through autophagy and proteasome pathways 61
  - 2.3.2 BES1 interacts with the ubiquitin receptor protein DSK2 63
  - 2.3.3 DSK2 acts as a receptor for BES1 degradation 64

2.3.4 DSK2 is phosphorylated by BIN2 and serves as a phosphor-regulated autophagy receptor 66
2.3.5 DSK2 is involved in BES1 degradation during drought stress 69
2.3.6 DSK2 is involved in BES1 degradation during fixed-carbon starvation 73
2.3.7 SINAT family E3 ubiquitin ligases are involved in BES1 degradation during starvation 75
2.4 Discussion 76
2.5 Acknowledgements 81
2.6 Author Contributions 81
2.7 Methods 82
2.8 References 94
2.9 Figures 103
2.10 Supplemental Figures and Tables 112

CHAPTER 3: NETWORK-BASED DISCOVERY OF BRASSINOSTEROID REGULATION OF PLANT GROWTH AND STRESS RESPONSES IN ARABIDOPSIS 126
3.1 Abstract 127
3.2 Introduction 128
3.3 Results and Discussion 131
3.3.1 BES1 and BZR1 direct a transcriptional network for BR responses 131
3.3.2 Construction of GRNs based on 11,760 transcriptome datasets 133
3.3.3 BR-TFs are enriched for BR and drought targets in the GRN 137
3.3.4 BR-TFs physically interact and may regulate common target genes 140
3.3.5 NEST analysis prioritizes BR-TFs for functional studies 141
3.3.6 BL and BRZ phenomics uncovers BR phenotypes of BR-TFs 143
3.3.7 BES1, PLATZ and ARID-HMG1 interact with a common set of TFs and control BR-regulated gene expression 147
3.3.8 BR and drought phenomics of soil-grown plants 150
3.4 Conclusions 154
3.5 Acknowledgements 155
3.6 Author Contributions 156
3.7 Methods 157
3.8 References 170
3.9 Figures and Tables 184

CHAPTER 4: DISCUSSION AND FUTURE WORK 203
4.1 Dissertation Discussion 203
4.2 References 211

APPENDIX A: RD26 MEDIATES CROSSTALK BETWEEN DROUGHT AND BRASSINOSTEROID SIGNALING PATHWAYS 216

APPENDIX B: ARABIDOPSIS WRKY46, WRKY54 AND WRKY70 TRANSCRIPTION FACTORS ARE INVOLVED IN BRASSINOSTEROID-REGULATED PLANT GROWTH AND DROUGHT RESPONSE 281

ACKNOWLDEGEMENTS

My deepest gratitude goes to my advisor, Yanhai Yin and my mentor Michelle Guo. Being in your lab has been one of the greatest experiences in my life. Thank for you believing in me, challenging me and providing the support and guidance to bring my ideas to life. You are both remarkable scientists and all-around human beings. There is no one I would have rather spent these years with.

My sincerest thanks go to my wife, Breanna Nolan. Your love, support and understanding have made all that I've done possible. I started my scientific career when our first daughter Adyline was born. In many ways, neither of us knew the work and sacrifice that this journey would entail. You have been the glue that has held our world together through these years and I will be forever grateful for everything you have done.

To my children Adyline and Hudson: You are what drives me to make the world a better place. I hope that one day you can share my passion for discovery in a way that suits your own personalities.

I want to thank the many people on and off campus that have enabled my scientific development. Thank you to Steve Rodermel for seeing my potential and inspiring me to become a scientist. You gave me an opportunity that completely changed my career trajectory. The way that you taught me to think was one of the greatest gifts a mentor can give a student. Aarthi Putarjunan – your patient mentorship, teaching and friendship were the cornerstone of my early scientific training.

Thank you to everyone in the Yin lab, Carver Co-lab and elsewhere on campus that have made coming to work every day to do science a joy. Especially Jiani Chen, Zhouli Xie, Hao Jiang, Buyun Tang, Lirong Xiang, Colton McNinch, Zaki Jubery,

Adedotun Akintayo, Ping Wang, Renu Srivastava, Jin Liao, Yunting Pu and Christian Montes-Serey.

I also want to thank all those that have made my research projects possible. I have been very fortunate to work with an extremely talented and motived group of students including Ben Brennan, Nicole Huser, Sean McLaughlin, Ashley Hurd, Paige Rassel, Jessica Parrott and Kyle Small. I'm so glad to see how you've all grown and accomplished your goals. Thank you to Diane Bassham, Justin Walley, Bing Yang, Steve Whitham, Dior Kelley, Stephen Howell, Pat Schnable, Lie Tang, Maneesha Aluru, Srinivas Aluru and many other ISU faculty. You all have been beyond generous with your time, resources and support.

Lastly, I want to thank my parents, Becky and Art Nolan, my in-laws, James and Lindha Steffen, and my brother Connor Nolan.

ABSTRACT

Understanding how plants balance growth and stress responses is essential to optimize crop yield in an ever-changing environment. Brassinosteroids (BRs) regulate plant growth and stress responses, including that of drought. BRs signal to control the activities of the BES1/BZR1 family transcription factors (TFs), which in turn mediate the expression of more than 5,000 BR-responsive genes. The network through which BES1 regulates the large number of target genes and the factors that modulate BES1 during stress are only beginning to be understood. In this thesis, I investigated several mechanisms that converge on BES1 to balance BR-regulated growth and stress responses. First, BES1 is degraded by selective autophagy during stress. BES1 interacts with the ubiquitin receptor protein DSK2 and is targeted to the autophagy pathway during stress via the interaction of DSK2 with ATG8, a ubiquitin-like protein directing autophagosome formation and cargo recruitment. DSK2 is phosphorylated by the GSK3-like kinase BIN2, a negative regulator in the BR pathway. BIN2 phosphorylation of DSK2 flanking its ATG8 interacting motifs (AIMs) promotes the interaction of DSK2 with ATG8, thereby targeting BES1 for degradation under stress conditions. Accordingly, loss-of-function *dsk2* plants accumulate BES1, have altered global gene expression profiles, and have compromised responses to drought and fixed-carbon starvation stresses.

In addition, BES1 interacts with other TFs to coordinate growth and drought responses. RD26 is induced by drought and inhibits the activity of BES1 on target gene promoters during drought conditions. In contrast, under growth promoting conditions BES1 cooperates with a large network of TFs including WRKY46/54/70 to inhibit

drought responses, thereby enabling BR-regulated growth. To more fully characterize the BR-regulatory network, we used genome-wide chromatin immunoprecipitation (ChIP), transcriptome and TF interactome datasets to identify 657 BR-related Transcription Factors (BR-TFs). We then took an integrated approach involving computational modeling, phenomics and functional genomics to study the networks through which BRs, BES1/BZR1 and BR-TFs function. Initially, 11,760 publicly available microarray datasets were used to build comprehensive gene regulatory networks (GRNs). BR-TFs are significantly enriched for BR and drought target genes in the GRNs, suggesting that these TFs function in growth and stress responses. BR-TFs were prioritized for functional studies using NEST (Network Essentiality Scoring Tool). Next, we developed BR response assays to conduct BR phenomics experiments for over 300 BR-TFs using more than 1000 knockout or overexpression lines. These studies identified numerous BR-TF mutants that displayed altered BR responses, allowing us to characterize the function of PLATZ and ARID-HMG1 as A/T-rich binding TFs that oppositely regulate BR-responsive gene expression. Finally, BR and drought phenomics experiments in soil-grown plants using time-lapse imaging and a robotic phenotyping system revealed that *tcp11* mutants have increased BR-regulated growth and improved survival during drought compared to wild-type. These studies provide a paradigm for network-based discovery and characterization of hormone response pathways through the integration of genomics, network analysis and phenomics. Taken together, BES1 is emerging as a critical hub for BR-drought crosstalk, allowing plants to efficiently balance growth and stress responses.

CHAPTER 1

GENERAL INTRODUCTION

CROSS-TALK OF BRASSINOSTEROID SIGNALING IN CONTROLLING GROWTH AND STRESS RESPONSES

A review published in *Biochemical Journal*

Trevor Nolan, Jiani Chen and Yanhai Yin

Department of Genetics, Development and Cell Biology, Iowa State University, Ames, IA 50011, U.S.A.

1.1 Abstract

Plants are faced with a barrage of stresses in their environment and must constantly balance their growth and survival. As such, plants have evolved complex control systems that perceive and respond to external and internal stimuli in order to optimize these responses, many of which are mediated by signaling molecules such as phytohormones. One such class of molecules called Brassinosteroids are an important group of plant steroid hormones involved in numerous aspects of plant life including growth, development and response to various stresses. The molecular determinants of the BR signaling pathway have been extensively defined, starting with the membrane localized receptor BRI1 and coreceptor BAK1 and ultimately culminating on the activation of BES1/BZR1 family transcription factors, which direct a transcriptional network controlling the expression of thousands of genes enabling BRs to influence growth and stress programs. Here, we highlight recent progress in understanding the relationship between the BR pathway and plant stress responses and provide an

integrated view of the mechanisms mediating crosstalk between BR and stress signaling.

1.2 Introduction

As sessile organisms, plants have the exquisite challenge to perceive and withstand the environmental conditions they encounter while optimizing their growth. Stress conditions arise as the consequence of environmental perturbations such as changes in temperature, light, water availability and solute concentrations as well as through interactions of plants with pathogens. Plants employ an array of signaling molecules including phytohormones and peptide regulators to coordinate their development and responses to the environment. Among growth promoting hormones, Brassinosteroids (BRs) are a group of polyhydroxylated plant steroid hormones that have emerged as key agonists and antagonists of pathways controlling growth and stress responses. Mutants deficient in BR signaling or biosynthesis exhibit marked defects in plant growth, reproduction and have altered stress responses [1-4]. Research over the last several decades has defined the BR biosynthesis and signaling pathways, which have been extensively reviewed elsewhere [5-7]. Subsequently, emerging research is characterizing the role of BRs in a tissue and context specific manner [8-10], including the way by which BR signaling is coordinated with stress and defense responses [11]. In this review, we focus our discussion on two important stresses that BRs have been implicated in: drought and response to pathogens.

1.2.1 Overview of BR signaling

Brassinosteroids are perceived by BRI1 (BRASSINOSTEROID INSENSITIVE 1) and its homologs BRL1 (BRI1-LIKE1) and BRL3 (BRI1-LIKE3), which are a family of

plasma membrane-localized leucine-rich repeat receptor kinases [4, 12, 13] along with co-receptor BAK1 (BRI1 ASSOCIATED KINASE 1) and related SERKs (SOMATIC EMBRYOGENESIS RECEPTOR KINASES) [14-16]. When BR levels are low, BR signaling is restrained by multiple mechanisms (Figure 1, left). Firstly, BKI1 (BRASSINOSTEROID KINASE INHIBITOR1) associates with BRI1 and prevents BRI1-BAK1 interactions [17]. Secondly, BIN2 (BRASSINOSTEORID INSENSITIVE 2), a GSK3-like kinase phosphorylates a collection of substrates [18] including BES1/BZR1 family transcription factors that function as master regulators of the BR pathway. Phosphorylation of BES1 and BZR1 leads to their inactivation through mechanisms that include cytoplasmic retention via interaction with 14-3-3 proteins [19, 20], reduced DNA binding [21] and protein degradation [22, 23].

When BRs are present, they bind to BRI1 and co-receptor BAK1 to initiate a series of signaling events that ultimately activate BES1/BZR1 family transcription factors (Figure 1, right). Binding of BL to the BRI1-BAK1 complex causes BRI1 to rapidly phosphorylate BKI1 [17], leading to BKI1 dissociation from BRI1 and sequestration of BKI1 by 14-3-3 proteins [24, 25]. BRI1 and BAK1 then sequentially phosphorylate and activate one another [26-28], which at least partially requires TWISTED DWARF1 (TWD1/FKBP42) an immunophilin-like protein that constitutively interacts with BRI1 but is required for BR-induced association and phosphorylation of the BRI1-BAK1 complex [29, 30]. Activated BRI1 phosphorylates receptor-like cytoplasmic kinases BR SIGNALING KINASES (BSKs) and CONSTITUTIVE GROWTH (CDG1) that activate the phosphatase BRI1-SUPPRESSOR 1 (BSU1) [31-34]. BSU1 is proposed to dephosphorylate BIN2 on Y200, leading to inactivation of BIN2 kinase activity [31].

Several additional mechanisms that also regulate BIN2 have been reported recently, which include targeted protein degradation in the presence of BRs by F-box E3 ubiquitin ligase KINK SUPPRESSED IN BZR1-1D (KIB1) [35, 36], cell-type specific sequestration of BIN2 at the plasma membrane by OCTOPUS (OPS) in the phloem [37] and inhibition of BIN2 by regulators such as HISTONE DEACTYLASE6 (HDA6) under energy-limiting conditions [38] and CONSTITUTIVELY PHOTOMORPHOGENIC 1 (COP1)/ SUPPRESSOR of *phyA-105* (SPA) in darkness [39]. The inactivation of BIN2 and the action of PROTEIN PHOSPHATASE 2A (PP2A) leads to the desphosphorylation of BES1/BZR1 family transcription factors [40]. Dephosphorylated BES1/BZR1 translocate from the cytoplasm to the nucleus where they function along with a suite of transcription factors and co-factors to regulate the expression of thousands of BR regulated genes [22, 23, 41-44].

1.2.2 BES1 and BZR1 function with other transcriptional regulators to promote growth.

Many studies have analyzed the BR-responsive transcriptome and have begun to reveal the extent to which BES1 and BZR1 modulate the BR-regulated transcriptional network [6]. Genome-wide ChIP-chip studies identified several thousand genes directly bound by BES1 and/or BZR1, including many BR-regulated genes and a number of transcription factors [44, 45], leading to the idea that BES1 and BZR1 may propagate BR signals by regulating transcription factors in a series of transcriptional waves. Indeed, numerous studies have identified downstream transcriptional regulators in the BR pathway. Many of these transcription factors are themselves regulated by BES1

and/or BZR1 and also physically interact with BES1/BZR1 to carry out BR-regulated gene expression [6, 46].

Early studies characterizing the function of BES1 as a transcription factor identified BES1-INTERACTING MYC-LIKE1 (BIM1) as a BES1 interacting transcription factor via yeast two-hybrid screening [43]. BES1 and BIM1 interact and bind synergistically to E-Box (CANNTG) sequences in BR target gene promoters, providing an early clue as to how BES1 cooperates with other transcription factors to regulate BR responsive gene expression. Further examples of these interactions provide mechanisms connecting the growth promoting hormones auxin and gibberellins (GA) with BRs as well as light signaling. PHYTOCHROME INTERACTING FACTORS (PIFs) are light regulated transcription factors that function as important regulators of growth and responses to the environment [47]. PIF4 physically interacts with BES1 and BZR1 and these transcription factors share over 2,000 common target genes as determined by genome-wide ChIP analysis, which led to a model in which BZR1 and PIFs interact to form heterodimers which bind to G-box (CACGTG) elements in BR target gene promoters [48]. Similar to PIFs, the auxin responsive transcription factors ARF6 and ARF8 interact with BZR1 [49]. ARF6 can also interact with PIF4, and over 40% of ARF6 target genes are shared with both BZR1 and PIF4. While BZR1 and PIFs cooperatively bind to G-box motifs, ARF6 binds to ARF binding motifs (TGTCTC). BR treatment or increased BZR1/PIF4 in *bzr1-d* and *PIF-OX* enhanced ARF binding, suggesting that the three transcription factors bind to target genes cooperatively [49]. Together, BZR1, PIFs and ARFs form the so called BZR1–ARF–PIF module [50] whose targets include the downstream tri-antagonistic bHLH system regulating both growth and defense gene

expression. This system includes ATBS1/PREs (ACTIVATION-TAGGED *bri1* SUPPRESSOR1/ PACLOBUTRAZOL-RESISTANCE) family proteins that antagonize AIFs/IBH1 (ATBS1-INTERACTING FACTORS/INCREASED LAMINA INCLINATION INTERACTING bHLH1) bHLH transcription factors, which in turn inhibit ACEs/HBI1 (ACTIVATORS FOR CELL ELONGATION/ HOMOLOG OF BEE2 INTERACTING WITH IBH 1) bHLH proteins that promote cell elongation [51-54].

BRs also function cooperatively with GA, which is at least partially mediated by the DELLA family of repressors inactivating BZR1, PIFs and ARFs to inhibit their function under low GA conditions [55-57]. BRs are also established to regulate GA metabolism and levels in both rice and *Arabidopsis* [58, 59]. Another element of BR-GA crosstalk is manifested through complex interactions revolving around the NAC (NO APICAL MERISTEM, ARABIDOPSIS TRANSCRIPTION ACTIVATION FACTOR AND CUP-SHAPED COTYLEDON) transcription factor JUNGBRUNNEN1 (JUB1). JUB1 also interacts with DELLA proteins, which allows JUB1 to repress transcription of BR and GA biosynthesis genes including *DWARF4 (DWF4*) and *GA3ox1* [60]. Moreover, it was found that BZR1 and PIF4 bind to a G-box in the *JUB1* promoter region to repress *JUB1* expression, revealing an important regulatory circuit between this NAC transcription factor and BR/GA signaling [60].

In addition to cooperatively binding to the same promoter element, BES1 also regulates target genes via interaction of transcription factors that bind different sites (Figure 1). Some examples include MYB30, and ARABODOPSIS THALIANA HOMEO-DOMAIN-LEUCINE ZIPPER PROTEIN 1 (HAT1) and ARF6/8. Both MYB30 and HAT1 are direct targets of BES1 and also physically interact with BES1. MYB30 functions with

BES1 to control BR-induced genes via binding of BES1 and MYB30 to E-box and MYB sites, respectively [61] whereas BES1 and HAT1 control BR repressed genes by binding BRRE and homeodomain binding sites. Therefore, there are numerous examples of how BES1 and BZR1 cooperate with other transcription factors to mediate various aspects of BR-responsive gene expression. BES1 also co-occupies promoters with transcription factors that exert opposite effects on gene expression. This is the case in the root stem cell niche where BR activation of cell division in the quiescent center (QC) is prevented via antagonism of BES1 with the R2R3-MYB transcription factor, BRAVO (BRASSINOSTEROIDS AT VASCULAR AND ORGANIZING CENTER) [9]. BES1 and BRAVO physically interact and together bind the *BRAVO* promoter via E-box and MYB sites, respectively. BES1 represses *BRAVO* expression via recruitment of co-repressor TOPLESS (TPL) [62] whereas BRAVO promotes its own expression. Together, BES1 and BRAVO create a switch that allows BR regulation of QC cell division to be tightly controlled. Given this paradigm for BES1-BRAVO interactions, it will be interesting to define the genome-wide roles of BES1 and BRAVO and the mechanisms of their interaction.

Several studies also indicated that BES1 regulates gene expression by recruiting histone modifying enzymes and a transcription elongation factor to differentially control BR-regulated gene expression at both transcription initiation and elongation steps [63-65]. Thus, there is accumulating evidence that BES1 interfaces with many other transcription factors and co-factors to regulate target gene expression and promote BR-mediated growth responses (Figure 1). In some cases, BES1/BZR1 interact with transcription factors to cooperatively or synergistically regulate target gene expression,

whereas in other cases BES1/BZR1 interact with other transcription factors in an antagonistic manner. Together, these interactions provide insight into how BES1/BZR1 regulate a large number of BR-responsive genes; however, the detailed mechanisms that allow BES1 and BRs to regulate specific subsets of BR regulated genes under different conditions and developmental stages are still under investigation. Future studies are needed to examine the full complement of transcription factors involved in the BR pathway and to define how BES1/BZR1 and other transcription factors interact to regulate various BR-induced and BR-repressed genes, which should yield significant insights into the structure and function of BR-controlled gene regulatory networks.

1.3 Crosstalk Between BR and Drought

In addition to regulating growth, BR signaling also interfaces with various stress outputs. Drought is a major stress that causes dramatic losses of crop yield, and thus a great deal of effort has been placed on studying drought stress responses [66, 67]. Recent progress in understanding the relationship between BR and drought have revealed several mechanisms by which BRs are inhibited during drought stress. Many of these operate to control BR-ABA antagonism at multiple levels of regulation ranging from the receptors complexes to downstream transcription factors. Central to this crosstalk are the BR signaling components BIN2 and BES1/BZR1, which have emerged as key factors promoting and antagonizing drought responses, respectively. Here we provide an update on the mechanisms controlling BR and drought crosstalk and highlight recent work defining the genetic interactions between these pathways.

1.3.1 Antagonism between BR and ABA pathways

ABA is an important hormone that regulates responses to abiotic stress including drought [67, 68]. ABA is synthesized from chloroplast derived carotenoid precursors, and during water deprivation the rate limiting enzyme in ABA biosynthesis, nine-cis-epoxycarotenoid dioxygenase (NCED), is rapidly upregulated [69, 70], leading to ABA accumulation that exerts a protective function through mechanisms including stomata closure, growth inhibition and synthesis of osmocompatible solutes [71]. In recent years, a core ABA signaling network has been pieced together. The predominant mechanism for sensing ABA is carried out by a large family of PYR/PLY/RCAR receptors that form a ternary complex with PP2C phosphatases, alleviating PP2C inhibition of SnRK2 kinase [72-75]. SnRK2 can then promote the function of ABA responsive SnRK2 targets, including AREB/ABF transcription factors and ion channels [76] (Figure 2, left).

From early in the BR literature, it has been noted that BR and ABA exhibit an antagonistic relationship. For example, it was shown that roots of BR mutants are hypersensitive to ABA treatment [4, 77] and seeds with reduced BR biosynthesis or signaling are more sensitive to ABA [78]. Upon examination of hormone responsive gene expression at the genome-wide level, it also became apparent that BR and ABA regulate common sets of genes [79]. ABA was shown to modulate BR response outputs including BES1 phosphorylation status and BR marker genes [80]. Since these effects were still observed in BR receptor mutants, but not when the more downstream kinase BIN2 was inhibited, it was postulated that crosstalk between ABA and BR pathways occurs downstream of BR perception, but at or upstream of BIN2 kinase in the BR signaling pathway. More recently, several studies have begun define these and other

molecular mechanisms of BR-ABA crosstalk, showing that BR and ABA pathways interface at multiple points ranging from inhibition of receptor complexes to downstream transcriptional regulation.

1.3.2 BR-ABA crosstalk at BR receptor complexes

Recent evidence in rice suggests that BR-ABA crosstalk may occur as early as the formation of BRI1-BAK1 receptor complexes [81, 82]. This occurs via the plant specific family of membrane anchored remorin proteins. Specifically, OsREM4.1, which is transcriptionally induced by ABA via the SnRK2 regulated transcription factor OsbZIP28 [81, 83] binds to the activation loop of OsSERK1 (homolog of BAK1). This interaction inhibits BRI1-BAK1 complex formation and thus BR signaling, which is reminiscent of the negative regulation provided by BKI1 [17, 24]. Similar to the inactivation of BKI1 by BRs, OsREM4.1 can be directly phosphorylated and inactivated by OsBRI1 in the presence of BRs [81]. Thus, OsREM4.1 is activated by ABA to shut down BR responses whereas BRs inactivate OsREM4.1, providing one mechanism to tradeoff growth and stress response programs depending on the relative amounts of BR and ABA present. It remains to be determined if a similar mechanism operates in *Arabidopsis* and if so, its contribution to overall ABA-BR crosstalk.

BAK1 is also involved in BR-ABA crosstalk to regulate stomata opening. A recent study found that *bak1* mutants lose water more quickly than wild type plants and are insensitive to ABA in terms of stomata closure [84]. This can be explained by the interaction of BAK1 with OST1/SnRK2.6, which is known to be a major contributor to ABA induced stomatal closure [85, 86]. This study also found that BAK1 can interact with the PP2C family protein ABI1. BAK1 and ABI1 oppositely regulate OST

phosphorylation (at least *in vitro*) and ABI1 interaction with BAK1 inhibits BAK1-OST1 complex formation. Therefore, the BAK1-OST1 complex is promoted by ABA which leads to stomatal closure, whereas this process is inhibited by BL treatment, providing another layer of BR-ABA crosstalk [84]. Further studies are needed to determine whether BAK1-OST1 interactions affect BR signaling outputs in response to ABA. While these studies seem to support antagonism of BR and ABA in terms of stomata closure, this effect has been somewhat controversial across studies and species and may depend on the relative concentrations of BRs used and whether BRs were exogenously applied or BR mutants were used [87-90]. For example, BR mutants showed increased response to ABA with enhanced stomatal closure [90-92]; however, BR application could cause stomata opening at low concentrations [89], but promoted stomatal closure at higher concentrations [87, 89, 90].

1.3.3 BIN2 kinase regulates multiple aspects of BR-ABA crosstalk

Further crosstalk among BR and ABA pathways occurs at the level of BIN2 kinase (Figure 2, left). BIN2 is a GSK3 kinase that functions as a negative regulator in the BR pathway by phosphorylating and inactivating BES1 and BZR1. In addition to BES1 and BZR1, BIN2 has a diverse array of substrates that allow it to regulate numerous processes involved in growth, development and stress responses [93]. Consistent with the reported ABA hypersensitivity of *bin2-1D* gain-of-function mutants [77], *bin2-1D* plants were found to be hypersensitive to ABA in root growth inhibition assays and ABA responsive gene expression and displayed increased phosphorylation of the SnRK2 substrate ABF2. Conversely, BIN2 loss-of-function *bin2-3 bil1 bil2* mutants showed compromised ABA responses [94]. A search for BIN2 interacting

proteins using immunoprecipitated BIN2-FLAG and liquid chromatography tandem mass spectrometry (LC-MS/MS) identified SnRK2s as BIN2 interactors. BIN2 was shown to specifically interact with SnRK2.2, SnRK2.3 and SnRK2.6 and phosphorylate SnRK2.2 and SnRK2.3 but not SnRK2.6. Mass spectrometry and follow up analysis identified T180 as a BIN2 phosphorylation site on SnRK2.3 (T181 of SnRK2.2), and a mutant SnRK2.3^{T180A} displayed decreased auto- and transphosphorylation activity, indicating that BIN2 phosphorylation is crucial for SnRK2 activity [94]. Therefore, BIN2 phosphorylation and activation of SnRK2 represents one mechanism by which BIN2 promotes ABA responses.

Another point of BR-ABA crosstalk mediated by BIN2 comes in the form of BIN2 interaction with a downstream transcription factor in the ABA pathway, ABI5 (Figure 2, left). ABI5 is a well-known target of SnRK2 kinases and is critical for ABA inhibition of seed germination [95, 96]. ABI5 was identified in a yeast two-hybrid screen using BIN2 as bait [97]. Subsequent analysis indicated that BIN2 phosphorylates ABI5 in an ABA dependent manner, likely on distinct residues from those phosphorylated by SnRK2. Genetic evidence indicated that BIN2 phosphorylation stabilizes ABI5, as ABI5 levels were increased in BIN2 gain-of-function mutants, but decreased in the absence of BIN2 or when plants were treated with BRs, which inactivates BIN2 [97]. Together with evidence that BIN2 and its homologs may be induced by stresses [80, 93, 98, 99], it is likely that BIN2 is activated during abiotic stress conditions and positively modulates ABA signaling through both phosphorylation and activation of SnRK2.2 and SnRK2.3 as well as by increasing ABI5 protein stability. Given that several other ABA regulated ABF transcription factors (ABF1 and ABF3) were found to interact with BIN2 [97], it will be

interesting for future studies to determine the extent to which the repertoire of BIN2 substrates extends into the ABA pathway.

1.3.4 Inhibition of ABA signaling by BES1 and BZR1

A more downstream aspect of BR-ABA interactions occurs between ABA and BR regulated transcription factors (Figure 2, right). Firstly, BES1 can antagonize ABA signaling via repression of *ABI3* expression by the BES1-TPL-HDAC19 complex [100]. The expression of ABA regulated transcription factors *ABI3*, and *ABI5* was shown to be decreased in *bes1-D* but upregulated in a *bes1* knockout mutant, which corresponded to the altered ABA sensitivities of these mutants. The mechanistic basis as to how BES1 can repress target gene expression can be explained by interactions of BES1 with TPL and TOPLESS-RELATED (TPR) repressors via an EAR motif that is conserved among BES1/BZR1 family transcription factors. Consistently, expression of a *BES1-D* construct contain EAR mutations was unable to produce BR or ABA related phenotypes normally associated with *BES1-D* overexpression, reinforcing the notion that the repression function of BES1 is crucial for BR signaling as well as BR-ABA crosstalk. Moreover, BES1 was found to bind to several E-box motifs in the *ABI3* promoter, repressing its expression by reducing histone acetylation that is normally associated with gene activation [100]. Since ABI3 functions to promote the expression of *ABI5*, repression of *ABI3* by BES1 could downregulate both of these transcription factors and thus ABA responses.

Subsequently, another related study also found that BZR1 can directly bind to the promoter of *ABI5* [101]. In this study, it was found mutant *bzr1-D* plants are also resistant to ABA treatments, which is at odds with previous reports that *bes1-D*, but not

bzr1-D displayed ABA insensitivity [100]. Interestingly, *bzr1-d/bin2-1D* double mutants showed decreased sensitivity to ABA compared to *bin2-1D* mutants, and a subset of ABA responsive genes including *ABI5* were differentially expressed in *bzr1-D/bin2-1D* compared to *bin2-1D* as monitored by RNA-seq experiments. Follow up experiments showed that BZR1 could directly bind to G-box elements within the *ABI5* promoter. These G-box elements were necessary for BZR1 repression of *ABI5* and overexpression of *ABI5* in *bzr1-d* partially rescued the ABA insensitive phenotype of *bzr1-d* [101]. These studies suggest that BES1 and BZR1 can transcriptionally modulate *ABI5* levels to control ABA signaling either through control of *ABI3* and/or via direct binding to the *ABI5* promoter. It remains to be determined if the differences between these two studies reflect the specificities of BES1 versus BZR1 or if they can be explained by other experimental differences.

MYB30, a target and interactor of BES1 [61], also functions in regulating ABA responses [102, 103]. Similar to BES1 and BZR1, MYB30 appears to negatively regulate ABA responses, which is consistent with BES1 and MYB30 cooperatively regulating BR gene expression. *myb30* mutants were more sensitive to ABA treatment, whereas overexpression of *MYB30* led to ABA insensitivity [103]. Interestingly, MYB30 is sumoylated by the small ubiquitin-like modifier (SUMO) E3 ligase SIZ1, which leads to stabilization of MYB30 [103]. Conversely, the E3 ubiquitin ligase MIEL1 (MYB30-Interacting E3 Ligase1) targets both MYB30 [104] and another ABA related transcription factor, MYB96 for degradation [102], but the ABA hypersensitive phenotype of *miel1* mutants in seed germination was found to be largely due to accumulation of MYB96 [102], which functions as a positive regulator in the ABA pathway [105]. In contrast,

MIEL1 appears to regulate both MYB30 and MYB96 stability in leaf tissue [102], which could have important implications in ABA and pathogen crosstalk. Thus, MYB30 is a negative regulator of ABA responses and is controlled by several post-translational modifications to fine-tune its activity in ABA and related pathways.

1.3.5 Interactions between the BR pathway and drought stress

While there is accumulating evidence that BR and ABA pathways function antagonistically, the relationship between BRs and drought is somewhat more complex. Several studies reported that application of exogenous BRs could actually promote tolerance to drought stress, which is seemingly contradictory to the BR-ABA antagonism [106-110]. However, the effects of BR on drought outcomes seem to depend on the concentrations of BRs used as well as the environment. When high concentrations of BRs are used, they may lead to feedback inhibition or other secondary effects as was noted in tomato, where exogenous BR application leads to elevated ABA levels due to H_2O_2 production [111].

While the effects of exogenous BRs may be complex, several recent studies have used a genetic approach to address the relationship of the BR pathway with drought responses, showing that the BR pathway inhibits drought response [112-114]. Knockdown of a *BRI1* homolog in *Brachypodium distachyon*, *BdBRI1*, led to increased tolerance to drought and altered drought responsive gene expression [115]. Furthermore, Northey et al. [114] connected BR to both ABA and drought by establishing the relationship between the farnesyl transferase ERA1 (ENHANCED RESPONSE TO ABSCISIC ACID 1) and CYP85A2, the cytochrome P450 enzyme that converts castasterone to brassinoloide in the last step of BR biosynthesis. A mutant in

CYP85A2 (*cyp85a2-2*) was identified from a screen targeting candidate ERA1 substrates that contained a motif typically targeted by farnesyl transferases. The *cyp85a2-2* mutant showed a phenotype similar to *era1-2* including increased response to ABA and drought tolerance. The known function of CYP85A2 in the BR pathway suggested that the phenotypes observed in *era1-2* might be due to decreased BR biosynthesis. Indeed, detailed analysis showed that *era1-2* mutants have reduced BR biosynthesis and ERA1 mediated farnesylation of CYP85A2 is required for proper localization and function of CYP85A2 [114]. This study supports the idea that reduced BR biosynthesis can lead to drought tolerance, however; the mechanisms that allow plants to balance BR-regulated growth when drought stress is encountered remained unclear until recently.

1.3.6 Reciprocal inhibition between BR and drought pathways mediated by BES1 and RD26

When plants encounter drought, it is important that growth be quickly inhibited such that resources can be devoted to stress response. Similarly, under optimal growth conditions, resources need not be wasted by unnecessarily activating drought stress responses [116]. Recent studies have shown that several mechanisms converge on BES1 to restrain growth when stress is encountered. One of these mechanisms was revealed through characterization of a BES1 target transcription factor, RESPONSIVE TO DESICCATION 26 (RD26), which allows plants balance these constrains through modulation of the transcriptional activity of BES1 [112] (Figure 2). *RD26* is a member of the NAC family of transcription factors and is induced under abiotic stress conditions including drought to promote drought tolerance [117-119].

BRs inhibit the expression of *RD26* and several of its homologs, which is mediated by BES1 binding to a region of *RD26* promoter containing the BES1 BRRE binding site. When overexpressed (*RD26 OX*), RD26 caused stunted growth, reduced BR response and suppressed the BR gain-of-function mutant *bes1-D*. These observations along with the fact that *RD26* is induced under abiotic stress [117-119] suggest that RD26 functions to inhibit BR-regulated growth when stress is encountered.

Global gene expression studies were instrumental in deciphering the mechanism of interactions between BES1 and RD26. BRs regulated ~5,000 genes, about 35% of which were regulated in an opposite fashion in *RD26 OX* plants. Investigation of these genes revealed that BR induced and *RD26 OX* repressed genes were enriched for E-box promoter elements, while BR repressed and *RD26 OX* induced genes were enriched for BRRE sites. Since these are BES1 binding sites and closely resembled those previously reported for RD26 and other NACs [117, 120] it was postulated that BES1 and RD26 might bind to a common site in these BR and RD26 regulated genes [112]. Indeed, BES1 and RD26 were found to physically interact and simultaneously bind to the same promoter element where they neutralized each other's activity on BES1 target genes. For example, BES1 promotes BR induced genes, whereas RD26 represses these genes, and together the combination of BES1 and RD26 has intermediate activity. The opposite was true on BR repressed genes, where BES1 repressed their expression and RD26 induced their expression.

The idea that BES1 and RD26 bind to a common target site is supported by an elegant study by Song et al. that provided the largest set of ABA-responsive ChIP-seq data to date [121]. This study confirmed that the motif enriched in RD26 target genes

matched known BES1 binding sites and provided a rich dataset allowing comparisons of RD26 target genes to various BES1 and BR datasets. We combined and analyzed these published datasets to provide a more comprehensive overview of the relationship between BES1 and RD26 target and regulated genes. As expected, RD26 targets from ABA treated plants [121] show extensive overlaps with *RD26 OX* regulated genes [112] (Figure 3A). Similarly, RD26 target genes have a high degree of overlap with BES1/BZR1 target [44, 49, 122] and BR regulated genes [63] (Figure 3A), which confirms the interactions between BES1 and RD26 reported by Ye et al. [112] at the genome wide level. Consistent with the role of RD26 in drought response, a significant amount of overlap is also observed with drought regulated genes [123] and *RD26 OX*/RD26 targets. Comparison of BES1/BZR1 and RD26 target genes with genes regulated by BRs, drought and in *RD26 OX* revealed a core set of 594 genes (Figure 3B) which are highly enriched for the BES1 and RD26 G-box binding site (CACGTG; a specific E-box, Figure 3C). We also performed clustering analysis of these 594 genes using published RNA-seq data from plants treated with or without BRs [112] which revealed that many BR repressed genes are induced in *RD26 OX* and repressed in *rd26q* mutants (especially after BR treatment, Figure 3D). Conversely, the subset of BR induced genes in this core set appear to be highly repressed in *RD26 OX*, but no longer induced by BRs in *rd26q*, raising the possibility that RD26 could actually be required for BR responsive induction of these genes. In any case, perturbation of *RD26* leads to dramatic changes in expression of BR and drought regulated genes that are targets of both BES1/BZR1 and RD26.

The genetic relationship between BR and drought was also confirmed and explained by crosstalk between BES1 and RD26. BR loss-of-function *bri1-5* mutants showed increased expression of *RD26* and homologs and resistance to drought, while the BR gain-of-function mutant *bes1-D* suppressed *RD26* gene expression and was more sensitive to drought [112]. A double mutant of *bes1-D RD26 OX* largely rescued the drought sensitive phenotype of *bes1-D*, suggesting that BR repression of *RD26* through BES1 plays a major role in controlling drought response. Together, these observations suggest a model in which BRs restrain drought responses under normal conditions by repressing the expression of *RD26* and other *NACs*. When drought is encountered, *RD26* is quickly induced [119] and interacts with BES1 to inhibit the function of BES1 on target gene promoters. Thus, BR and drought pathways converge by interaction of BES1 and RD26 on a common promoter element, leading to inactivation of BES1, which ensures a proper growth-stress balance. While BES1 and RD26 oppose each other's function on many genes, a subset of genes affected by BRs and in *RD26 OX* are regulated in the same direction [112], suggesting that BES1 and RD26 may function cooperatively in certain contexts. Thus, it will be of great interest to determine the mechanisms that lead to antagonism or cooperation between BES1 and RD26. These sets of genes may explain why BRs can sometimes promote resistance to drought [124] and could provide an opportunity to engineer crops for optimal growth and stress responses.

1.3.7 Degradation of BES1 by selective autophagy during drought stress

In addition to inhibition of the activity of BES1 on target gene promoters, more recent evidence suggests that BES1 can also be inhibited during stress by targeted

degradation. One pathway that is involved in protein degradation, especially during stress is autophagy [125, 126]. Autophagy can be highly selectively by employing receptor proteins that bind to both cargos destined for degradation and also to the autophagy protein ATG8 (AUTOPHAGY-RELATED8) [127-129]. Using autophagy inhibitors and autophagy deficient mutants Nolan at al showed that BES1 accumulates when autophagy is blocked, especially during drought and starvations stresses [113], which is in line with studies showing that TOR, a central regulator of growth and inhibitor of autophagy promotes accumulation of BZR1 [130].

A mechanistic basis for how BES1 is degraded by autophagy was revealed through yeast two-hybrid screening for BES1 interacting proteins, which led to the discovery that DSK2 (DOMINANT SUPPRESSOR OF KAR2) functions as the autophagy receptor targeting BES1 for degradation [113] and also defined SINAT (SINA of Arabidopsis thaliana) E3 ubiquitin ligases for their role in targeting BES1 for degradation during stress [113] and in response to changing light conditions [131]. DSK2 interacts with ubiquitinated BES1 and is required for recruitment of BES1 to ATG8-labeled autophagosomes, but does not affect bulk autophagy, suggesting that DSK2 is involved in selective autophagy of BES1. Consistently, DSK2 interacts with ATG8 through two regions containing ATG8 interacting motifs (AIMs). DSK2 is phosphorylated by BIN2 kinase around its AIMs, which enhances the interaction between DSK2 and ATG8, thus promoting BES1 degradation [113].

Impairment of BES1 degradation in autophagy mutants or loss-of-function *dsk2 RNAi* plants led to increased growth in the presence of BR inhibitors compared to wild type plants, whereas survival during drought stress was compromised in these mutants.

Survival of *dsk2 RNAi* plants could be restored by reduction of BES1 in a *dsk2 RNAi bes1 RNAi* double mutant, suggesting that BES1 degradation during drought provides a key mechanism to shut down growth in favor of drought responses. This idea is supported by global gene expression studies which showed that thousands of drought-related genes were misregulated in *dsk2 RNAi* plants during stress, many of which are BES1 targets [113]. A similar trend was observed during fixed-carbon starvation, indicating that BES1 degradation through autophagy is also critical to balance growth during starvation conditions. Additionally, the SINAT E3 ubiquitin ligases was shown to be induced during starvation stress and control BES1 degradation through autophagy during fixed-carbon starvation [113], however; whether SINAT and/or additional E3 ubiquitin ligases function during drought to degrade BES1 remains to be determined.

Degradation of BES1 during drought conditions was recently confirmed and extended to another family of transcription factors by Chen et al [132] who characterized the role of WRKY46, WRKY54 and WRKY70 (WRKY46/54/70) in both BR-regulated growth and drought responses. WRKY transcription factors have been extensively studied for their roles in diverse stress responses [133-137], but a role in BR-regulated growth had not been shown previously. Expression of *WRKY46/56/70* was induced by BRs in and *bes1-D* plants and the dwarf phenotype of a *wrky54wrky46wrky70 (wrky54t)* mutant indicated that WRKYs are also required for BR-regulated growth. WRKY46/54/70 modulate both BR biosynthesis and also BR-signaling, where they interact with BES1 to cooperatively regulate the expression of thousands of genes [132]. A large number of drought-responsive genes are affected in *wrky54t* mutants, and changes in drought responsive gene expression corresponded with increased drought

resistance of *wrky54t* mutants. These studies indicate that similar to BES1, WRKY46/54/70 are negative regulators of drought response. WRKY46/54/70 are substrates of BIN2 kinase, and BIN2 phosphorylation of these WRKYs led to their destabilization. During drought conditions, both BES1 and WRKY54 protein levels dramatically decreased [132]. These observations suggest that degradation of growth promoting transcription factors during drought stress is likely an important mechanism to shut down BR responses, and the transcription factors affected by this process might extend beyond BES1, but the detailed pathways and components that control WRKY46/54/70 stability remain to be investigated.

Taken together, several studies have established BES1 as a key component for BR-drought crosstalk, and BES1 is inhibited through multiple mechanisms when drought stress is encountered. These include inhibition of BES1 transcriptional activity on target gene promoters through interactions with RD26 [112], degradation of BES1 through DSK2-mediated selective autophagy [113] and destabilization of transcription factors that cooperate with BES1 such as WRKY46/54/70 during drought [132]. Additionally, BIN2 kinase has been implicated in several regulatory events that comprise BR-drought crosstalk. BIN2 promotes ABA signaling components such as ABI5 and SnRK2 kinases and also inhibits a BES1 both directly and through modulating BES1 degradation via modulation of DSK2-ATG8 interactions that promote autophagy mediated degradation of BES1. BIN2 also leads to the destabilization of several other positive regulators of the BR pathway. Thus, it appears that BIN2 is a critical component involved in promoting stress response while inhibiting growth and future studies should reveal the exact mechanisms that control BIN2 activation during stress.

In summary, BR and drought pathways interact at multiple levels (Figure 2). This multi-layer crosstalk happens in both directions (i.e. drought/ABA pathway can inhibit BR signaling and likewise, BR can inhibit drought/ABA signaling), which likely operate to slow down plant growth under drought conditions and also prevent unnecessary activation of drought response during active plant growth. It is likely that the multi-layer crosstalk is needed to provide both genetic redundancy as well as fine-tune the growth and stress responses depending on the nature and severity of the imposed stresses.

1.4 Crosstalk Between BR and Plant Immunity

In addition to drought, plants are faced with an array of other interactions with their environment, including those with pathogens. Response to pathogen attack must be swift to ensure survival of the plant, but also needs to be carefully controlled to optimize allocation of resources. The BR pathway is extensively intertwined with immunity, and crosstalk starts at receptor complexes that share a number of components and extends to downstream transcriptional regulators. In this section, we provide an update BR and immune crosstalk with a focus on the molecular mechanisms controlling interactions between these two pathways.

1.4.1 Interactions between BR signaling and immunity at receptor complexes and the receptor-kinase substrates

One major aspect of immune signaling that the BR pathway is involved in is Pathogen-Associated Molecular Pattern (PAMP)-Triggered Immunity (PTI) [11]. PAMPs are recognized by pattern-recognition receptors (PRRs), which result in the activation of PTI responses. For instance, FLAGELLIN SENSING2 (FLS2), a well-studied receptor

kinase, recognizes flagellin from bacterial flagella [138]. Recent studies revealed that several signaling components are involved in BR and PTI crosstalk, including receptor-like kinases (RLK) BAK1 and BIR1, receptor-like cytoplasmic kinases (RLCK) BSK1 and BIK1, and transcription factors BES1/BZR1 (Figure 4).

BAK1 has been considered as a possible candidate to mediate tradeoffs between BR-regulated plant growth and immunity due to its function as a co-receptor in both the BR and PTI pathways. In the BR pathway, BAK1 promotes growth by interacting with BRI1 to initiate BR signal transduction at the plasma membrane [14, 139], and knockout of *BAK1* and its homologs led to *bri1*-like BR-insensitive dwarf phenotypes [16]. BAK1 also function as a co-receptor for several LRR-RLKs (FLS2, EFR and PEPR1) to perceive various PAMP signals (flg22, elf26 and AtPep1) [140-143] and promote PTI responses. In line with this idea, *bak1* mutants showed reduced response to PAMPs, suggesting that BAK1 positively regulates PTI in *Arabidopsis* [140]. Additionally, *bak1* mutants suppress the autoimmune phenotype of *bir1* (BAK1-INTERACTING RECEPTOR-LIKE KINASE1), a RLK that functions as a negative regulator of plant immunity [144]. Thus, one possibility is that BR signaling and the immunity antagonize each other is through competition for BAK1 in their receptor complexes.

Two independent groups reported that the BR pathway inhibits PTI (Albrecht et al., 2012, Belkhadira, 2012). However, these two studies had opposite conclusions regarding the role of BAK1 in this process. Belkhadir et al. reported that BAK1 was required for the antagonistic effect of BRs on PTI based on the following observations [145, 146]. First, plants overexpressing the BR receptor *BRI1* displayed compromised

oxidative burst in response to flg22, elf19 and PGN treatment, but not to chitin, a component of the fungal cell wall that activates BAK1-independent defense response. The BRI1 suppression of PTI requires BAK1. Consistent with these observations, overexpression of BR biosynthetic gene *DWF4* also showed compromised response to flg22 [145]. Moreover, expression of a hyperactive *BRI* allele, *BRI1sud1*, led to enhanced PTI response, likely due to the fact that activated BAK1 (from constitutive active BRI1sud1) could also activate PTI response.

Consistent with a negative role of BRs in PTI response, Albrecht et al. reported that treating *Arabidopsis* leaves with BR inhibited FLS2-mediated disease resistance to Pseudomonas synringae pv. tomato DC3000 (Pst DC3000), with compromised flg22 or elf18-triggered ROS burst and PTI marker gene expression [147]. BR signaling outputs including BES1 phosphorylation and BR marker gene expression were unaltered by flg22 treatment, suggesting the regulation between BR and PTI is unidirectional [147]. Therefore, both of these studies support negative regulation of PTI by the BR pathway. However, the results of Albrecht et al. suggest that BAK1 is not a rate-limiting factor that causes competition between BR and immune signaling. Co-treatment of BR and flg22 did not reduce the amount of FLS2 that associated with BAK1 [147], which is consistent with a model in which competition for BAK1 by BRI1 and FLS2 does not play a major role balancing growth and immunity. One possibility for the opposite conclusions on the requirement of BAK1 in BR/PTI interaction might be the different approaches, treatments and mutants used in these studies.

Similar to the results regarding the role of BAK1 in immunity, application of BRs versus the use of BR mutants can lead to opposite conclusions about the effect of the

BR pathway on plant immune responses. In *Hordeum vulgare*, BR treatment enhanced the plant tolerance to Fusarium Head Blight (FHB) disease caused by fungi *Fusarium culmorum* [148]. In *Brassica napus*, overexpression of *AtDWF4* displayed increased tolerance to several fungal pathogens, confirming the results from the BR application experiments [149]. However, semi-dwarf '*uzu*' barley mutant, which has a mutation (H857A) in the kinase domain of BRI1 and compromised BR signaling, displayed enhanced resistance to a broad range of viral and fungal pathogens, including *Fusarium culmorum* [150]. The genetic studies indicate a negative role of BR signaling in fungal defense. Similarly, disruption of *BRI1* in *Brachypodium distachyon* led to increased tolerance to necrotrophic and hemibiotrophic pathogens but not to biotrophic pathogens [151]. Taken together, these physiological and genetic studies suggest that BRs can play either a negative or positive role in biotic stress responses. The opposite results derived from plants exposed to the exogenous BR and from BR mutants suggest that many factors such as plant age, environment, BR concentrations applied (i.e. signaling strengths) and activation of additional pathways may determine the different outcomes.

Several receptor-like cytoplasmic kinases (RLCKs) are involved in both BR signaling and immunity response (Figure 4). One RLCK member, BOTRYTIS-INDUCED KINASE1 (BIK1), is phosphorylated by BAK1 upon flagellin perception and transphosphorylates FLS2/BAK1 via direct interaction to transduce the flagellin signal [152]. *bik1* mutants displayed compromised resistance to Pst DC300 infection, indicating that BIK1 also positively regulates flg22-induced immunity [152]. BSK1, another RLCK member, is associated with BR receptor BRI1 upon BR activation and is phosphorylated by BRI1 to transduce the signal to downstream targets [153]. *bsk1*

knockout mutants display increased susceptibility to pathogens including *Pst DC3000* with reduced levels of salicylic acid (SA) [154]. Furthermore, BSK1 directly interacts with FLS2 and is required for ROS burst, indicating a positive role of BSK1 in flg22-induced PTI [154, 155]. In contrast to BSK1, BIK1 plays a negative role in BR signaling since *bik1* mutants are hypersensitive to BRs, accumulate dephosphorylated-BES1 and have decreased expression of BR biosynthesis genes *BR6OX*, *CPD* and *DWF4* [156]. BIK1 associates with BRI1 and is directly phosphorylated by BRI1, which is enhanced upon BL treatment [156]. In both BR signaling and FLS2 signaling, BIK1 dissociates from BRI1 and FLS2 receptors upon ligand perception. BAK1 is required for the dissociation of BIK1 with FLS2 in flg22-induced immunity but not in BR signaling [156]. It was further shown that BIK1 regulates flg22-triggered immunity via phosphorylation of the NADPH oxidase RBOHD, which activates ROS burst and controls stomatal movement [157, 158].

Both BAK1 and BIK1 were reported to be negatively regulated by phosphatases, which could be alleviated by PAMP treatment [159, 160]. PP2A associates with BAK1, negatively regulating BAK1's activity [160], whereas PP2C38 negatively regulates the activity of BIK1 in immunity [159]. PP2C38 associates with BIK1 and directly dephosphorylates BIK1, leading to a reduction of PAMP-induced ROS production and stomatal immunity. Upon PAMP perception, PP2C38 is phosphorylated, likely by BIK1, which leads to dissociation of PP2C38 from BIK1 thus enabling BIK1 to activate ROS burst [159].

In summary, several points of crosstalk occur between PTI response and BR signaling at the receptor complexes and downstream RLCKs. Given the number of

shared signaling components between BR and immunity, understanding how specificity is achieved between the two pathways is an active area of research. Indeed, recent work has suggested that BRI1 and FLS2 receptor complexes are spatial separated at the plasma membrane [161]. Along these lines, it would be interesting to determine why BSK1 and BIK1 both play positive roles in PTI but have positive and negative functions in BR signaling, respectively.

1.4.2 Interactions between BR signaling and immunity at transcription levels

It has been reported that the crosstalk between BR and PTI occurs downstream of BIN2, a central negative regulator in the BR signaling pathway (Figure 4). Flg22-triggered ROS burst was inhibited by BIN2 kinase inhibitors LiCl/28hosph treatment or in loss-of-function of *BIN2* mutants [162]. One part of the pathways that this crosstalk occurs at is the downstream transcriptional regulators. The BR-regulated transcription factor BZR1 appears to suppress bacterial defense through several mechanisms. First, BZR1 activates the expression of several WRKY transcription factors, *WRKY11*, *WRKY15* and *WRKY18*, which negatively control the immunity response [163]. Second, BZR1 interacts with WRKY40 to directly suppress genes required for PTI responses [163]. Finally, the bHLH transcription factor HBI1, which is required for BZR1-PIF4 mediated cell elongation and the activation of BR biosynthetic genes *CPD*, *DWF4* and *BR6OX1*, inhibits the expression of PTI marker genes and is therefore proposed to mediate the trade-off between plant growth and bacterial defense [164].

BZR1 is also implicated in fungal and insect defense, which likely involves the plant hormones jasmonic acid (JA) and GA (Figure 4). Gain-of-function *bzr1-D* mutants, exhibited enhanced resistance against thrip feeding with elevated expression of JA-

inducible *VSP* genes [165], indicating that BZR1 positively regulates insect defense, likely by activating JA signaling. In addition, as discussed above, BZR1 acts through NAC transcription factor JUB1 to increase the biosynthesis of GA/BR as well as the expression of *DELLA* genes, which probably act together to promote fungal defense [60]. Finally, overexpression of *JUB1* led to enhanced susceptibility to *Pst DC3000* [166]. The contribution of JUB1 to BR-regulation of PTI remains to be defined, and may represent an indirect mechanism for BZR1 to positively regulate PTI via JUB1. In rice, BRs can antagonize GA-mediated fungal defenses by stabilizing SLR1, an ortholog of *Arabidopsis* DELLA protein [167, 168]; BRs can also suppress SA response to root oomycete *Pythium graminicola* inoculation [168]. It's proposed that *P. graminicola* uses BRs as a decoy to suppress SA 29hosphor29, operating downstream of SA biosynthesis but upstream of OsNPR1 and OsWRKY45, to achieve pathogenesis [168].

In contrast to BZR1, BES1 was reported to play a positive role in bacterial immunity and a negative role in fungal defense. Loss-of-function of *bes1* mutants showed decreased resistance to *Pst DC3000* and BES1 was identified as a direct substrate of MPK6 [169]. Mutation of the MPK6 phosphorylation sites in BES1 ($BES1^{SSAA}$) led to impaired disease resistance, suggesting a positive role of BES1 in plant immunity downstream of the MAPK pathway [169]. BES1 has been found to negatively regulate the defense response to fungal pathogens as *bes1-D* gain-of-function mutants showed enhanced susceptibility to a necrotrophic fungus *Alternaria brassicicola* [170]. The BES1 target transcription factor MYB30 positively regulates the hypersensitive cell death program in plants in response to bacterial and fungal pathogens [171, 172], likely mediating some of the function of BES1 in bacterial

defense. MYB30-Interacting E3 Ligase1, MIEL1, interacts with and ubiquitinates MYB30, leading to MYB30 degradation, thus weakening MYB30-mediated hypersensitive cell death response [104]. Taken together, there is significant evidence that TRANSCRIPTION FACTORs involved in the BR pathway mediate crosstalk with immune responses. Given that BES1 and BZR1 function similarly in controlling BR-regulated growth, it will be interesting to further explore their seemingly contradictory functions in immune responses, which might lead to insights into the complex relationship between BR and immunity.

1.4.3 BR signaling and virus immunity

Early studies in *Nicotiana benthamiana* indicated that exogenous application of BR enhanced disease resistance to a broad range of pathogens, including virus (TMV), bacteria (*Pst DC3000*) and fungus (*Oidium sp*) [173]. A recent study using the Virus Induced Gene Silencing (VIGS) system revealed potential mechanisms of crosstalk between BR and virus resistance [174]. It was shown that foliar application of BL increased the tolerance of tobacco plants to TMV with accumulation of BR-induced *MAPK* and *RBOHB* (NADPH oxidase B) gene expression, which is accompanied by ROS burst and defense-related gene expression. The BR-induced virus tolerance was compromised in *BRI1* and *BSK1*-silenced plants [174]. These results indicated that BRs function through BRI1 and BSK1 to activate MAPK cascade and ROS production to confer TMV tolerance (Fig 4). On the other hand, BR activated BES1/BZR1 was shown to inhibit *RBOHB* gene expression, thereby reducing virus resistance and promoting plant growth [174]. The elevated expression of several defense-responsive genes was also observed in the overexpression transgenic line of wheat *TaBRI1* in *Arabidopsis*,

confirming the results from VIGS studies [174, 175]. BRs thus have dual roles in virus defense and the final outcome is probably determined by the relative signaling strengths of the two branches as well as plant growth and environmental conditions (Figure 4).

Taken together, research into BR and immune crosstalk has shown that BRs and plant defense signaling pathways crosstalk at multiple levels in a complex network at the receptors/coreceptors, their immediate signaling intermediates as well as downstream transcription factors. The outcome of the crosstalk in terms of plant growth and immune response is probably determined by the sum of several interactions. One common feature is that different family members may have different functions (such as BSK1/BIK1 and BES1/BZR1) likely based on their substrates and/or targets.

1.5 Summary and future directions

In summary, there is accumulating evidence for crosstalk of BR with both drought and pathogen defense at multiple tiers of these complex signaling pathways. It seems that the role of BRs in drought stress depends on the environment, as well as if the BR pathway is manipulated via genetic means or by exogenous application. Similarly, the relationship between BRs and plant immunity may depend on the different pathogens, hosts and the systems used for studies (i.e. exogenously supplied hormone or mutants). The mechanisms controlling the regulation of plant immunity and drought stress by BRs likely operate through complex regulatory networks, including crosstalk with other hormonal pathways. Understanding how these networks function represents a significant challenge for the BR field that should be the focus of future research. Given that many factors involved in BR signaling have already been identified, further studies with systems level approaches are needed to define how the large number of BR

signaling components function together and how they are modulated by other pathways, environments and in different developmental contexts. Establishing a global and integrated view of the BR pathway may help clarify the functions and mechanisms of BRs in regulating the both plant immunity and drought pathways, allowing for optimization of BR-regulated growth without compromising resistance to these important stresses.

1.6 Acknowledgements

The work in the Yin lab is supported by grants from NIH (1R01GM120316-01A1), NSF (IOS-1257631), and the Plant Sciences Institute at Iowa State University. We apologize to colleagues for not being able to cite all related papers in the review due to space limitations.

1.7 References

1 Li, J., Nagpal, P., Vitart, V., McMorris, T. C. and Chory, J. (1996) A role for brassinosteroids in light-dependent development of *Arabidopsis*. Science. 272, 398-401

2 Szekeres, M., Németh, K., Koncz-Kálmán, Z., Mathur, J., Kauschmann, A., Altmann, T., Rédei, G. P., Nagy, F., Schell, J. and Koncz, C. (1996) Brassinosteroids rescue the deficiency of CYP90, a cytochrome P450, controlling cell elongation and de-etiolation in *Arabidopsis*. Cell. 85, 171-182

3 Noguchi, T., Fujioka, S., Takatsuto, S., Sakurai, A., Yoshida, S., Li, J. M. and Chory, J. (1999) Arabidopsis det2 is defective in the conversion of (24R)-24-methylcholest-4-En-3-One to (24R)-24-methyl-5 alpha-cholestan-3-one in brassinosteroid biosynthesis. Plant Physiology. 120, 833-839

4 Clouse, S. D., Langford, M. and McMorris, T. C. (1996) A brassinosteroid-insensitive mutant in Arabidopsis thaliana exhibits multiple defects in growth and development. Plant Physiology. 111, 671-678

5 Belkhadir, Y. and Jaillais, Y. (2015) The molecular circuitry of brassinosteroid signaling. The New phytologist. 206, 522-540

6 Guo, H., Li, L., Aluru, M., Aluru, S. and Yin, Y. (2013) Mechanisms and networks for brassinosteroid regulated gene expression. Curr. Opin. Plant Biol. 16, 545-553

7 Wang, W., Bai, M. Y. and Wang, Z. Y. (2014) The brassinosteroid signaling network-a paradigm of signal integration. Curr Opin Plant Biol. 21C, 147-153

8 Jaillais, Y. and Vert, G. (2016) Brassinosteroid signaling and BRI1 dynamics went underground. Curr Opin Plant Biol. 33, 92-100

9 Vilarrasa-Blasi, J., Gonzalez-Garcia, M. P., Frigola, D., Fabregas, N., Alexiou, K. G., Lopez-Bigas, N., Rivas, S., Jauneau, A., Lohmann, J. U., Benfey, P. N., Ibanes, M. and Cano-Delgado, A. I. (2014) Regulation of Plant Stem Cell Quiescence by a Brassinosteroid Signaling Module. Developmental cell. 30, 36-47

10 Vragovic, K., Sela, A., Friedlander-Shani, L., Fridman, Y., Hacham, Y., Holland, N., Bartom, E., Mockler, T. C. and Savaldi-Goldstein, S. (2015) Translatome analyses capture of opposing tissue-specific brassinosteroid signals orchestrating root meristem differentiation. Proceedings of the National Academy of Sciences of the United States of America. 112, 923-928

11 Lozano-Duran, R. and Zipfel, C. (2015) Trade-off between growth and immunity: role of brassinosteroids. Trends Plant Sci. 20, 12-19

12 Cano-Delgado, A., Yin, Y. H., Yu, C., Vafeados, D., Mora-Garcia, S., Cheng, J. C., Nam, K. H., Li, J. M. and Chory, J. (2004) BRL1 and BRL3 are novel brassinosteroid receptors that function in vascular differentiation in Arabidopsis. Development. 131, 5341-5351

13 Li, J. M. and Chory, J. (1997) A putative leucine-rich repeat receptor kinase involved in brassinosteroid signal transduction. Cell. 90, 929-938

14 Nam, K. H. and Li, J. M. (2002) BRI1/BAK1, a receptor kinase pair mediating brassinosteroid signaling. Cell. 110, 203-212

15 Li, J., Wen, J. Q., Lease, K. A., Doke, J. T., Tax, F. E. and Walker, J. C. (2002) BAK1, an Arabidopsis LRR receptor-like protein kinase, interacts with BRI1 and modulates brassinosteroid signaling. Cell. 110, 213-222

16 Gou, X. P., Yin, H. J., He, K., Du, J. B., Yi, J., Xu, S. B., Lin, H. H., Clouse, S. D. and Li, J. (2012) Genetic Evidence for an Indispensable Role of Somatic Embryogenesis Receptor Kinases in Brassinosteroid Signaling. PloS genetics. 8

17 Wang, X. L. and Chory, J. (2006) Brassinosteroids regulate dissociation of BKI1, a negative regulator of BRI1 signaling, from the plasma membrane. Science. 313, 1118-1122

18 Youn, J. H. and Kim, T. W. (2015) Functional Insights of Plant GSK3-like Kinases: Multi-Taskers in Diverse Cellular Signal Transduction Pathways. Molecular Plant. 8, 552-565

19 Gampala, S. S., Kim, T. W., He, J. X., Tang, W. Q., Deng, Z. P., Bai, M. Y., Guan, S. H., Lalonde, S., Sun, Y., Gendron, J. M., Chen, H. J., Shibagaki, N., Ferl, R. J., Ehrhardt, D., Chong, K., Burlingame, A. L. and Wang, Z. Y. (2007) An essential role for 14-3-3 proteins in brassinosteroid signal transduction in Arabidopsis. Developmental cell. 13, 177-189

20 Ryu, H., Kim, K., Cho, H., Park, J., Choe, S. and Hwang, I. (2007) Nucleocytoplasmic shuttling of BZR1 mediated by phosphorylation is essential in Arabidopsis brassinosteroid signaling. Plant Cell. 19, 2749-2762

21 Vert, G. and Chory, J. (2006) Downstream nuclear events in brassinosteroid signalling. Nature. 441, 96-100

22 He, J. X., Gendron, J. M., Yang, Y. L., Li, J. M. and Wang, Z. Y. (2002) The GSK3-like kinase BIN2 phosphorylates and destabilizes BZR1, a positive regulator of the brassinosteroid signaling pathway in Arabidopsis. P Natl Acad Sci USA. 99, 10185-10190

23 Yin, Y. H., Wang, Z. Y., Mora-Garcia, S., Li, J. M., Yoshida, S., Asami, T. and Chory, J. (2002) BES1 accumulates in the nucleus in response to brassinosteroids to regulate gene expression and promote stem elongation. Cell. 109, 181-191

24 Wang, H. J., Yang, C. J., Zhang, C., Wang, N. Y., Lu, D. H., Wang, J., Zhang, S. S., Wang, Z. X., Ma, H. and Wang, X. L. (2011) Dual Role of BKI1 and 14-3-3 s in Brassinosteroid Signaling to Link Receptor with Transcription Factors. Developmental cell. 21, 825-834

25 Jaillais, Y., Hothorn, M., Belkhadir, Y., Dabi, T., Nimchuk, Z. L., Meyerowitz, E. M. and Chory, J. (2011) Tyrosine phosphorylation controls brassinosteroid receptor activation by triggering membrane release of its kinase inhibitor. Genes & Development. 25, 232-237

26 Wang, X. F., Goshe, M. B., Soderblom, E. J., Phinney, B. S., Kuchar, J. A., Li, J., Asami, T., Yoshida, S., Huber, S. C. and Clouse, S. D. (2005) Identification and functional analysis of in vivo phosphorylation sites of the Arabidopsis BRASSINOSTEROID-INSENSITIVE1 receptor kinase. Plant Cell. 17, 1685-1703

27 Wang, X. F., Kota, U., He, K., Blackburn, K., Li, J., Goshe, M. B., Huber, S. C. and Clouse, S. D. (2008) Sequential transphosphorylation of the BRI1/BAK1 receptor kinase complex impacts early events in brassinosteroid signaling. Developmental cell. 15, 220-235

28 Oh, M. H., Wang, X. F., Kota, U., Goshe, M. B., Clouse, S. D. and Huber, S. C. (2009) Tyrosine phosphorylation of the BRI1 receptor kinase emerges as a component of brassinosteroid signaling in Arabidopsis. Proceedings of the National Academy of Sciences of the United States of America. 106, 658-663

29 Zhao, B. L., Lv, M. H., Feng, Z. X., Campbell, T., Liscum, E. and Li, J. (2016) TWISTED DWARF 1 Associates with BRASSINOSTEROID-INSENSITIVE 1 to Regulate Early Events of the Brassinosteroid Signaling Pathway. Molecular Plant. 9, 582-592

30 Chaiwanon, J., Garcia, V. J., Cartwright, H., Sun, Y. and Wang, Z. Y. (2016) Immunophilin-like FKBP42/TWISTED DWARF1 Interacts with the Receptor Kinase BRI1 to Regulate Brassinosteroid Signaling in Arabidopsis. Molecular Plant. 9, 593-600

31 Kim, T. W., Guan, S. H., Sun, Y., Deng, Z. P., Tang, W. Q., Shang, J. X., Sun, Y., Burlingame, A. L. and Wang, Z. Y. (2009) Brassinosteroid signal transduction from cell-surface receptor kinases to nuclear transcription factors. Nature cell biology. 11, 1254-U1233

32 Kim, T. W., Guan, S. H., Burlingame, A. L. and Wang, Z. Y. (2011) The CDG1 Kinase Mediates Brassinosteroid Signal Transduction from BRI1 Receptor Kinase to BSU1 Phosphatase and GSK3-like Kinase BIN2. Molecular cell. 43, 561-571

33 Tang, W. Q., Kim, T. W., Oses-Prieto, J. A., Sun, Y., Deng, Z. P., Zhu, S. W., Wang, R. J., Burlingame, A. L. and Wang, Z. Y. (2008) BSKs mediate signal transduction from the receptor kinase BRI1 in Arabidopsis. Science. 321, 557-560

34 Sreeramulu, S., Mostizky, Y., Sunitha, S., Shani, E., Nahum, H., Salomon, D., Ben Hayun, L., Gruetter, C., Rauh, D., Ori, N. and Sessa, G. (2013) BSKs are partially redundant positive regulators of brassinosteroid signaling in Arabidopsis. Plant Journal. 74, 905-919

35 Peng, P., Yan, Z. Y., Zhu, Y. Y. and Li, J. M. (2008) Regulation of the Arabidopsis GSK3-like kinase brassinosteroid-insensitive 2 through proteasome-mediated protein degradation. Molecular Plant. 1, 338-346

36 Zhu, J. Y., Li, Y., Cao, D. M., Yang, H., Oh, E., Bi, Y., Zhu, S. and Wang, Z. Y. (2017) The F-box Protein KIB1 Mediates Brassinosteroid-Induced Inactivation

and Degradation of GSK3-like Kinases in Arabidopsis. Molecular cell. 66, 648-657 e644

37 Anne, P., Azzopardi, M., Gissot, L., Beaubiat, S., Hematy, K. and Palauqui, J. C. (2015) OCTOPUS Negatively Regulates BIN2 to Control Phloem Differentiation in Arabidopsis thaliana. Curr. Biol. 25, 2584-2590

38 Hao, Y. H., Wang, H. J., Qiao, S. L., Leng, L. N. and Wang, X. L. (2016) Histone deacetylase HDA6 enhances brassinosteroid signaling by inhibiting the BIN2 kinase. Proceedings of the National Academy of Sciences of the United States of America. 113, 10418-10423

39 Ling, J. J., Li, J., Zhu, D. and Deng, X. W. (2017) Noncanonical role of Arabidopsis COP1/SPA complex in repressing BIN2-mediated PIF3 phosphorylation and degradation in darkness. Proc Natl Acad Sci U S A. 114, 3539-3544

40 Tang, W., Yuan, M., Wang, R., Yang, Y., Wang, C., Oses-Prieto, J. A., Kim, T.-W., Zhou, H.-W., Deng, Z., Gampala, S. S., Gendron, J. M., Jonassen, E. M., Lillo, C., DeLong, A., Burlingame, A. L., Sun, Y. and Wang, Z.-Y. (2011) PP2A activates brassinosteroid-responsive gene expression and plant growth by dephosphorylating BZR1. Nature cell biology. 13, 124-U149

41 Wang, Z. Y., Nakano, T., Gendron, J., He, J. X., Chen, M., Vafeados, D., Yang, Y. L., Fujioka, S., Yoshida, S., Asami, T. and Chory, J. (2002) Nuclear-localized BZR1 mediates brassinosteroid-induced growth and feedback suppression of brassinosteroid biosynthesis. Developmental cell. 2, 505-513

42 Zhao, J., Peng, P., Schmitz, R. J., Decker, A. D., Tax, F. E. and Li, J. M. (2002) Two putative BIN2 substrates are nuclear components of brassinosteroid signaling. Plant Physiology. 130, 1221-1229

43 Yin, Y., Vafeados, D., Tao, Y., Yoshida, S., Asami, T. and Chory, J. (2005) A new class of transcription factors mediates brassinosteroid-regulated gene expression in Arabidopsis. Cell. 120, 249-259

44 Yu, X., Li, L., Zola, J., Aluru, M., Ye, H., Foudree, A., Guo, H., Anderson, S., Aluru, S., Liu, P., Rodermel, S. and Yin, Y. (2011) A brassinosteroid transcriptional network revealed by genome-wide identification of BESI target genes in Arabidopsis thaliana. Plant Journal. 65, 634-646

45 Sun, Y., Fan, X. Y., Cao, D. M., Tang, W. Q., He, K., Zhu, J. Y., He, J. X., Bai, M. Y., Zhu, S. W., Oh, E., Patil, S., Kim, T. W., Ji, H. K., Wong, W. H., Rhee, S. Y. and Wang, Z. Y. (2010) Integration of Brassinosteroid Signal Transduction with the Transcription Network for Plant Growth Regulation in Arabidopsis. Developmental cell. 19, 765-777

46 Li, J. M. (2010) Regulation of the nuclear activities of brassinosteroid signaling. Curr. Opin. Plant Biol. 13, 540-547

47 de Lucas, M. and Prat, S. (2014) PIFs get Brright: PHYTOCHROME INTERACTING FACTORs as integrators of light and hormonal signals. The New phytologist. 202, 1126-1141

48 Oh, E., Zhu, J.-Y. and Wang, Z.-Y. (2012) Interaction between BZR1 and PIF4 integrates brassinosteroid and environmental responses. Nature cell biology. 14, 802-U864

49 Oh, E., Zhu, J.-Y., Bai, M.-Y., Arenhart, R. A., Sun, Y. and Wang, Z.-Y. (2014) Cell elongation is regulated through a central circuit of interacting transcription factors in the Arabidopsis hypocotyl. Elife. 3

50 Wang, Z.-Y., Bai, M.-Y., Oh, E. and Zhu, J.-Y. (2012) Brassinosteroid Signaling Network and Regulation of Photomorphogenesis. Annual Review of Genetics, Vol 46. 46, 701-724

51 Zhang, L. Y., Bai, M. Y., Wu, J. X., Zhu, J. Y., Wang, H., Zhang, Z. G., Wang, W. F., Sun, Y., Zhao, J., Sun, X. H., Yang, H. J., Xu, Y. Y., Kim, S. H., Fujioka, S., Lin, W. H., Chong, K., Lu, T. G. and Wang, Z. Y. (2009) Antagonistic HLH/bHLH Transcription Factors Mediate Brassinosteroid Regulation of Cell Elongation and Plant Development in Rice and Arabidopsis. Plant Cell. 21, 3767-3780

52 Wang, H., Zhu, Y. Y., Fujioka, S., Asami, T., Li, J. Y. and Li, J. M. (2009) Regulation of Arabidopsis Brassinosteroid Signaling by Atypical Basic Helix-Loop-Helix Proteins. Plant Cell. 21, 3781-3791

53 Bai, M. Y., Fan, M., Oh, E. and Wang, Z. Y. (2012) A Triple Helix-Loop-Helix/Basic Helix-Loop-Helix Cascade Controls Cell Elongation Downstream of Multiple Hormonal and Environmental Signaling Pathways in Arabidopsis. Plant Cell. 24, 4917-4929

54 Ikeda, M., Fujiwara, S., Mitsuda, N. and Ohme-Takagi, M. (2012) A Triantagonistic Basic Helix-Loop-Helix System Regulates Cell Elongation in Arabidopsis. Plant Cell. 24, 4483-4497

55 Bai, M.-Y., Shang, J.-X., Oh, E., Fan, M., Bai, Y., Zentella, R., Sun, T.-p. and Wang, Z.-Y. (2012) Brassinosteroid, gibberellin and phytochrome impinge on a common transcription module in Arabidopsis. Nature cell biology. 14, 810-U878

56 Gallego-Bartolome, J., Minguet, E. G., Grau-Enguix, F., Abbas, M., Locascio, A., Thomas, S. G., Alabadi, D. and Blazquez, M. A. (2012) Molecular mechanism for the interaction between gibberellin and brassinosteroid signaling pathways in

Arabidopsis. Proceedings of the National Academy of Sciences of the United States of America. 109, 13446-13451

57 Li, Q. F., Wang, C. M., Jiang, L., Li, S., Sun, S. S. M. and He, J. X. (2012) An Interaction Between BZR1 and DELLAs Mediates Direct Signaling Crosstalk Between Brassinosteroids and Gibberellins in Arabidopsis. Science Signaling. 5

58 Unterholzner, S. J., Rozhon, W., Papacek, M., Ciomas, J., Lange, T., Kugler, K. G., Mayer, K. F., Sieberer, T. and Poppenberger, B. (2015) Brassinosteroids Are Master Regulators of Gibberellin Biosynthesis in Arabidopsis. Plant Cell. 27, 2261-2272

59 Tong, H. N., Xiao, Y. H., Liu, D. P., Gao, S. P., Liu, L. C., Yin, Y. H., Jin, Y., Qian, Q. and Chu, C. C. (2014) Brassinosteroid Regulates Cell Elongation by Modulating Gibberellin Metabolism in Rice. Plant Cell. 26, 4376-4393

60 Shahnejat-Bushehri, S., Tarkowska, D., Sakuraba, Y. and Balazadeh, S. (2016) Arabidopsis NAC transcription factor JUB1 regulates GA/BR metabolism and signalling. Nat Plants. 2, 16013

61 Li, L., Yu, X., Thompson, A., Guo, M., Yoshida, S., Asami, T., Chory, J. and Yin, Y. (2009) Arabidopsis MYB30 is a direct target of BES1 and cooperates with BES1 to regulate brassinosteroid-induced gene expression. Plant Journal. 58, 275-286

62 Espinosa-Ruiz, A., Martinez, C., de Lucas, M., Fabregas, N., Bosch, N., Cano-Delgado, A. I. and Prat, S. (2017) TOPLESS mediates brassinosteroid control of shoot boundaries and root meristem development in Arabidopsis thaliana. Development. 144, 1619-1628

63 Wang, X., Chen, J., Xie, Z., Liu, S., Nolan, T., Ye, H., Zhang, M., Guo, H., Schnable, P. S., Li, Z. and Yin, Y. (2014) Histone Lysine Methyltransferase SDG8 Is Involved in Brassinosteroid-Regulated Gene Expression in Arabidopsis thaliana. Molecular Plant. 7, 1303-1315

64 Li, L., Ye, H., Guo, H. and Yin, Y. (2010) Arabidopsis IWS1 interacts with transcription factor BES1 and is involved in plant steroid hormone brassinosteroid regulated gene expression. Proceedings of the National Academy of Sciences of the United States of America. 107, 3918-3923

65 Yu, X., Li, L., Li, L., Guo, M., Chory, J. and Yin, Y. (2008) Modulation of brassinosteroid-regulated gene expression by jumonji domain-containing proteins ELF6 and REF6 in Arabidopsis. Proceedings of the National Academy of Sciences of the United States of America. 105, 7618-7623

66 Nakashima, K., Yamaguchi-Shinozaki, K. and Shinozaki, K. (2014) The transcriptional regulatory network in the drought response and its crosstalk in abiotic stress responses including drought, cold, and heat. Frontiers in Plant Science. 5

67 Yoshida, T., Mogami, J. and Yamaguchi-Shinozaki, K. (2014) ABA-dependent and ABA-independent signaling in response to osmotic stress in plants. Curr Opin Plant Biol. 21, 133-139

68 Raghavendra, A. S., Gonugunta, V. K., Christmann, A. and Grill, E. (2010) ABA perception and signalling. Trends Plant Sci. 15, 395-401

69 Espasandin, F. D., Maiale, S. J., Calzadilla, P., Ruiz, O. A. and Sansberro, P. A. (2014) Transcriptional regulation of 9-cis-epoxycarotenoid dioxygenase (NCED) gene by putrescine accumulation positively modulates ABA synthesis and drought tolerance in Lotus tenuis plants. Plant Physiol Biochem. 76, 29-35

70 Iuchi, S., Kobayashi, M., Taji, T., Naramoto, M., Seki, M., Kato, T., Tabata, S., Kakubari, Y., Yamaguchi-Shinozaki, K. and Shinozaki, K. (2001) Regulation of drought tolerance by gene manipulation of 9-cis-epoxycarotenoid dioxygenase, a key enzyme in abscisic acid biosynthesis in Arabidopsis. The Plant Journal. 27, 325-333

71 Cutler, S. R., Rodriguez, P. L., Finkelstein, R. R. and Abrams, S. R. (2010) Abscisic acid: emergence of a core signaling network. Annual review of plant biology. 61, 651-679

72 Ma, Y., Szostkiewicz, I., Korte, A., Moes, D., Yang, Y., Christmann, A. and Grill, E. (2009) Regulators of PP2C Phosphatase Activity Function as Abscisic Acid Sensors. Science. 324, 1064-1068

73 Park, S.-Y., Fung, P., Nishimura, N., Jensen, D. R., Fujii, H., Zhao, Y., Lumba, S., Santiago, J., Rodrigues, A., Chow, T.-f. F., Alfred, S. E., Bonetta, D., Finkelstein, R., Provart, N. J., Desveaux, D., Rodriguez, P. L., McCourt, P., Zhu, J.-K., Schroeder, J. I., Volkman, B. F. and Cutler, S. R. (2009) Abscisic Acid Inhibits Type 2C Protein Phosphatases via the PYR/PYL Family of START Proteins. Science. 324, 1068-1071

74 Nishimura, N., Sarkeshik, A., Nito, K., Park, S.-Y., Wang, A., Carvalho, P. C., Lee, S., Caddell, D. F., Cutler, S. R., Chory, J., Yates, J. R. and Schroeder, J. I. (2010) PYR/PYL/RCAR family members are major in-vivo ABI1 protein phosphatase 2C-interacting proteins in Arabidopsis. The Plant Journal. 61, 290-299

75 Santiago, J., Rodrigues, A., Saez, A., Rubio, S., Antoni, R., Dupeux, F., Park, S.-Y., Márquez, J. A., Cutler, S. R. and Rodriguez, P. L. (2009) Modulation of

drought resistance by the abscisic acid receptor PYL5 through inhibition of clade A PP2Cs. The Plant Journal. 60, 575-588

76 Yoshida, T., Mogami, J. and Yamaguchi-Shinozaki, K. (2015) Omics Approaches Toward Defining the Comprehensive Abscisic Acid Signaling Network in Plants. Plant Cell Physiol. 56, 1043-1052

77 Li, J. M., Nam, K. H., Vafeados, D. and Chory, J. (2001) BIN2, a new brassinosteroid-insensitive locus in Arabidopsis. Plant Physiology. 127, 14-22

78 Steber, C. M. and McCourt, P. (2001) A role for brassinosteroids in germination in Arabidopsis. Plant Physiology. 125, 763-769

79 Nemhauser, J. L., Hong, F. and Chory, J. (2006) Different Plant Hormones Regulate Similar Processes through Largely Nonoverlapping Transcriptional Responses. Cell. 126, 467-475

80 Zhang, S., Cai, Z. and Wang, X. (2009) The primary signaling outputs of brassinosteroids are regulated by abscisic acid signaling. Proc Natl Acad Sci U S A. 106, 4543-4548

81 Gui, J., Zheng, S., Liu, C., Shen, J., Li, J. and Li, L. (2016) OsREM4.1 Interacts with OsSERK1 to Coordinate the Interlinking between Abscisic Acid and Brassinosteroid Signaling in Rice. Developmental cell. 38, 201-213

82 Clouse, S. D. (2016) Brassinosteroid/Abscisic Acid Antagonism in Balancing Growth and Stress. Developmental cell. 38, 118-120

83 Zong, W., Tang, N., Yang, J., Peng, L., Ma, S., Xu, Y., Li, G. and Xiong, L. (2016) Feedback Regulation of ABA Signaling and Biosynthesis by a bZIP Transcription Factor Targets Drought-Resistance-Related Genes. Plant Physiol. 171, 2810-2825

84 Shang, Y., Dai, C., Lee, M. M., Kwak, J. M. and Nam, K. H. (2016) BRI1-Associated Receptor Kinase 1 Regulates Guard Cell ABA Signaling Mediated by Open Stomata 1 in Arabidopsis. Molecular Plant. 9, 447-460

85 Acharya, B. R., Jeon, B. W., Zhang, W. and Assmann, S. M. (2013) Open Stomata 1 (OST1) is limiting in abscisic acid responses of Arabidopsis guard cells. The New phytologist. 200, 1049-1063

86 Mustilli, A. C. (2002) Arabidopsis OST1 Protein Kinase Mediates the Regulation of Stomatal Aperture by Abscisic Acid and Acts Upstream of Reactive Oxygen Species Production. The Plant Cell Online. 14, 3089-3099

87 Shi, C. Y., Qi, C., Ren, H. Y., Huang, A. X., Hei, S. M. and She, X. P. (2015) Ethylene mediates brassinosteroid-induced stomatal closure via G alpha protein-activated hydrogen peroxide and nitric oxide production in Arabidopsis. Plant Journal. 82, 280-301

88 Haubrick, L. L., Torsethaugen, G. and Assmann, S. M. (2006) Effect of brassinolide, alone and in concert with abscisic acid, on control of stomatal aperture and potassium currents of Vicia faba guard cell protoplasts. Physiol Plantarum. 128, 134-143

89 Xia, X. J., Gao, C. J., Song, L. X., Zhou, Y. H., Shi, K. and Yu, J. Q. (2014) Role of H2O2 dynamics in brassinosteroid-induced stomatal closure and opening in Solanum lycopersicum. Plant Cell and Environment. 37, 2036-2050

90 Ha, Y., Shang, Y. and Nam, K. H. (2016) Brassinosteroids modulate ABA-induced stomatal closure in Arabidopsis. Journal of Experimental Botany. 67, 6297-6308

91 Ephritikhine, G., Pagant, S., Fujioka, S., Takatsuto, S., Lapous, D., Caboche, M., Kendrick, R. E. and Barbier-Brygoo, H. (1999) The sax1 mutation defines a new locus involved in the brassinosteroid biosynthesis pathway in Arabidopsis thaliana. Plant Journal. 18, 315-320

92 Xue, L. W., Du, J. B., Yang, H., Xu, F., Yuan, S. and Lin, H. H. (2009) Brassinosteroids Counteract Abscisic Acid in Germination and Growth of Arabidopsis. Zeitschrift Fur Naturforschung Section C-a Journal of Biosciences. 64, 225-230

93 Youn, J. H. and Kim, T. W. (2014) Functional Insights of Plant GSK3-like Kinases: Multi-Taskers in Diverse Cellular Signal Transduction Pathways. Mol Plant

94 Cai, Z., Liu, J., Wang, H., Yang, C., Chen, Y., Li, Y., Pan, S., Dong, R., Tang, G., Barajas-Lopez Jde, D., Fujii, H. and Wang, X. (2014) GSK3-like kinases positively modulate abscisic acid signaling through phosphorylating subgroup III SnRK2s in Arabidopsis. Proc Natl Acad Sci U S A. 111, 9651-9656

95 Finkelstein, R. R. and Lynch, T. J. (2000) The arabidopsis abscisic acid response gene ABI5 encodes a basic leucine zipper transcription factor. Plant Cell. 12, 599-609

96 Skubacz, A., Daszkowska-Golec, A. and Szarejko, L. (2016) The Role and Regulation of ABI5 (ABA-Insensitive 5) in Plant Development, Abiotic Stress Responses and Phytohormone Crosstalk. Frontiers in Plant Science. 7

97 Hu, Y. and Yu, D. (2014) BRASSINOSTEROID INSENSITIVE2 interacts with ABSCISIC ACID INSENSITIVE5 to mediate the antagonism of brassinosteroids to abscisic acid during seed germination in Arabidopsis. Plant Cell. 26, 4394-4408

98 Charrier, B., Champion, A., Henry, Y. and Kreis, M. (2002) Expression profiling of the whole Arabidopsis shaggy-like kinase multigene family by real-time reverse transcriptase-polymerase chain reaction. Plant Physiol. 130, 577-590

99 Dal Santo, S., Stampfl, H., Krasensky, J., Kempa, S., Gibon, Y., Petutschnig, E., Rozhon, W., Heuck, A., Clausen, T. and Jonak, C. (2012) Stress-induced GSK3 regulates the redox stress response by phosphorylating glucose-6-phosphate dehydrogenase in Arabidopsis. Plant Cell. 24, 3380-3392

100 Ryu, H., Cho, H., Bae, W. and Hwang, I. (2014) Control of early seedling development by BES1/TPL/HDA19-mediated epigenetic regulation of ABI3. Nature communications. 5

101 Yang, X., Bai, Y., Shang, J., Xin, R. and Tang, W. (2016) The antagonistic regulation of abscisic acid-inhibited root growth by brassinosteroids is partially mediated via direct suppression of ABSCISIC ACID INSENSITIVE 5 expression by BRASSINAZOLE RESISTANT 1. Plant, cell & environment. 39, 1994-2003

102 Lee, H. G. and Seo, P. J. (2016) The Arabidopsis MIEL1 E3 ligase negatively regulates ABA signalling by promoting protein turnover of MYB96. Nature communications. 7

103 Zheng, Y., Schumaker, K. S. and Guo, Y. (2012) Sumoylation of transcription factor MYB30 by the small ubiquitin-like modifier E3 ligase SIZ1 mediates abscisic acid response in Arabidopsis thaliana. Proceedings of the National Academy of Sciences of the United States of America. 109, 12822-12827

104 Marino, D., Froidure, S., Canonne, J., Ben Khaled, S., Khafif, M., Pouzet, C., Jauneau, A., Roby, D. and Rivas, S. (2013) Arabidopsis ubiquitin ligase MIEL1 mediates degradation of the transcription factor MYB30 weakening plant defence. Nature communications. 4, 1476

105 Seo, P. J., Xiang, F. N., Qiao, M., Park, J. Y., Lee, Y. N., Kim, S. G., Lee, Y. H., Park, W. J. and Park, C. M. (2009) The MYB96 Transcription Factor Mediates Abscisic Acid Signaling during Drought Stress Response in Arabidopsis. Plant Physiology. 151, 275-289

106 Divi, U. K., Rahman, T. and Krishna, P. (2016) Gene expression and functional analyses in brassinosteroid-mediated stress tolerance. Plant Biotechnology Journal. 14, 419-432

107 Kagale, S., Divi, U. K., Krochko, J. E., Keller, W. A. and Krishna, P. (2007) Brassinosteroid confers tolerance in Arabidopsis thaliana and Brassica napus to a range of abiotic stresses. Planta. 225, 353-364

108 Bajguz, A. and Hayat, S. (2009) Effects of brassinosteroids on the plant responses to environmental stresses. Plant Physiology and Biochemistry. 47, 1-8

109 Yuan, G. F., Jia, C. G., Li, Z., Sun, B., Zhang, L. P., Liu, N. and Wang, Q. M. (2010) Effect of brassinosteroids on drought resistance and abscisic acid concentration in tomato under water stress. Sci Hortic-Amsterdam. 126, 103-108

110 Anjum, S. A., Wang, L. C., Farooq, M., Hussain, M., Xue, L. L. and Zou, C. M. (2011) Brassinolide Application Improves the Drought Tolerance in Maize Through Modulation of Enzymatic Antioxidants and Leaf Gas Exchange. J Agron Crop Sci. 197, 177-185

111 Zhou, J., Wang, J., Li, X., Xia, X. J., Zhou, Y. H., Shi, K., Chen, Z. X. and Yu, J. Q. (2014) H2O2 mediates the crosstalk of brassinosteroid and abscisic acid in tomato responses to heat and oxidative stresses. Journal of Experimental Botany. 65, 4371-4383

112 Ye, H., Liu, S., Tang, B., Chen, J., Xie, Z., Nolan, T. M., Jiang, H., Guo, H., Lin, H.-Y., Li, L., Wang, Y., Tong, H., Zhang, M., Chu, C., Li, Z., Aluru, M., Aluru, S., Schnable, P. S. and Yin, Y. (2017) RD26 mediates crosstalk between drought and brassinosteroid signalling pathways. Nature communications. 8, 14573

113 Nolan, T. M., Brennan, B., Yang, M., Chen, J., Zhang, M., Li, Z., Wang, X., Bassham, D. C., Walley, J. and Yin, Y. (2017) Selective Autophagy of BES1 Mediated by DSK2 Balances Plant Growth and Survival. Developmental cell. 41, 33-46 e37

114 Northey, J. G., Liang, S., Jamshed, M., Deb, S., Foo, E., Reid, J. B., McCourt, P. and Samuel, M. A. (2016) Farnesylation mediates brassinosteroid biosynthesis to regulate abscisic acid responses. Nat Plants. 2, 16114

115 Feng, Y., Yin, Y. and Fei, S. (2015) Down-regulation of BdBRI1, a putative brassinosteroid receptor gene produces a dwarf phenotype with enhanced drought tolerance in Brachypodium distachyon. Plant Sci. 234, 163-173

116 Claeys, H. and Inze, D. (2013) The agony of choice: how plants balance growth and survival under water-limiting conditions. Plant Physiol. 162, 1768-1779

117 Tran, L. S. P., Nakashima, K., Sakuma, Y., Simpson, S. D., Fujita, Y., Maruyama, K., Fujita, M., Seki, M., Shinozaki, K. and Yamaguchi-Shinozaki, K. (2004) Isolation and functional analysis of Arabidopsis stress-inducible NAC

transcription factors that bind to a drought-responsive cis-element in the early responsive to dehydration stress 1 promoter. Plant Cell. 16, 2481-2498

118 Chung, Y., Kwon, S. I. and Choe, S. (2014) Antagonistic regulation of Arabidopsis growth by brassinosteroids and abiotic stresses. Mol Cells. 37, 795-803

119 Fujita, M., Fujita, Y., Maruyama, K., Seki, M., Hiratsu, K., Ohme-Takagi, M., Tran, L. S. P., Yamaguchi-Shinozaki, K. and Shinozaki, K. (2004) A dehydration-induced NAC protein, RD26, is involved in a novel ABA-dependent stress-signaling pathway. Plant Journal. 39, 863-876

120 Guan, Q. M., Yue, X. L., Zeng, H. T. and Zhu, J. H. (2014) The Protein Phosphatase RCF2 and Its Interacting Partner NAC019 Are Critical for Heat Stress-Responsive Gene Regulation and Thermotolerance in Arabidopsis. Plant Cell. 26, 438-453

121 Song, L., Huang, S. C., Wise, A., Castanon, R., Nery, J. R., Chen, H., Watanabe, M., Thomas, J., Bar-Joseph, Z. and Ecker, J. R. (2016) A transcription factor hierarchy defines an environmental stress response network. Science. 354

122 Sun, Y., Fan, X.-Y., Cao, D.-M., Tang, W., He, K., Zhu, J.-Y., He, J.-X., Bai, M.-Y., Zhu, S., Oh, E., Patil, S., Kim, T.-W., Ji, H., Wong, W. H., Rhee, S. Y. and Wang, Z.-Y. (2010) Integration of Brassinosteroid Signal Transduction with the Transcription Network for Plant Growth Regulation in Arabidopsis. Developmental cell. 19, 765-777

123 Maruyama, K., Takeda, M., Kidokoro, S., Yamada, K., Sakuma, Y., Urano, K., Fujita, M., Yoshiwara, K., Matsukura, S., Morishita, Y., Sasaki, R., Suzuki, H., Saito, K., Shibata, D., Shinozaki, K. and Yamaguchi-Shinozaki, K. (2009) Metabolic Pathways Involved in Cold Acclimation Identified by Integrated Analysis of Metabolites and Transcripts Regulated by DREB1A and DREB2A. Plant Physiology. 150, 1972-1980

124 Divi, U. K., Rahman, T. and Krishna, P. (2010) Brassinosteroid-mediated stress tolerance in Arabidopsis shows interactions with abscisic acid, ethylene and salicylic acid pathways. Bmc Plant Biology. 10

125 Michaeli, S., Galili, G., Genschik, P., Fernie, A. R. and Avin-Wittenberg, T. (2015) Autophagy in Plants – What's New on the Menu? Trends Plant Sci.

126 Floyd, B. E., Morriss, S. C., MacIntosh, G. C. and Bassham, D. C. (2012) What to Eat: Evidence for Selective Autophagy in Plants. Journal of integrative plant biology. 54, 907-920

127 Kraft, C., Peter, M. and Hofmann, K. (2010) Selective autophagy: ubiquitin-mediated recognition and beyond. Nature cell biology. 12, 836-841

128 Liu, X. D., Yao, J., Tripathi, D. N., Ding, Z., Xu, Y., Sun, M., Zhang, J., Bai, S., German, P., Hoang, A., Zhou, L., Jonasch, D., Zhang, X., Conti, C. J., Efstathiou, E., Tannir, N. M., Eissa, N. T., Mills, G. B., Walker, C. L. and Jonasch, E. (2014) Autophagy mediates HIF2alpha degradation and suppresses renal tumorigenesis. Oncogene

129 Gao, C., Cao, W., Bao, L., Zuo, W., Xie, G., Cai, T., Fu, W., Zhang, J., Wu, W., Zhang, X. and Chen, Y. G. (2010) Autophagy negatively regulates Wnt signalling by promoting Dishevelled degradation. Nature cell biology. 12, 781-790

130 Zhang, Z., Zhu, J. Y., Roh, J., Marchive, C., Kim, S. K., Meyer, C., Sun, Y., Wang, W. and Wang, Z. Y. (2016) TOR Signaling Promotes Accumulation of BZR1 to Balance Growth with Carbon Availability in Arabidopsis. Current biology : CB. 26, 1854-1860

131 Yang, M., Li, C., Cai, Z., Hu, Y., Nolan, T., Yu, F., Yin, Y., Xie, Q., Tang, G. and Wang, X. (2017) SINAT E3 Ligases Control the Light-Mediated Stability of the Brassinosteroid-Activated Transcription Factor BES1 in Arabidopsis. Developmental cell. 41, 47-58 e44

132 Chen, J., Nolan, T., Ye, H., Zhang, M., Tong, H., Xin, P., Chu, J., Chu, C., Li, Z. and Yin, Y. (2017) Arabidopsis WRKY46, WRKY54 and WRKY70 Transcription Factors Are Involved in Brassinosteroid-Regulated Plant Growth and Drought Response. The Plant Cell, tpc.00364.02017

133 Li, J., Brader, G. and Palva, E. T. (2004) The WRKY70 transcription factor: a node of convergence for jasmonate-mediated and salicylate-mediated signals in plant defense. Plant Cell. 16, 319-331

134 Li, J., Brader, G., Kariola, T. and Palva, E. T. (2006) WRKY70 modulates the selection of signaling pathways in plant defense. Plant J. 46, 477-491

135 Hu, Y., Dong, Q. and Yu, D. (2012) Arabidopsis WRKY46 coordinates with WRKY70 and WRKY53 in basal resistance against pathogen Pseudomonas syringae. Plant Sci. 185-186, 288-297

136 Ding, Z. J., Yan, J. Y., Xu, X. Y., Yu, D. Q., Li, G. X., Zhang, S. Q. and Zheng, S. J. (2014) Transcription factor WRKY46 regulates osmotic stress responses and stomatal movement independently in Arabidopsis. Plant J. 79, 13-27

137 Li, J., Besseau, S., Toronen, P., Sipari, N., Kollist, H., Holm, L. and Palva, E. T. (2013) Defense-related transcription factors WRKY70 and WRKY54 modulate

osmotic stress tolerance by regulating stomatal aperture in Arabidopsis. New Phytol. 200, 457-472

138 Gomez-Gomez, L. and Boller, T. (2000) FLS2: An LRR receptor-like kinase involved in the perception of the bacterial elicitor flagellin in Arabidopsis. Molecular cell. 5, 1003-1011

139 Li, J., Wen, J., Lease, K. A., Doke, J. T., Tax, F. E. and Walker, J. C. (2002) BAK1, an Arabidopsis LRR receptor-like protein kinase, interacts with BRI1 and modulates brassinosteroid signaling. Cell. 110, 213-222

140 Chinchilla, D., Zipfel, C., Robatzek, S., Kemmerling, B., Nurnberger, T., Jones, J. D., Felix, G. and Boller, T. (2007) A flagellin-induced complex of the receptor FLS2 and BAK1 initiates plant defence. Nature. 448, 497-500

141 Zipfel, C., Kunze, G., Chinchilla, D., Caniard, A., Jones, J. D., Boller, T. and Felix, G. (2006) Perception of the bacterial PAMP EF-Tu by the receptor EFR restricts Agrobacterium-mediated transformation. Cell. 125, 749-760

142 Yamaguchi, Y. P., G.; Ryan, C.A. (2006) The cell surface leucine-rich repeat receptor for AtPep1, an endogenous peptide elicitor in Arabidopsis, is functional in transgenic tobacco cells. Proc Natl Acad Sci U S A. 103, 10104-10109

143 Schulze, B., Mentzel, T., Jehle, A. K., Mueller, K., Beeler, S., Boller, T., Felix, G. and Chinchilla, D. (2010) Rapid heteromerization and phosphorylation of ligand-activated plant transmembrane receptors and their associated kinase BAK1. J Biol Chem. 285, 9444-9451

144 Liu, Y., Huang, X., Li, M., He, P. and Zhang, Y. (2016) Loss-of-function of Arabidopsis receptor-like kinase BIR1 activates cell death and defense responses mediated by BAK1 and SOBIR1. New Phytol

145 Belkhadir, Y., Jaillais, Y., Epple, P., Balsemao-Pires, E., Dangl, J. L. and Chory, J. (2012) Brassinosteroids modulate the efficiency of plant immune responses to microbe-associated molecular patterns. Proceedings of the National Academy of Sciences of the United States of America. 109, 297-302

146 Belkhadir, Y., Yang, L., Hetzel, J., Dangl, J. L. and Chory, J. (2014) The growth-defense pivot: crisis management in plants mediated by LRR-RK surface receptors. Trends Biochem Sci. 39, 447-456

147 Albrecht, C., Boutrot, F., Segonzac, C., Schwessinger, B., Gimenez-Ibanez, S., Chinchilla, D., Rathjen, J. P., de Vries, S. C. and Zipfel, C. (2012) Brassinosteroids inhibit pathogen-associated molecular pattern-triggered immune signaling independent of the receptor kinase BAK1. Proc Natl Acad Sci U S A. 109, 303-308

148 Ali, S. S., Kumar, G. B., Khan, M. and Doohan, F. M. (2013) Brassinosteroid enhances resistance to fusarium diseases of barley. Phytopathology. 103, 1260-1267

149 Sahni, S., Prasad, B. D., Liu, Q., Grbic, V., Sharpe, A., Singh, S. P. and Krishna, P. (2016) Overexpression of the brassinosteroid biosynthetic gene DWF4 in Brassica napus simultaneously increases seed yield and stress tolerance. Sci Rep. 6, 28298

150 Ali, S. S., Gunupuru, L. R., Kumar, G. B. S., Khan, M., Scofield, S., Nicholson, P. and Doohan, F. M. (2014) Plant disease resistance is augmented in uzu barley lines modified in the brassinosteroid receptor BRI1. Bmc Plant Biology. 14

151 Goddard, R., Peraldi, A., Ridout, C. and Nicholson, P. (2014) Enhanced Disease Resistance Caused by BRI1 Mutation Is Conserved Between Brachypodium distachyon and Barley (Hordeum vulgare). Molecular Plant-Microbe Interactions. 27, 1095-1106

152 Lu, D., Wu, S., Gao, X., Zhang, Y., Shan, L. and He, P. (2010) A receptor-like cytoplasmic kinase, BIK1, associates with a flagellin receptor complex to initiate plant innate immunity. Proc Natl Acad Sci U S A. 107, 496-501

153 Tang, W., Kim, T. W., Oses-Prieto, J. A., Sun, Y., Deng, Z., Zhu, S., Wang, R., Burlingame, A. L. and Wang, Z. Y. (2008) BSKs mediate signal transduction from the receptor kinase BRI1 in Arabidopsis. Science. 321, 557-560

154 Shi, H., Shen, Q., Qi, Y., Yan, H., Nie, H., Chen, Y., Zhao, T., Katagiri, F. and Tang, D. (2013) BR-SIGNALING KINASE1 physically associates with FLAGELLIN SENSING2 and regulates plant innate immunity in Arabidopsis. Plant Cell. 25, 1143-1157

155 Shi, H., Yan, H., Li, J. and Tang, D. (2013) BSK1, a receptor-like cytoplasmic kinase, involved in both BR signaling and innate immunity in Arabidopsis. Plant Signal Behav. 8

156 Lin, W., Lu, D., Gao, X., Jiang, S., Ma, X., Wang, Z., Mengiste, T., He, P. and Shan, L. (2013) Inverse modulation of plant immune and brassinosteroid signaling pathways by the receptor-like cytoplasmic kinase BIK1. Proc Natl Acad Sci U S A. 110, 12114-12119

157 Li, L., Li, M., Yu, L., Zhou, Z., Liang, X., Liu, Z., Cai, G., Gao, L., Zhang, X., Wang, Y., Chen, S. and Zhou, J. M. (2014) The FLS2-associated kinase BIK1 directly phosphorylates the NADPH oxidase RbohD to control plant immunity. Cell Host Microbe. 15, 329-338

158 Kadota, Y., Sklenar, J., Derbyshire, P., Stransfeld, L., Asai, S., Ntoukakis, V., Jones, J. D., Shirasu, K., Menke, F., Jones, A. and Zipfel, C. (2014) Direct regulation of the NADPH oxidase RBOHD by the PRR-associated kinase BIK1 during plant immunity. Mol Cell. 54, 43-55

159 Couto, D., Niebergall, R., Liang, X., Bucherl, C. A., Sklenar, J., Macho, A. P., Ntoukakis, V., Derbyshire, P., Altenbach, D., Maclean, D., Robatzek, S., Uhrig, J., Menke, F., Zhou, J. M. and Zipfel, C. (2016) The Arabidopsis Protein Phosphatase PP2C38 Negatively Regulates the Central Immune Kinase BIK1. PloS Pathog. 12, e1005811

160 Segonzac, C., Macho, A. P., Sanmartin, M., Ntoukakis, V., Sanchez-Serrano, J. J. and Zipfel, C. (2014) Negative control of BAK1 by protein phosphatase 2A during plant innate immunity. Embo Journal. 33, 2069-2079

161 Bucherl, C. A., Jarsch, I. K., Schudoma, C., Segonzac, C., Mbengue, M., Robatzek, S., MacLean, D., Ott, T. and Zipfel, C. (2017) Plant immune and growth receptors share common signalling components but localise to distinct plasma membrane nanodomains. Elife. 6

162 Lozano-Duran, R., Macho, A. P., Boutrot, F., Segonzac, C., Somssich, I. E. and Zipfel, C. (2013) The transcriptional regulator BZR1 mediates trade-off between plant innate immunity and growth. Elife. 2

163 Lozano-Duran, R., Macho, A. P., Boutrot, F., Segonzac, C., Somssich, I. E. and Zipfel, C. (2013) The transcriptional regulator BZR1 mediates trade-off between plant innate immunity and growth. Elife. 2, e00983

164 Fan, M., Bai, M. Y., Kim, J. G., Wang, T. N., Oh, E., Chen, L., Park, C. H., Son, S. H., Kim, S. K., Mudgett, M. B. and Wang, Z. Y. (2014) The bHLH Transcription Factor HBI1 Mediates the Trade-Off between Growth and Pathogen-Associated Molecular Pattern-Triggered Immunity in Arabidopsis. Plant Cell. 26, 828-841

165 Miyaji, T., Yamagami, A., Kume, N., Sakuta, M., Osada, H., Asami, T., Arimoto, Y. and Nakano, T. (2014) Brassinosteroid-related transcription factor BIL1/BZR1 increases plant resistance to insect feeding. Biosci Biotechnol Biochem. 78, 960-968

166 Shahnejat-Bushehri, S., Nobmann, B., Devi Allu, A. and Balazadeh, S. (2016) JUB1 suppresses Pseudomonas syringae-induced defense responses through accumulation of DELLA proteins. Plant Signal Behav. 11, e1181245

167 Navarro, L., Bari, R., Achard, P., Lison, P., Nemri, A., Harberd, N. P. and Jones, J. D. (2008) DELLAs control plant immune responses by modulating the balance of jasmonic acid and salicylic acid signaling. Curr Biol. 18, 650-655

168 De Vleesschauwer, D., Van Buyten, E., Satoh, K., Balidion, J., Mauleon, R., Choi, I. R., Vera-Cruz, C., Kikuchi, S. and Hofte, M. (2012) Brassinosteroids antagonize gibberellin- and salicylate-mediated root immunity in rice. Plant Physiol. 158, 1833-1846

169 Kang, S., Yang, F., Li, L., Chen, H., Chen, S. and Zhang, J. (2015) The Arabidopsis Transcription Factor BRASSINOSTEROID INSENSITIVE1-ETHYL METHANESULFONATE-SUPPRESSOR1 Is a Direct Substrate of MITOGEN-ACTIVATED PROTEIN KINASE6 and Regulates Immunity. Plant Physiol. 167, 1076-1086

170 Shin, S. Y., Chung, H., Kim, S. Y. and Nam, K. H. (2016) BRI1-EMS-suppressor 1 gain-of-function mutant shows higher susceptibility to necrotrophic fungal infection. Biochem Biophys Res Commun. 470, 864-869

171 Vailleau, F. (2002) A R2R3-MYB gene, AtMYB30, acts as a positive regulator of the hypersensitive cell death program in plants in response to pathogen attack. Proc Natl Acad Sci U S A. 99, 10179-10184

172 Li, L., Yu, X., Thompson, A., Guo, M., Yoshida, S., Asami, T., Chory, J. and Yin, Y. (2009) Arabidopsis MYB30 is a direct target of BES1 and cooperates with BES1 to regulate brassinosteroid-induced gene expression. Plant J. 58, 275-286

173 Nakashita, H. Y. M., Nitta T, Asami T, Fujioka S, Arai Y, Sekimata K, Takatsuto S, Yamaguchi I, Yoshida S. (2003) Brassinosteroid functions in a broad range of disease resistance in tobacco and rice. Plant Journal. 33, 887-898

174 Deng, X. G., Zhu, T., Peng, X. J., Xi, D. H., Guo, H. Q., Yin, Y. H., Zhang, D. W. and Lin, H. H. (2016) Role of brassinosteroid signaling in modulating Tobacco mosaic virus resistance in Nicotiana benthamiana. Sci Rep-Uk. 6

175 Deng, X. G., Zhu, T., Zou, L. J., Han, X. Y., Zhou, X., Xi, D. H., Zhang, D. W. and Lin, H. H. (2016) Orchestration of hydrogen peroxide and nitric oxide in brassinosteroid-mediated systemic virus resistance in Nicotiana benthamiana. Plant Journal. 85, 478-493

176 Bailey, T. L. (2011) DREME: motif discovery in transcription factor ChIP-seq data. Bioinformatics. 27, 1653-1659

1.8 Figures

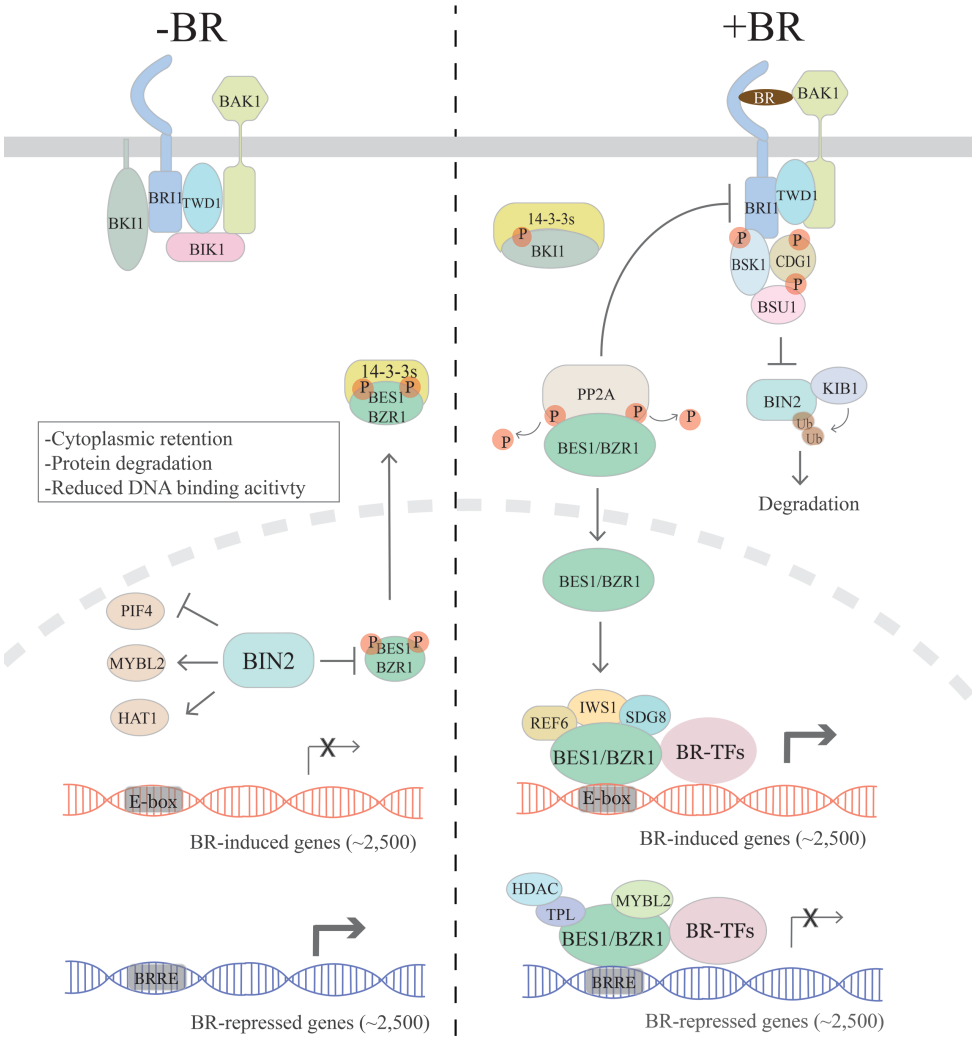

Figure 1: Overview of the BR signaling pathway
In the absence of BR, several negative regulators (BKI1 and BIK1) act to inhibit BR signaling at BRI1/BAK1 receptors, and BIN2 phosphorylates BES1/BZR1 family transcription factors to inhibit their function through several mechanisms. BIN2 also phosphorylates other transcription factors such as PIF4, MYBL2 and HAT1 to regulate their activities. Without BR signaling, expression of BR-induced genes is relatively low whereas BR-repressed genes are more highly expressed, leading to suppressed BR responses. When present, BRs bind to receptor BRI1 and coreceptor BAK1, which leads to the disassociation of BKI1 and BIK1 as well as phosphorylation and activation of BRI1/BAK1, which activates BSK1, CDG1 and BSU1. BSU1 then functions to inhibit BIN2 kinase function while KIB1 ubiquitinates BIN2. PP2A activates BES1/BZR1 by dephosphorylation and cytoplasmic BKI1 sequesters 14-3-3s that otherwise sequester BES1/BZR1 in cytoplasm. These events lead to accumulation of dephosphorylated BES1/BZR1 in the nucleus. BES1/BZR1 bind to E-box elements and interact with cofactors (such as histone modifying enzymes REF6 and SDG8 and transcription elongation factor IWS1) and BR-related transcription factors (BR-TFs, such as PIF4, BIM1) to activate BR-induced gene expression. On the other hand, BES1/BZR1 bind to BRRE sites and interact with co-repressors (TPL and MYBL2), histone deacetylase (HDAC) and likely other BR-TFs to inhibit BR-repressed genes. The large number of BR-regulated genes (~5,000) enable cell elongation and other BR-regulated processes.

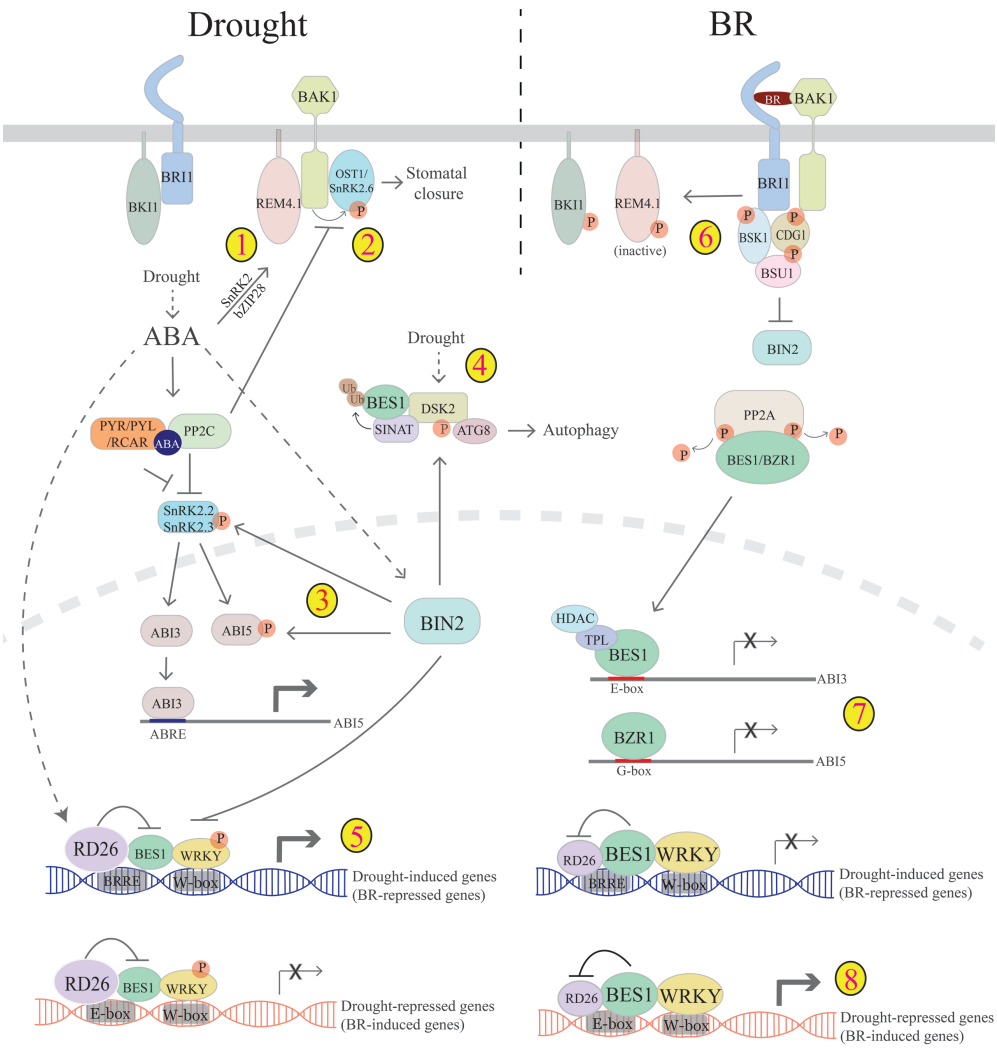

Figure 2: Crosstalk between BR and drought pathways
Drought induces ABA accumulation, which promotes drought responses. ABA acts through receptors (PYR/PYL/RCAR) to inhibit PP2C-repression of SnRKs, allowing SnRKs to phosphorylate downstream TRANSCRIPTION FACTORs (ABI3/ABI5 and others) which regulate genes for drought responses. ABA-activated OST1/SnRK2.6 also functions to regulate stomatal closure. There are several mechanisms of crosstalk between drought/ABA and BR pathways that involve the negative regulator of the BR pathway BIN2 and converge on BES1/BZR1. 1. ABA induces the expression of REM4.1 through SnRK2 and bZIP28; and REM4.1 acts to inhibit BRI1/BAK1 and thus BR signaling. 2. BAK1 and ABI1/PP2C oppositely regulate OST1/SnRK2.6 to modulate stomatal closure, providing another layer to BR-ABA crosstalk. 3. Under drought conditions, BIN2 is active, which phosphorylates and activates SnRK2.2/2.3 and ABI5. 4. During stress conditions, BES1 is ubiquitinated by SINAT E3 ubiquitin ligases and targeted for degradation through selective autophagy via 51hosphor-regulated autophagy receptor DSK2. Phosphorylation of DSK2 by BIN2 enhances DSK2-ATG8 interactions, therefore promoting BES1 degradation. 5. Drought and ABA activate NAC family TRANSCRIPTION FACTOR RD26 that inhibits BES1 activity to promote drought-induced (BR-repressed) genes and inhibit drought-repressed (BR-induced) genes. 6. In contrast, under BR-promoted growth conditions, BRI1 phosphorylates and inactivates REM4.1. 7. BR-activated BES1/BZR1 inhibit *ABI5* expression to inhibit ABA responses either through *ABI3* (top) or by directly binding ABI5 promoter (bottom). 8. On the other hand, BES1 also inhibits RD26 transcriptional activity to promote BR-induced (drought-repressed) genes and inhibit drought-induced (BR-repressed) genes, thereby promoting BR-regulated growth.

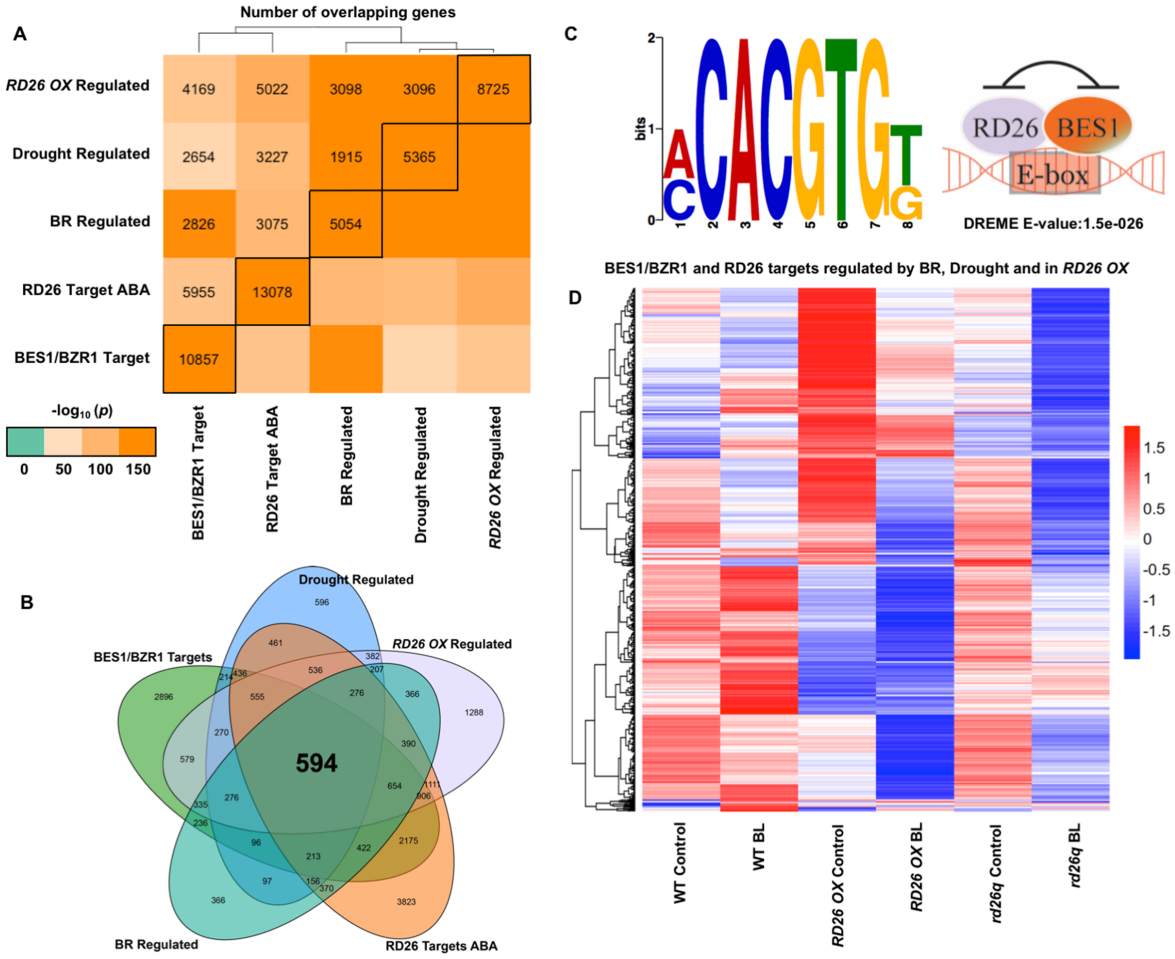

Figure 3: RD26 and BES1 regulate a common set of BR and drought genes
(A) Comparisons of RD26 and BES1/BZR1 target genes with those regulated by *RD26 OX*, BRs or drought . Gene lists were obtained from previously published datasets [7, 44, 49, 112, 121, 122] and statistical significance of their intersection was assessed using Fisher's exact test. Color legend indicates –log10 transformed p-values for the intersection between the given pair of genes; black boxes indicate the total number of genes in each list (B) Venn diagram showing core set of 594 genes that are both BES1/BZR1 and RD26 targets and regulated in *RD26OX* as well as by BRs and drought. (C) The G-box motif is enriched in the core set of genes shown in (B) in DREME promoter motif analysis [176] (left), which supports a model in which BES1 and RD26 bind to a common promoter element to inhibit each other's function (right). (D) Clustering analysis of BR responsive gene expression for 594 core genes from (B) using published *RD26 OX* and *rd26q* RNA-seq data [112] showing that these genes are strongly influenced by RD26.

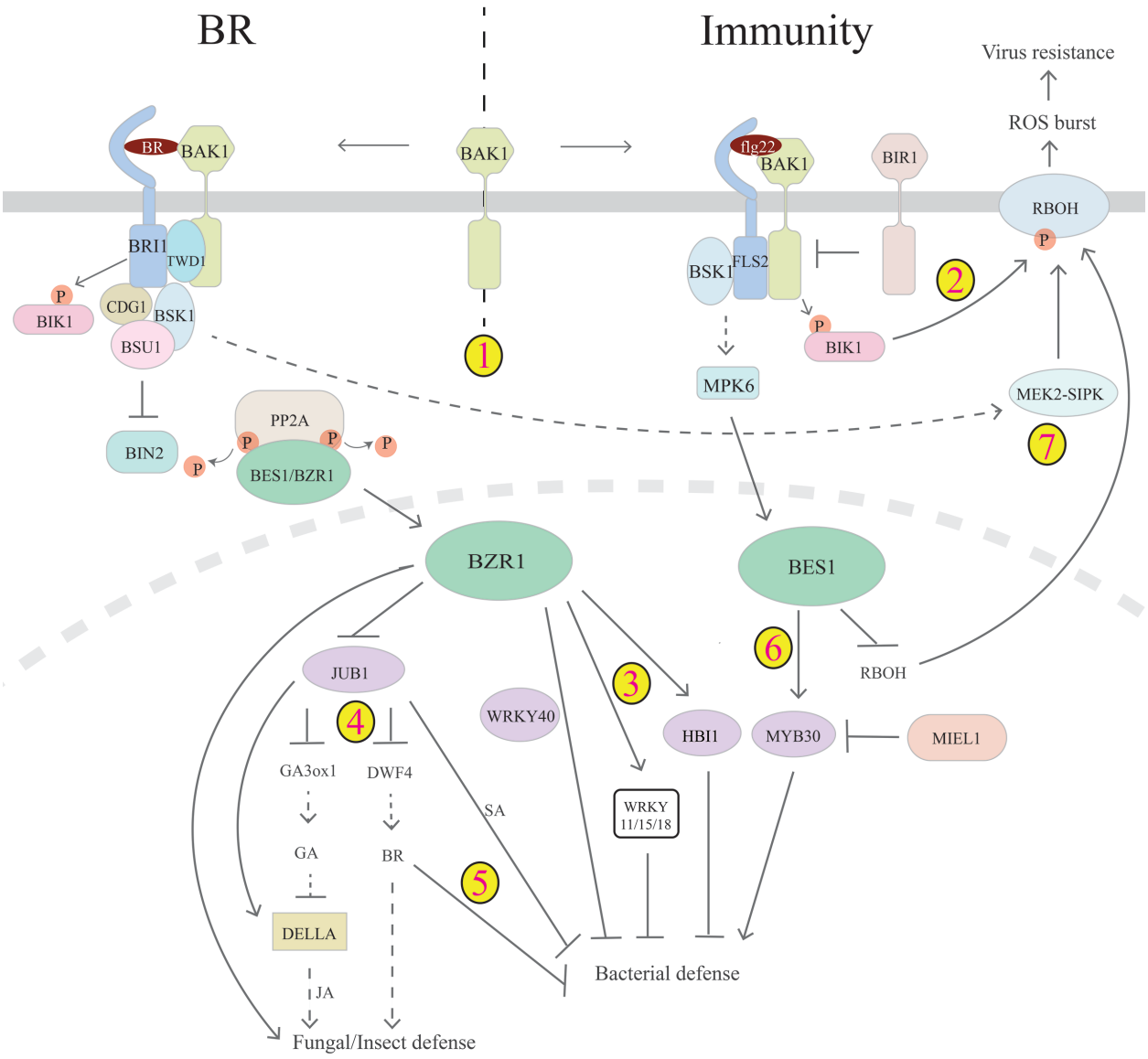

Figure 4: Crosstalk between BR and immunity

There is multi-layer crosstalk between BR and plant immunity pathways. 1. Genetic studies indicated that BR and PAMP receptors may compete for common co-receptor BAK1, thus enabling BR-repression of PTI. 2. Bacterial infection leads to phosphorylation and activation of BIK1, which activates RBOH and ROS burst to confer hypersensitive response. 3. In the nucleus, BR-activated BZR1 can inhibit PTI-mediated defense gene expression through WRKY11/15/18, HBI1, or in collaboration with WRKY40. 4. BZR1 can also function through JA and GA pathways (directly or through NAC transcription factor JUB1) to regulate fungal defense. 5. JUB1 can modulate BR and SA pathways to inhibit bacterial defense. 6. In contrast, BES1 is activated by MAPK pathway and plays a positive role in bacterial defense, which involves MYB30, its E3 ligase MIEL1 and likely other regulators. 7. Recent studies also suggest that BR signals to activate MEK2-SIPK through BRI1 and BSK1, which in turn triggers RBOH to generate ROS to confer virus resistance. On the other branch, BES1 inhibits the expression of RBOH and thus virus resistance, mediating trade-offs between BES1-promoted growth and virus resistance.

1.9 Dissertation Organization

This dissertation summarizes my work on the mechanisms and networks of BES1 function in Brassinosteroid-mediated growth and stress responses in *Arabidopsis thaliana*.

Chapter 1 provides an introduction to the Brassinosteroid pathway and summarizes Brassinosteroid crosstalk with stress responses including drought and immunity. I wrote this review that was published in *Biochemical Journal* along with Jiani Chen. I led the Brassinosteroid and drought sections whereas Jiani focused on the immunity portion.

Chapter 2 describes my finding that BR and autophagy pathways crosstalk in the regulation of plant growth and several stress responses. I found that BES1 interacts with a ubiquitin receptor protein DSK2, which targets BES1 to the autophagy pathway through the interaction between DSK2 and the autophagy protein ATG8 under drought or fixed carbon starvation stresses. The BES1-DSK2-ATG8 interaction provided a molecular link for the degradation of a critical BR signaling component by the autophagy pathway. DSK2 is a highly conserved protein among plant and animal kingdoms and has been implicated in protein degradation, but the mechanism of its action remained elusive. My results established DSK2 as a selective autophagy receptor for BES1. I found that DSK2-ATG8 interaction is modulated by BIN2 kinase, a GSK3-like kinase and negative regulator of BR signaling. This result provided another layer of crosstalk between the BR and autophagy pathways and new insight into the regulation of selective autophagy by a specific hormone signaling pathway. Moreover, I characterized SINAT2 as an E3 ubiquitin ligase that ubiquitinates BES1 during fixed-carbon starvation

stress. These studies filled important gaps in BR and autophagy pathways and provided significant new insights into the coordination of plant growth and stress responses. I performed the majority of the experiments and writing for these studies. Further details are included in the author contributions described along with this chapter.

Chapter 3 addresses the question of how BRs are able to function through BES1/BZR1 to control the expression of 5,000 to 8,000 genes. Complex gene expression programs such as those regulated by BRs are carried out through intricate gene regulatory networks (GRNs). These GRNs are comprised of TF-target interactions that control gene expression. BES1 and BZR1 are the central transcriptional regulators in the BR pathway, but the complete networks that allow BRs and BES1/BZR1 to control thousands of genes remained to be identified. To address this challenge, I led a team of researchers and used an integrated approach involving computational modeling, phenomics and functional genomics. We used genome-wide chromatin immunoprecipitation (ChIP), transcriptome and TF interactome datasets to identify 657 BR-related Transcription Factors (BR-TFs). Next, we built comprehensive GRNs to prioritize BR-TFs for functional studies and conducted BR phenomics experiments for over 300 BR-TFs using more than 1000 knockout or overexpression lines. These studies identified numerous BR-TF mutants with altered BR responses, allowing us to characterize the function of PLATZ and ARID-HMG1 as A/T-rich binding TFs that oppositely regulate BR-responsive gene expression. Finally, we developed BR and drought phenomics experiments in soil-grown plants using time-lapse imaging and a fully automated robotic system called Robotic Assay for Drought (RoAD). These studies identified *tcp11* mutants which have increased BR-regulated growth and increased

survival during drought. Taken together, this work provides a paradigm for network-based discovery and characterization of hormone response pathways through the integration of omics data, network analysis and phenomics. I was involved in nearly all aspects of this project, which entailed highly collaborative and interdisciplinary work. I assembled, summarized and interpreted the data and wrote the manuscript. The role of each member of this project is listed within the author contributions of this chapter.

Chapter 4 summarizes the conclusions, implications and future directions from these studies.

Included in the appendix are two additional manuscripts I contributed to. Appendix A is a research paper by Ye et al. that demonstrates the antagonistic relationship between Brassinosteroids and drought. This study showed that a transcription factor called RD26 functions as a negative regulator of growth and positive regulator of drought by interacting with BES1 and blocking the activity of BES1 on target gene expression. I performed gene clustering analysis, BiFC experiments and assisted with revising the manuscript for this study. Appendix B is a research paper by Jiani Chen et al. that describes the role of WRKY46/54/70 transcription factors that cooperate with BES1 to promote growth and inhibit stress responses. I worked with Jiani to conduct RNA-seq, performed gene clustering analysis, microscopy and assisted in writing and revising portions of the manuscript.

CHAPTER 2

SELECTIVE AUTOPHAGY OF BES1 MEDIATED BY DSK2 BALANCES PLANT GROWTH AND SURVIVAL

A paper published in *Developmental Cell*

Trevor M. Nolan[1], Benjamin Brennan[1], Mengran Yang[2], Jiani Chen[1], Mingcai Zhang[3], Zhaohu Li[3], Xuelu Wang[2] , Diane C. Bassham[1], Justin Walley[4] and Yanhai Yin[1, 5, *]

[1] Department of Genetics, Development and Cell Biology, Iowa State University, Ames, IA, United States

[2] College of Life Science and Technology, Huazhong Agricultural University, Wuhan, China

[3] College of Agronomy, China Agricultural University, Beijing, China

[4] Department of Plant Pathology and Microbiology, Iowa State University, Ames, IA, United States

[5] Lead Contact

*Corresponding author: yin@iastate.edu

2.1 Abstract

Plants encounter a variety of stresses and must fine-tune their growth and stress response programs to best suit their environment. BES1 functions as a master regulator in the Brassinosteroid (BR) pathway that promotes plant growth. Here, we

show that BES1 interacts with the ubiquitin receptor protein DSK2 and is targeted to the autophagy pathway during stress via the interaction of DSK2 with ATG8, a ubiquitin-like protein directing autophagosome formation and cargo recruitment. Additionally, DSK2 is phosphorylated by the GSK3-like kinase BIN2, a negative regulator in the BR pathway. BIN2 phosphorylation of DSK2 flanking its ATG8 interacting motifs (AIMs) promotes the interaction of DSK2 with ATG8, thereby targeting BES1 for degradation. Accordingly, loss-of-function *dsk2* mutants accumulate BES1, have altered global gene expression profiles, and have compromised stress responses. Our results thus reveal that plants coordinate growth and stress responses by integrating BR and autophagy pathways and identify the molecular basis of this crosstalk.

2.2 Introduction

Organisms encounter constantly changing environments and must respond appropriately in order to optimize their fitness and ensure survival. Growth and stress response programs generally antagonize one another, and as such need to be balanced (Claeys and Inze, 2013; Lopez-Maury et al., 2008). This need is exacerbated in sessile organisms such as plants that cannot easily relocate to escape adverse environmental conditions. Plants are therefore an excellent system to study coordination of growth and stress responses, and research in this area has important implications in optimizing plant growth under adverse environments (Skirycz et al., 2011).

Brassinosteroids (BRs) are one major family of growth-promoting plant hormones (Kir et al., 2015; Li and Chory, 1997; Sun et al., 2015). BRs are perceived by a receptor kinase, BRASSINOSTERIOID INSENSITIVE1 (BRI1), and many other signaling components to regulate the BRI1-EMS SUPRESSOR1 (BES1) and BRASSINAZOLE-

RESISTANT1 (BZR1) family of transcription factors (Clouse, 2011; Wang et al., 2011). In the absence of BRs, a GSK3-like kinase BIN2 (Li and Nam, 2002) phosphorylates and inhibits BES1/BZR1 function through multiple mechanisms (Li and Jin, 2007). In the presence of BR, BIN2 kinase activity is inhibited, thus leading to the accumulation of dephosphorylated BES1/BZR1 in the nucleus to regulate target gene expression (Belkhadir and Jaillais, 2015; Guo et al., 2013). Recently, BR signaling has also been linked with stress responses, in part through BIN2 activity (Hao et al., 2013; Vardhini and Anjum, 2015; Youn and Kim, 2015), but many molecular details are still unclear.

Posttranslational regulation adds another level of complexity to BR signaling. BES1 and BZR1 can be degraded by the proteasome (He et al., 2002; Wang et al., 2013), and gain-of-function *bes1-D* or *bzr1-D* mutants exhibit stabilized BES1 or BZR1, respectively (Wang et al., 2002; Yin et al., 2002). BES1 is targeted for ubiquitin mediated degradation by the Skp-CULLIN-F-box (SCF) E3 ubiquitin ligase MORE AXILLARY GROWTH LOCUS 2 (MAX2) during strigolactone-mediated control of shoot branching (Wang et al., 2013), and BZR1 is degraded in a COP1-dependent manner in response to darkness (Kim et al., 2014). These results demonstrated that regulated proteolysis of BES1/BZR1 plays important roles in diverse plant responses and the key downstream components required for such processes remain to be fully defined.

Typically, ubiquitin mediated protein degradation occurs through proteasome or autophagy pathways (Floyd et al., 2012; Kraft et al., 2010). Autophagy functions in the degradation and recycling of macromolecules and cytoplasmic organelles, often in response to stress conditions (Yang and Bassham, 2015). Proteins required for autophagy (encoded by *ATG* genes) include, among others, ubiquitin-like conjugation

systems required for autophagosome formation and expansion (Xie and Klionsky, 2007). These include the attachment of ATG8 to the autophagosome membrane through covalent linkage to the membrane lipid phosphatidylethanolamine (PE) (Ichimura et al., 2000). There is also recent evidence for selective autophagy in plants, whereby specific proteins or organelles are recognized by receptor proteins and degraded**,** although many details remain to be elucidated (Michaeli et al., 2016). A subset of these receptors contain a ubiquitin-binding domain and an ATG8 interacting motif (AIM), allowing them to recruit ubiquitinated cargo to ATG8-labeled autophagosomes (Floyd et al., 2012). Two such receptors in Arabidopsis are the NEXT TO BRCA1 GENE 1 (NBR1) homolog, which mediates degradation of ubiquitinated protein aggregates (Svenning et al., 2011; Zhou et al., 2013; Zientara-Rytter et al., 2011), and REGULATORY PARTICLE NON-ATPASE 10 (RPN10), which can target ubiquitinated proteasomes for autophagic degradation (Marshall et al., 2015).

DOMINANT SUPPRESSOR OF KAR2 (DSK2) is a ubiquitin-binding receptor protein with known connections to protein degradation pathways in yeast, animals and plants (Funakoshi et al., 2002; Lee and Brown, 2012; Lin et al., 2011). In Arabidopsis, two DSK2 paralogs exist as a result of tandem duplication (DSK2A and DSK2B), with 87% amino acid identity (Farmer et al., 2010). Both DSK2 proteins contain a N-terminal ubiquitin-like (UBL) domain that mediates their interaction with the proteasome and a C-terminal ubiquitin-associated (UBA) domain that can bind both K48 and K63 polyubiquitin chains (Lin et al., 2011). Interestingly, studies of the human DSK2 homologs (Ubiquilins) revealed that they can function in autophagy as LC3-interacting partners (Lee et al., 2013).

In this study, we found direct evidence linking the regulation and activity of DSK2 to BR signaling which leads to altered plant growth under drought and fixed-carbon starvation conditions. Specifically, we show that BES1 is targeted for autophagy-mediated degradation by direct interaction with DSK2 following abiotic stress. Additionally, the interaction between BES1 and DSK2 is regulated by BIN2 phosphorylation of DSK2. Loss-of-function *dsk2* mutants have increased BES1 protein levels, altered global gene expression profiles and compromised survival during stresses. Our results thus provide a previously unknown mechanism by which plants coordinate growth and stress responses by targeting a central growth regulator to the selective autophagy pathway via a phosphor-regulated receptor protein.

2.3 Results

2.3.1 BES1 is degraded through autophagy and proteasome pathways

Although BES1 is known to be degraded in a ubiquitin-dependent manner, the role of autophagy in this process has not been extensively examined. To test the possibility that BES1 is regulated by autophagy in addition to the proteasome, we first investigated BES1 protein levels after treatment with Concanamycin A (ConA), the cysteine protease inhibitor E64d, or MG132. ConA and E64d cause accumulation of proteins degraded via autophagy whereas MG132 blocks proteasomal degradation (Droese et al., 1993; Inoue et al., 2006; Kisselev et al., 2012). Remarkably, BES1 accumulated in response to inhibitors of both pathways (Figure 1A) while another transcription factor, RD26, accumulated after MG132 treatment, but not following treatment with ConA or E64d (Figure S1A). This indicates that BES1 can be degraded by both the autophagy and proteasome pathways, similar to HIF2α in hypoxia response

(Liu et al., 2014) and β-catenin in the Wnt signaling pathway (Petherick et al., 2013). To further verify that BES1 is degraded via autophagy we examined BES1 accumulation in the autophagy-deficient mutants *atg5-1* and *atg7-2* (Chung et al., 2010). Consistently, we found that BES1 protein levels accumulated in these autophagy-deficient mutants during mock treatments and the application of autophagy inhibitors had no effect in these mutant backgrounds (Figure 1B). Quantification of BES1 protein levels showed that *atg5-1* and *atg7-2* plants had higher BES1 levels after treatment with MG132 compared to mock treated controls (Figure S1B). Further, co-application of MG132 with ConA in WT plants led to slightly increased levels of BES1 compared to the application of either inhibitor alone (Figure S1C, lanes 2, 3 and 5). These results indicate that BES1 can be degraded by both proteasome and autophagy pathways, but that the two pathways do not function completely redundantly, which is consistent with previous reports regarding proteins targeted by both proteasome and autophagy-mediated degradation (Liu et al., 2014).

Since ubiquitination often triggers degradation through the proteasome and autophagy pathways, we analyzed BES1 ubiquitination. Immunoprecipitated BES1-GFP showed extensive high molecular weight laddering after MG132 or E64d treatment, reminiscent of ubiquitination (Figure 1C). These high molecular weight forms of BES1 cross-reacted with anti-Ubiquitin antibody, indicating that ubiquitinated BES1 accumulates in response to proteasome and autophagy inhibitors. Furthermore, treatments of protoplasts expressing BES1-YFP with ConA resulted in accumulation of BES1-YFP in puncta within the vacuole, consistent with BES1 degradation through autophagy (Figure 1D). Similar results were obtained using BES1P:BES1-GFP

transgenic lines in which BES1 expression was driven by its native promoter (Figures 1E and 1F), supporting the idea that BES1 puncta observed in protoplasts were not the result of artificially high levels of BES1 expression. Taken together, these results demonstrate that BES1 can be degraded by autophagy.

2.3.2 BES1 interacts with the ubiquitin receptor protein DSK2

To further explore the mechanisms of BES1 degradation, we performed yeast two-hybrid screening and identified one of the BES1 interactors as DSK2A, a ubiquitin-binding receptor. We hypothesized that DSK2 might be involved in targeting BES1 for degradation. We first confirmed that BES1 interacts with both DSK2A and DSK2B *in vitro* using GST pulldown and pairwise yeast-two hybrid assays (Figures 1G and S1D) and also *in planta* with BiFC and Co-immunoprecipitation (Co-IP) (Figures 1H, S1E and S1F). Coexpression of BES1-YFPN with DSK2A-YFPC resulted in strong YFP fluorescence signals (Figure 1H, left panels), some of which were present in mobile puncta (Figure 1I). Fluorescence signals were not observed in negative controls (Figure 1H, middle panels and S1E, lower panels) and were greatly diminished when the Ubiquitin binding UBA domain of DSK2 was deleted (DSK2ΔUBA) (Figure 1H, right panels), indicating that efficient binding of BES1 to DSK2 *in vivo* may be promoted by ubiquitination of BES1. Consistent with this idea, Co-IP using DSK2A-GFP transgenic lines treated with the autophagy inhibitor ConA demonstrated that DSK2A-GFP immunoprecipitated with anti-GFP antibodies pulled down high molecular weight forms of BES1 (Figure S1F) that likely represent ubiquitinated BES1. We also tested the effect of BES1 phosphorylation on the BES1-DSK2 interaction using BES1 phosphorylated *in vitro* with BIN2 kinase. DSK2 interacted with both phosphorylated and

unphosphorylated BES1, indicating that phosphorylation does not markedly influence the interaction between DSK2 and BES1 *in vitro* (Figure S1G).

To examine if BES1-DSK2 BiFC puncta were of autophagic origin, we performed colocalization experiments using the autophagosome marker Cerulean-ATG8e (Liu et al., 2012). Reconstituted YFP signal resulting from coexpression of BES1-YFPN with DSK2A-YFPC colocalized extensively with the Cerulean-ATG8e (Figure 1J). DSK2 could also interact with itself (Figures S1E and S1H), in common with several autophagy receptors that often dimerize or multimerize to recruit their cargo for autophagic degradation (Birgisdottir et al., 2013; Ciuffa et al., 2015; Floyd et al., 2012). YFP signals resulting from interaction of DSK2A-YFPN with DSK2A-YFPC also colocalized with Cerulean-ATG8e whereas controls expressing DSK2A-YFPN with DSK2A-YFPC or Cerulean-ATG8e alone did not result in any colocalization signal (Figure S1H). DSK2 therefore interacts with BES1 and the DSK2-BES1 complex can localize to autophagosomes, suggesting that DSK2 recruits BES1 to the autophagy pathway.

2.3.3 DSK2 acts as a receptor for BES1 degradation

To test the possibility that DSK2 functions as an autophagy receptor mediating BES1 degradation, we examined colocalization of BES1-YFP with Cerulean-ATG8e in Arabidopsis protoplasts under starvation and osmotic stress conditions in which autophagy is induced (Doelling et al., 2002; Hanaoka et al., 2002; Liu et al., 2009). Strong colocalization of BES1-YFP and Cerulean-ATG8e in autophagic bodies occurred upon sucrose starvation (Figure 2A, top panels) or osmotic stress with mannitol treatment (Figure 2A, bottom panels), but not in unstressed controls (Figure 2A, middle

panels). The colocalization was not observed in single transformations of BES1-YFP or Cerulean-ATG8e (Figure S2A) indicating that colocalization signals were not an artifact of crosstalk between YFP and CFP channels. Both BES1-YFP and Cerulean-ATG8e puncta were absent in autophagy-deficient *atg7-2* mutants (Figure 2B). On the other hand, *DSK2 RNAi* protoplasts in which both DSK2A and DSK2B were knocked down (Figure S2B) displayed normal ATG8e puncta, but failed to recruit BES1 to ATG8-labeled autophagosomes (Figure 2C), suggesting that DSK2 is required to target BES1 to autophagy but is not required for proper function of the core autophagy machinery. These observations were supported by quantification of protoplasts with visible BES1 autophagy, which was reduced in *DSK2 RNAi* as compared to WT under starvation (-suc) or osmotic (mannitol) stress (Figures 2D and S2C). In contrast, quantification of protoplasts displaying ATG8e autophagy did not reveal significant differences between WT and *DSK2 RNAi* (Figure S2D); confirming that bulk autophagy is not impaired in *DSK2 RNAi.* Furthermore, accumulation of BES1 was observed in *DSK2 RNAi* lines during mock inhibitor treatments, and *DSK2 RNAi* had reduced response to application of E64d or MG132 (Figure 3A), consistent with a role for DSK2 in degrading BES1.

To investigate the effects of stress induced BES1 degradation on BR mediated plant growth responses, we measured hypocotyl lengths of WT, *DSK2 RNAi, atg7-2* and *bes1-D* treated with sucrose starvation or mannitol induced osmotic stress. Under stress conditions, *DSK2 RNAi* and *atg7-2* displayed decreased sensitivity to the BR biosynthesis inhibitor Brassinazole (BRZ) (Asami et al., 2000) (Figures 3B and 3C). *DSK2 RNAi* seedlings showed a mild BRZ resistant phenotype under normal conditions, whereas *atg7-2* was not significantly different than WT, and *bes1-D* was resistant to

BRZ under all of the tested conditions (Figures 3D, S3A and S3B). The BR response phenotype was consistent across two *DSK2 RNAi* lines (Figure S3C) that have been previously well characterized (Lin et al., 2011) and showed depleted DSK2 levels as monitored by immunodetection with anti-DSK2 antibodies (Figure S1D). These results indicate that DSK2 functions as an autophagy receptor during stress conditions to reduce BR-mediated plant growth and imply that DSK2 may also operate in an autophagy-independent manner in non-stress conditions, which is consistent with the known role of DSK2 in other protein degradation pathways (Farmer et al., 2010).

2.3.4 DSK2 is phosphorylated by BIN2 and serves as a phosphor-regulated autophagy receptor

Since autophagy receptor proteins typically interact with ATG8, we tested the interaction of DSK2 with several representative ATG8 family members (Marshall et al., 2015; Yoshimoto et al., 2004). DSK2 physically interacted with all ATG8 members tested in GST pulldown assays, including ATG8e (Figure 4A). To further characterize the role of DSK2 as a possible autophagy receptor, we examined the DSK2 protein sequence for predicted ATG8-interacting motifs (AIMs) using iLIR prediction software (Kalvari et al., 2014). AIMs are typified by the consensus sequence W/F/Y-X-X-L/I/V, which is often adjacent to acidic or phosphorylated residues (Herhaus and Dikic, 2015; Kalvari et al., 2014). DSK2A has two regions with high scoring AIMs, each of which is surrounded by multiple BIN2 consensus phosphorylation sites (S/T-X-X-X-S/T) (Figure 4B) (Zhao et al., 2002). This observation led us to hypothesize that DSK2 might be phosphorylated proximal to its AIM sequences by BIN2, thereby promoting physical interaction between DSK2 and ATG8 (Farre et al., 2013; Wild et al., 2011; Zhu et al.,

2013). Further examination of the DSK2A (hereafter referred to as DSK2) protein sequence revealed 22 potential BIN2 phosphorylation sites (Figure 4B). We first performed phosphatase treatments of immunoprecipitated DSK2-GFP protein, which caused DSK2 to shift from a higher- to lower-migrating form. Thus, DSK2 can be phosphorylated *in vivo* (Figure 4C).

Next, we found that DSK2 interacts with and is phosphorylated by BIN2, consistent with the predicted BIN2 phosphorylation sites. Specifically, we observed physical association between DSK2 and BIN2 in BiFC assays (Figure 4D), yeast two-hybrid assays (Figure S4A) and *in vitro* pulldown assays (Figure S4B). BIN2 efficiently phosphorylated DSK2 in *in vitro* kinase assays (Figure 4E). Phosphorylation was unaffected by deletion of the N-terminal UBL domain of DSK2 (DSK2 C1, AA 90-538), but was blocked in a truncated version of DSK2 (DSK2 C2, AA 402-538) that removed 18 of the 22 predicted BIN2 sites (Figure 4E).

We confirmed that BIN2 phosphorylates DSK2 *in vivo* by western blotting using anti-DSK2 antibodies coupled with Phostag SDS-PAGE, which causes slower migration of phosphorylated proteins (Kinoshita et al., 2006). In this assay, BIN2 loss-of-function *bin2-3 bil1 bil2* triple mutants (*bin2-T*) (Yan et al., 2009) displayed decreased DSK2 phosphorylation (Figure 4F). Conversely, gain-of-function (*bin2-1D*) mutants (Li and Nam, 2002) showed slower migration of DSK2 due to increased phosphorylation (Figure 4F).

To test the effect of BIN2 phosphorylation on DSK2 function, we generated a series of mutants, changing BIN2 sites to aspartic acid (D) or alanine (A) to mimic or to abolish phosphorylation, respectively. We found that at least a portion of these sites can

be phosphorylated *in vivo* since coexpression of DSK2-MYC with BIN2 in *Nicotiana benthamiana* led to a higher migrating form of DSK2, but no shift was observed when BIN2 was expressed with DSK2^{A}, a construct where all putative BIN2 phosphorylation sites were mutated to Alanine (Figure S4C).

Given the precedence for phosphorylation in increasing autophagy receptor interactions with ATG8 (Wild et al., 2011), we selected ATG8e as a representative ATG8 family member for the investigation of the effect of phosphorylation on interaction of DSK2 with ATG8 (Figures 4G and 4H). Using yeast two hybrid assays we found that WT DSK2 interacted with ATG8e, and a phosphomimic version of DSK2 (DSK2^{D}) had increased interaction with ATG8e (Fig 4H, columns 2 and 3). In contrast, loss-of-function (DSK2^{A}) mutants showed decreased interaction (Figure 4H, column 4). The phosphomimic mutation of the putative phosphorylation sites proximal to the AIM domains (DSK2^{D12}) was sufficient to increase the interaction of DSK2 with ATG8e (Figure 4H, column 7). Moreover, mutation of the AIM sequences of DSK2 abolished the interaction with ATG8e (Figure 4H, columns 5-6). These DSK2 mutants showed a similar trend when tested in plants using BiFC. Specifically, DSK2^{D} showed increased interaction with ATG8e compared to DSK2 while mutation of DSK2 AIMs in DSK2^{mAIM} also abolished the interaction *in planta* (Figures 4I and 4J). Furthermore, Co-IP assays demonstrated that immunoprecipitated Cerulean-ATG8e interacted more strongly with phosphomimic DSK2^{D}-MYC than with DSK2-MYC (Figure 4K), confirming that phosphorylation of DSK2 promotes interaction with ATG8 in vivo.

We next confirmed site-specific phosphorylation of DSK2 by BIN2 using peptide mass spectrometry. Several phosphorylated peptides were detected from DSK2-MBP

phosphorylated *in vitro* with BIN2-MBP (Tables S1 and S2), whereas no phosphorylation was detected in mock treated DSK2-MBP. These phosphorylation sites include at least four phosphorylated residues near AIM1 (4 sites between amino acids 5-41) and two residues around AIM2 (S240 and S244), suggesting that BIN2 can phosphorylate DSK2 proximal to its AIM domains. In order to investigate the function of DSK2 phosphorylation on plant growth and BES1 stability, we generated transgenic plants overexpressing phosphomimic DSK2 ($DSK2^{D}$). These lines exhibited reduced growth compared to WT plants and had decreased BES1 protein levels (Figures 4L and 4M), consistent with the role of phosphorylated DSK2 in promoting BES1 degradation. In contrast, transgenic lines expressing inactive $DSK2^{A}$ or $DSK2^{mAIM}$ variants did not cause dramatic changes in plant growth or BES1 protein levels under the conditions tested (Figures S4D and S4E). Taken together, these results demonstrate that DSK2 is a phosphor-regulated ATG8-interacting receptor protein mediating BES1 degradation.

2.3.5 DSK2 is involved in BES1 degradation during drought stress

Autophagy is induced by numerous stimuli, including nutrient stress and osmotic or drought stress (Li and Vierstra, 2012; Liu et al., 2009). Thus, we hypothesized that autophagic degradation of BES1 may occur under such stress conditions. We confirmed that autophagy-defective *atg7-2* plants were susceptible to drought (Zhou et al., 2013) (Figure 5A). We next tested the role of BR responses in drought. Constitutive activation of BR responses in *bes1-D* led to increased susceptibility to drought, while *bri1-301,* a loss-of-function mutant in the BR pathway was resistant to drought treatments (Figure 5A). Based on these findings, we examined how BES1 levels may be regulated during drought conditions. To simulate drought conditions in a controlled and reproducible

manner, we subjected plants to dehydration treatments, which have been widely used to examine plant drought responses (Nakashima et al., 2009; Sakuma et al., 2006; Urao et al., 1993). Following four hours of dehydration, BES1 levels were substantially reduced in WT plants, while BES1 accumulated in *atg7-2* and *DSK2 RNAi* under control conditions and minimal reduction was observed in response to dehydration (Figure 5B). BES1 levels followed a similar trend in plants treated with sub-lethal drought in soil (Figure 5C), showing accumulation in *DSK2 RNAi* and *atg7-2* backgrounds. Accumulation of BES1 in the mutant backgrounds was not due to increased transcription, as BES1 expression levels were not markedly increased in *DSK2 RNAi* or *atg7-2* compared to WT during control or stress conditions (Figures S5A and S5B). Moreover, experiments in which translation was inhibited via cycloheximide (CHX) treatment showed that BES1 stability was decreased to a greater extent in drought vs. control treated WT plants, especially at later time points of CHX treatment (Figures 5D, top panels and S5C), whereas a similar reduction in BES1 was not observed after drought and CHX treatment in *DSK2 RNAi* or *atg7-2* plants (Figure 5D, middle and bottom panels). These results demonstrate that BES1 is regulated at the post-translational level during drought stress.

Since *DSK2 RNAi* plants have elevated BES1 levels under drought conditions, we expected them to behave similarly to *bes1-D*. In support of this hypothesis, *DSK2 RNAi* plants also had drastically reduced survival in drought assays (Figures 5A, 5E and S6A), and lost water more quickly in detached leaf water loss assays (Figure 5F). Meanwhile, *DSK2* expression remained decreased in *DSK2 RNAi* compared to WT under stress conditions (Figures S5D and S5E).

Given the strong phenotype of *DSK2 RNAi* under drought conditions, we next examined changes in the transcriptome during control and dehydration conditions using RNA-seq. In dehydrated WT plants, 554 genes were differentially expressed (DE) compared to mock treated controls (dehydration DE genes; Table S3). These dehydration responsive transcripts exhibit a high concordance with previously published dehydration datasets and an enrichment of drought related GO terms (Figures S6B and S6C). We observed few genes that were DE in *DSK2 RNAi* plants compared to WT under control conditions (Table S3), but strikingly, 2522 genes were DE in *DSK2 RNAi* compared to WT under dehydration stress (referred to as *DSK2 RNAi* dehydration DE genes). The DE genes in dehydrated *DSK2 RNAi* lines opposed dehydration regulated genes (Figure 5G) and were enriched for drought and/or dehydration-related GO terms (Figure 5H). Furthermore, clustering analysis of *DSK2 RNAi* dehydration DE genes (Figures 5I and S6D) revealed many genes with increased expression during dehydration in WT that showed lower expression patterns in *DSK2 RNAi* and minimal induction by the treatment (Group I), while others were repressed in WT dehydration but had higher expression in *DSK2 RNAi* (Group II). These transcriptional changes following dehydration are consistent with the drought hypersensitive phenotype of the *DSK2 RNAi* mutant.

Many previously published drought-regulated genes (Maruyama et al., 2009) were present in these datasets and showed altered expression in *DSK2 RNAi* lines (Figure S6E). There is also a high degree of overlap between BES1/BZR1 target genes and DSK2-regulated genes (Figure 6J and Table S3). Comparison of BR- and dehydration-regulated genes indicated that drought and BR pathways antagonize each

other (Figures S6F, S6G and S6H). These results demonstrate that perturbation of BES1 levels in *DSK2 RNAi* plants coincides with the dramatic changes in drought phenotypes and drought-related gene expression.

We further confirmed the role of BES1 in drought stress resistance by testing the drought phenotype of previously described *BES1-RNAi* plants (Yin et al., 2005). *BES1 RNAi* had increased resistance to drought as compared with WT (Figures S7A and S7B) and decreased BES1 protein levels (Figure S7C). We then generated *DSK2 RNAi BES1 RNAi* double transgenic plants in which both BES1 and DSK2 were reduced (Figure S8A) in order to determine the extent to which BES1 accumulation was responsible for the increased drought sensitivity in *DSK2 RNAi.* Drought survival assays indicated that decreased BES1 in *DSK2 RNAi BES1 RNAi* plants could restore the drought survival phenotype of *DSK2 RNAi* to near WT levels (Figures S8B and S8C). These observations indicate that BES1 accumulation in *DSK2 RNAi* is a major contributor to the impaired survival of *DSK2 RNAi* plants during drought stress.

We also tested the effect of modulating BIN2 activity on BES1 protein levels and plant survival during drought stress. We found that loss-of-function *bin2-T* mutants had higher BES1 protein levels compared to WT after dehydration treatment, whereas BES1 levels were reduced in gain-of-function *bin2-1D* mutants during dehydration (Figure S9A). Furthermore, *bin2-1D* plants were resistant to drought stress as compared to WT. However, *bin2-T* mutants did not show obviously decreased drought survival under the conditions tested (Figures S9B and S9C), likely due to the large array of substrates targeted by BIN2 kinase (Youn and Kim, 2015). Taken together, these results support a role for BIN2 in modulating BES1 protein levels and survival under stress conditions.

2.3.6 DSK2 is involved in BES1 degradation during fixed-carbon starvation

In addition to drought, autophagy is strongly induced under nutrient-limiting conditions, including fixed-carbon starvation, and autophagy deficient mutants have reduced survival under carbon or nitrogen starvation (Contento et al., 2004; Thompson et al., 2005). Recently, it has been shown that BRs are required for sugar-promoted hypocotyl elongation in the dark and that BZR1 is both transcriptionally and post-translationally regulated by sucrose, which suggests that BES1/BZR1 protein levels may be controlled under low energy conditions (Zhang et al., 2015). We confirmed the sensitivity of *atg7-2* to starvation stress in our assays and found that constitutive BR response in *bes1-D* led to enhanced sensitivity to fixed-carbon starvation (Figures 6A and 6B). We next examined BES1 protein levels after 5 days of dark treatment. Fixed-carbon starvation reduced the level of BES1 in WT plants, whereas BES1 was reduced to a lesser extent in *atg7-2* and *DSK2 RNAi* (Figures 6C and S10A). Regulation of BES1 under these conditions was at least partially due to reduced energy availability rather than dark conditions since addition of sucrose during starvation treatments increased BES1 levels (Figure S10B). Furthermore, we tested the fixed-carbon starvation survival phenotypes of *DSK2 RNAi* lines. In line with the BES1 protein accumulation, *DSK2 RNAi* plants had markedly reduced recovery compared to WT in a fixed-carbon starvation time course with seedlings grown on medium without sucrose (Figure 6B and S10C) or after 8 days of dark treatment on soil-grown plants (Figure 6A). Additionally, we tested the role of BIN2 in starvation stress by examining the phenotypes of *bin2* mutants in starvation survival assays. Similar to our observations in

drought stress, gain-of-function *bin2-1D* mutants were resistant to starvation; however, *bin2-T* mutants were also more resistant than WT to starvation, raising the possibility that additional BIN2 homologs or substrates may be regulated during starvation in *bin2-T* mutants (Figure S10D).

We also performed RNA-seq experiments under starvation conditions and found 6,737 genes that were DE in *DSK2 RNAi* lines compared to WT (designated *DSK2 RNAi* starvation DE genes). Examination of these genes showed that starvation responsive gene expression was attenuated in *DSK2 RNAi* plants as illustrated by the opposing pattern of overlap observed between *DSK2 RNAi* starvation DE genes and genes regulated by starvation in WT. 1,677/4,070 *DSK2 RNAi* starvation upregulated genes and 1,400/2,667 *DSK2 RNAi* starvation downregulated genes overlapped with genes downregulated or upregulated in WT starvation, respectively (Figures 6D and S10E). These differential changes were also evident from clustering analysis (Figure 6E). The DE genes in starved *DSK2 RNAi* lines were enriched for GO terms related to plant growth and stress responses (Figure 6F). Further comparisons revealed that many DE genes in starved *DSK2 RNAi* lines are BES1/BZR1 targets (24.7%, 1,664/6,737 genes) (Figure S10F). Moreover, we observed a large degree of overlap among *DSK2 RNAi* starvation DE genes and those DE in *atg7-2* and *bes1-D* during starvation (Figures S10G and S10H), suggesting functional overlap among these genes. Furthermore, 41% of BR induced genes (1,601/3,898) and 33.6% of BR repressed genes (1,274/3,789) were regulated in opposite directions (down and up-regulated, respectively) during starvation (Figures S10I, S10J and S10K), indicating a mostly inverse relationship between BR function and starvation response. Taken together,

these results demonstrate that BES1 and BRs play a negative role in survival during fixed-carbon limitation and that BES1 is degraded by DSK2 and autophagy pathways under these conditions.

2.3.7 SINAT family E3 ubiquitin ligases are involved in BES1 degradation during starvation

In addition to DSK2, we also recovered a RING E3 ubiquitin ligase, SINAT2, as a BES1 interacting partner via yeast-two hybrid screening. Several SINAT family members directly interact with and ubiquitinate BES1 (Yang et al., accompanying manuscript). To test the possible role of SINAT2 in DSK2-mediated degradation of BES1, we first examined the physical interaction of SINAT2 with DSK2. Strikingly, SINAT2 strongly interacted with DSK2 in BiFC assays (Figure 7A), likely in the nucleus and also in puncta. GST pulldown assays demonstrated that the DSK2-SINAT2 interaction is direct (Figure 7B). These data indicate that SINAT2 and DSK2 form a complex to carry out BES1 degradation and suggest that SINAT family E3 ligases might be involved in targeting BES1 for degradation during stress. SINAT E3 ligases have been previously implicated in stress responses (Bao et al., 2014), and we found that 3/6 SINAT family members were transcriptionally induced by starvation (Figure 7C). Furthermore, BES1 protein accumulated following starvation treatment in *SINAT RNAi* lines compared to WT (Figures 7D and S11A) and *SINAT RNAi* plants exhibited a starvation hypersensitive phenotype, showing dramatically reduced survival in fixed-carbon starvation assays (Figure 7E). Accordingly, BES1 ubiquitination was reduced in *SINAT RNAi* plants compared to WT under starvation conditions when autophagy-mediated degradation was blocked with E64d (Figure S11B). These findings reveal that

SINAT E3 ubiquitin ligases are involved in targeting BES1 for degradation during starvation (Figure 7F).

2.4 Discussion

Organisms develop strategies to coordinate growth and stress responses. Multiple mechanisms have been reported that allow for inhibition of growth when stress is encountered, including global reprogramming of gene expression (Clauw et al., 2015; Harb et al., 2010), RNA processing or sequestration (Weber et al., 2008) and translation inhibition (Ren et al., 2011). Our studies established a major mechanism for the coordination of plant growth and stress responses. We demonstrated that targeting of a central growth regulator BES1 to autophagy-mediated degradation by ubiquitin receptor DSK2 plays an important role in slowing down plant growth under dehydration and fixed-carbon starvation (Figure 7F). We showed that GSK kinase BIN2, which is repressed by growth hormone BRs and activated by stresses (Charrier et al., 2002; Dal Santo et al., 2012; Youn and Kim, 2015; Zhang et al., 2009), controls BES1 autophagy by modulating DSK2-ATG8 interaction. Our studies also revealed a new function for *SINATs*, which encode E3 ubiquitin ligases that target the active unphosphorylated form of BES1 to influence BR-regulated growth in a light dependent manner (Yang et al., accompanying manuscript). Our results indicate that *SINATs* are induced by starvation stress and are involved in targeting BES1 for degradation under starvation conditions. Thus, both BIN2 and SINATs are activated by stress to potentiate BES1 degradation.

Our results revealed crosstalk between autophagy and plant steroid hormone signaling pathways. Both autophagy (Doelling et al., 2002; Hanaoka et al., 2002; Liu et al., 2009) and BRs (Hao et al., 2013; Zhang et al., 2015) have been linked to drought

and starvation, but the role of BRs in controlling plant survival and mechanisms regulating BES1 during these stresses are not completely understood. Recently, it was reported that TARGET OF RAPAMYCIN (TOR) functions to activate BR signaling under energy replete conditions by stabilizing BZR1 and that *tor rnai*-induced BZR1 degradation was attenuated by treatment with 3-methyladenine, an inhibitor of autophagy (Zhang et al., 2016). These results suggest that BZR1 may be degraded through autophagy, but genetic and cell biological evidence for autophagy-mediated degradation of BES1/BZR1 family transcription factors as well as the E3 ligase and autophagy receptor that mediate this process remained to be established. The BES1-DSK2-ATG8 interaction demonstrated in this study provides a molecular mechanism connecting autophagy and BR pathways, which allows plants to slow down growth under stress conditions. Our studies revealed that BES1 negatively regulates plant survival under drought and starvation and that DSK2 mediates degradation of BES1 under these conditions (Figures 5 and 6). Accumulation of BES1 in *DSK2 RNAi* or *atg7-2* mutants coincided with decreased plant survival under both drought and fixed-carbon starvation. In contrast, *DSK2 RNAi* and *atg7-2* mutants were resistant to the inhibition of BR biosynthesis during stress (Figure 3), suggesting that BES1 accumulation in these mutants promotes plant growth during stress. Furthermore, expression of a constitutive active DSK2 ($DSK2^{D}$, mimicking BIN2 phosphorylation) led to reduced BES1 protein levels and decreased plant growth (Figure 4). Taken together, these genetic and physiological studies indicate that DSK2-mediated BES1 degradation leads to reduced plant growth under stress conditions and is required for optimal plant responses to stresses.

This study established DSK2 as a selective autophagy receptor. DSK2 has ties to both proteasome and autophagy pathways. The human homologs of DSK2, called Ubiquilins, have been implicated in protein degradation pathways including autophagy as LC3 (ortholog of ATG8) interactors (Lee et al., 2013), but their specific functions in autophagy have not been fully defined. In Arabidopsis, DSK2 was shown to participate in ubiquitinated cargo delivery to the proteasome, along with other receptors (Farmer et al., 2010; Lin et al., 2011; Vierstra, 2009). Our results demonstrate that DSK2 targets BES1 through selective autophagy. DSK2 is required for recruitment of BES1 to autophagy, but ATG8-labeled autophagosomes are not affected in *DSK2* RNAi lines (Figure 2), suggesting that DSK2 functions in selective degradation of BES1, but does not regulate bulk autophagy. Although selective autophagy has been shown to function in plant systems, the full repertoire of autophagy receptors and their specific cargos is only beginning to be fully appreciated (Michaeli et al., 2016). Multiple lines of evidence demonstrated that BES1-DSK2-ATG8 interactions function to target BES1 to selective autophagy during stress (Figures 1 and 2). Considered together, our results expand the role of DSK2 in ubiquitin-mediated proteolysis by showing DSK2's role in selective autophagy and by providing a molecular basis for DSK2 in targeting specific proteins such as BES1 for degradation.

Another significant finding of this study is that DSK2-ATG8 interaction is modulated by BIN2 kinase, a negative regulator of the BR pathway. BIN2 phosphorylates BES1/BZR1 as well as numerous other substrates involved in diverse aspects of plant growth, development and stress responses (Belkhadir and Jaillais, 2015; Youn and Kim, 2014). DSK2 is phosphorylated by BIN2 flanking its AIM domains

(Figure 4 and S4), which is a typical pattern of autophagy receptors that are regulated by phosphorylation (Farre et al., 2013; Wild et al., 2011; Zhu et al., 2013). Mutational analysis indicated that DSK2 phosphomimic forms had increased interaction with ATG8, suggesting that BIN2 induces BES1 degradation by phosphorylating DSK2 and enhancing its interaction with the autophagy protein ATG8. These results provide a new layer of regulation of BES1 by BIN2 kinase.

This scenario of phosphorylation-regulated autophagy receptor function is consistent with previous studies, such as that observed for Optineurin, where phosphorylation around the LIR (LC3 interacting region; equivalent to AIM) of Optineurin promoted interaction with LC3, potentiating this receptor's ability to degrade ubiquitinated intracellular bacteria (Wild et al., 2011). Structural studies indicate that the negative charge produced by phosphorylation of Optineurin interfaces with Arg11 and Lys51 residues of LC3B (Rogov et al., 2013), providing a mechanistic basis as to how phosphorylation can increase interactions between autophagy receptors and ATG8 family proteins. The regulation of DSK2-ATG8 interaction by BIN2 phosphorylation provides the first example of a phosphor-regulated autophagy receptor in plant systems.

The role of DSK2 in the regulation of BES1 during stress responses is further corroborated by global gene expression studies. Our RNA-seq analyses showed that BES1 accumulation in *DSK2 RNAi* was associated with altered expression of a large number of genes under dehydration and starvation conditions. In contrast, few genes were affected in *DSK2 RNAi* plants in unstressed control conditions, indicating that DSK2 functions primarily during stresses. BES1 and BZR1 bind to the promoters of about 6600 target genes as determined by genome-wide ChIP studies (Sun et al., 2010;

Yu et al., 2011). Strikingly, a large proportion of the misregulated genes under both stress conditions were BES1/BZR1 targets (Figures 5 and S11). These results suggest that BES1 accumulation under stress conditions in *DSK2 RNAi* is associated with changes in BES1/BZR1 target gene expression. Moreover, the expression of stress-regulated genes in dehydration and starvation generally opposed that of BR-regulated genes, suggesting that BR responses might be reduced during stress through degradation of BES1 by DSK2 and autophagy.

In metazoans, regulation of β-catenin, a positive regulator of cell proliferation in the Wnt pathway provides another excellent example of how growth and stress pathways can crosstalk through targeted protein degradation. β-catenin reduces autophagy and inhibits the expression of the autophagy receptor p62 under normal conditions, but it is targeted for degradation through interaction with the autophagy protein LC3 under autophagy inducing conditions (Petherick et al., 2013). Our results showed that autophagy-mediated degradation of BES1 under stress conditions affects BR-regulated growth and stress responses, which suggests that negative regulation of growth promoting factors during stress by autophagy-mediated degradation might be a general mechanism used to shut down growth responses. Given the similarities in signaling mechanisms between the Wnt and BR signaling pathways (Yin et al., 2002), it would be interesting to investigate if there is a reciprocal regulation of autophagy by BRs, which could provide additional means for plants to balance growth and stress responses. In the future, identification of additional DSK2 substrates, examination of the function of DSK2 in both proteasome and autophagy-mediated BES1 degradation and

exploration of possible regulation of the autophagy pathway by BR signaling should further our understanding of crosstalk between growth and stress response pathways.

2.5 Acknowledgements

The identification of DSK2 and SINAT2 as BES1 interactors by yeast two-hybrid screens was performed in Dr. J. Chory's laboratory at the Salk Institute for Biological Studies with support from Howard Hughes Medical Institute (HHMI). DSK2 antibodies and *DSK2 RNAi* seeds were a generous gift from Hongyong Fu. We thank Drs. Patrick S. Schnable and Sanzhen Liu (Data2Bio, Inc.) for assistance in analyzing RNA-seq data and Dior Kelly and Hongqing Guo for critical comments on the manuscript. The work is supported by grants from NSF (IOS-1257631) and Plant Science Institute at Iowa State University.

2.6 Author Contributions

T.N. performed most of the experiments with the following exceptions: B.B. produced recombinant proteins, performed some of the GST pulldown assays and assisted in generating DSK2 transgenic lines. M.Y. and X.W. generated *SINAT RNAi* lines and analyzed BES1 accumulation in SINAT RNAi during starvation. T.N., J.C., M.Z. and J.L. conducted the RNA-seq experiments. D.C.B. provided autophagy mutants and materials and assisted in analyzing autophagy experiments. J.W. conducted mass spectrometry for identification of DSK2 phosphorylation sites. T.N. and Y.Y. wrote the manuscript with D.C.B. and J.W.

2.7 Methods

Plant materials and growth conditions

Arabidopsis thaliana accession Columbia (Col-0) was used along with previously described mutants: *atg5-1* (Thompson et al., 2005)*, atg7-2* (Chung et al., 2010)*, bri1-301*(Li and Nam, 2002)*, bes1-D* (Vilarrasa-Blasi et al., 2015; Yin et al., 2002)*, bin2-1D* (Li et al., 2001)*, bin2-3 bil1 bil2* (Yan et al., 2009). Well characterized DSK2 *RNAi* lines (Lin et al., 2011) were used in this study. The majority of experiments in this manuscript were conducted with *DSK2 RNAi 2-6* (referred to as *DSK2 RNAi*) and another independent line (*DSK2 RNAi 1-4*) was used to verify the phenotype. *DSK2 RNAi BES1 RNAi* plants were generated by crossing *DSK2 RNAi* with *BES1 RNAi* and F1 progeny used to examine BES1 and DSK2 protein levels as well as drought phenotypes. Plants were grown on 0.5X Linsmaier and Skoog (LS; Caisson Laboratories) plates or in soil under long day (16 h light/8 h dark) conditions at 22°C unless otherwise specified.

Inhibitor treatments

Treatment with proteasome or autophagy inhibitors was performed by soaking plants in 0.5X LS liquid medium containing DMSO, 50μM MG132, 20μM E64d or 1μM ConA. Plants were vacuum infiltrated for 5 minutes and then kept under light for 6 hours before sample collection. Similarly, cycloheximide treatments were performed by soaking plants in 0.5X LS medium containing 500μM cycloheximide for the indicated time points. For BES1 ubiquitination, BES1-YFP was expressed in *N. benthamiana.* 24 hours post-inoculation, infiltration medium (10mM $MgCl_2$, 10mM MES, pH 5.7) containing DMSO, 50μM MG132, or 20μM E64d was infiltrated into the lower side of the leaves. Samples were collected 16 hours after addition of inhibitors.

BRZ response assays

For BRZ response assays under normal (non-stressed) conditions, sterilized seeds were planted directly on 0.5X LS medium with 1% sucrose containing DMSO or indicated concentrations of BRZ (Asami et al., 2000). Plates were exposed to light for 6-8 hours and then kept in darkness for 7 days. Seedlings were then imaged and hypocotyls quantified using ImageJ software (http://imagej.nih.gov/ij/). For BRZ response under stress conditions, seedlings were grown under light for 5 days on 0.5X LS medium and then transferred to medium containing DMSO or 1μM BRZ in combination with control (+ suc; containing 1% sucrose), starvation (without sucrose) or mannitol (350mM mannitol) stresses. The seedlings were incubated in darkness for 3 days following transfer and then hypocotyl length was quantified as described above.

Drought and dehydration assays

Drought survival assays were performed by withholding water for 2-3 weeks to impose drought stress followed by rewatering. 7 days after rewatering plants were scored for survival as judged by the presence of new green leaves. Equal water and soil amounts were assured in drought assays by weighing the amount of dry soil for each pot and watering with equal amounts of water. Pots were randomized in trays to control for varying water loss due to position. Dehydration treatments were performed as previously described (Qin et al., 2008). Briefly, whole rosettes of 4-week-old plants were removed from pots and placed in empty petri dishes (dehydration) or in petri dishes containing moistened kimwipes (mock control) and sealed with parafilm for 4 hours. Detached leaf water loss assays were performed with 4-5 week old plants grown under short day conditions as previously described (Bao et al., 2014).

Fixed-carbon starvation assays

Fixed-carbon starvation survival assays in seedlings were performed as described by (Chung et al., 2010). Seedlings were grown on 0.5X LS plates without sucrose in light for one week and then transferred to darkness for 8-12 days as indicated. After dark treatment, the seedlings were placed back in light conditions for one week. Plants with new growth were counted as surviving. For fixed-carbon starvation treatments of plants in soil, plants were grown for 4-5 weeks under short day conditions and then transferred to a dark chamber at 22°C. After 8 or 9 days dark incubation, plants were transferred back into light for one week recovery before being scored for survival.

Immunoprecipitation

The majority of immunoprecipitation experiments were carried out as follows: plant leaf tissue was ground to a fine powder and resuspended in 2-3 volumes of protein extraction buffer. Extracts were then filtered through Miracloth (Calbiochem), and insoluble debris removed by centrifugation for 10 minutes at 5000g, 4°C. The protein extracts were incubated for 2-4 hours with GFP-trap agarose beads (Chromotek) or with anti-GFP antibody followed by Protien-A agarose beads (Pierce). Beads were then washed 3-5 times with protein extraction buffer containing 0.1%-0.5% Triton X-100 and eluted by boiling in 2X SDS sample buffer. CIP treatments were performed at 37 degrees for one hour using Alkaline phosphatase (Roche) as described (Yin et al., 2002). Cerulean-ATG8 was Immunoprecipitated from the membrane fraction by grinding 5g fresh *N. benthamiana* tissue (48 hours post-innoculation) in 20mL cold extraction buffer (0.3M Sucrose, 0.1M Tris-HCl, pH7.5, 1mM EDTA, 1mM PMSF). The

extract was then passed through Miracloth (Calbiochem) and centrifuged for 5 minutes at 1,000g, 4°C to remove insoluble material. The supernatant was then centrifuged at 100,000g for 30 minutes, 4°C. The membrane pellet was resuspended in Phosphate buffered saline (PBS) supplemented with 1% Triton X-100, 10mM Beta-mercaptoethanol and Roche complete mini protease inhibitor cocktail by gentle rocking for 2 hours at 4°C. The extract was centrifuged again at 100,000g for 30 minutes, 4°C and the supernatant was incubated with 20μL GFP-Trap agarose beads (Chromotek) overnight. Beads were then washed 5 times with PBS containing 0.1% Triton X-100 and eluted by boiling in 2X SDS sample buffer.

TUBE ubiquitination assays

To detect BES1 ubiquitination, Tandem Ubiquitin Binding Entities (TUBEs; LifeSensors) were used to enrich total ubiquitinated proteins. Harvested tissue was ground to a fine powder in liquid nitrogen and extracted in protein extraction buffer (50mM Tris-Cl, pH 7.4, 150mM NaCl, 10% glycerol) supplemented with complete mini protease inhibitor cocktail (Roche) and deubiquitinase inhibitor (50μM PR-619; LifeSensors). Extract was clarified by two rounds of centrifugation at 13,000g for 10 minutes at 4°C and the supernatant was incubated with blocked agarose (control) or TUBE2 agarose beads for 3 hours with gentle rocking at 4°C. Beads were then washed 4 times with protein extraction buffer and eluted by boiling in 2X SDS sample buffer.

Western blotting

Protein was extracted in protein extraction buffer (50mM Tris-Cl, pH 7.4, 150mM NaCl, 10% glycerol) supplemented with complete mini protease inhibitor cocktail (Roche) followed by quantification using Bradford assay or by fresh weight through

directly adding 2-3 volumes of 2X SDS sample buffer to ground plant tissue. Western blotting was performed using standard laboratory techniques. Phostag SDS-PAGE was conducted by adding 1mM $MnCl_2$ to protein samples and running SDS-PAGE gels containing 100μM Phostag reagent (Wako) according to the manufacturer's instructions. The following antibodies were used in this study in conjunction with appropriate secondary antibody-HRP conjugates : anti-BES1 (Yu et al., 2011), anti-DSK2 (Lin et al., 2011), anti-HERK1 (Guo et al., 2009), anti-GFP, anti-Tubulin (Sigma), anti-Ubiquitin (Pratelli et al., 2012), anti-MYC (Sigma or Cell Signaling Technology), anti-MBP (NEB).

RNA-seq

RNA-seq experiments were performed using 4-week old plants under control, 4 hour dehydration, or 5 days dark treatment for starvation. 3 biological replicates were performed for control and dehydration conditions and 2 biological replicates for starvation. For each replicate, whole rosette tissue from 3-4 plants was pooled. RNA was then extracted using Trizol, followed by DNAse digestion and RNA cleanup using Qiagen Rneasy kit. Purified RNA was subject to quality control on an Agilent 2100 Bioanalyzer. Library preparation and RNA sequencing were performed by BGI Americas using an Illumina HiSeq 2000 with 50bp single-end reads and ~30 million reads per sample. Details of data processing and statistical analysis of RNA-seq data are provided in the Quantification and Statistical Analysis section.

Yeast-two hybrid

Yeast-two hybrid screening for BES1 interacting proteins using the Clontech matchmaker system was described previously (Yin et al., 2005). DSK2A was recovered from a screen using BES1-N domain as bait (amino acid residues 1-99) and SINAT2

was recovered using BES1-P domain (amino acid residues 100-150). For pairwise yeast-two hybrid assays, full length BES1, ATG8e, BIN2 and DSK2 were cloned into GBKT7 or GADT7 vectors and transformed into yeast strain Y187. Yeast cells were grown in medium lacking Trp and Leu and assayed for LacZ activity as described in the Yeast Protocols Handbook (Clontech) using X-gal (5- bromo-4-chloro-3-indolyl-b-D-galactopyranoside).

***in vitro* pulldown assays**

For GST-pulldown assays, GST or MBP fusions were generated by cloning into pET42a, pET-MALc-H or pET-MBP-H vectors. DSK2A-HIS fusion protein constructs were generated by cloning DSK2A into pET28a. Recombinant proteins were produced in *E. coli* strain BL21, and tested for interaction as described previously (Yin et al., 2002). GST or each GST tagged fusion were incubated with indicated MBP fusion proteins in 1mL GST-pulldown buffer (50mM Tris-HCl pH 7.5, 200mM NaCl, 0.5% Trition X-100 and 0.5 mM Beta-mercaptoethanol, Roche complete mini protease inhibitor cocktail) at room temperature for 2 hours on a tube rotator. Following incubation, 20uL GST beads pre-blocked overnight with 1mg/mL BSA and BL21 extract were added and the incubation was continued for an additional 30 minutes. GST beads were washed in GST-pulldown buffer 5-6 times and then eluted in 2X SDS sample buffer. For pulldown reactions exhibiting high background, an alternative pulldown buffer was substituted (25 mM HEPES-KOH [pH 8.0], 1 mM DTT, 50 mM KCL, 10% glycerol and 1% NP-40). GST-pulldown experiments were repeated 2-3 times with similar results. For pulldown of DSK2A-HIS, phosphorylated BES1-MBP protein was generated by incubating BES1-MBP with BIN2-GST in kinase buffer containing 10mM ATP

(rotated 5 hours at 37 degrees). Non-phosphorylated BES1 control was produced with an identical reaction lacking ATP. Pulldown assays were carried out as described above, except that blocked amylose resin (NEB) was used to capture the MBP proteins. DSK2A-HIS was detected with anti-DSK2 antibodies.

BiFC assays

BiFC assays were conducted using constructs for the N- or C-terminus of YFP (Yu et al., 2008). BES1, DSK2, ATG8e, BIN2, and SINAT2 were cloned upstream of YFP fragments and transformed into *Agrobacterium tumefaciens* (strain GV3101). Agrobacterium cultures were grown overnight in LB medium containing 200μM acetosyringone, washed with infiltration medium (10mM $MgCl_2$, 10mM MES, pH 5.7, 200μM acetosyringone) and resuspended to an OD600 of 1.0. Agrobacterium carrying NYFP and CYFP constructs were mixed in equal ratios, and the Agrobacterium mixtures were infiltrated into the lower surface of *N. benthamiana* leaves. After 36-48 hours, YFP signal was detected using a Leica SP5 X MP confocal microscope equipped with an HCS PL APO CS 20.0×0.70 oil objective. YFP was excited with a 514-nm laser line and detected from 530 to 560 nm. Images were acquired with LAS AF software (Leica Microsystems) using identical settings for samples and controls. For BiFC colocalization studies, Agrobacterium carrying Cerulean-ATG8e was mixed along with NYFP and CYFP constructs at equal ratios and infiltrated into *N. benthamiana* as described above. Confocal microscopy was used to image YFP and CFP sequentially to reduce cross-excitation. YFP was excited with a 514nm laser line and detected from 530-560nm. CFP was excited at 405nm and detected from 460-490nm. BiFC experiments were repeated 2-3 times.

Coexpression of DSK2 and BIN2 in tobacco

DSK2-MYC or DSK2 A-MYC (containing putative BIN2 phosphorylation sites mutated to alanine) was co-expressed with BIN2-D-YFP (bin2-1) (Li et al., 2001) or empty YFP vector in *N. benthamiana* as described for BiFC assays. Leaf tissue was collected for protein extraction 2 days post-infiltration.

Plasmid constructs and generation of transgenic plants

Plasmid constructs were generated using standard laboratory techniques via restriction enzyme digestion or Gateway technology (Invitrogen) and were confirmed by DNA sequencing. pET-MBP-H vector was generated by modifying pETMALc-H (Pryor and Leiting, 1997) via digestion with SacI and XhoI and replacement of the multiple cloning site with a redesigned sequence (GAGCTCCNGCGAATTCACGGGATCCCTGGGTACCCGCAAGCTTCGAGTCGACTACCTCGAG). gBlocks gene synthesis (IDT) was used to generate DSK2 mutants. An overview of mutated DSK2 sites and oligonucleotides used in this study is provided (Tables S4 and S5). DSK2-MYC constructs were generated by fusing DSK2 or mutated DSK2 variants with a C-terminal 2X MYC tag driven by the strong constitutive BRI1 promoter (Li and Chory, 1997; Li et al., 2009). Plasmid constructs were transferred into *Agrobacterium tumefaciens* (strain GV3101) and used to transform plants by the floral-dip method (Clough and Bent, 1998). Transgenic plants were screened on 0.5X LS plates supplemented with 50mg/L kanamycin and further confirmed via western blotting using anti-MYC antibodies.

Protoplast transient expression assays

Protoplasts were prepared from Arabidopsis rosette leaves grown under short day conditions and transformed using 30-50μg of plasmid DNA via the PEG method (Wu et al., 2009; Yoo et al., 2007). Transformed protoplasts were incubated in darkness for 36-48 hours with control (+sucrose; .5% sucrose added), starvation (-sucrose; without sucrose) or mannitol (350mM mannitol) treatments and concanamycin A (Sigma) or dimethyl sulfoxide (DMSO) were added 12 hours before visualization by confocal microscopy. Confocal microscopy was performed with a Leica (Leica Microsystems) SP5 X MP confocal microscope equipped with a resonance scanner and HPX PL APO CS 63.0x1.40 oil objective. For colocalization assays, YFP and CFP were imaged sequentially to avoid cross-detection between channels. Excitation and detection wavelengths were the same as those described for BiFC colocalization assays.

Confocal microscopy of Arabidopsis roots

For imagine of BES1-GFP signal, homozygous BES1P:BES1-GFP lines were grown for 5 days in light and then transferred to -sucrose plates for 2-day starvation treatments. DMSO or 1μM conA was applied by transferring the plants to liquid 0.5X LS medium 16 hours prior to imaging. Confocal microscopy was performed with a Leica (Leica Microsystems) SP5 X MP confocal microscope equipped with a HCX PL APO CS 40.0x1.25 oil objective. GFP was excited with a 489nm laser line and detected from 500-580nm.

Phosphorylation assays

For *in vitro* kinase assays, MBP or DSK2-MBP proteins were mixed with BIN2-HIS in 20μL kinase buffer (20 mM Tris, pH 7.5, 100 mM NaCl, 12 mM MgCl2 and 10μCi ^{32}P-γATP) as previously described (Yin et al., 2002). For Mass spectrometry analysis of phosphorylated proteins, DSK2-MBP was phosphorylated using BIN2-MBP in kinase buffer containing 20mM ATP.

Protein digestion and LC-MS/MS

Proteins were reduced with 5 mM TCEP in ammonium biocarbonate for 5 min at 94 °C. Proteins were then digested using either Glu-C (ThermoFisher) or trypsin (Roche) at 37 °C overnight and then alkylated with 12.5 mM iodacetamide for 15 min at 37 °C in the dark. Peptides were further digested using an additional aliquot of Glu-C or trypsin for 2 hrs. Samples were then acidified to a pH of ~3 with formic acid. Digested peptides were purified using Waters Oasis MCX cartridges and eluted using 45%IPA/500mM NH_4HCO_3. Eluted peptides were dried using a speedvac (Thermo) and resuspended in 0.1% formic acid. Peptide amount was then quantified using the Pierce BCA Protein assay kit.

An Agilent 1260 quaternary HPLC was used to deliver a flow rate of ~600 nL min^{-1} to a 3-phase capillary chromatography column through a splitter. The 3-phase capillary chromatography was assembled as follows. Using a Next Advance pressure cell a fused silica capillary column was packed with 5 μM Zorbax SB-C18 (Agilent) to form the first dimension reverse phase column (RP1). A 5 cm long strong cation exchange (SCX) column packed with 5 μm PolySulfoethyl (PolyLC) was connected to RP1 using a zero dead volume 1 μm filter (Upchurch, M548) attached to the exit of the

RP1 column. A nanospray fused silica capillary was pulled to a sharp tip using a laser puller (Sutter P-2000) and packed with 2.5 µM C18 (Waters) to form RP2 and then connected to the SCX column. The 3 sections were joined and mounted on a custom electrospray source for on-line nested elutions. A new set of columns was used for every sample. Peptides were loaded onto RP1 using the Next Advance pressure cell. Peptides were eluted from RP1 unto the SCX column using a 0 to 80% acetonitrile gradient over 60 min. Peptides were then fractionated using the SCX column using a series of 9 salt gradients (0, 30, 50, 60, 70, 80, 90, 100 and 1000 mM ammonium acetate), followed by high resolution reverse phase separation using an acetonitrile gradient of 0-80% for 150 min.

Spectra were acquired on a Thermo Scientific Q-Exactive high-resolution quadrupole Orbitrap mass spectrometer. Data dependent acquisition was obtained using Xcalibur 3.0.63 software in positive ion mode with a spray voltage of 2.00 kV and a capillary temperature of 275 °C. MS1 spectra were measured at a resolution of 70,000, an automatic gain control (AGC) of 3e6 with a maximum ion time of 100 ms and a mass range of 400-2000 m/z. Up to 15 MS2 were triggered at a resolution of 17,500, an AGC of 1e5 with a maximum ion time of 50 ms and a normalized collision energy of 28. MS1 that triggered MS2 scans were dynamically excluded for 15 s.

The raw data were extracted and searched using Spectrum Mill v4.01 (Agilent Technologies). MS/MS spectra with a sequence tag length of 1 or less were considered to be poor spectra and were discarded. The remaining MS/MS spectra were searched against the Arabidopsis TAIR10 proteome. The enzyme parameter was limited to tryptic peptides with a maximum mis-cleavage of 2. Carbamidomethylation was set as a fixed

modification while Ox-Met, and phosphorylation on Serine, Threonine, or Tyrosine were defined as variable modifications. A maximum of 6 phosphorylation events per peptide was used. A 1:1 concatenated forward-reverse database was constructed to calculate the false discovery rate (FDR). The tryptic peptides in the reverse database were compared to the forward database, and were shuffled if they matched to any tryptic peptides from the forward database. Cutoff scores were dynamically assigned to each dataset to obtain a peptide false discovery rate (FDR) of 0.1%. Phosphorylation sites were localized to a particular amino acid within a phosphopeptide using the variable modification localization (VML) score in Agilent's Spectrum Mill software (Chalkley and Clauser, 2012).

RNA-seq Data Processing and Statistics

Raw reads were subject to quality control and trimming and aligned to the Arabidopsis TAIR10 reference genome using GSNAP (Wu and Nacu, 2010). Uniquely aligned reads were used to obtain read counts per gene. Only genes with an average read count greater than 1 across all samples were used for differential expression analysis. Normalization was conducted automatically by DESeq2, which corrects for biases introduced by differences in the total number of uniquely mapped reads between samples. Normalized read counts were used to calculate fold changes and test for differential expression. The R package Deseq2 (https://bioconductor.org/packages/release/bioc/html/DESeq2.html) was used to test the null hypothesis that expression of a given gene is not different between two genotypes or conditions being compared. This null hypothesis was tested using a model with a negative binomial distribution. P-values of all statistical tests were converted to adjusted

p-values (q-values) (Benjamini and Hochberg, 1995). A false discovery rate of 10% (q-value) was used to account for multiple testing. Comparisons of gene lists were performed using Venny (http://bioinfogp.cnb.csic.es/tools/venny/index.html) and overrepresentation in overlapping gene lists tested using the Genesect tool in VirtualPlant (Katari et al., 2010). Reported overlaps were statistically significant at a $p < 0.05$ level. Clustering was performed using the 'aheatmap' function of the NMF package in R (https://cran.r-project.org/web/packages/NMF/index.html). Log2 reads per million mapped reads (RPM) values were used for clustering analysis and values were normalized for each gene by centering and scaling each row of the heatmap. GO analysis was performed using BINGO (Maere et al., 2005).

Data and software availability

RNA-seq data has been deposited into the Gene Expression Omnibus (GEO # GSE93420). Proteomics data relating to DSK2 phosphorylation by BIN2 has been deposited in the MassIVE repository (MassIVE ID: MSV000079641).

2.8 References

Asami, T., Min, Y.K., Nagata, N., Yamagishi, K., Takatsuto, S., Fujioka, S., Murofushi, N., Yamaguchi, I., and Yoshida, S. (2000). Characterization of brassinazole, a triazole-type brassinosteroid biosynthesis inhibitor. Plant Physiology *123*, 93-99.

Bao, Y., Wang, C., Jiang, C., Pan, J., Zhang, G., Liu, H., and Zhang, H. (2014). The tumor necrosis factor receptor-associated factor (TRAF)-like family protein SEVEN IN ABSENTIA 2 (SINA2) promotes drought tolerance in an ABA-dependent manner in Arabidopsis. The New phytologist *202*, 174-187.

Belkhadir, Y., and Jaillais, Y. (2015). The molecular circuitry of brassinosteroid signaling. The New phytologist *206*, 522-540.

Benjamini, Y., and Hochberg, Y. (1995). Controlling the False Discovery Rate – a Practical and Powerful Approach to Multiple Testing. J Roy Stat Soc B Met *57*, 289-300.

Birgisdottir, A.B., Lamark, T., and Johansen, T. (2013). The LIR motif – crucial for selective autophagy. Journal of Cell Science *126*, 3237-3247.

Chalkley, R.J., and Clauser, K.R. (2012). Modification site localization scoring: strategies and performance. Molecular & cellular proteomics : MCP *11*, 3-14.

Charrier, B., Champion, A., Henry, Y., and Kreis, M. (2002). Expression profiling of the whole Arabidopsis shaggy-like kinase multigene family by real-time reverse transcriptase-polymerase chain reaction. Plant Physiol *130*, 577-590.

Chung, T., Phillips, A.R., and Vierstra, R.D. (2010). ATG8 lipidation and ATG8-mediated autophagy in Arabidopsis require ATG12 expressed from the differentially controlled ATG12A AND ATG12B loci. Plant J *62*, 483-493.

Ciuffa, R., Lamark, T., Tarafder, A.K., Guesdon, A., Rybina, S., Hagen, W.J.H., Johansen, T., and Sachse, C. (2015). The Selective Autophagy Receptor p62 Forms a Flexible Filamentous Helical Scaffold. Cell Reports *11*, 748-758.

Claeys, H., and Inze, D. (2013). The agony of choice: how plants balance growth and survival under water-limiting conditions. Plant Physiol *162*, 1768-1779.

Clauw, P., Coppens, F., De Beuf, K., Dhondt, S., Van Daele, T., Maleux, K., Storme, V., Clement, L., Gonzalez, N., and Inze, D. (2015). Leaf Responses to Mild Drought Stress in Natural Variants of Arabidopsis thaliana. Plant Physiol.

Clough, S.J., and Bent, A.F. (1998). Floral dip: a simplified method for Agrobacterium-mediated transformation of Arabidopsis thaliana. Plant Journal *16*, 735-743.

Clouse, S.D. (2011). Brassinosteroid Signal Transduction: From Receptor Kinase Activation to Transcriptional Networks Regulating Plant Development. Plant Cell *23*, 1219-1230.

Contento, A.L., Kim, S.J., and Bassham, D.C. (2004). Transcriptome profiling of the response of Arabidopsis suspension culture cells to Suc starvation. Plant Physiology *135*, 2330-2347.

Dal Santo, S., Stampfl, H., Krasensky, J., Kempa, S., Gibon, Y., Petutschnig, E., Rozhon, W., Heuck, A., Clausen, T., and Jonak, C. (2012). Stress-induced GSK3 regulates the redox stress response by phosphorylating glucose-6-phosphate dehydrogenase in Arabidopsis. Plant Cell *24*, 3380-3392.

Doelling, J.H., Walker, J.M., Friedman, E.M., Thompson, A.R., and Vierstra, R.D. (2002). The APG8/12-activating enzyme APG7 is required for proper nutrient recycling and senescence in Arabidopsis thaliana. J Biol Chem *277*, 33105-33114.

Droese, S., Bindseil, K.U., Bowman, E.J., Siebers, A., Zeeck, A., and Altendorf, K. (1993). Inhibitory effect of modified bafilomycins and concanamycins on P- and V-type adenosinetriphosphatases. Biochemistry *32*, 3902-3906.

Farmer, L.M., Book, A.J., Lee, K.-H., Lin, Y.-L., Fu, H., and Vierstra, R.D. (2010). The RAD23 Family Provides an Essential Connection between the 26S Proteasome and Ubiquitylated Proteins in Arabidopsis. Plant Cell *22*, 124-142.

Farre, J.C., Burkenroad, A., Burnett, S.F., and Subramani, S. (2013). Phosphorylation of mitophagy and pexophagy receptors coordinates their interaction with Atg8 and Atg11. EMBO reports *14*, 441-449.

Floyd, B.E., Morriss, S.C., MacIntosh, G.C., and Bassham, D.C. (2012). What to Eat: Evidence for Selective Autophagy in Plants. J Integr Plant Biol *54*, 907-920.

Funakoshi, M., Sasaki, T., Nishimoto, T., and Kobayashi, H. (2002). Budding yeast Dsk2p is a polyubiquitin-binding protein that can interact with the proteasome. Proc Natl Acad Sci U S A *99*, 745-750.

Guo, H., Li, L., Aluru, M., Aluru, S., and Yin, Y. (2013). Mechanisms and networks for brassinosteroid regulated gene expression. Curr. Opin. Plant Biol. *16*, 545-553.

Guo, H., Ye, H., Li, L., and Yin, Y. (2009). A family of receptor-like kinases are regulated by BES1 and involved in plant growth in Arabidopsis thaliana. Plant signaling & behavior *4*, 784-786.

Hanaoka, H., Noda, T., Shirano, Y., Kato, T., Hayashi, H., Shibata, D., Tabata, S., and Ohsumi, Y. (2002). Leaf senescence and starvation-induced chlorosis are accelerated by the disruption of an Arabidopsis autophagy gene. Plant Physiol *129*, 1181-1193.

Hao, J., Yin, Y., and Fei, S.Z. (2013). Brassinosteroid signaling network: implications on yield and stress tolerance. Plant Cell Rep *32*, 1017-1030.

Harb, A., Krishnan, A., Ambavaram, M.M., and Pereira, A. (2010). Molecular and physiological analysis of drought stress in Arabidopsis reveals early responses leading to acclimation in plant growth. Plant Physiol *154*, 1254-1271.

He, J.X., Gendron, J.M., Yang, Y., Li, J., and Wang, Z.Y. (2002). The GSK3-like kinase BIN2 phosphorylates and destabilizes BZR1, a positive regulator of the brassinosteroid signaling pathway in Arabidopsis. Proc Natl Acad Sci U S A *99*, 10185-10190.
Herhaus, L., and Dikic, I. (2015). Expanding the ubiquitin code through post-translational modification. EMBO reports *16*, 1071-1083.

Ichimura, Y., Kirisako, T., Takao, T., Satomi, Y., Shimonishi, Y., Ishihara, N., Mizushima, N., Tanida, I., Kominami, E., Ohsumi, M.*, et al.* (2000). A ubiquitin-like system mediates protein lipidation. Nature *408*, 488-492.

Inoue, Y., Suzuki, T., Hattori, M., Yoshimoto, K., Ohsumi, Y., and Moriyasu, Y. (2006). AtATG genes, homologs of yeast autophagy genes, are involved in constitutive autophagy in Arabidopsis root tip cells. Plant Cell Physiol *47*, 1641-1652.

Kalvari, I., Tsompanis, S., Mulakkal, N.C., Osgood, R., Johansen, T., Nezis, I.P., and Promponas, V.J. (2014). iLIR. Autophagy *10*, 913-925.

Katari, M.S., Nowicki, S.D., Aceituno, F.F., Nero, D., Kelfer, J., Thompson, L.P., Cabello, J.M., Davidson, R.S., Goldberg, A.P., Shasha, D.E*., et al.* (2010). VirtualPlant: A Software Platform to Support Systems Biology Research. Plant Physiology *152*, 500-515.

Kim, B., Jeong, Y.J., Corvalan, C., Fujioka, S., Cho, S., Park, T., and Choe, S. (2014). Darkness and gulliver2/phyB mutation decrease the abundance of phosphorylated BZR1 to activate brassinosteroid signaling in Arabidopsis. The Plant journal : for cell and molecular biology *77*, 737-747.

Kinoshita, E., Kinoshita-Kikuta, E., Takiyama, K., and Koike, T. (2006). Phosphate-binding tag, a new tool to visualize phosphorylated proteins. Molecular & cellular proteomics : MCP *5*, 749-757.

Kir, G., Ye, H.X., Nelissen, H., Neelakandan, A.K., Kusnandar, A.S., Luo, A.D., Inze, D., Sylvester, A.W., Yin, Y.H., and Becraft, P.W. (2015). RNA Interference Knockdown of BRASSINOSTEROID INSENSITIVE1 in Maize Reveals Novel Functions for Brassinosteroid Signaling in Controlling Plant Architecture. Plant Physiology *169*, 826-+.

Kisselev, A.F., van der Linden, W.A., and Overkleeft, H.S. (2012). Proteasome inhibitors: an expanding army attacking a unique target. Chem Biol *19*, 99-115.

Kraft, C., Peter, M., and Hofmann, K. (2010). Selective autophagy: ubiquitin-mediated recognition and beyond. Nat Cell Biol *12*, 836-841.

Lee, D.Y., Arnott, D., and Brown, E.J. (2013). Ubiquilin4 is an adaptor protein that recruits Ubiquilin1 to the autophagy machinery. Embo Rep *14*, 373-381.

Lee, D.Y., and Brown, E.J. (2012). Ubiquilins in the crosstalk among proteolytic pathways. Biological chemistry *393*, 441-447.

Li, F.Q., and Vierstra, R.D. (2012). Autophagy: a multifaceted intracellular system for bulk and selective recycling. Trends Plant Sci *17*, 526-537.

Li, J., and Chory, J. (1997). A putative leucine-rich repeat receptor kinase involved in brassinosteroid signal transduction. Cell *90*, 929-938.

Li, J., and Jin, H. (2007). Regulation of brassinosteroid signaling. Trends Plant Sci *12*, 37-41.

Li, J., and Nam, K.H. (2002). Regulation of Brassinosteroid Signaling by a GSK3/SHAGGY-Like Kinase. Science *295*, 1299-1301.

Li, J.M., Nam, K.H., Vafeados, D., and Chory, J. (2001). BIN2, a new brassinosteroid-insensitive locus in Arabidopsis. Plant Physiology *127*, 14-22.

Li, L., Yu, X., Thompson, A., Guo, M., Yoshida, S., Asami, T., Chory, J., and Yin, Y. (2009). Arabidopsis MYB30 is a direct target of BES1 and cooperates with BES1 to regulate brassinosteroid-induced gene expression. Plant Journal *58*, 275-286.

Lin, Y.L., Sung, S.C., Tsai, H.L., Yu, T.T., Radjacommare, R., Usharani, R., Fatimababy, A.S., Lin, H.Y., Wang, Y.Y., and Fu, H. (2011). The defective proteasome but not substrate recognition function is responsible for the null phenotypes of the Arabidopsis proteasome subunit RPN10. Plant Cell *23*, 2754-2773.

Liu, X.D., Yao, J., Tripathi, D.N., Ding, Z., Xu, Y., Sun, M., Zhang, J., Bai, S., German, P., Hoang, A.*, et al.* (2014). Autophagy mediates HIF2alpha degradation and suppresses renal tumorigenesis. Oncogene.

Liu, Y.M., Burgos, J.S., Deng, Y., Srivastava, R., Howell, S.H., and Bassham, D.C. (2012). Degradation of the Endoplasmic Reticulum by Autophagy during Endoplasmic Reticulum Stress in Arabidopsis. Plant Cell *24*, 4635-4651.

Liu, Y.M., Xiong, Y., and Bassham, D.C. (2009). Autophagy is required for tolerance of drought and salt stress in plants. Autophagy *5*, 954-963.

Lopez-Maury, L., Marguerat, S., and Bahler, J. (2008). Tuning gene expression to changing environments: from rapid responses to evolutionary adaptation. Nature reviews. Genetics *9*, 583-593.

Maere, S., Heymans, K., and Kuiper, M. (2005). BiNGO: a Cytoscape plugin to assess overrepresentation of Gene Ontology categories in Biological Networks. Bioinformatics *21*, 3448-3449.

Marshall, R.S., Li, F., Gemperline, D.C., Book, A.J., and Vierstra, R.D. (2015). Autophagic Degradation of the 26S Proteasome Is Mediated by the Dual ATG8/Ubiquitin Receptor RPN10 in Arabidopsis. Molecular cell.

Maruyama, K., Takeda, M., Kidokoro, S., Yamada, K., Sakuma, Y., Urano, K., Fujita, M., Yoshiwara, K., Matsukura, S., Morishita, Y.*, et al.* (2009). Metabolic pathways involved in cold acclimation identified by integrated analysis of metabolites and transcripts regulated by DREB1A and DREB2A. Plant Physiol *150*, 1972-1980.

Michaeli, S., Galili, G., Genschik, P., Fernie, A.R., and Avin-Wittenberg, T. (2016). Autophagy in Plants – What's New on the Menu? Trends Plant Sci *21*, 134-144.

Nakashima, K., Ito, Y., and Yamaguchi-Shinozaki, K. (2009). Transcriptional regulatory networks in response to abiotic stresses in Arabidopsis and grasses. Plant Physiol *149*, 88-95.

Petherick, K.J., Williams, A.C., Lane, J.D., Ordonez-Moran, P., Huelsken, J., Collard, T.J., Smartt, H.J., Batson, J., Malik, K., Paraskeva, C.*, et al.* (2013). Autolysosomal beta-catenin degradation regulates Wnt-autophagy-p62 crosstalk. EMBO J *32*, 1903-1916.

Pratelli, R., Guerra, D.D., Yu, S., Wogulis, M., Kraft, E., Frommer, W.B., Callis, J., and Pilot, G. (2012). The ubiquitin E3 ligase LOSS OF GDU2 is required for GLUTAMINE DUMPER1-induced amino acid secretion in Arabidopsis. Plant Physiol *158*, 1628-1642.

Pryor, K.D., and Leiting, B. (1997). High-level expression of soluble protein in Escherichia coli using a His(6)-tag and maltose-binding-protein double-affinity fusion system. Protein Expres Purif *10*, 309-319.

Qin, F., Sakuma, Y., Tran, L.S., Maruyama, K., Kidokoro, S., Fujita, Y., Fujita, M., Umezawa, T., Sawano, Y., Miyazono, K.*, et al.* (2008). Arabidopsis DREB2A-interacting proteins function as RING E3 ligases and negatively regulate plant drought stress-responsive gene expression. Plant Cell *20*, 1693-1707.

Ren, M., Qiu, S., Venglat, P., Xiang, D., Feng, L., Selvaraj, G., and Datla, R. (2011). Target of rapamycin regulates development and ribosomal RNA expression through kinase domain in Arabidopsis. Plant Physiol *155*, 1367-1382.

Rogov, V.V., Suzuki, H., Fiskin, E., Wild, P., Kniss, A., Rozenknop, A., Kato, R., Kawasaki, M., McEwan, D.G., Lohr, F.*, et al.* (2013). Structural basis for phosphorylation-triggered autophagic clearance of Salmonella. Biochem J *454*, 459-466.

Sakuma, Y., Maruyama, K., Osakabe, Y., Qin, F., Seki, M., Shinozaki, K., and Yamaguchi-Shinozaki, K. (2006). Functional analysis of an Arabidopsis transcription factor, DREB2A, involved in drought-responsive gene expression. Plant Cell *18*, 1292-1309.

Skirycz, A., Vandenbroucke, K., Clauw, P., Maleux, K., De Meyer, B., Dhondt, S., Pucci, A., Gonzalez, N., Hoeberichts, F., Tognetti, V.B.*, et al.* (2011). Survival and growth of Arabidopsis plants given limited water are not equal. Nat Biotechnol *29*, 212-214.
Sun, S.Y., Chen, D.H., Li, X.M., Qiao, S.L., Shi, C.N., Li, C.X., Shen, H.Y., and Wang, X.L. (2015). Brassinosteroid Signaling Regulates Leaf Erectness in Oryza sativa via the Control of a Specific U-Type Cyclin and Cell Proliferation. Developmental cell *34*, 220-228.

Sun, Y., Fan, X.-Y., Cao, D.-M., Tang, W., He, K., Zhu, J.-Y., He, J.-X., Bai, M.-Y., Zhu, S., Oh, E.*, et al.* (2010). Integration of Brassinosteroid Signal Transduction with the Transcription Network for Plant Growth Regulation in Arabidopsis. Developmental cell *19*, 765-777.

Svenning, S., Lamark, T., Krause, K., and Johansen, T. (2011). Plant NBR1 is a selective autophagy substrate and a functional hybrid of the mammalian autophagic adapters NBR1 and p62/SQSTM1. Autophagy *7*, 993-1010.

Thompson, A.R., Doelling, J.H., Suttangkakul, A., and Vierstra, R.D. (2005). Autophagic nutrient recycling in Arabidopsis directed by the ATG8 and ATG12 conjugation pathways. Plant Physiol *138*, 2097-2110.

Urao, T., Yamaguchi-Shinozaki, K., Urao, S., and Shinozaki, K. (1993). An Arabidopsis myb homolog is induced by dehydration stress and its gene product binds to the conserved MYB recognition sequence. Plant Cell *5*, 1529-1539.

Vardhini, B.V., and Anjum, N.A. (2015). Brassinosteroids make plant life easier under abiotic stresses mainly by modulating major components of antioxidant defense system. Frontiers in Environmental Science *2*.

Vierstra, R.D. (2009). The ubiquitin-26S proteasome system at the nexus of plant biology. Nature reviews. Molecular cell biology *10*, 385-397.

Vilarrasa-Blasi, J., Gonzalez-Garcia, M.P., Frigola, D., Fabregas-Vallve, N., Alexiou, K.G., Lopez-Bigas, N., Rivas, S., Jauneau, A., Lohmann, J.U., Benfey, P.N.*, et al.* (2015). Regulation of Plant Stem Cell Quiescence by a Brassinosteroid Signaling Module (vol 30, pg 36, 2014). Developmental cell *33*, 238-238.

Wang, H., Yang, C., Zhang, C., Wang, N., Lu, D., Wang, J., Zhang, S., Wang, Z.X., Ma, H., and Wang, X. (2011). Dual role of BKI1 and 14-3-3 s in brassinosteroid signaling to link receptor with transcription factors. Developmental cell *21*, 825-834.

Wang, Y., Sun, S., Zhu, W., Jia, K., Yang, H., and Wang, X. (2013). Strigolactone/MAX2-induced degradation of brassinosteroid transcriptional effector BES1 regulates shoot branching. Developmental cell *27*, 681-688.

Wang, Z.Y., Nakano, T., Gendron, J., He, J.X., Chen, M., Vafeados, D., Yang, Y.L., Fujioka, S., Yoshida, S., Asami, T.*, et al.* (2002). Nuclear-localized BZR1 mediates brassinosteroid-induced growth and feedback suppression of brassinosteroid biosynthesis. Developmental cell *2*, 505-513.

Weber, C., Nover, L., and Fauth, M. (2008). Plant stress granules and mRNA processing bodies are distinct from heat stress granules. The Plant journal : for cell and molecular biology *56*, 517-530.

Wild, P., Farhan, H., McEwan, D.G., Wagner, S., Rogov, V.V., Brady, N.R., Richter, B., Korac, J., Waidmann, O., Choudhary, C.*, et al.* (2011). Phosphorylation of the Autophagy Receptor Optineurin Restricts Salmonella Growth. Science *333*, 228-233.

Wu, F.-H., Shen, S.-C., Lee, L.-Y., Lee, S.-H., Chan, M.-T., and Lin, C.-S. (2009). Tape-Arabidopsis Sandwich – a simpler Arabidopsis protoplast isolation method. Plant Methods *5*.

Wu, T.D., and Nacu, S. (2010). Fast and SNP-tolerant detection of complex variants and splicing in short reads. Bioinformatics *26*, 873-881.

Xie, Z., and Klionsky, D. (2007). Autophagosome formation: core machinery and adaptations. Nat Cell Biol *9*, 1102-1109.

Yan, Z.Y., Zhao, J., Peng, P., Chihara, R.K., and Li, J.M. (2009). BIN2 Functions Redundantly with Other Arabidopsis GSK3-Like Kinases to Regulate Brassinosteroid Signaling. Plant Physiology *150*, 710-721.

Yin, Y., Vafeados, D., Tao, Y., Yoshida, S., Asami, T., and Chory, J. (2005). A new class of transcription factors mediates brassinosteroid-regulated gene expression in Arabidopsis. Cell *120*, 249-259.

Yin, Y.H., Wang, Z.Y., Mora-Garcia, S., Li, J.M., Yoshida, S., Asami, T., and Chory, J. (2002). BES1 accumulates in the nucleus in response to brassinosteroids to regulate gene expression and promote stem elongation. Cell *109*, 181-191.

Yoo, S.D., Cho, Y.H., and Sheen, J. (2007). Arabidopsis mesophyll protoplasts: a versatile cell system for transient gene expression analysis. Nat Protoc *2*, 1565-1572.

Yoshimoto, K., Hanaoka, H., Sato, S., Kato, T., Tabata, S., Noda, T., and Ohsumi, Y. (2004). Processing of ATG8s, ubiquitin-like proteins, and their deconjugation by ATG4s are essential for plant autophagy. Plant Cell *16*, 2967-2983.

Youn, J.H., and Kim, T.W. (2014). Functional Insights of Plant GSK3-like Kinases: Multi-Taskers in Diverse Cellular Signal Transduction Pathways. Mol Plant.

Youn, J.H., and Kim, T.W. (2015). Functional Insights of Plant GSK3-like Kinases: Multi-Taskers in Diverse Cellular Signal Transduction Pathways. Molecular Plant *8*, 552-565.

Yu, X., Li, L., Li, L., Guo, M., Chory, J., and Yin, Y. (2008). Modulation of brassinosteroid-regulated gene expression by jumonji domain-containing proteins ELF6 and REF6 in Arabidopsis. Proceedings of the National Academy of Sciences of the United States of America *105*, 7618-7623.

Yu, X., Li, L., Zola, J., Aluru, M., Ye, H., Foudree, A., Guo, H., Anderson, S., Aluru, S., Liu, P.*, et al.* (2011). A brassinosteroid transcriptional network revealed by genome-wide identification of BESI target genes in Arabidopsis thaliana. Plant Journal *65*, 634-646.

Zhang, S., Cai, Z., and Wang, X. (2009). The primary signaling outputs of brassinosteroids are regulated by abscisic acid signaling. Proc Natl Acad Sci U S A *106*, 4543-4548.

Zhang, Y., Liu, Z., Wang, J., Chen, Y., Bi, Y., and He, J. (2015). Brassinosteroid is required for sugar promotion of hypocotyl elongation in Arabidopsis in darkness. Planta *242*, 881-893.

Zhang, Z., Zhu, J.Y., Roh, J., Marchive, C., Kim, S.K., Meyer, C., Sun, Y., Wang, W., and Wang, Z.Y. (2016). TOR Signaling Promotes Accumulation of BZR1 to Balance Growth with Carbon Availability in Arabidopsis. Current biology : CB *26*, 1854-1860.

Zhao, J., Peng, P., Schmitz, R.J., Decker, A.D., Tax, F.E., and Li, J. (2002). Two putative BIN2 substrates are nuclear components of brassinosteroid signaling. Plant Physiol *130*, 1221-1229.

Zhou, J., Wang, J., Cheng, Y., Chi, Y.J., Fan, B., Yu, J.Q., and Chen, Z. (2013). NBR1-mediated selective autophagy targets insoluble ubiquitinated protein aggregates in plant stress responses. PloS genetics *9*, e1003196.

Zhu, Y., Massen, S., Terenzio, M., Lang, V., Chen-Lindner, S., Eils, R., Novak, I., Dikic, I., Hamacher-Brady, A., and Brady, N.R. (2013). Modulation of serines 17 and 24 in the LC3-interacting region of Bnip3 determines pro-survival mitophagy versus apoptosis. The Journal of biological chemistry *288*, 1099-1113.

Zientara-Rytter, K., Lukomska, J., Moniuszko, G., Gwozdecki, R., Surowiecki, P., Lewandowska, M., Liszewska, F., Wawrzynska, A., and Sirko, A. (2011). Identification and functional analysis of Joka2, a tobacco member of the family of selective autophagy cargo receptors. Autophagy *7*, 1145-1158.

2.9 Figures

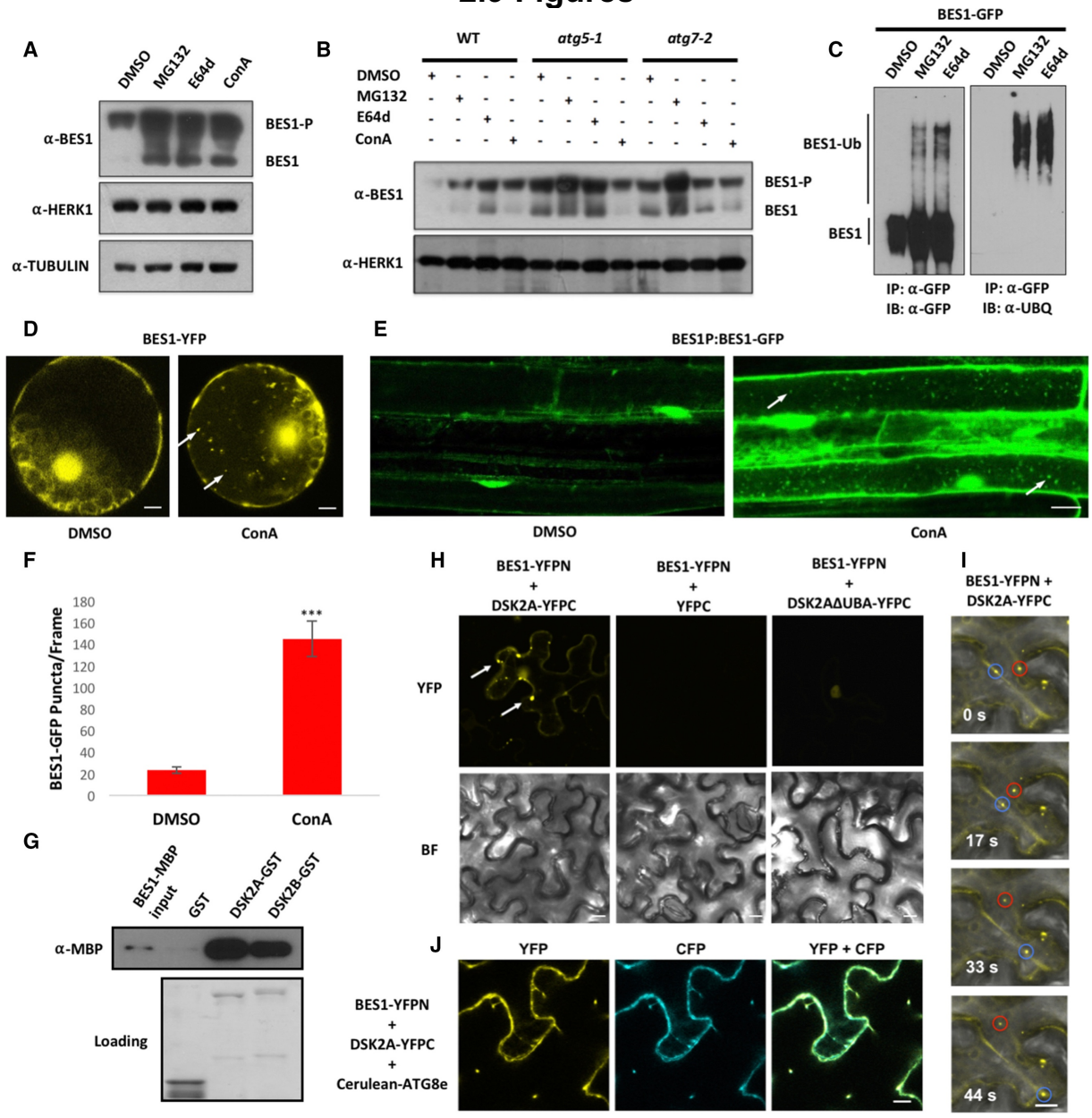

Figure 1: BES1 is degraded by proteasome and autophagy pathways and interacts with ubiquitin receptor protein DSK2

(A) Response of 10-day-old WT seedlings to proteasome and autophagy inhibitors. Seedlings treated for 6 hours in 1/2 MS liquid with DMSO, 50μM MG132, 20μM E64d or 1μM ConA were analyzed by western blotting with anti-BES1 antibodies. HERK1 and Tubulin served as loading controls. See also Figure S1A. (B) Response of BES1 to inhibitors as described above in 4-week-old WT, *atg5-1 or atg7-2* leaf tissue. See also Figure S1B. (C) Ubiquitination of BES1. BES1-GFP was expressed in *N. benthamiana* and treated with mock solvent or inhibitors for 16 hours. Immunoprecipitated BES1-GFP analyzed by western blotting with GFP or Ubiquitin antibodies. (D) Confocal microscopy images of Arabidopsis protoplasts expressing BES1-YFP under -sucrose conditions treated with DMSO or 1μM ConA for 12 hours. Scale bars indicate 5μm. I Confocal microscopy of *BES1* Promoter: *BES1-GFP* (*BES1P:BES1-GFP*) transgenic plants grown for 5 days in light followed by 2 day sucrose starvation. DMSO or 1μM ConA was applied 16

hours prior to microscopy. Scale bars indicate 20μm. (F) Quantification of BES1P:BES1-GFP puncta. Data represent mean ± SEM, n=8, *** indicates p<0.001 (t-test). (G) GST pulldown showing interactions of GST-DSK2A and GST-DSK2B with BES1-MBP. BES1-MBP was detected using anti-MBP antibody. Loading indicates amounts of GST proteins used in the pulldown reactions. (H) Interaction of BES1 with DSK2 in BiFC assays in *N. benthamiana.* Bright field images are shown (BF). See also Figure S1E. (I) Time course showing movement of BES1-DSK2 BiFC signals. Time of image acquisition is shown in seconds. (J) Colocalization of BES1-DSK2 BiFC signals (YFP channel) with Cerulean-ATG8e (CFP channel). Scale bars for BiFC experiments indicate 10μm. (See also Figures S1E and S1H).

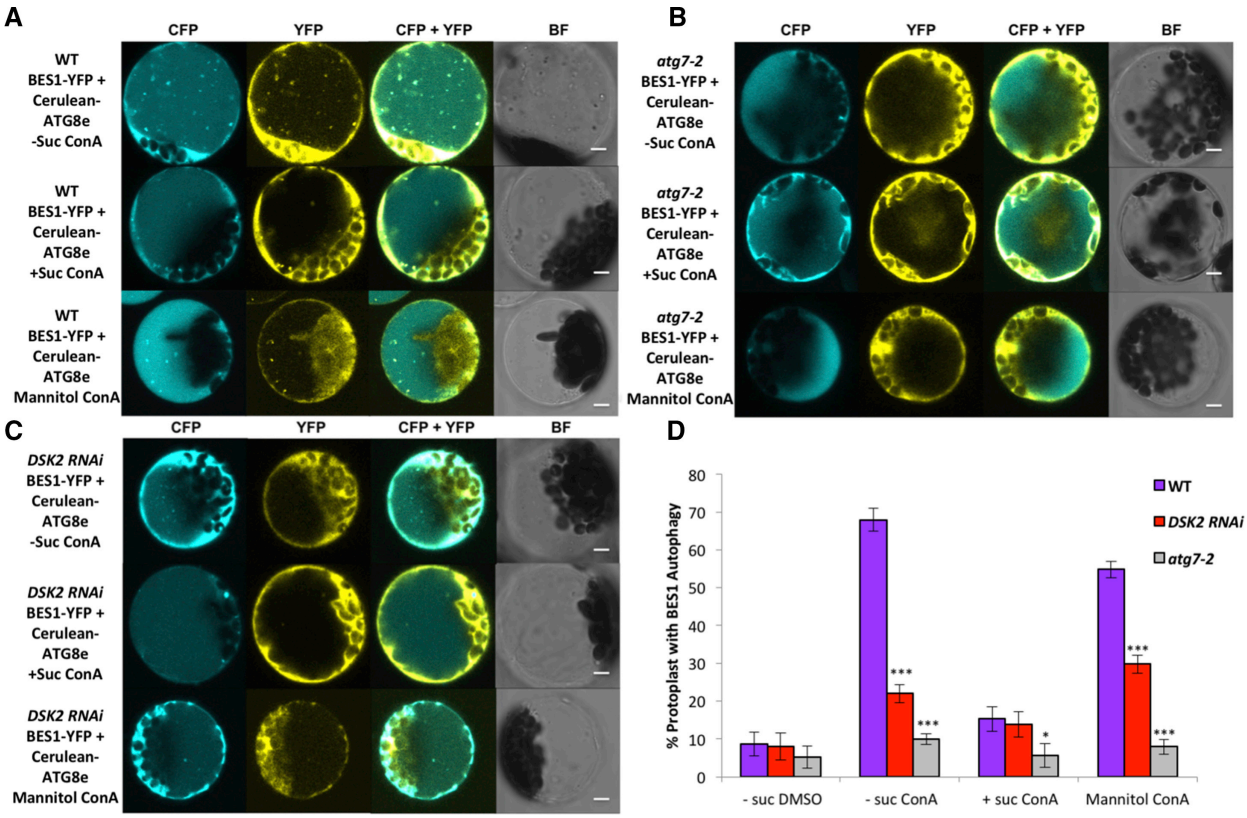

Figure 2: DSK2 recruits BES1 to ATG8-labeled autophagosomes during stress

(A) Representative images showing colocalization of BES1-YFP and Cerulean-ATG8 in WT Arabidopsis protoplasts. Protoplasts treated with control (+Suc), starvation (-Suc) or mannitol stress conditions were incubated with 1μM ConA for 12 hours and imaged by confocal microscopy. CFP, YFP or merged (CFP + YFP) fluorescence channels are shown along with bright field images (BF). See also Figure S2A. (B) Colocalization of BES1-YFP and Cerulean-ATG8 in *atg7-2* protoplasts. (C) Colocalization of BES1-YFP and Cerulean-ATG8 in *DSK2 RNAi* protoplasts. See also Figure S2B. (D) Quantification of protoplasts with BES1 autophagy. Protoplasts expressing BES1-YFP were treated with indicated treatments as described above. BES1 autophagy was defined by the presence ≥3 autophagosomes per protoplast. Data represent mean of 3 biological replicates ± SEM, n ≥ 50. (*$p < 0.05$ and ***$p < 0.001$, t test). See also Figure S2D.

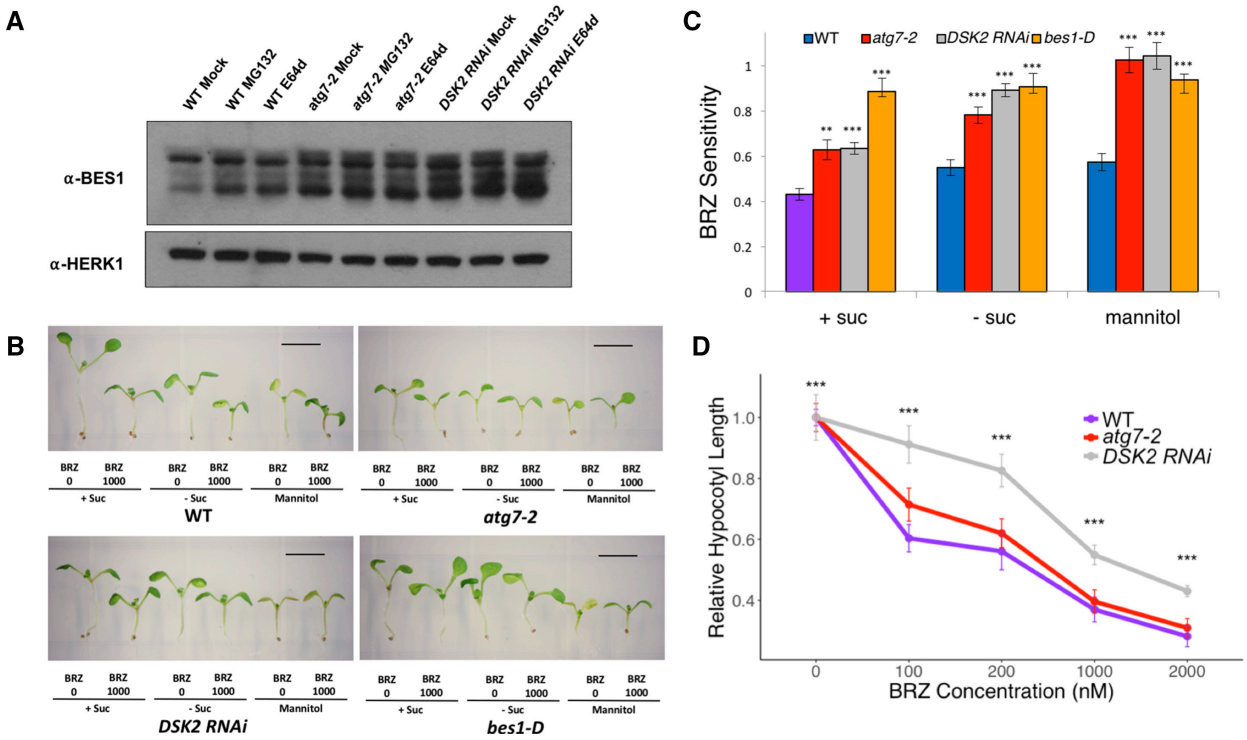

Figure 3: BES1 degradation by DSK2 and autophagy affects BR-regulated plant growth responses

(A) BES1 accumulation in 4-week-old Arabidopsis plants following 6-hour inhibitor treatments. HERK1 was used as a loading control (B) BRZ treatments under stress conditions. 5-day-old plants were transferred to medium with indicated combinations of BRZ with or without sucrose or 350mM mannitol to induce stress. Plants were incubated in darkness for 3 days followed by imaging and hypocotyl measurements. (C) Quantification of BRZ sensitivity (hypocotyl length BRZ1000nM/ hypocotyl length BRZ0) from (B). (D) Response to BRZ under non-stress conditions. Data represent mean ± SEM. (***p < 0.001, t test). See also Figures S3A,S3B and S3C.

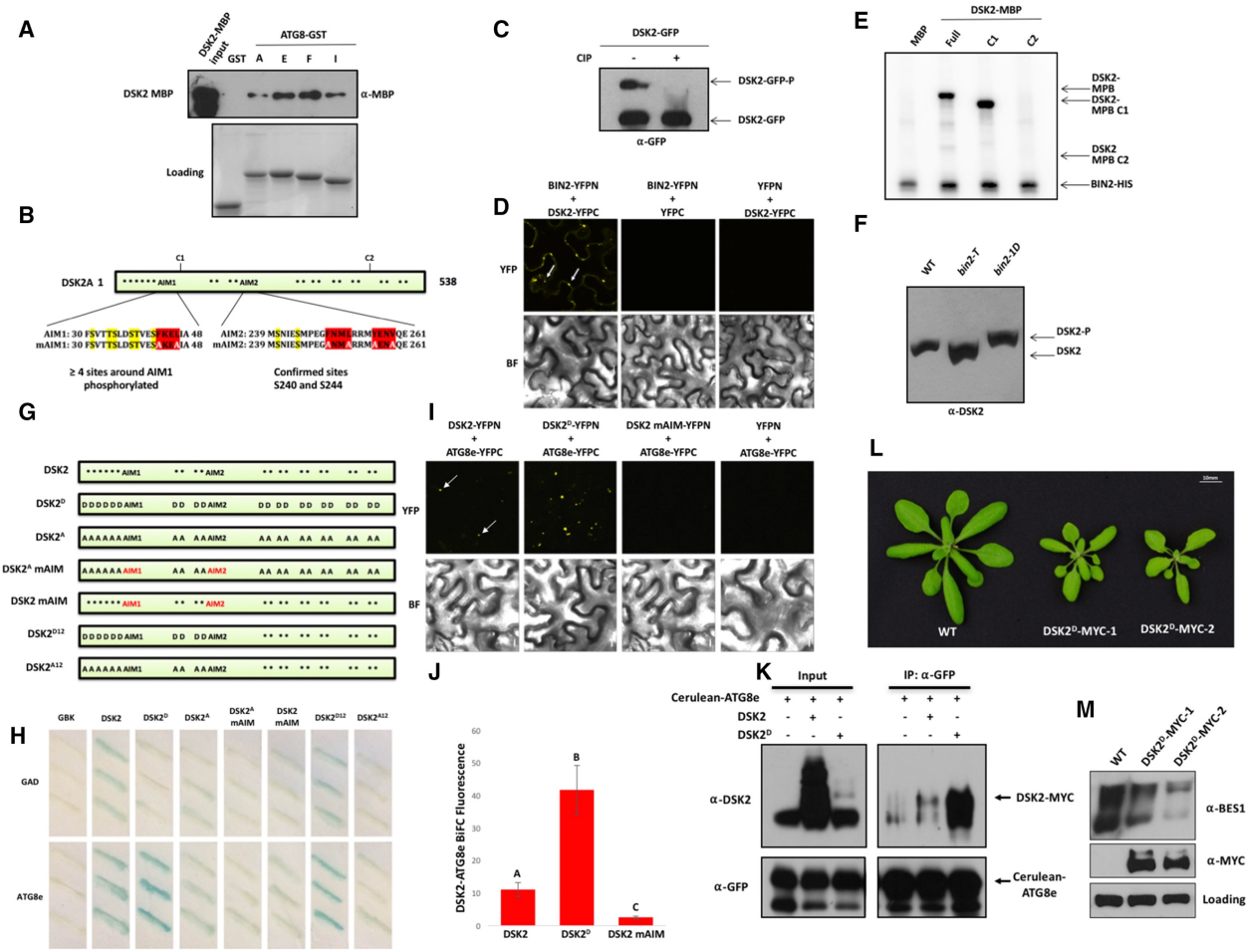

Figure 4: DSK2 interacts with ATG8 and is phosphorylated by BIN2 kinase around AIMs

(A) Interaction of DSK2 with ATG8 (letters indicate ATG8 family members) in GST pulldown assays. DSK2A-MBP was detected with anti-MBP antibodies. Loading indicates amounts of GST proteins used in pulldown reactions. (B) Schematic diagram showing DSK2A protein sequence. Text colors indicate the following: red, predicted ATG8 Interacting Motifs (AIMs); white, AIM mutations present in DSK2 mAIM constructs; yellow, putative BIN2 phosphorylation sites. Predicted BIN2 phosphorylation sites are also marked with an asterisk (*) in the schematic. (C) Phosphatase treatment of DSK2-GFP expressed in *N. benthamiana,* immunoprecipitated with anti-GFP antibodies and treated with (+) or without (-) Calf Intestinal Alkaline Phosphatase (CIP) followed by Phostag SDS-PAGE and western blotting with anti-GFP antibodies. (D) Interaction of BIN2 (BIN2-YFPN) with DSK2 (DSK2-YFPC) in *N. benthamiana* BiFC experiments. See also Figures S4A and S4B.

(E) *in vitro* phosphorylation of DSK2 by BIN2. MBP or DSK2-MBP proteins (Full, AA1-538; C1, AA90-538; C2, AA403-538) were phosphorylated by BIN2 kinase. Arrows indicate phosphorylated DSK2A or BIN2 autophosphorylation. (F) Modulation of DSK2 phosphorylation by BIN2 *in* vivo as monitored by Phostag SDS-PAGE and western blotting with anti-DSK2 antibody. Arrows denote gel shifts indicating phosphorylated or unphosphorylated DSK2. (G) Schematic diagrams of DSK2 proteins showing mutated BIN2 phosphorylation sites and AIM mutations. Predicted BIN2 phosphorylation sites are marked with an asterisk (*). When mutated, residues are represented as A (Ser or Thr to Ala) or D (Ser or Thr to Asp). ATG8 interacting motif (AIM) domains are indicated, with red color representing mutant AIMs (mAIM). (See also Figures S4C and S4D). (H) Yeast-two hybrid interaction of DSK2 with ATG8e as detected by β-galactosidase (LacZ) activity. (I) BiFC assays of DSK2 (DSK2-YFPN), phosphomimic forms of DSK2 ($DSK2^{D}$ -YFPN) or DSK2 AIM mutant ($DSK2^{mAIM}$-YFPN) with ATG8e (ATG8e-YFPC) in *N. benthamiana.* (J) Quantification of DSK2-ATG8e BiFC signal from (I). Fluorescence was measured using ImageJ and normalized to controls expressing DSK2-YFPN with YFPC or ATG8e-YFPC with YFPN. Data represent

mean of 4 independent images ± SEM. Different letters indicate statistically significant differences at $p<0.05$ (t test). (K) Co-Immunoprecipitation in *N. benthamiana* showing Cerulean-ATG8e immunoprecipiated with GFP-Trap interacts more strongly with DSK2^{D}-MYC than DSK2-MYC**.** (L) Phenotype of two independent T2 transgenic lines overexpressing phosphomimic DSK2 plants (DSK2^{D}-MYC). (M) BES1 protein levels in DSK2^{D}-MYC lines. Protein extracts from indicated lines were analyzed by western blotting. DSK2^{D}-MYC was detected with anti-MYC antibodies, while BES1 was detected with anti-BES1. A non-specific band from anti-MYC was used as a loading control. All DSK2 constructs presented in this figure are derived from the *DSK2A* gene. See also Figures S4E and S4F.

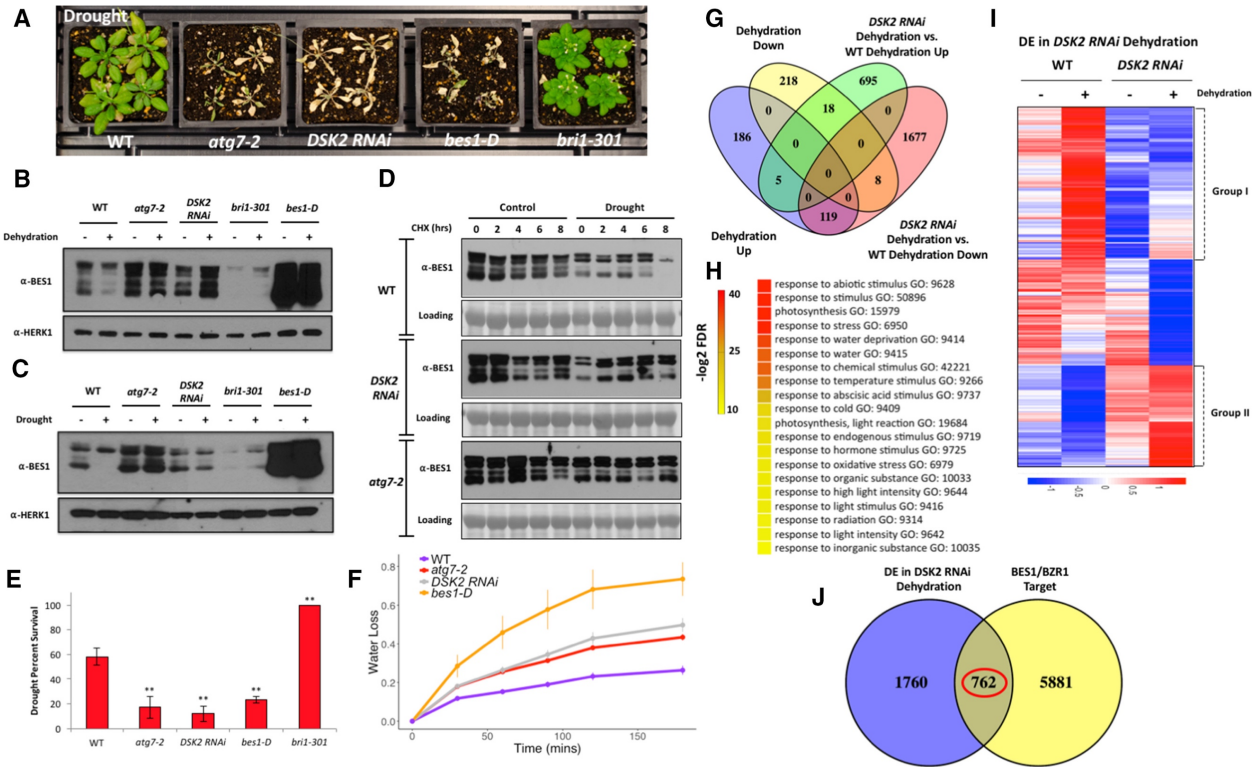

Figure 5: Degradation of BES1 mediated by DSK2 and autophagy during drought stress

(A) Plant phenotypes for indicated lines after drought recovery assays. See also Figure S6A. (B) BES1 protein levels during dehydration. Plants were subjected to control or 4-hour dehydration conditions and BES1 levels analyzed by western blotting. HERK1 was used as a loading control. (C) BES1 protein levels during drought in soil. Plants were treated with control (well-watered) or sub-lethal drought conditions and protein was extracted from plant leaf tissue for analysis by western blotting as described above. (D) BES1 protein levels following cycloheximide (CHX) treatment during control or drought treatments. Indicated genotypes were grown for 4 weeks in control or sub-lethal drought conditions followed by treatment with 500μM CHX for the indicated time points. Ponceua S staining was used as loading control. See also Figure S5C. (E) Quantification of percent survival following drought recovery. Plants producing new leaves after the 7-day recovery period were scored as survivors. Data represent mean survival of 3 biological replicates of 12-16 plants ± SEM, (**p < 0.01, t test). (F) Detached leaf water loss assays. Water loss represents proportion of total weight lost compared to initial weight. Data represent mean ± SEM from 2-3 biological replicates. Differences between WT and mutants are statistically significant at p<0.05 for all time points shown except 30 mins (t test). (G) Comparison of dehydration regulated and *DSK2 RNAi* dehydration DE genes in whole transcriptome RNA-seq. (H) Top 20 significantly enriched GO terms in *DSK2 RNAi* dehydration DE genes as ranked by false discovery rate (FDR). (I) Clustering of 2522 genes differentially expressed in *DSK2 RNAi* dehydration vs. WT dehydration. Color legend indicates normalized gene expression values. See also Figures S6D and S6E. (J) Comparison of DSK2 RNAi dehydration DE genes with BES1/BZR1 target genes from genome-wide Chromatin immunoprecipitation (ChIP) datasets. About 30% (762/2522) of *DSK2 RNAi* dehydration DE genes are BES1 or BZR1 targets which is comparable to that of BR responses, where 33.5% (2579/7687) of BR regulated genes are BES1/BZR1 targets.

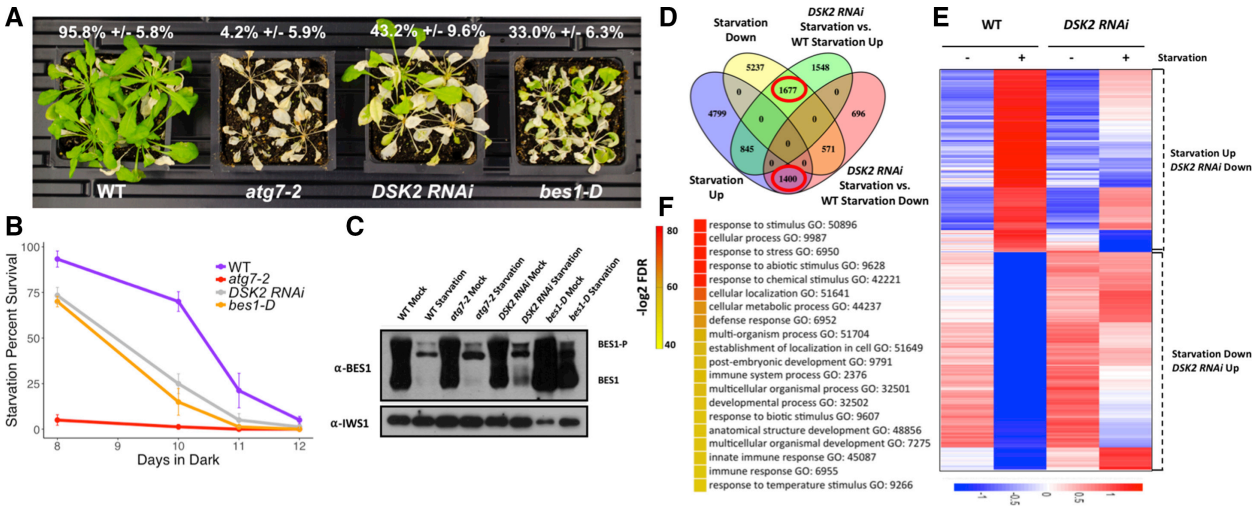

Figure 6: Degradation of BES1 under fixed-carbon starvation via DSK2 and autophagy

(A) Representative images of plant survival following 8 day fixed-carbon starvation treatment. Percentage survival is indicated from 2 biological repeats of 7-12 plants ± SD. Differences between WT and mutants are statistically significant $p<0.05$ (t test). (B) Time course of fixed-carbon starvation survival. Plants were grown on 1/2 LS plates without sucrose for one week and transferred to darkness for indicated time points followed by one-week recovery under light. Data represent mean ± SEM for 3-4 biological replicates of 20 plants each. Differences between WT and mutants are statistically significant $p<0.05$ (t test). See also Figure S10C. (C) Western blot analysis of BES1 protein levels following 5-day dark treatment. A general transcription factor, IWS1, served as a loading control. See also Figures S10A and S10B. (D) Comparison of starvation regulated and *DSK2 RNAi* starvation DE genes in whole transcriptome RNA-seq. See also Figure S10E. (E) Clustering analysis of 3077 genes that are starvation upregulated and downregulated in *DSK2 RNAi* starvation or starvation downregulated and upregulated in *DSK2 RNAi* starvation. Color legend indicates normalized gene expression values. (F) Top 20 significantly enriched GO terms in *DSK2 RNAi* starvation DE genes as ranked by false discovery rate (FDR).

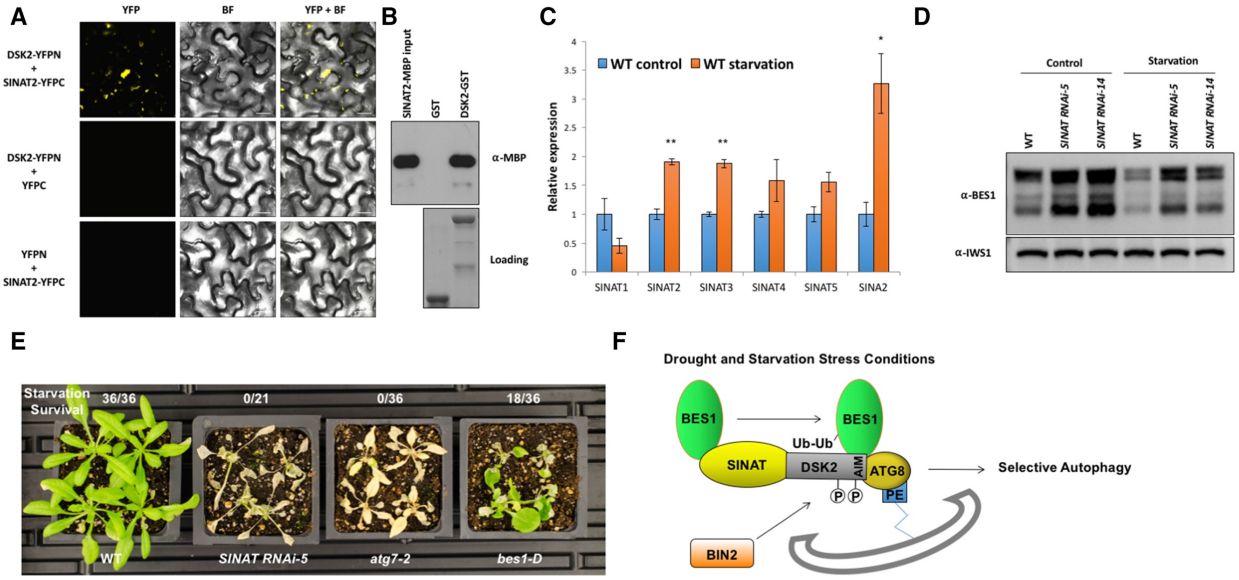

Figure 7: SINAT E3 ligases are involved in BES1 degradation during starvation.

(A) Interaction of DSK2 and SINAT2 in BiFC assays in *N. benthamiana.* Bright field images are shown (BF). (B) GST pulldown assays showing interaction of SINAT2 with DSK2. SINAT2-MBP was detected with anti-MBP antibodies. Loading indicates amounts of GST proteins used. (C) Expression levels of SINAT family E3 ligases from starvation RNA-seq experiments. Data represent mean ± SEM. (*p < .05 and **p < 0.01, t test). (D) Western blot analysis of BES1 protein levels following 3-day starvation treatment. IWS1 served as a loading control. (E) Representative images of plant survival following 8 day fixed-carbon starvation treatment. Numbers indicate recovered plants after one-week recovery period. The experiment was repeated twice with similar results. (F) A Model for BES1 protein degradation through selective autophagy. Under stress conditions, BES1 is ubiquitinated and targeted for degradation by SINAT E3 ubiquitin ligases, partly due to the induction of *SINAT* genes by stresses (see C). Ubiquitin receptor DSK2 interacts with BES1 and recruits BES1 to autophagy through DSK2-ATG8 interactions. When activated under stress conditions, BIN2 phosphorylates DSK2 flanking DSK2's AIM domains and potentiates DSK2-ATG8 interactions, promoting BES1 degradation through selective autophagy.

2.10 Supplemental Figures and Tables

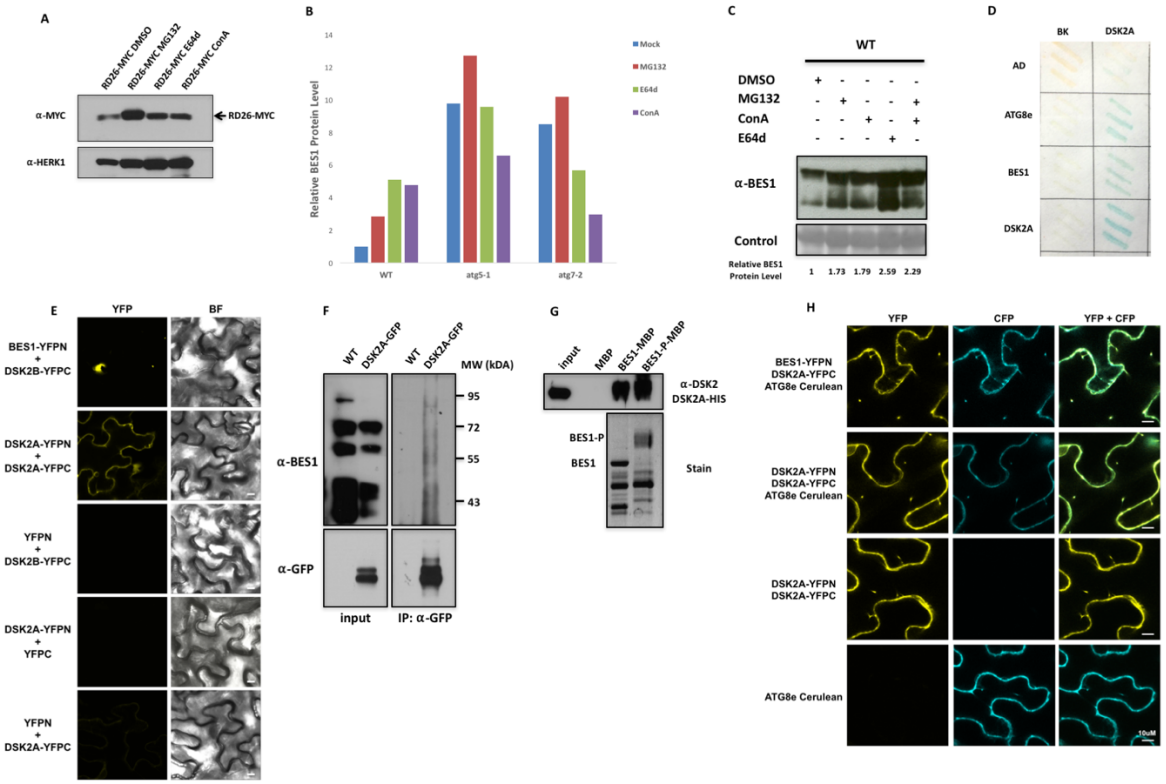

Figure S1, Related to Figure1. BES1 and DSK2 interaction experiments.

(A) Control for proteasome and autophagy inhibitor treatments in Figure 1A and B. MYC-tagged RD26 transgenic plants were treated for 6 hours in 1/2 MS liquid with DMSO, 50μM MG132, 20μM E64d or 1μM ConA. RD26-MYC protein was detected by western blotting with anti-MYC antibodies. HERK1 served as a loading control. (B) Quantification of BES1 protein levels following inhibitor treatments from Figure 1B. (C) BES1 accumulation after combined proteasome and autophagy inhibitor treatment. Plants were treated for 6 hours in 1/2 MS liquid with DMSO, 50μM MG132, 20μM E64d or 1μM ConA, or both 50μM MG132 and 1μM ConA. (D) LacZ assays showing yeIst-two hIbIid interactions of DSK2A wIth BES1 or ATG8e and self-association of DSK2A. (E) BiFC assays in *N. benthamiana* showing interactions of BES1 with DSK2B (top panel) or DSK2A self-association (second panel). Negative controls are shown in bottom panels. (F) Co-Immunoprecipiation showing interaction of DSK2-GFP with high-molecular weight forms of BES1. WT or 35S:DSK2-GFP plants were treated with 1μM ConA and 2μM Brassinazole (BRZ) for 16 hours. Co-IP was performed with anti-GFP antibodies and BES1 detected with anti-BES1 antibody. (G) Interaction of DSK2-HIS with BES1-MBP and phosphorylated BES1-MBP. Equal amounts of BES1-MBP protein were incubated with BIN2-GST in the absence (unphosphorylated BES1) or presence of ATP (phosphorylated BES1). Pulldown reactions were then carried out by incubating DSK2A-HIS with MBP, BES1-MBP or phosphorylated BES1-MBP. MBP proteins were bound with amylose resin and interacting DSK2-HIS detected with anti-DSK2 antibodies. SYBR Ruby staining was used to verify the phosphorylation status of BES1 (lower panel). (H) BiFC colocalization assays in *N. benthamiana* showing colocalization of BES1-DSK2A or DSK2A-DSK2A complexes (YFP channel) with autophagy marker Cerulean-ATG8e (CFP channel). Top panel showing DSK2A-BES1 colocalization with Cerulean-ATG8 is repeated from Figure 1H to show specificity of channels. Bottom panels indicate expression of YFP signals only (DSK2A-YFPN with DSK2A-YFPC) or CFP signals only (Cerulean-ATG8e). Scale bars for BiFC experiments indicate 10μm.

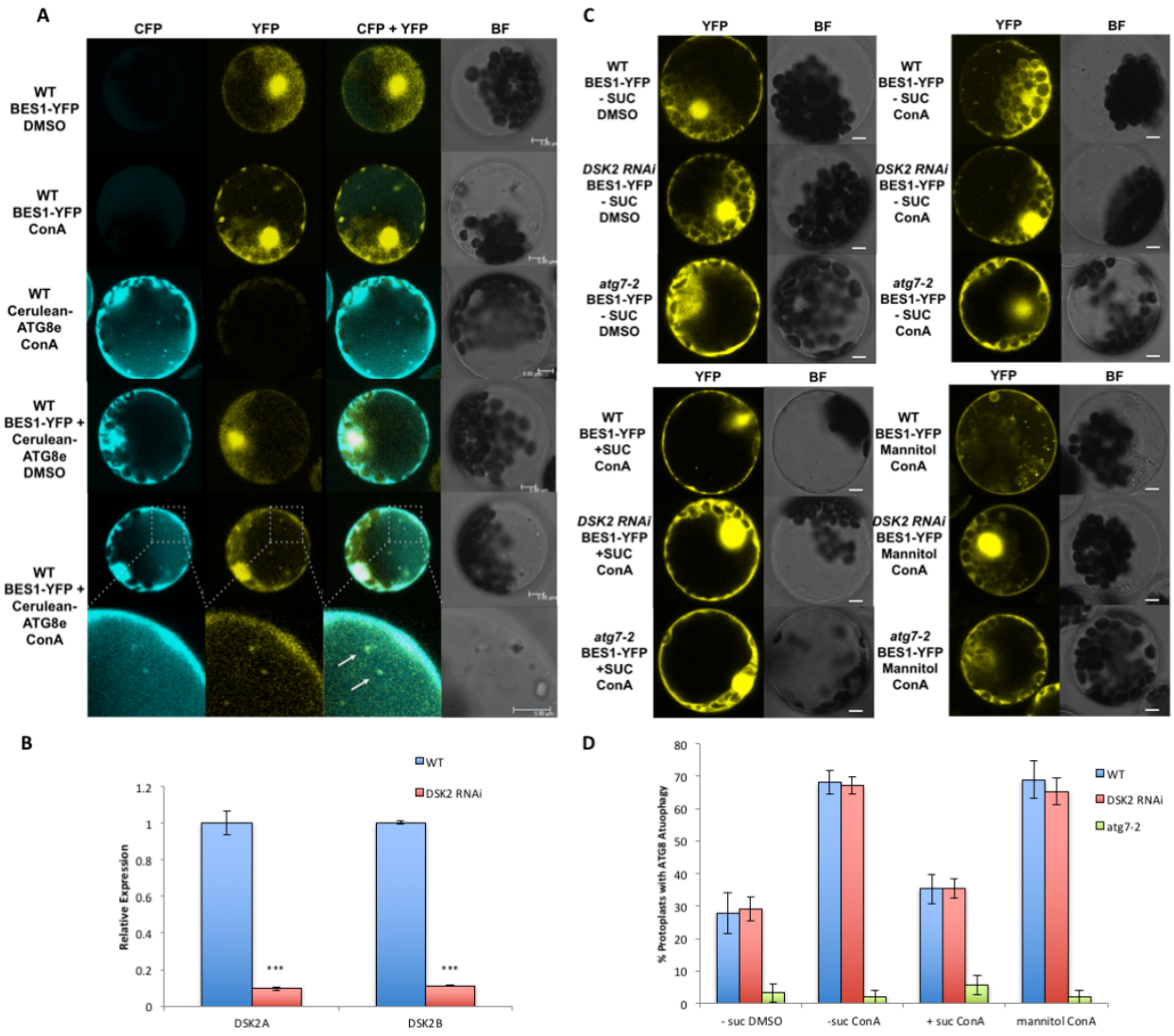

Figure S2, related to Figure 2. Confocal microscopy of BES1 and ATG8 in Arabidopsis protoplasts.

(A) Protoplasts treated with starvation (-Suc) conditions were incubated with control solvent (DMSO) or 1μM ConA for 12 hours and imaged by confocal microscopy. CFP, YFP or merged (CFP + YFP) fluorescence channels are shown along with bright field images (BF). Single transformations of BES1-YFP (top two panels) or Cerulean-ATG8e (third panel) indicate that CFP and YFP channels are specific. Arrows denote ATG8-labeled autophagosomes that colocalize with BES1 (bottom panel). Bright field images are shown (BF). (B) mRNA expression levels of DSK2A and DSK2B in WT or *DSK2 RNAi* plants from whole transcriptome RNA-seq. Error bars represent SEM (***, $p < 0.001$, t test). (C) Representative images of protoplasts expressing BES1-YFP used for quantification of protoplasts containing BES1 autophagy in Figure 2D. WT expressing BES1-YFP under -Suc DMSO conditions was a shared control and is also presented in Figure 1D. (D) Quantification of protoplasts containing ATG8 autophagy using Cerulean-ATG8e marker. ATG8 autophagy was defined by the presence ≥3 Cerulean-ATG8 labeled autophagosomes per protoplast.

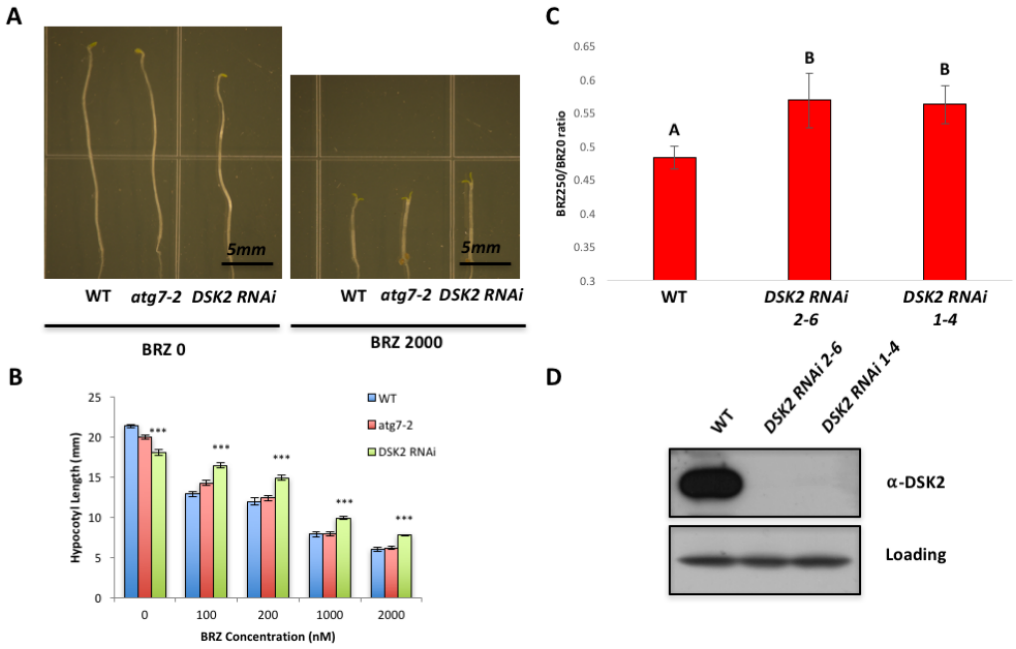

Figure S3, related to Figure 3. BRZ response of *atg7-2* and *DSK2 RNAi* under non-stressed conditions.

(A) Plant phenotypes in BRZ response assay. Plants were grown on control or BRZ containing medium in darkness for 7 days followed by imaging and hypocotyl length measurements. (B) Quantification of hypocotyl length from BRZ response assays. Data represent mean ± SEM from at least 10 seedlings. (***, $p < 0.001$, t test.). (C) BRZ response under non-stress conditions with an additional independent DSK2 RNAi line. DSK2 RNAi 2-6 is otherwise referred to as DSK2 RNAi throughout this study. (D) DSK2 protein levels in DSK2 RNAi lines detected using anti-DSK2 antibodies. IWS1 was used as a loading control.

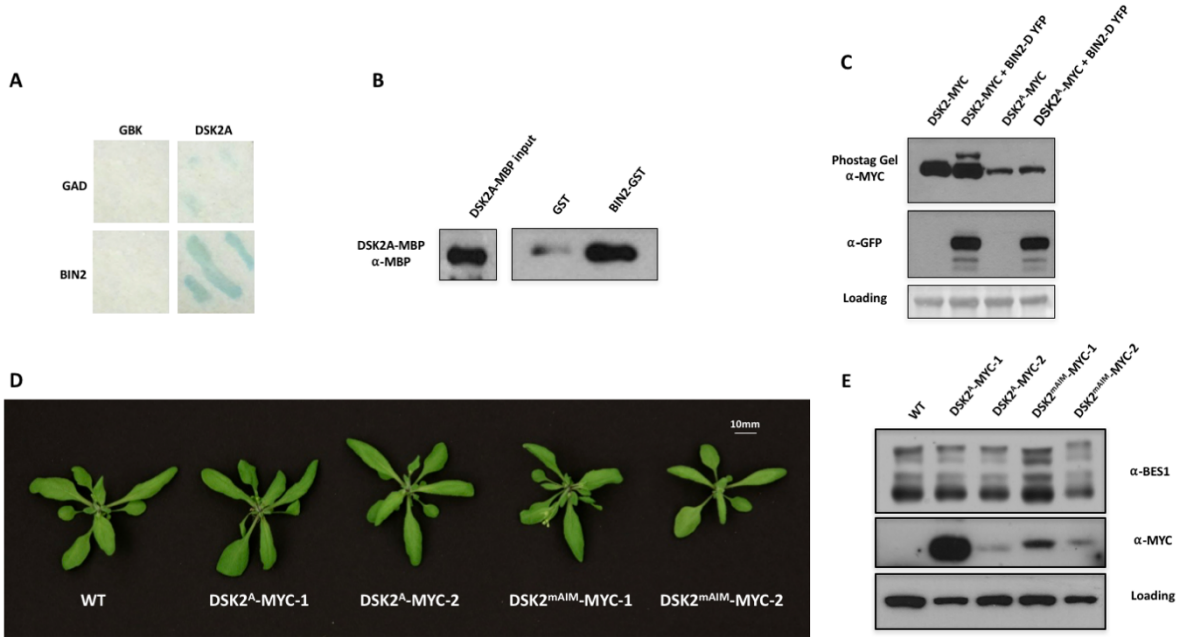

Figure S4, related to Figure 4. Interaction and phosphorylation of DSK2 by BIN2.
(A) Interaction of DSK2A with BIN2 in yeast-two hybrid LacZ assays. (B) GST pulldown showing interaction of DSK2A-MBP with BIN2-GST. DSK2A-MBP was detected using anti-MBP antibody. (C) Phosphorylation of DSK2 upon coexpression with BIN2 in *N. benthamiana.* DSK2-MYC or DSK2^{A}-MYC (with predicted BIN2 phosphorylation sites mutated to Ala) was co-expressed with empty vector control or with BIN2-D YFP. After 48 hours, protein was extracted and analyzed by SDS-PAGE using anti-GFP antibodies to detect BIN2-YFP or by Phostag SDS-PAGE with anti-MYC antibodies to detect DSK2-MYC fusion proteins. (D) Phenotype T2 transgenic lines overexpressing DSK2 mutant forms shown in Figure 1D. (E) BES1 protein levels in DSK2-MYC lines. Protein extracts from indicated lines were analyzed by western blotting. DSK2-MYC mutant forms were detected with anti-MYC antibodies, while BES1 was detected with anti-BES1. A non-specific band from anti-MYC was used as a loading control.

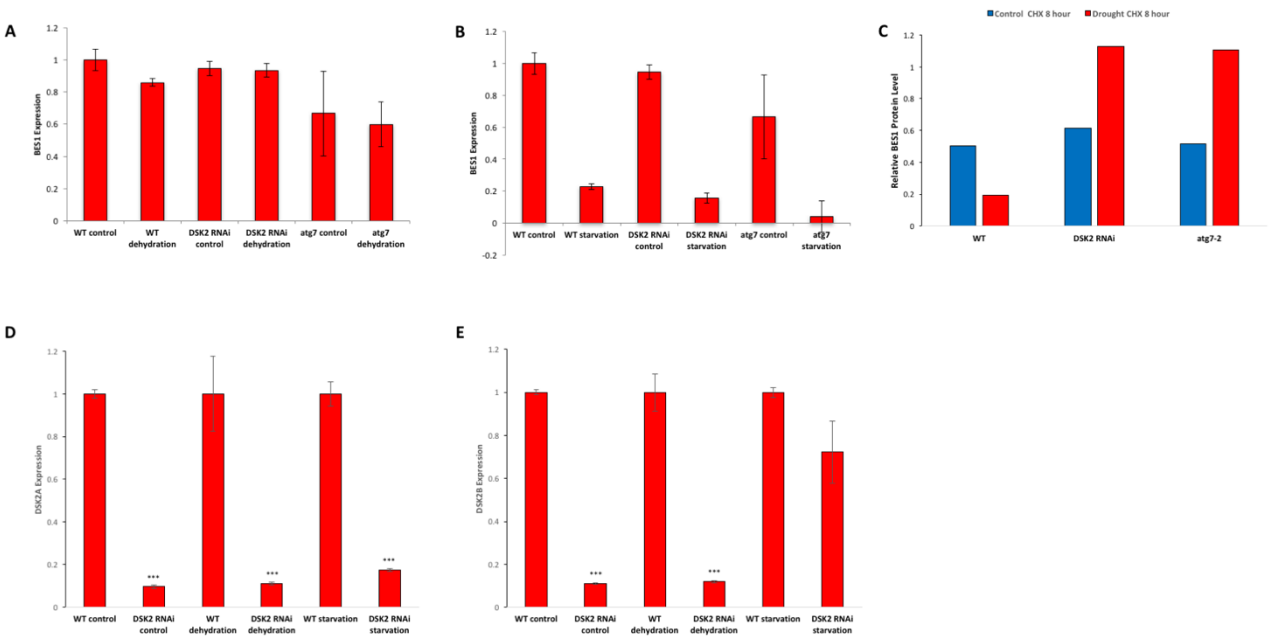

Figure S5, Related to Figure 5. BES1 transcript levels during stress treatments.
(A) BES1 transcript levels during dehydration treatments as monitored by whole transcriptome RNA-seq. (B) BES1 transcript during starvation treatments as monitored by whole transcriptome RNA-seq. (C) Quantification of BES1 protein levels from cycloheximide (CHX) treatments shown in Figure 5D. Relative BES1 level is defined as BES1 after 8hr CHX treatment/BES1 at 0 hr. (D) DSK2A transcript levels during control and indicated stress treatments as monitored by whole transcriptome RNA-seq. (E) DSK2B transcript levels during Itrol and indicated stress treatments as monitored by whole transcriptome RNA-seq. All error bars in this figure indicate SEM (***, $p<0.001$, t test).

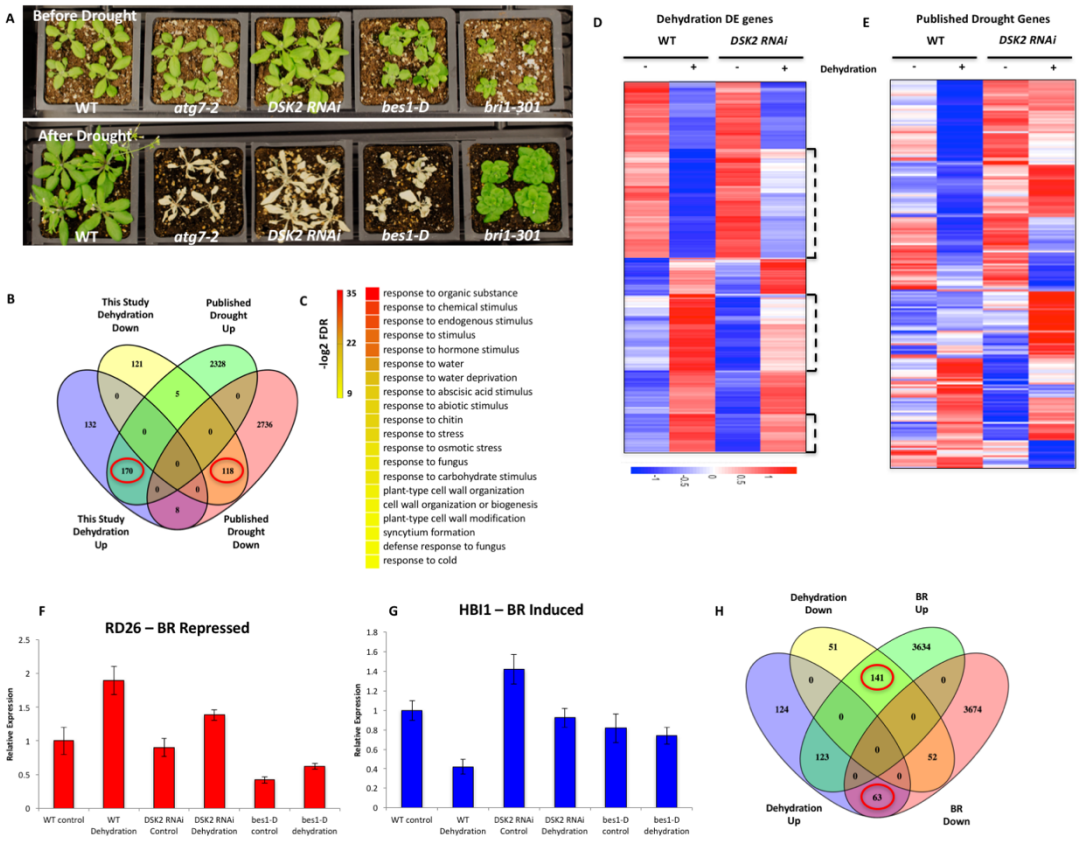

Figure S6, related to Figure 5. Phenotypic and transcriptome changes during drought or dehydration stress.

(A) Additional drought phenotype images from drought assay described in Figure 6A. Plants were imaged before significant drought stress was imposed (Before Drought) followed by drought treatment and rewatering. Plants were imaged again 7 days subsequent to rewatering (After Rewatering). (B) Comparison of RNA-seq dehydration regulated genes to previously published drought regulated genes. (C) Top 20 significantly enriched GO terms in Dehydration regulated genes as ranked by false discovery rate (FDR). (D) Clustering analysis of 554 genes DE during WT dehydration treatments. Brackets indicate clusters of genes with altered expression patterns in *DSK2 RNAi* plants. (E) Clustering of 5,365 genes previlly implicated in drought response using dehydration RNA-seq data from this study. Color legend indicates normalized gene expression values. (F) Expression levels of RD26 from RNA-seq experiments. RD26 is a known dehydration induced gene that is down regulated in *DSK2 RNAi* and *bes1-D* during compared to WT dehydration. Error bars indicate SEM. (G) Expression levels of HBI1 from RNA-seq experiments. HBI1 is a positive regulator in growth that is downregulated during dehydration in WT, but not in *DSK2 RNAi* and *bes1-D.* Error bars indicate SEM. (H) Overlap of dehydration DE genes with Brassinosteroid (BR) regulated genes showing enrichment of dehydration down regulated genes that were upregulated by BRs (57.8%, 141/244) and dehydration upregulated genes that were downregulated by BRs (20.3%, 63/310).

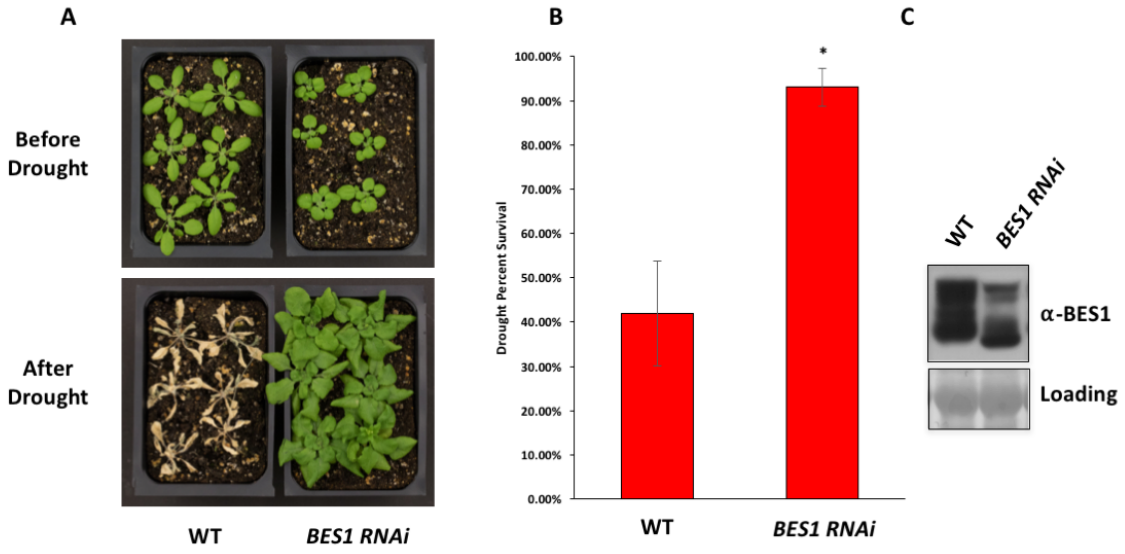

Figure S7, related to Figure 5. Drought phenotype of BES1 RNAi plants.
(A) Phenotype of *BES1 RNAi* during drought stress. Plants were imaged before significant drought stress was imposed (Before Drought) followed by drought treatment and rewatering. Plants were imaged again 7 days subsequent to rewatering (After Rewatering). (B) Quantification of percent survival following drought recovery. Plants producing new leaves after the 7-day recovery period were scored as survivors. Data represent mean survival of 3 biological replicates of at least 12 plants ± SEM, (*$p < 0.05$, t test). (C) BES1 protein levels are reduced in *BES1 RNAi* plants as monitored by western blotting with anti-BES1 antibody.

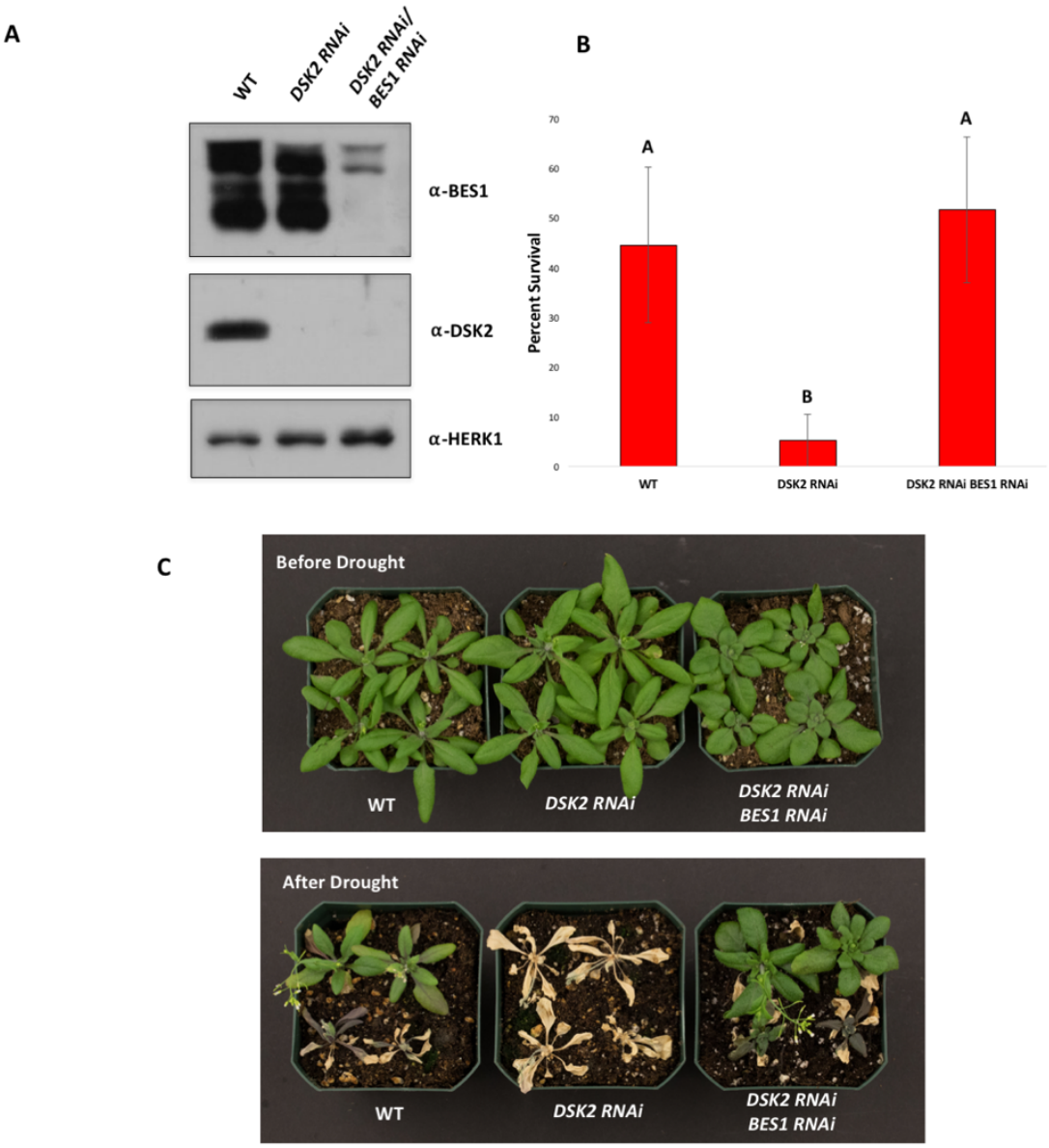

Figure S8, related to Figure 5. The drought phenotype of *DSK2 RNAi* can be reversed by knockdown of BES1.

(A) Both BES1 and DSK2 protein levels are reduced in *DSK2 RNAi BES1 RNAi* plants. (B) Quantification of percent survival following drought recovery. Plants producing new leaves after the 7-day recovery period were scored as survivors. Data represent mean survival of 3 biological replicates of at least 8 plants ± SEM. Different letters indicate statistically significant differences $p<0.05$, t test. (C) Drought stress phenotypes of *DSIRNAi* and *DSK2 RNAi BES1 RNAi* double mutants. Plants were imaged before significant drought stress was imposed (Before Drought) followed by drought treatment and rewatering. Plants were imaged again 7 days subsequent to rewatering (After Rewatering).

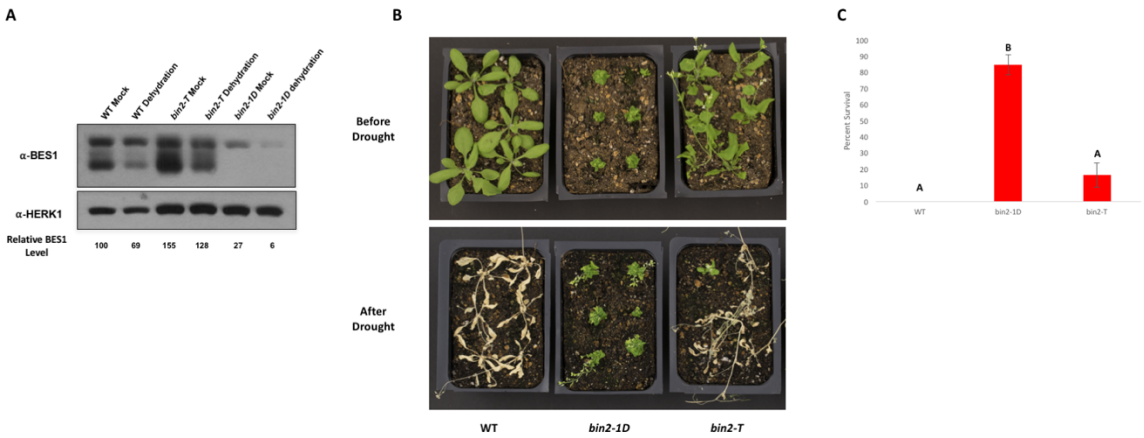

Figure S9, related to Figure 5. Effect of BIN2 on BES1 protein levels and drought stress phenotypes.

(A) BES1 protein levels in *bin2* gain-of-function (*bin2-1D)* and loss-of-function (*bin2-T)* mutants during dehydration treatments. Plants were subjected to control or 4-hour dehydration conditions and BES1 levels analyzed by western blotting. HERK1 was used as a loading control. (B) Drought stress phenotypes of *bin2* mutants. Plants were imaged before significant drought stress was imposed (Before Drought) followed by drought treatment and rewatering. Plants were imaged again 7 days subsequent to rewatering (After Rewatering). (C) Quantification of percent survival following drought recovery. Plants producing new leaves after the 7-day recovery period were scored as survivors. Data represent mean survival of 3 biological replicates of at least 10 plants ± SEM. Different letters indicate statistically significant differences $p<0.05$, t test.

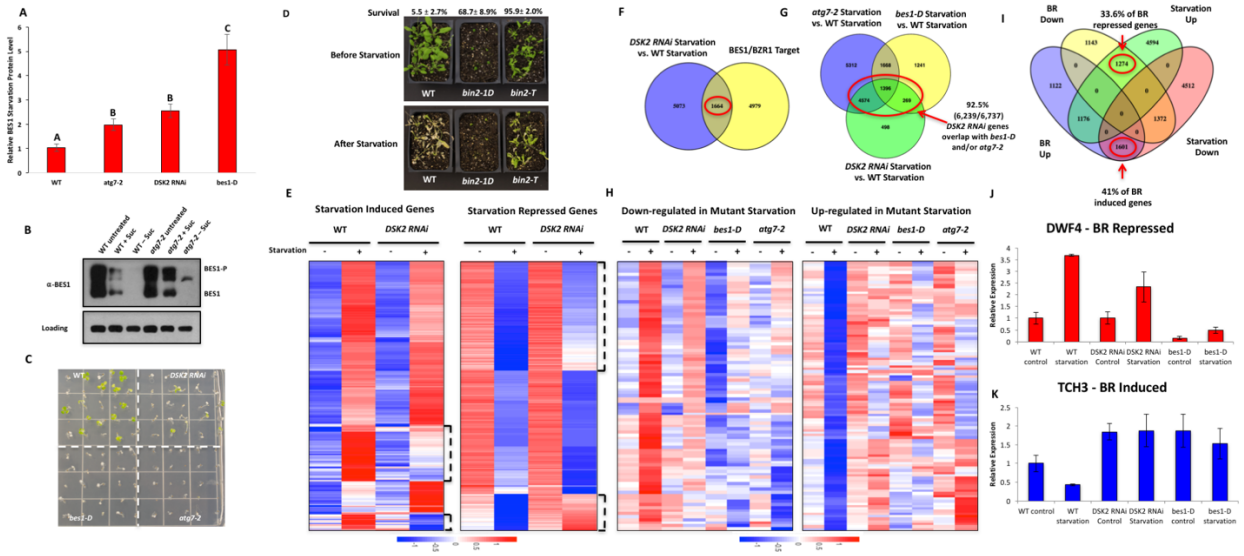

Figure S10, related to Figure 6. Phenotypic and transcriptome changes during starvation stress.

(A) Quantification of BES1 protein levels during starvation as shown in Figure 6C. Data represent mean BES1 protein level ± SEM from 3 biological replicates (for WT, *atg7-2* and *DSK2 RNAi*) or 2 biological replicates (*bes1-D*). Different letters indicate statistically significant differences $p<0.05$, t test. (B) BES1 protein levels are regulated by energy availability in dark conditions. Protein samples were collected from 7 day-old WT or *atg7-2* seedlings that were untreated or transferred to plates with (+ Suc) or without sucrose (-Suc) and incubated in darkness for three days. Western blotting was performed with anti-BES1 antibodies or anti-HERK1 (loading control). (C) Representative image showing fixed-carbon starvation survival phenotypes after 10 days darkness as presented in Figure 7B. (D) Phenotypes of *bin2* mutants after starvation stress. Representative images of plant survival following 9 day fixed-carbon starvation treatment. Percentage survival is indicated from 3 biological repeats of at least 12 plants ± SEM. Differences between WT and mutants are statistically significant $p<0.05$ (t test). (E) Clustering of 7044 starvation ulgulated genes (left panel) or 7485 starvation downregulated genes (right panel). Brackets indicate clusters of genes with altered expression patterns in *DSK2 RNAi* plants. (F) Comparison of *DSK2 RNAi* starvation DE genes with BES1/BZR1 target genes. (G) Overlap of genes DE in *atg7-2, bes1-D,* or *DSK2 RNAi* starvation compared to WT starvation. (H) Clustering of 89 genes upregulated during starvation but downregulated in *DSK2 RNAi, bes1-D,* and *atg7-2* starvation (left panel) or 106 genes downregulated during starvation but upregulated in *DSK2 RNAi, bes1-D,* and *atg7-2* starvation (right panel). (I) Comparison of starvation DE genes with Brassinosteroid (BR) regulated genes. (J) Expression levels of DWF4 from RNA-seq experiments. Error bars indicate SEM. (K) Expression levels of TCH3 from RNA-seq experiments. Error bars indicate SEM.

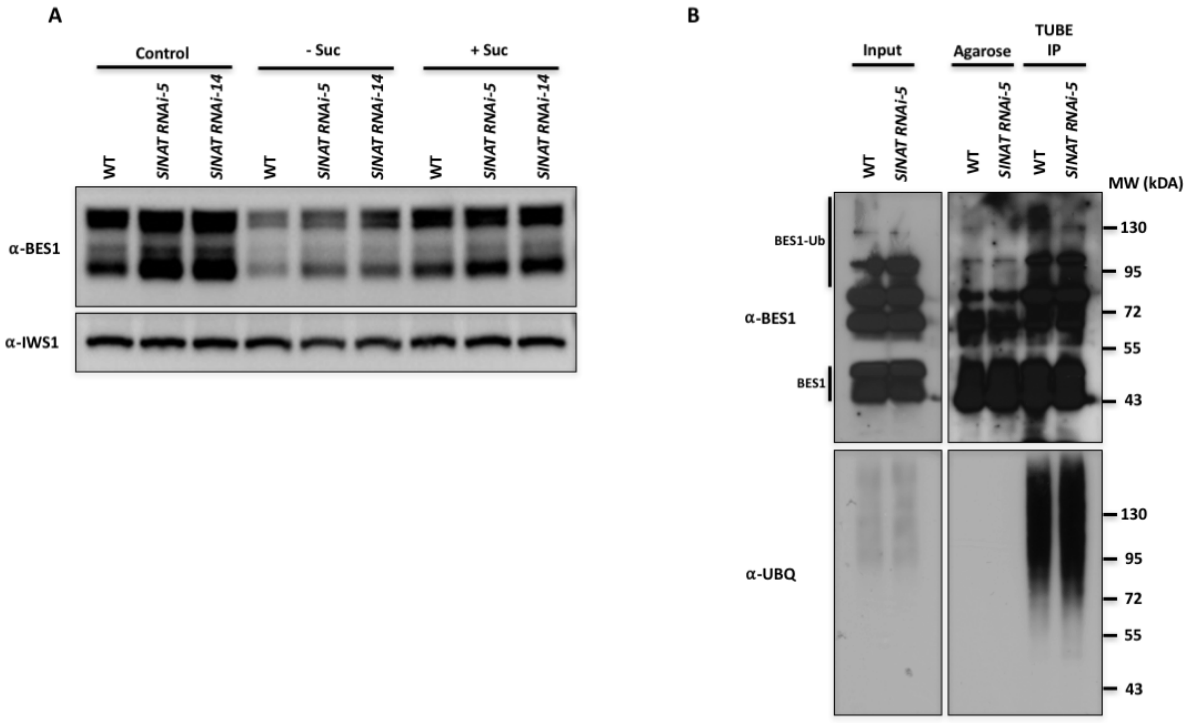

Figure S11, related to Figure 7. Effect of *SINAT RNAi* on BES1 accumulation and ubiquitination in during starvation.

(A) Western blot analysis of BES1 protein levels from 10-day seedlings in WT and two independent *SINAT RNAi* lines. Plants were harvested directly after 10 days of growth (Control) or transferred to plates without sucrose (-Suc) or with sucrose (+Suc) and incubated for 3 days in darkness. IWS1 served as a loading control. (B) Ubiquitinated BES1 is reduced in *SINAT RNAi* during starvation. Tandem Ubiquitin Binding Entities (TUBE) ubiquitination assays were performed with 10-day old WT or *SINAT RNAi* seedlings treated with – sucrose and 20μM E64d in darkness for 24 hours. Input, control (Agarose) and ubiquitin enriched (TUBE IP) samples were analyzed by western blotting with BES1 and Ubiquitin (UBQ) antibodies.

Table S1, related to Figure 4. DSK2 phosphorylation sites identified by mass spectrometry following *in vitro* phosphorylation with BIN2.

Phosphorylation sites flanking DSK2 AIM domains are bold. When phosphorylation sites could not be localized due to peptide fragmentation patterns, all possible residues are listed. Number of phosphorylated residues indicates sites detected within a single peptide. No phosphorylation was detected in mock DSK2 phosphorylation reactions lacking BIN2. For complete output of DSK2 mass spectrometry data see Table S2.

DSK2 Phosphorylation Site(s)	Number of Phosphorylated Residues	Peptide Sequence
S7	1	(2)GGEADsRQPLTAEGVAVAVNVR (23)
T12	1	(9)QPLtAEGVAVAVNVR(23)
S7 or T12 or T28 or S31 or T33 or T34 or S35 or S38 or T39	**4**	**(5)ADSRQPLTAEGVAVAVNVRCS NGTKFSVTTSLDSTVE(41)**
S31 or T33 or T34 or S35 or S38 or T39 or S42	**1**	**(30)FSVTTSLDSTVESFK(44)**
T172	1	(168)EMMNTPAIQNLMNNPEFM R(186)
S213	1	(197)ELVDRNPELGHVLNDPSILR(2 16)
S213 or T218	1	(205)LGHVLNDPSILRQTLE(220)
S240	**1**	**(238)AMSNIESMPEGFNMLR(253)**
S244	**1**	**(238)AMSNIESMPEGFNMLR(253)**
S425 or S426	1	(414)MMQNPDFLRQFSSPE(428)
S425 or S426 or S435 or S439 or S442	1	(423)QFSSPEMMQQMMSLQQSLFS QNR(445)
T447 or T453 or T455 or T459 or T461 or S476 or S483 or T485	3	(446)NTAGQDPTQTGAATGTANN GGLDLLMNMFGSLGAGGLSGTNQ PNVPPEER(495)
T521	1	(514)NIRALLAtNGNVNAAVE(530)

Table S2: DSK2 mass spectrometry Spectrum Mill output.
Table S3: Differentially expressed gene lists from RNA-seq experiments.
Table S4: Summary of DSK2A variants used in this study.

Construct	Phosphorylation site mutations	AIM mutations	Region
DSK2^{D}	S31D T34D S35D S38D T39D S42D S114D S118D S240D S244D T292D S296D S299D S303D T324D T328D T362D S366D S435D S439D T455D T459D	None	Full Length 1-538
DSK2^{A}	S31A T34A S35A S38A T39A S42A S114A S118A S240A S244A T292A S296A S299A S303A T324A T328A T362A S366A S435A S439A T455A T459A	None	Full Length 1-538
DSK2^{A} mAIM	S31A T34A S35A S38A T39A S42A S114A S118A S240A S244A T292A S296A S299A S303A T324A T328A T362A S366A S435A S439A T455A T459A	F43A L46A F249A L252A Y256A V259A	Full Length 1-538
DSK2 mAIM	None	F43A L46A F249A L252A Y256A V259A	Full Length 1-538
DSK2^{D12}	S31D T34D S35D S38D T39D S42D S114D S118D S240D S244D	None	Full Length 1-538
DSK2^{A12}	S31A T34A S35A S38A T39A S42A S114A S118A S240A S244A	None	Full Length 1-538
DSK2 C1	None	None	90-538
DSK2 C2	None	None	403-538
DSK2AΔUBA	None	None	1-497

Table S5: Oligonucleotides used in this study.

Oligo Name	Sequence
DSK2AF	CACCGAATTCGGTACCATGGGTGGTGAAGCAGATTCGAGG
DSK2AR	CACCGTCGACCTGGCCAATACTCCCCAAGAGTCGT
DSK2AGSTF	CACGAATTCATGGGTGGTGAAGCAGATTCGAGG
DSK2AGSTR	CACGTCGACTTACTGGCCAATACTCCCCAAGA
DSK2AC1F	CACCGAATTCTTTGTGCCTTCTTCTCCTTCTGCTCC
DSK2AC2F	CACCGAATTCAGCATGCTAGATATGAATCCTCAGT
DSK2AUBAdel	CACCGTCGACCGCAAATCGCTCTTCAGGAGGAACA
DSK2BGSTF	CACCGAATTCATGGGTGGAGAGGGAGATTCAAGTCA
DSK2GSTR	CACCGTCGACCTACTGTCCGATACTCCCCAAGA
ATG8aF	CACCGGATCCATGATCTTTGCTTGCTTGAAATTCGCA
ATG8aR	CACCGTCGACTCAAGCAACGGTAAGAGATCCAAAAGT
ATG8eGSTF	CACCGGATCCATGAATAAAGGAAGCATCTTTAAGATGGACA
ATG8eGSTR	CACCGCGGCCGCTTAGATTGAAGAAGCACCGAATGT
ATG8fF	CACCGAATTCATGGCAAAAAGCTCGTTCAAGCAAGA
ATG8fR	CACCGTCGACTTATGGAGATCCAAATCCAAATGTGT
ATG8iF	CACCGAATTCATGAAATCGTTCAAGGAACAATACACGT
ATG8iR	CACCGTCGACTCAACCAAAGGTTTTCTCACTGCTA
BIN2F	CACCGGATCCACCATGGCTGATGATAAGGAGATGCCTGC
BIN2R	CACCGTCGACTTAAGTTCCAGATTGATTCAAGAAGCT

CHAPTER 3

NETWORK-BASED DISCOVERY OF BRASSINOSTEROID REGULATION OF PLANT GROWTH AND STRESS RESPONSES IN ARABIDOPSIS

Trevor M. Nolan[1], Sriram Chockalingam[2], Lirong Xiang[3], Zaki Jubery[4], Mathew G. Lewsey[5], Nicole Huser[1], Sean McLaughlin[1], Ashley Hurd[1], Zhouli Xie[1], Hongqing Guo[1], Hao Jiang[1], Yin Bao[3], Taylor Tuel[3], Hung-Ying Lin[6], Dior Kelley[1], Ping Wang[1], Adedotun Akintayo[4], Shruti Shivakumar[2], Hyeongseon Jeon[6], Maneesha Aluru[7], Dan Nettleton[6], Soumik Sarkar[4], Baskar Ganapathysubramanian[4], Diane C. Bassham[1], Patrick S. Schnable[8], Justin W. Walley[9], Joseph R. Ecker[10], Lie Tang[3], Srinivas Aluru[2], and Yanhai Yin[1]

[1]Department of Genetics, Development and Cell Biology, Iowa State University.

[2]School of Computational Science and Engineering, Georgia Institute of Technology.

[3]Department of Agriculture and Biosystems Engineering, Iowa State University.

[4]Department of Mechanical Engineering, Iowa State University. [5]Centre for AgriBioscience, La Trobe University, Bundoora, Vic., Australia.

[6]Deparement of Statistics, Iowa State University.

[7]School of Biology, Georgia Institute of Technology.

[8]Department of Agronomy, Iowa State University.

[9]Department of Plant Pathology and Microbiology, Iowa State University.

[10]Howard Hughes Medical Institute and The Salk Institute for Biological Studies La Jolla, CA.

3.1 Abstract

Understanding gene regulatory networks (GRNs) that control plant growth and stress responses is essential to optimize plant growth in an ever-changing environment. Brassinosteroids (BRs) regulate plant growth and stress responses, including that of drought. BRs signal to regulate the activities of the BES1 and BZR1 (BES1/BZR1) family transcription factors (TFs), which in turn mediate the expression of more than 5,000 BR-responsive genes. To understand how BES1/BZR1 regulate the large number of BR targets we used genome-wide chromatin immunoprecipitation (ChIP), transcriptome and TF interactome datasets to identify 657 BR-related Transcription Factors (BR-TFs). We then took an integrated approach involving computational modeling, phenomics and functional genomics to study the networks through which BRs, BES1/BZR1 and BR-TFs function. First, we built comprehensive GRNs using 11,760 publicly available microarray datasets. BR-TFs are significantly enriched for BR and drought target genes in the GRNs, suggesting they function in growth and drought responses. We prioritized BR-TFs for functional studies using Network Essentiality Scoring Tool (NEST). Next, we optimized BR response assays to conduct BR phenomics experiments for over 300 BR-TFs using more than 1000 knockout or overexpression lines. These studies identified numerous BR-TF mutants that displayed altered BR responses, allowing us to characterize the function of PLATZ and ARID-HMG1 as A/T-rich binding TFs which oppositely regulate BR-responsive gene expression. Finally, our BR and drought phenomics experiments in soil-grown plants revealed that *tcp11* mutants have increased BR-regulated growth and increased survival during drought. These studies provide a paradigm for network-based discovery

and characterization of hormone response pathways through the integration of omics data, network analysis and phenomics.

3.2 Introduction

Brassinosteroids (BRs) are a group of plant steroid hormones that play key roles in growth, stress responses and various developmental processes (Clouse et al., 1996; Li et al., 1996; Noguchi et al., 1999; Szekeres et al., 1996). The molecular determinants of BR signaling have been traced from the plasma membrane localized receptor BRI1 (BRASSINOSTEROID INSENSITIVE 1) and co-receptor BAK1 (BRI1 ASSOCIATED KINASE 1) to downstream BES1 (BRI1-EMS-SUPPRESSOR1) and BZR1 (BRASSINAZOLE-RESISTANT 1) family transcription factors (TFs) (Cano-Delgado et al., 2004; Clouse, 2011; Clouse et al., 1996; Gou et al., 2012; He et al., 2005; He et al., 2002; Kim et al., 2009; Li et al., 2002; Li and Chory, 1997; Nam and Li, 2002; Wang et al., 2002; Yin et al., 2005; Yin et al., 2002). In the presence of BRs a series of signal transduction steps inactivates the negative acting kinase BIN2 (BRASSINOSTEORID INSENSITIVE 2) (Kim et al., 2009), allowing PP2A (PROTEIN PHOSPHATASE 2A) to dephosphorylate BES1 and BZR1 (Tang et al., 2011). Dephosphorylated BES1 and BZR1 function with a variety of other co-factors and TFs in the nucleus to mediate the expression of 5,000-8,000 BR-responsive genes (Guo et al., 2013; Nolan et al., 2017c).

TF-target interactions form the basis for gene regulatory networks (GRNs) that control gene expression. The underlying GRN that allows BRs to control thousands of genes is a major topic in the BR field. Several studies have analyzed BR-responsive gene expression, beginning to reveal how BES1 and BZR1 modulate the BR-regulated transcriptional network (Guo et al., 2013; Sun et al., 2010; Yu et al., 2011). Genome-

wide chromatin immunoprecipitation (ChIP) identified thousands of genes directly bound by BES1 and/or BZR1, including many BR-regulated genes and TFs (Sun et al., 2010; Yu et al., 2011). This suggests that BES1 and BZR1 propagate BR signals by regulating downstream TFs. Indeed, a number of TFs involved in BR responses have been identified and individually characterized. Many of these TFs are transcriptionally regulated by BES1 and/or BZR1 and also physically interact with BES1/BZR1 to carry out BR-regulated gene expression (Guo et al., 2013; Li et al., 2010). These include positive regulators that cooperate with BES1 and BZR1 such as BIM1 (Yin et al., 2005), MYB30 (Li et al., 2009a), MYBL2 (Ye et al., 2012), PIF4 (Oh et al., 2012), and ARF6 (Oh et al., 2014), as well as negative regulators that function oppositely to BES1. For example, BES1 and BRAVO function in an antagonistic manner to control QC cell division in the stem cell niche (Vilarrasa-Blasi et al., 2014) and reciprocal inhibition between BES1 and RD26 balance BR-regulated growth and drought responses (Ye et al., 2017). Thus, there is accumulating evidence that BES1 and BZR1 interface with many other TFs to regulate target gene expression and promote BR-mediated growth responses. These interactions provide clues as to how BES1/BZR1 regulate a large number of BR-responsive genes; however, systems level approaches including predictive modeling of BR networks and large-scale characterization of TFs in the BR pathway are needed to gain a more complete understanding of how BES1 and BZR1 direct the transcriptional network controlling thousands of BR-regulated genes.

In addition to regulating growth, the BRs pathway has extensive crosstalk with drought stress responses (Nolan et al., 2017a). Recent studies have shown that BR and drought response pathways antagonize one another through several mechanisms.

Under growth promoting conditions, BES1 inhibits the drought-induced TF RD26 (Ye et al., 2017) and cooperates with several WRKY TFs including WRKY54 to promote growth and restrain drought responses (Chen et al., 2017). Conversely, when drought stress is encountered BES1 is degraded by selective autophagy (Nolan et al., 2017c) and BES1 activity on target gene promoters is inhibited through interaction of BES1 with RD26 (Ye et al., 2017). Despite these mechanisms for BR-drought antagonism, there are over 900 genes that are regulated by BRs and drought in the same direction (Ye et al., 2017), suggesting it may be possible to identify factors that promote both BR and drought responses.

In this study we leverage omics data including genome-wide ChIP, transcriptome and TF interactome datasets to identify TFs involved in BR signaling. We then use 11,760 categorized transcriptome datasets to construct GRNs and prioritize TFs predicted to be crucial for BR responses. Next, we test the network predictions through the use of high-throughput BR phenomics assays conducted with over 1,000 knockout or overexpression lines spanning 300 TFs. We characterize the function of two A/T-rich binding TFs – PLATZ and ARID-HMG1 – that oppositely regulate BR-responsive gene expression by interacting with BES1 and numerous other TFs. Finally, we develop BR and drought phenomics assays for soil-grown plants using time-lapse imaging and a fully-automated robotic platform. These systems reveal that *tcp11* mutants have increased BR-regulated growth accompanied by increased survival during drought rather than drought susceptibility that is typically observed for plants with increased BR-regulated growth (Ye et al., 2017). Our studies provide a paradigm for the

characterization of hormone response pathways through the integration of genomics, network analysis and phenomics.

3.3 Results and Discussion

3.3.1 BES1 and BZR1 direct a transcriptional network for BR responses

Global gene expression studies demonstrated that BRs can regulate 5,000-8,000 genes under different growth stages and conditions (Guo et al., 2013; Nolan et al., 2017b; Nolan et al., 2017c; Wang et al., 2014; Ye et al., 2017). To identify additional TFs regulated by BRs and BES1/BZR1, we compiled BES1 and BZR1 target genes identified by genome-wide ChIP studies (Oh et al., 2014; Sun et al., 2010; Yu et al., 2011) which indicated that 10,858 genes are direct BES1 or BZR1 targets (BES1/BZR1 Target genes, Table S1). To verify the BES1/BZR1 ChIP-targets, we generated BES1-YPet lines through recombineering (Alonso and Stepanova, 2015) and performed ChIP-seq with 3-day-old BES1-YPet etiolated seedlings. These ChIP experiments had significant overlap with previously identified BES1 or BZR1 targets, including BES1 target TFs such as HAT1 (HOMEOBOX ARABIDOPSIS THALIANA 1, Figure 1A). We previously identified 7,687 genes that can be regulated by BRs from microarray and/or RNA-sequencing (RNA-seq) transcriptome datasets (Nolan et al., 2017c). BES1/BZR1 target genes include 4,047 BR-regulated genes (Figure S1A) and 535 BR-regulated BES1/BZR1 target TFs (BTFs, Figure 1B). Of the 535 BTFs, 265 BTFs are induced and 270 BTFs repressed by BRs, respectively (Figure S1B).

BES1 and BZR1 also physically interact with other TFs to regulate target gene expression (Guo et al., 2013; Li et al., 2010; Li et al., 2009a; Nolan et al., 2017a; Ye et

al., 2012; Ye et al., 2017; Zhang et al., 2014). To further our understanding of this level of gene regulation in the BR pathway, we performed pairwise yeast-two hybrid (Y2H) screening with BES1 against a library of 1956 TFs (Pruneda-Paz et al., 2014) and identified 129 putative BES1 interacting TFs (Table S2). The BES1 interacting TFs identified by Y2H include several families known to interact with BES1 such as MYB (Li et al., 2009a), WRKY (Chen et al., 2017) and NACs, including RD26, which physically interacts with BES1 by binding a common promoter element on BR-responsive genes (Ye et al., 2017). Combined with publicly available interaction data from BioGrid and the Arabidopsis TF interactome (Trigg et al., 2017), we identified a total of 169 putative BES1 or BZR1 interacting TFs (BES1/BZR1 interacting TFs, Figure 1C and Table S2). Consistent with a role in the BR pathway, BES1/BZR1 interacting TFs are enriched for BES1/BZR1 target genes (Figure S1C, 53.8%, 91/169 TFs, p-value: 1.19e-04, Fisher's exact test) as well as BR regulated genes (Figure S1D, 39.0%, 66/169 TFs, p-value: 1.25e-03, Fisher's exact test). By combining BTFs and BES1/BZR1 interacting TFs we identified a total of 657 BR-related TFs (BR-TFs, Table S3). Together with BES1 and BZR1, these BR-TFs likely function to allow BRs to modulate the expression of thousands of BR-regulated genes (Figure 1D).

We examined regulation of *BR-TFs* through clustering and comparisons of genes differentially expressed in gain-of-function *bes1-D* or *bzr1-1D* mutants (Bai et al., 2012a; Chen et al., 2017; Nolan et al., 2017c; Sun et al., 2010; Tian et al., 2018; Wang et al., 2014; Yu et al., 2011). These analyses indicated that there is significant overlap between *BR-TFs* and genes differentially expressed in *bes1-D* or *bzr1-1D* and that the direction of regulation of *BR-TFs* by BRs and BES1/BZR1 is similar (Figure S1E). Given

that BRs have been implicated in drought stress responses (Nolan et al., 2017a), we investigated if *BR-TFs* are regulated by drought. *BR-TFs* showed significant overlap with drought responsive genes (Maruyama et al., 2009) with 113 *BR-TFs* induced by drought (Figure S1F, p-value 3.22e-11, Fisher's exact test) and 97 *BR-TFs* repressed by drought (Figure S1F, p-value 1.54e-6, Fisher's exact test). We also examined the patterns of *BR-TF* regulation in response to a time-course drought treatment in both roots and shoots (Rasheed et al., 2016). Clustering analysis showed that both BR induced and BR repressed *BR-TFs* respond to drought; however, we observed a tendency for antagonism between BR and drought regulation. Specifically, a larger proportion of BR induced *BR-TFs* were repressed by drought whereas BR repressed *BR-TFs* showed increased expression in response to drought (Figure 1E and S1E). These results are consistent with an antagonistic relationship between BRs and drought (Chen et al., 2017; Nolan et al., 2017c; Ye et al., 2017) which includes reciprocal inhibition between BES1 and RD26 (Ye et al., 2017). These data also point towards complex regulation between BR and drought. Some *BR-TFs* are induced or repressed by both BRs and drought in the same direction, indicating that it may be possible to identify factors that simultaneously affect BR and drought responses in a positive manner. Together, our data suggest that BES1 and BZR1 interface with a complex network of TFs through both transcriptional regulation and protein-protein interactions.

3.3.2 Construction of GRNs based on 11,760 transcriptome datasets

In order to investigate the relationship between BES1/BZR1 and BR-TFs in regulating BR-responsive gene expression we constructed GRNs, which consist of interactions between TFs and target genes. We collected 13,386 non-redundant

Affymetrix ATH1 expression profiles from various public microarray databases. After removal of duplicate entries, manual inspection of the CEL files and quality control analyses (Aluru et al., 2013), 11,760 CEL files remained for construction of gene regulatory networks (Figure 2A). The datasets were further classified into 12 categories - 5 tissue (Flower, Leaf, Root, Seedling, Whole Plant) and 7 biological process (Chemical, Development, Hormone, Light, Metabolism, Pathogen, Stress) functional categories (Chockalingam et al., 2016). This process of categorization was necessary to see the dynamic range of interactions between all genes in the genome and to compute biologically relevant gene-gene coexpression (Chockalingam et al., 2016; Chockalingam et al., 2017). We considered 2,492 Arabidopsis TFs (Pruneda-Paz et al., 2014) as potential regulators for GRN reconstruction, 1,915 of which were present in the transcriptome datasets. We applied three different inference methods - Tool for Inferring Networks of Genes (TINGe) (Aluru et al., 2013; Chockalingam et al., 2017), Gene Network Inference with Ensemble of trees (GENIE3) (Huynh-Thu et al., 2010) and GRNBoost (Aibar et al., 2017) to first reconstruct separate networks for each tissue and biological process following which, a union network was constructed for each method by considering the maximum edge weight from all 12 networks (Figure 2B).

To evaluate the predictive power of the GRNs generated we constructed receiver operating characteristic (ROC) and precision-versus-recall (PR) curves using seven benchmark reference network datasets and calculated area under the ROC curve (AUROC) and area under the PR curve (AUPR) (Table S4). The benchmark datasets used include TF binding data from DNA affinity purification sequencing (DAP-seq) (Bartlett et al., 2017; O'Malley et al., 2016), ChIP-seq (Kulkarni et al., 2017; Song et al.,

2016a) or yeast one-hybrid (Y1H) assays (Li et al., 2014; Shani et al., 2017; Sparks et al., 2016; Taylor-Teeples et al., 2015). We also included benchmark datasets described along with the TF2Network algorithm (Kulkarni et al., 2017) that predicts potential regulators for gene sets using TF binding site information. These additional validation datasets consist of genes bound in ChIP assays (TF2N ChIP) or differentially expressed upon TF perturbation (TF2N DE). Additionally, we reanalyzed expression quantitative trait loci (eQTL) for BR-responsive genes using RNA-seq data from the Arabidopsis 1001 genomes project (Kawakatsu et al., 2016). Finally, we identified 5022 RD26 target genes that are bound in ChIP-seq and regulated upon *RD26* overexpression in RNA-seq experiments (Nolan et al., 2017a; Song et al., 2016a; Ye et al., 2017).

The network validation results showed the utility of constructing union networks, which retain the highest edge-weight from each of the 5 tissue and 7 process specific networks. Union networks had the highest AUROC in 4 out of 7 validation datasets (Table 1), indicating that union networks often perform favorably. Among the GRN reconstruction methods used, TINGe had the highest AUROC for 5 out of 7 validation datasets (Table 1). These observations suggest that the TINGe union network performs well with our validation datasets. Next, we focused on RD26 as a specific example since both ChIP-seq and RNA-seq data are available for this TF. NAC family TFs, including RD26 are involved in plant responses to various stresses including drought, heat and bacterial infection (Bu et al., 2008; Chung et al., 2014; Fujita et al., 2004; Guan et al., 2014; Nakashima et al., 2012; Tran et al., 2004; Zheng et al., 2012). First, we compared AUROC and AUPR for the RD26 validation dataset using the full union networks for each GRN reconstruction method. The TINGe union network had an AUROC of 0.719

(Figure 2C-E) whereas GRNBoost and GENIE3 had AUROC of 0.681 and 0.658, respectively. TINGe also performed best in terms of RD26 AUPR (Figure 2D). Comparison across the 39 networks (union network, 5 tissue and 7 process specific networks for each GRN construction method) revealed that TINGe union had the highest performance for RD26 AUROC (Figure S2A, top). In contrast, the GRNBoost hormone subnetwork had the highest AUPR for RD26 (Figure S2A, bottom), consistent with the previously described role of RD26 in hormone responses (Song et al., 2016a; Ye and al., 2017). Given the advantageous performance of the TINGe union network we chose to focus on this network for subsequent analysis.

We recently showed that RD26 functions in a partially redundant manner with several related TFs including NAC019, NAC055 and NAC102 (Ye and al., 2017). Therefore, we constructed a subnetwork with RD26, NAC019, NAC055 and NAC102, which shows that these BR-TFs are connected to 1,394 genes in the network including many BR and drought regulated genes (Fig 2F-G). Our genetic and genomic studies demonstrated that RD26 and its close homologs inhibit BR-regulated plant growth, representing an important crosstalk point between BR and drought response pathways (Ye et al., 2017). Comparison of the RD26 subnetwork to *RD26OX* RNA-seq (Ye et al., 2017) or RD26 ChIP-seq (Song et al., 2016a) datasets revealed that 1,122/1394 (80.5%, p-value: 4.01e-77, Fisher's exact test) of the genes in the RD26 subnetwork are indeed bound and/or regulated by RD26 (Figure 2G). Next, we expanded our analysis to 21 ABA-related TFs that were profiled for genome-wide binding events via ChIP-seq in the presence or absence of Abscisic Acid (ABA) (Song et al., 2016a). We examined the overlap of the top 1000 edges for each of these 21 TFs from the TINGe union network

and counted the number that were experimentally confirmed in the ChIP-seq experiments. The network predictions for all 21 TFs examined showed significant enrichment for ChIP-seq target genes (Figure 2H, p-value <0.001, Fisher's exact test). NF-YB2 had the largest number of validated predictions, with 836 out of the top 1000 edges experimentally confirmed by ChIP-seq (Figure 2H). We also performed GO enrichment analysis for the top 1000 edges for each of the 21 TFs (Figure S2B, Table S5). The regulons of the 21 ABA-related TFs showed enrichment for GO terms including "response to abiotic stimulus" (FDR correct p-value <0.05 for 21/21 TFs), "response to water" (FDR correct p-value <0.05 for 17/21 TFs) and "response to abscisic acid" (FDR correct p-value <0.05 for 16/21 TFs). Thus, our GRN predicts validated ChIP-seq target genes and GO terms that are consistent with the functions of these 21 TFs in ABA and stress responses. Taken together, these results strongly suggest that the predictions in our GRNs are biologically meaningful.

3.3.3 BR-TFs are enriched for BR and drought targets in the GRN

To understand how BR-TFs mediate BR-regulated gene expression, we integrated our own and publicly available protein-protein interaction (PPI) data with BES1/BZR1 ChIP targets and the TINGe union GRN. The combined network was used to investigate the relationship among BES1/BZR1 and BR-TFs in BR and drought target gene regulation (Figure 3A, Table S6). First, we focused on the relationship between BR-TFs and potential BR regulated targets in the GRN. The potential targets of a TF in the GRN make up the regulon for that TF. If BR-TFs are involved in controlling BR-responsive gene expression, then the regulons of BR-TFs would be expected to contain a large number of BR-regulated target genes. To systematically test this, we

implemented master regulator analysis (MRA) (Fletcher et al., 2013; Margolin et al., 2006) to determine the gene signatures enriched in the regulons of each TF (Figure 3B-D). MRA uses a hypergeometric test to detect enrichment of a given gene list in each TF's regulon. Thus, the TF controlling a regulon with significant MRA is a candidate regulator for the set of genes in the gene list being examined (Castro et al., 2016; Fletcher et al., 2013). We performed MRA with 1,841 TFs present in our GRN with sufficiently large regulons to be analyzed by this analysis, including 581 BR-TFs. We then calculated a p-value and odds ratio for BR-TF regulon enrichment with respect to each gene set by comparing the number BR-TFs that were significant MRA hits versus the total number of TFs that were significant MRA hits (Figure 3B). Consistent with a role in BR-regulated gene expression, we found that 448 BR-TFs were significantly enriched for BR-regulated genes from RNA-seq experiments (Figure 3B, p-value: 1.51e-59, Fisher's exact test). Importantly, these BR RNA-seq data are independent of the microarray data used to generate the network (Wang et al., 2014). Moreover, 466 BR-TFs were significantly enriched for drought regulated genes in MRA (Figure 3B, p-value: 7.23e-38, Fisher's exact test) (Maruyama et al., 2009). Together 502 BR-TFs were significant MRA hits for BR- or drought-regulated genes (Figure S3A), supporting the idea that BR-TFs are involved in regulating growth and stress responses. We also performed MRA using other hormone- or stress-regulated gene sets (Albihlal et al., 2018; Bai et al., 2012b; de Zélicourt et al., 2018; Guo et al., 2018; Hickman et al., 2017; Maruyama et al., 2009; Park et al., 2015; Song et al., 2016a; Xie et al., 2018; Zhang et al., 2018). We compared the number of significant BR-TFs from MRA using each gene

set and found a high concordance between BR-TFs enriched for BR, ABA, Jasmonic Acid (JA) and heat stress signatures (Figure 3C).

In addition to BR regulated genes, BR-TFs would be expected to be enriched for BES1/BZR1 targets. The regulons of 396 BR-TFs were significantly enriched for BES1/BZR1 target genes in MRA (Figure 3B and Table S7, p-value: 1.047614e-70, Fisher's exact test). Clustering of MRA p-values for BR-TFs versus other TFs (non-BR-TFs) clearly revealed the pattern of enrichment of BES1/BZR1 targets for the BR-TF group (Figure 3D). Among those enriched were several TFs previously shown to interact with BES1 and control BR-regulated gene expression (Bai et al., 2012b; Li et al., 2009a; Lozano-Duran et al., 2013; Ye et al., 2017; Yin et al., 2005; Zhang et al., 2014; Zhou et al., 2013) (Table 2). For example, HAT1 showed the strongest enrichment for BES1/BZR1 targets among BR-TFs (Table S7) which is consistent with the role of HAT1 in mediating BR-repressed gene expression (Zhang et al., 2014). The majority of BR-TFs enriched for BES1/BZR1 targets also showed enrichment for BR and drought-regulated genes, with a total of 364 BR-TFs enriched for all three of these gene sets (Figure S3A). These results support a role for BES1/BZR1 and BR-TFs in mediating BR-regulated gene expression and suggest extensive cross-talk with other hormone and stress response pathways.

To further confirm the relationship between BR-TFs and BR-regulated genes we used an independent dataset consisting of eQTLs for BR-responsive genes reanalyzed from the *Arabidopsis* 1001 Genomes project transcriptome datasets (Kawakatsu et al., 2016). We found significant enrichment for eQTL hits for BR-responsive genes in the genomic regions surrounding BR-TFs (p-value: 3.038e-09, Table S8) In total, we

identified 2,740 significant eQTL hits corresponding to 630 BR-TFs for 791 BR-responsive genes. Moreover, we tested if eQTL hits for BR responsive genes are enriched in the binding sites of BR-TFs as determined by DAP-seq (Bartlett et al., 2017; O'Malley et al., 2016). DAP-seq binding peaks are available for 171 BR-TFs. In total 30,977 (62.9%) of eQTLs for BR-regulated genes are located in BR-TF binding sites (odds ratio: 1.88, p-value: 2.2e-16, Fisher's exact test). This analysis indicates that SNPs near *BR-TF* genes and in BR-TF binding sites are enriched for eQTLs corresponding to BR-regulated genes. These results add an additional layer of support for BR-TFs in BR-regulated gene expression. Altogether, our results provide multiple lines of evidence implicating BR-TFs in BR-regulated gene expression.

3.3.4 BR-TFs physically interact and may regulate common target genes

To investigate co-regulation of genes by BR-TFs we performed regulon overlap analysis which tests if each pair of TFs share a larger proportion of predicted targets genes in the GRN than would be expected by chance (Fletcher et al., 2013). We observed enrichment of shared predicted targets among BR-TFs, with 50,634 significant overlaps between the regulons of 581 BR-TFs that were included in this analysis (Figure S3B and Table S9, p-value <0.0001). These results suggest that BR-TFs function together in controlling BR-regulated gene expression. Next, we examined physical interactions among BR-TFs. An extensive TF interaction network was recently constructed using Cre-reporter-mediated Y2H coupled with next-generation sequencing (CrY2H-seq) (Trigg et al., 2017) to generate the 'Arabidopsis thaliana transcription factor interaction network, version 1' (AtTFIN-1). Since BR-TFs share many predicted target genes in our GRNs we reasoned that BR-TFs may physically interact in

controlling BR-responsive gene expression. Consistent with this idea, we observed significant enrichment for PPIs among BR-TFs, with 1705 interactions between the 472 BR-TFs present in the AtTFIN-1 (Figure S3C and Table S10, $p<0.0001$). BR-TFs that physically interact tend to share predicted targets in the GRN. In particular, of the 1321 BR-TF PPIs that were also examined in our overlap analysis, 597 of these showed significant overlaps between the regulons of the interacting BR-TFs in the GRN (Table S9, p-value: 6.26e-14, Fisher's exact test). These observations suggest that BR-TFs physically interact and are likely to function together in controlling overlapping sets of BR-regulated genes.

3.3.5 NEST analysis prioritizes BR-TFs for functional studies

Given the large number of BR-TFs identified, we next prioritized the TFs for further functional studies. Recently, NEST (Network Essentiality Scoring Tool) was developed to analyze gene essentiality with genome-wide CRISPR screens in a mammalian system (Jiang et al., 2015). It was found that the sum of expression levels of connected genes in a biological network correlates well with the essentiality of that hub gene (Jiang et al., 2015). To adapt NEST to study the BR pathway, we first extracted a subnetwork consisting of 2,160 genes that are regulated by BRs in microarray and RNA-seq experiments. We then performed NEST analysis using BR-specific gene expression data (Guo et al., 2009) with 1,841 TFs that were present in our networks and connected to the BR-regulated genes (referred to as BR-NEST). We first examined the BR-NEST scores for known regulators of the BR pathway. Notably, several TFs with established functions in BR signaling were highly ranked from the BR-NEST analysis. These included BEE2 (BR ENHANCED EXPRESSION 2; BR-NEST

rank: 2) (Friedrichsen et al., 2002), HBI1 (HOMOLOG OF BEE2 INTERACTING WITH IBH1, BR-NEST rank: 3) (Bai et al., 2012a; Fan et al., 2014; Malinovsky et al., 2014) and PIF5 (PHYTOCHROME INTERACTING FACTOR 5; BR-NEST rank: 12) (Bernardo-Garcia et al., 2014; Oh et al., 2012). RD26 and its close homologs were also highly ranked in BR-NEST, which is consistent with our functional studies that have characterized NACs as negative regulators of BR-regulated growth (Ye and al., 2017) (Table S11). The recovery of known regulators in the BR pathway suggests that BR-NEST scores have a good potential in identifying important genes for BR responses. Next, we examined the distribution of BR-NEST scores among All TFs, BR-TFs and other TFs (Figure 3E). BR-TFs had the highest BR-NEST scores among these groups with a mean BR-NEST of 140.8, compared to All TFs that had a mean BR-NEST of 91.5 (Table S11). Similarly, when we binned TFs according to their BR-NEST score ranking BR-TFs were significantly enriched in the top 200 TFs (Figure 3F, p-value: 8.29e-10, Fisher's exact test). Given the high rankings of both known TFs involved in the BR pathway and BR-TFs as a group we opted to rank BR-TFs according to their BR-NEST scores and chose the top BR-TFs for functional studies (Figure 3G). In addition to BR-TFs, BR-NEST analysis allowed us to identify several high-ranked non-BR-TFs that might be involved in BR responses. Thus, these TFs were also included in the BR phenomics assays described below. These results demonstrate that analysis of gene networks has great potential in identifying genes and pathways mediating BR-regulated gene expression and responses. Given that MRA and NEST can be applied to any gene set or pathway of interest, we expect that our GRNs and this tool set to be a broadly applicable hypothesis generating tool for the Arabidopsis community. The entire set of

GRNs, analysis tools used and documentation are made freely available in the R packages wgn.athaliana and wgntools.

3.3.6 BL and BRZ phenomics uncovers BR phenotypes of BR-TFs

In order to translate predictions from our GRNs into knowledge of the BR pathway an important step is to characterize the genes identified by genetic and genomic methods. To this end, we set out to investigate the functions of BR-TFs in BR responses by conducting phenomics experiments using more than 1000 homozygous knockout (KO) mutants (Alonso et al., 2003) or overexpression lines (Coego et al., 2014) for over 300 TFs. We established high-throughput BR phenomics assays in both petri plates and with soil-grown plants (Figure S4A-D). First, we employed the BR inhibitor, Brassinazole (BRZ) that has been widely used to study BR responses (Asami et al., 2000). In BRZ response assays, the ratio between treated (BRZ250nM) and control (BRZ0) hypocotyl length is measured as a proxy for BR response (Yu et al., 2011). We optimized BRZ response assays such that they could be conducted in a high throughput and quantitative manner. While WT controls produced highly consistent results across 10 independent experiments (mean BRZ250/BRZ0 ratio $\pm$ SD: 0.511 $\pm$ 0.030, Figure S4E-F), 93 out of 296 (31.4%) TFs tested showed ratio differences of at least 0.05 in BRZ ratios compared to WT controls (Figure 4A and Table S12). In contrast, a cohort of 20 randomly chosen control TFs showed little difference from WT (Figure 4B; Control Mutants), whereas BR-TF mutants showed a wider distribution of phenotypic differences, including a number of negative regulators with increased BRZ ratios and positive regulators with decreased BRZ ratios (Figure 4B). We also assayed BRZ response for 696 inducible overexpression (OE) lines from the Transplanta

collection (Coego et al., 2014) spanning 269 top ranking TFs from NEST analysis. In line with the KO phenotypes, 170 out of 269 (63.2%) TFs tested displayed BRZ phenotypes when overexpressed (Figure 4A and Table S13). Finally, we performed BL response experiments in light-grown seedlings, assaying the extent to which hypocotyls elongate after BL treatment. Consistent with the BRZ phenotypes, 80 out of 300 (26.7%) TFs tested showed BL response phenotypes (Figure 4A and Table S14). We identified 30 TF mutants with both BL and BRZ response phenotypes and 17 TFs with BRZ response phenotypes in both KO and OE lines (Figure 4C).

To confirm the mutant BL and BRZ phenotypes we performed two additional rounds of phenotyping with 8 independent biological replicates of 12 plants for each line and treatment combination. We included *bri1-301* (Xu et al., 2008), a weak loss-of-function mutant for the BR receptor *BRI1* as well as *BES1-RNAi,* which has reduced expression of *BES1* and *BZR1* (Yin et al., 2005) as controls in BRZ response experiments. As expected, *bri1-301* was shorter than WT and significantly more sensitive to BRZ treatment (Figure 4D-F and Table 3); however, *BES1 RNAi* was not more sensitive to BRZ in terms of BRZ250/BRZ0 ratio. Rather, *BES1 RNAi* plants were significantly shorter than WT under both control (BRZ0) and treated (BRZ250) conditions (Figure 4E-F and Table 3). Given that BES1 is well established as a critical regulator for BR responses (Yin et al., 2005; Yin et al., 2002), these data suggest that hypocotyl length under BRZ treatment is an important BR phenotype. Thus, we chose to consider differences in both BRZ250/BRZ0 ratio and hypocotyl length after BRZ250 treatment as BR phenotypes in BRZ assays. Using these criteria, we confirmed a total

of 18 TF mutants with significant BRZ phenotypes (Figure 4E-F, Table 3 and Table S15, $p<0.05$, Dunnett's method).

Among the mutants with altered BRZ phenotypes were two TFs implicated in binding A/T-rich sequences. These included PLATZ (PLANT A/T-RICH SEQUENCE AND ZINC-BINDING PROTEIN) (Nagano et al., 2001) whose homologs have been reported to be induced by abiotic stresses including drought (So et al., 2015) and ARID-HMG1 (A/T-RICH INTERACTION DOMAIN HIGH MOBILITY GROUP1) (Hansen et al., 2008), a TF that may be involved in DNA bending and enhanceosome formation (Agresti and Bianchi, 2003). Interestingly, although both of these TFs bind to AT-rich sequences (Antosch et al., 2012; Nagano et al., 2001) they exhibit opposite phenotypes in terms of BR response. *platz* mutants display characteristic BR loss-of-function phenotypes in the dark such as dwarfism and de-etiolation (Figure 4D-F), indicating that PLATZ is a positive regulator in the BR pathway. In contrast, *arid-hmg1* mutants are resistant to BRZ (Figure 4D-F), indicating that HMG functions as a negative regulator of BR signaling. Additionally, *tcp11* exhibited the strongest BRZ ratio resistance phenotype among the confirmed TF mutants (Figure 4D-F), indicating the TCP11 functions as a negative regulator in the BR pathway.

Next, we confirmed the results of our BL response assays. We employed gain-of-function *bes1-D* (Vilarrasa-Blasi et al., 2015; Yin et al., 2002) and loss-of-function *BES1-RNAi* plants as controls for BL response (Figure 4G-H). *BES1-RNAi* was shorter than WT under control (BL0) and treated (BL100) conditions whereas *bes1-D* was longer than WT under BL100 treatment. Neither *BES1-RNAi* or *bes1-D* had a dramatically altered BL100/BL0 ratio (Figure 4G). These data suggest that hypocotyl

length under BL0 and BL100 treatments are also important phenotypes to identify BR pathway components. We confirmed a total of 7 TF mutants with altered hypocotyl lengths or BL ratios in the BL assays (Figure 4G-H, Tables 4 and S16, $p<0.05$, Dunnett's method). For example, *ath1* (*homeobox gene 1*) displayed constitutively long hypocotyls that only marginally responded to BL (Figure 4G-H), which is consistent with the previously characterized function of *ATH1* in repressing growth along with light activated genes (Gomez-Mena and Sablowski, 2008). *gtl1* (*gt-2-like1*) mutants were hypersensitive to BL treatment and displayed the longest hypocotyls of the confirmed mutants under BL100 treated conditions (Figure 4G-H). *GTL1* controls cell growth in trichomes and root hairs (Breuer et al., 2009; Shibata et al., 2018) and *gtl1* mutants are resistant to drought stress (Yoo et al., 2010). Therefore, *gtl1* mutants have both increased BR-regulated growth and drought stress responses, making GTL1 a potential target to improve BR-regulated growth and stress responses. *platz* mutants also displayed phenotypes in BL assays, with constitutively short hypocotyls that could be partially restored upon BL treatment (Figure 4H). *arid-hmg1* mutants displayed a non-significant trend of longer hypocotyls compared to WT under BL treated conditions (Table S16). These phenotypes are consistent with PLATZ functioning as a positive regulator of BR responses and ARID-HMG1 functioning as a negative regulator.

We confirmed the OE BRZ phenotypes of 39 TFs with one additional replicate of 12 plants per treatment (Tables 5 and S17). Our overexpression studies identified several BES1/BZR1 interacting TFs with confirmed BRZ phenotypes. These include an uncharacterized C2H2 Zinc Finger TF (AT4G17810), the TCP family TF BRANCHED1 (BRC1, AT3G18550) implicated in flowering time control (Niwa et al., 2013) and the

suppression of auxiliary bud outgrowth in shade (Gonzalez-Grandio et al., 2013) and WRKY25 (AT2G30250), which is involved in pathogen defense and abiotic stress responses (Jiang and Deyholos, 2009; Li et al., 2009b; Zheng et al., 2007). Interestingly, all of the OE lines confirmed in our assays resulted in decreased hypocotyl length compared to WT under BRZ treatment. These data suggest that putative negative regulators of the BR pathway are often uncovered via TF overexpression studies.

Next, we examined the BR-NEST network scores of TFs with confirmed mutant or OE BR phenotypes. If BR-NEST is a strong predictor of TF function in BR responses then TFs with phenotypes would be expected to be highly ranked by BR-NEST. Consistent with this idea, TFs with mutant phenotypes in BRZ or BL assays showed higher BR-NEST rankings compared to all TFs or BR-TFs (Figure 4I), whereas TFs with OE phenotypes had only slightly higher BR-NEST rankings (Fig. 4I). We also examined enrichment for BR regulated genes (Figure 4J) or BES1/BZR1 target genes (Figure 4K) in the regulons of BR-TFs with confirmed phenotypes from MRA. Mutants with confirmed BL or BRZ phenotypes often had high MRA ranks, but to a lesser degree than that observed for BR-NEST. In sum, our BL and BRZ phenomics experiments suggest that BR-NEST and MRA network prioritization is a tractable strategy to identify TFs with phenotypes.

3.3.7 BES1, PLATZ and ARID-HMG1 interact with a common set of TFs and control BR-regulated gene expression

To further uncover the mechanisms by which BES1 and BR-TFs function, we analyzed the molecular roles of two top ranking TFs from our phenomics analysis –

PLATZ and ARID-HMG1. Although both of these TFs bind to AT-rich sequences (Antosch et al., 2012; Nagano et al., 2001) they display opposite phenotypes in terms of BR response. Therefore, we hypothesized that PLATZ and ARID-HMG1 have opposite functions in BR-regulated gene expression. PLATZ and ARID-HMG1 physically associate with BES1 in BiFC and Co-IP assays (Figure 5A-B), suggesting that these TFs may be involved in BES1-mediated gene expression. Since HMG group proteins are involved in enhanceosome formation (Agresti and Bianchi, 2003), we reasoned that ARID-HMG1 and PLATZ could function along with BES1 to assemble transcriptional complexes on the promoters of BR-regulated genes. We used Blue-Native Polyacrylamide Gel-Electrophoresis (BN-PAGE) (Eubel et al., 2005) and found that BES1 was present in several large (400-500kDa) nuclear complexes (Figure 5C). If PLATZ and ARID-HMG1 are involved in BES1 transcriptional complexes, they would be predicted to interact with a common set of TFs. To test this hypothesis, we performed Y2H screening with PLATZ and ARID-HMG1 using a library of 1956 TFs (Pruneda-Paz et al., 2014). We identified 87 PLATZ interacting TFs as well as 71 ARID-HMG1 interacting TFs. When combined with BES1/BZR1 interacting TFs, our analysis revealed a total of 251 TFs that interact with PLATZ, ARID-HMG1 or BES1/BZR1 (Figure 5D). 164 of these interacting TFs are BES1/BZR1 targets or regulated by BRs (Figure 5D). BES1/BZR1 and PLATZ interact with a common set of 32 TFs, whereas BES1/BZR1 and ARID-HMG1 have 24 shared TF interactors. For instance, PLATZ interacts with PHYTOCHROME-INTERACTING FACTORs PIF1 and PIF5, which have been shown to associate with BZR1 and BES1 and are crucial for cell elongation in darkness (Oh et al., 2012). The strong phenotype of *platz* mutants in dark-grown

seedlings suggests that interactions between BES1, PLATZ and PIFs may facilitate BR-regulated growth in the dark. Together, our results suggest that BES1, PLATZ and ARID-HMG1 interact with a large number of other TFs to mediate BR-regulated gene expression.

Next, we performed global gene expression studies using dark-grown *platz* and *arid-hmg1* mutants under control or BRZ-treated conditions. We included gain-of-function *bes1-D* mutants (Yin et al., 2005; Yin et al., 2002) so that comparisons could be made to BES1 regulated genes within the same experiment. In agreement with PLATZ and ARID-HMG1 interaction with BES1, the genes differentially expressed (DE) in *platz* and arid-*hmg1* mutants showed a high degree of overlap with BES1/BZR1 targets and *bes1-D* regulated genes. Specifically, 68.9% (1,443/2,094) of *platz* DE genes and 65.5% (495/755) of arid-*hmg1* DE genes are bound and/or regulated by BES1 (Figure 5E-F). Moreover, clustering analysis revealed that *bes1-D* induced genes are repressed in *platz* mutants but show increased expression levels in *arid-hmg1* mutants compared to WT under BRZ treatment. Similarly, *bes1-D* repressed genes showed increased expression levels in *platz* and decreased expression in arid-*hmg1* (Figure 5G). These commonly affected genes between *platz, arid-hmg1,* and *bes1-D* are enriched for known binding motifs of BES1 (Figure 5H) as well as AT-rich motifs that are consistent with PLATZ and ARID-HMG1 binding regions (Figure 5I). Our global gene expression studies suggest that PLATZ cooperates with BES1 whereas ARID-HMG1 inhibits BES1 function (Figure 5J). Together, our results indicate that PLATZ and ARID-HMG1 modulate BR responses by interacting with BES1 and other BR-TFs to form BR transcriptional complexes and control BR regulated genes.

3.3.8 BR and drought phenomics of soil-grown plants

Although BRs are emerging as crucial regulators of plant growth and stress responses (Nolan et al., 2017a), the majority of BR response experiments have been carried out with plants grown on petri plates which may not reflect conditions experienced in soil. Thus, a quantitative system to study BR and drought responses of plants in soil is needed. To this end, we established phenomics assays to interrogate BR responses in soil grown plants using time-lapse imaging or a fully automated robotic system called Robotic assay for drought (RoAD) which is capable of performing BR and drought response experiments. We then applied these assays to determine the role of a subset of BR-TFs in BR responses in the adult growth stage.

First, we established BR response experiments in soil using the economical BR inhibitor Propiconazole (PCZ) (Hartwig et al., 2012). PCZ can be effectively applied to *Arabidopsis* plants by watering soil with PCZ solution. We analyzed the PCZ response of 102 TF mutants along with WT, *bri1-301* and *bes1-D* controls. In total, we phenotyped 1,288 plants, collecting more than 49,000 images over ~5 weeks of plant growth in a greenhouse setting. The use of greenhouse conditions allowed for a natural lighting environment and increased throughput in the PCZ response assays, however; the fluctuating light in the greenhouse presented a challenge for image processing and segmentation. We developed a semi-automated pipeline to crop and segment individual plants for trait extraction, which was implemented to process one image from each of 12 days between 10 and 21 days after planting (DAP). This resulted in a total of 13,672 images of individually cropped plants for which traits could be extracted (Table S18).

Additionally, we manually measured plant height once all plants had ceased growth (Table S19).

To understand how PCZ influences plant growth under our experimental conditions we analyzed the various traits measured for control and PCZ treated plants. Although PCZ dramatically affected plant morphology (Figure S5A) we found that the area of control and PCZ treated plants was indistinguishable through most of the greenhouse experiment (Figures 6A and S5A-B). On the other hand, solidity, a measure of plant compactness, could efficiently separate WT control and PCZ treated plants**.** PCZ treatment led to increased solidity compared to control conditions, especially at later time points (Figure 6B**)**. If increased solidity corresponds to a decrease in BR response, then loss-of-function *bri1-301* mutants should resemble PCZ treated WT plants. Consistently, *bri1-301* had increased solidity compared to WT under both control and PCZ treated conditions (Figures 6C-E and S5A**)**. PCZ treatment also decreased plant height in WT compared to control conditions (Figure 6F) suggesting that plant height can also serve as a proxy for BR response in PCZ assays. Surprisingly, we were unable to detect gain-of-function BR phenotypes for *bes1-D* using plant height or solidity at traits (Figure 6E-F and S5A). The rosette of *bes1-D* is highly curved, which may obscure solidity phenotypes at the whole rosette level. Additional traits such as those in 3D or on individual leaves will be needed to distinguish the BR phenotypes of *bes1-D.*

A number of *BR-TF* mutants with phenotypes in the seedling stage also exhibited PCZ phenotypes in the adult stage. For example, under PCZ treatment *tcp11* had increased plant height and decreased solidity (Figure 6E-F) and *arid-hmg1* had increased plant height (Figure 6F). To validate the phenotype of *tcp11* revealed by PCZ

assays we crossed *tcp11* with *bri1-301.* Since *tcp11* is resistant to PCZ we expected that loss of *TCP11* would suppress the dwarf phenotype of *bri1-301* mutants. Indeed, we found that *tcp11 bri1-301* double mutants partially restored the growth phenotype of *bri1-301,* showing longer and narrower leaves (Figure 6G-H). These results identify BR phenotypes for *arid-hmg1* and *tcp11* in soil-grown plants that are consistent with ARID-HMG1 and TCP11 functioning as negative regulators in the BR pathway. Similar to *bri1-301, platz* mutants displayed increased solidity under control conditions in PCZ experiments (Figure 6E), consistent with PLATZ functioning as a positive regulator in the BR pathway.

In addition, our PCZ experiments allowed us to uncover additional mutants that did not have readily detectable phenotypes in BL or BRZ response assays. We found that loss-of-function of *ULTRAPETALA1 (ULT1)* in *ult1* mutants (Carles et al., 2005) led to a PCZ resistant plant height phenotype (Figure 6F). ULT1 was highly ranked in BR-NEST analysis (BR-NEST Rank 92/1,841 TFs, Table S11) and the regulon of ULT1 is enriched for BR regulated and BES1/BZR1 target genes in the GRN (Table S7). ULT1 is a trithorax group protein that counteracts polycomb mediating repression through epigenetic modifications (Carles and Fletcher, 2009). ULT1 is known to regulate developmental phenotypes including meristem activity (Carles et al., 2005) and also functions in stress responses (Pu et al., 2013). Interestingly, ULT1 is implicated in limiting H3K27 trimethylation, a repressive histone mark. H3K27 demethylases ELF6 (EARLY FLOWERING 6) and REF6 (RELATIVE OF EARLY FLOWERING 6) interact with BES1 and function as positive regulators of the BR pathway by promoting the expression of BR activated genes (Lu et al., 2011; Yu et al., 2008). The identification of

ULT1 suggests that network prioritization strategies such as BR-NEST can be applied to identify mutants with phenotypes in PCZ response assays. Future studies should explore if ULT1 is involved in activating BR repressed genes, which would explain the potential function of ULT1 as a negative regulator of the BR pathway.

Next, we analyzed the PCZ and mild drought response phenotypes of WT, *tcp11*, *arid-hmg1, platz* and *ult1* using the RoAD system. RoAD is a robotic rover capable of administering PCZ and drought assays by performing weighing, watering and non-destructive imaging of plants in 2D and 3D (Figure S4D). Using RoAD, we observed PCZ phenotypes of *tcp11, arid-hmg1*, *platz* and *ult1* that were consistent with those found in the greenhouse PCZ experiments (Figure 6I). We performed mild drought experiments with the RoAD system and found that drought treated *tcp11* mutants tend to have reduced plant area compared to WT (Figure 6J), suggesting that TCP11 may be involved in drought response. *TCP11* is transcriptionally repressed by drought (Rasheed et al., 2016) and is the second highest ranked TF in drought MRA (Figure 6K, drought MRA rank: 2 /1,841 TFs, adjusted p-value 1.0e-125). Thus, we hypothesized that TCP11 functions as a negative regulator of drought response. In line with this idea, we performed water withholding drought assays and observed that *tcp11* mutants had increased survival rates compared to WT (Figure 6L-M). These phenomics experiments establish a system to study BR-drought crosstalk in soil grown plants and reveal that *tcp11* mutants have increased BR-regulated growth while maintaining resistance to drought stress.

3.4 Conclusions

In this study, we devised a comprehensive approach to characterize the function of BES1, BZR1 and BR-TFs in BR responses through network analysis, genetics, genomics and phenomics approaches. We used ChIP, transcriptome and TF interactome datasets to identify 657 BR-TFs implicated in BR-regulated gene expression. Next, we built comprehensive GRNs based on 11,760 transcriptome datasets which showed that BR-TFs are regulators of BR and stress responsive genes. These networks to allowed us to prioritize BR-TFs for functional studies using NEST and MRA network scoring metrics. We tested the network predictions by analyzing BR responses for more than 1000 mutant or overexpression lines for 300 TFs using high-throughput phenotyping. These studies identified PLATZ and ARID-HMG1 as two novel A/T-rich binding BR-TFs that interact with BES1 and a host of other BR-TFs, controlling BR-mediated gene expression. Finally, we showed that BR and drought response experiments in soil can reveal regulators such as TCP11 that can alter BR and drought responses in the same direction, allowing for increased growth and drought stress resistance.

Why do BR responses involve such a large number of TFs? One possibility is that the plethora of BR-TFs allows the BR pathway to effectively interface with other hormone and stress signaling pathways under different conditions and developmental stages. Indeed, the BR pathway has been shown to be integrated with many other hormones including Auxin (Chaiwanon and Wang, 2015; Vert et al., 2008), Gibberellins (Bai et al., 2012b; Gallego-Bartolome et al., 2012; Shahnejat-Bushehri et al., 2016; Tong et al., 2014; Unterholzner et al., 2015), ABA (Clouse, 2016; Gui et al., 2016; Hu

and Yu, 2014; Zhang et al., 2009), JA (He et al., 2017; Shin et al., 2016), Ethylene (De Grauwe et al., 2005; Gendron et al., 2008), and Strigolactones (Wang et al., 2013). There is also growing evidence for tissue-specific BR responses (Singh and Savaldi-Goldstein, 2015; Vilarrasa-Blasi et al., 2014; Vragovic et al., 2015). These studies illustrate the complexity of BR signaling and our results demonstrate that systems approaches including network analysis can begin to provide insight into these processes.

In this study we investigated BR-TF functions using multiple phenomics assay that span different developmental stages (seedling and adult) and environmental conditions (light, dark and drought). For example, we found that the phenotype of *platz* mutants was weaker in the adult stage compared to the strong dwarf phenotype of dark-grown *platz* seedlings. This suggests that different phenotyping assays can provide complementary information which is of particular interest given the potential to uncover downstream factors in the BR pathway that alter only a subset of BR responses. In line with this idea, our drought phenomics experiments allowed us to identify that *tcp11* mutants have increased BR-regulated growth along with improved drought resistance. Thus, understanding the downstream aspects of BR signaling may have great potential for improving plant growth and stress resilience. In the future, temporal aspects of BR-TF responses to BRs and stress should allow for a more precise understanding and manipulation of the BR-regulated growth and stress pathways.

3.5 Acknowledgements

We thank the Iowa State Genomic Technologies Facility (GTF) for equipment use, Pete Lelonek and Jennifer Johnson for supporting RoAD efforts, Colton McNinch

for enabling greenhouse PCZ experiments and past Yin lab researchers that assisted with phenotyping efforts including Nick Smith, Jie Tang, Max McReynolds, Ashley Paulsen, Kyle Small, Basanta Bista, Jessica Parrott and Paige Rassel. This research was supported by grants from Plant Sciences Institute at Iowa State University and NSF (MCB 1818160)

3.6 Author Contributions

T.N. and Y. Y. conceived the project. T.N. designed, analyzed, and performed or supervised most of the experiments. S.C, M.A and S.A classified the transcriptome datasets, constructed TINGe and GENIE3 networks and created network analysis tools in wgn.tools and wgn.athaliana packages with input from T.N. Sh.S., M.A. S.C and S.A assembled network validation datasets and performed AUC analysis. M.L. conducted BES1 ChIP-seq in J.E. lab. D.K., P.W. and T.N. performed Y2H screening experiments with the TF library. T.N., N.H., S.M., Z.X. Ha.J., H.G., P.S. and A.H conducted BR phenomics experiments. T.N. and Z.X conducted the RNA-seq experiments. H.L. and P.S performed eQTL analysis. T.N., A.A. and So.S. analyzed BRZ phenotyping images. Z.J. S.M., N.H., A.H., and T.N. analyzed greenhouse PCZ images. L.X., T.T., Y.B. and L.T. designed and built RoAD with input from T.N. and Y.Y. L.X. process RoAD images. Hy. J and D.N. assisted T.N. with statistical analysis. T.N. wrote the manuscript input from Y.Y and H.G.

3.7 Methods

Plant materials and growth conditions

Arabidopsis thaliana accession Columbia (Col-0) was used along with previously described lines: *bri1-301* (Xu et al., 2008), *bes1-D* (Vilarrasa-Blasi et al., 2015; Yin et al., 2002), *BES1-RNAi* (Yin et al., 2005), *myc2myc3myc4* (Schweizer et al., 2013) and *ult1-3* (Carles et al., 2005). The complete list of homozygous TF mutants from the SALK Homozygote T-DNA Collection used in this study is included along with BL and BRZ phenotyping results in Tables S12 and S14. The mutants were ordered from the Arabidopsis Biological Resource Center (ABRC) and used directly in BRZ and BL phenotyping assays. To confirm the presence of homozygous T-DNA insertions in the mutants, we genotyped a subset of 49 mutants using primers listed in Table S20 and found that 44 mutants could be confirmed as homozygous. For TF OE assays, homozygous lines from the Transplanta collection (Coego et al., 2014) which express a single TF driven by a beta-estradiol inducible promoter were used. Seeds were sterilized for 2-4 hours using chlorine gas. Following stratification at 4°C to synchronize germination, plants were grown on 0.5X Linsmaier and Skoog (1/2 LS; Caisson Laboratories) plates supplemented with 1% (w/v) sucrose for 7-10 days followed by transfer to soil under long day (16 h light/8 h dark) conditions at 22°C unless otherwise specified.

Network construction and validation

We collected ~13,000 non-redundant Affymetrix ATH1 expression profiles from various public microarray databases. After removal of duplicate entries, manual

inspection of the CEL files and quality control analyses (Aluru et al., 2013), 11,760 CEL files remained for construction of GRNs. The datasets were further classified into 12 categories - 5 tissue and 7 biological process (Chockalingam et al., 2016). Probesets and/or genes with IQR values exceeding an empirically computed threshold for each category were removed from subsequent steps. We applied three different inference methods – TINGe (Aluru et al., 2013), GENIE3 (Huynh-Thu et al., 2010) and GRNBoost (Aibar et al., 2017) to first reconstruct separate networks for each tissue and biological process following which, a union network(s) was constructed for each method by considering the maximum edge weight from all 12 networks for each gene-gene interaction. The network(s) were constructed using a list of 2492 Arabidopsis TFs (Pruneda-Paz et al., 2014), in conjunction with the entire gene expression matrix from the microarray data. Based on our data processing and filtering, and dataset categorization methods, we were able to include a total of 1915 TFs in the final union network(s). We selected a subset of nodes/edges from the complete list of edges in the union network as deemed necessary for further analyses.

To evaluate performance of the 3 inference methods, we measured precision/recall (PR); precision (percent correct edges among all edges inferred) and recall (percent correct edges predicted) of each inference method, as well as the receiver operating characteristic (ROC) which measures the true positive rate against the false positive rate for different possible thresholds. We used seven different sets of TF-target interactions as reference sets for comparing the three methods: TF binding data from (1) DAP-seq (Bartlett et al., 2017; O'Malley et al., 2016), (2) ChIP-seq (Kulkarni et al., 2017; Song et al., 2016a) or (3) Y1H (Li et al., 2014; Shani et al., 2017;

Sparks et al., 2016; Taylor-Teeples et al., 2015); TF2Network (Kulkarni et al., 2017) benchmark datasets for (4) ChIP (TF2N ChIP) or (5) differentially expressed genes upon TF perturbation (TF2N DE); (6) eQTLs for BR-responsive genes from the Arabidopsis 1001 genomes project (Kawakatsu et al., 2016); and (7) 5022 RD26 target genes that are bound in ChIP-seq and regulated upon *RD26* overexpression (Nolan et al., 2017a; Song et al., 2016a; Ye et al., 2017). For fair comparison, we constrained the predicted interactions to include only those TF's present in the reference set(s), and any gene identified as a TF-target (all first-order neighbors of the TF's) by the corresponding network construction method. These subnetworks were then determined for the presence/absence of each edge between a TF-target in the given validation set(s) in a combined manner, and to compute and plot the PR and ROC curves. Such a cross-comparison allowed for determination of cases where a gene might be accepted as a valid target by one network construction method, but rejected by another method.

MRA and regulon overlap analysis were conducted in R (version 3.4.1) using the 'RTN' package (Bioconductor release 3.7) as previously described (Castro et al., 2016; Fletcher et al., 2013). Enrichment of BR-TFs with significant MRA was determined by comparing BR-TFs with significant MRA to all TFs with significant MRA for each gene set using Fisher's exact test in the 'GeneOverlap' R package. The resulting p-values were -log10 transformed and visualized using the 'ComplexHeatmap' R package (version 1.14.0) with the row and column orders determined by hierarchical clustering. Intersections between lists of BR-TFs with significant MRA from different hormone or stress gene sets were analyzed in the same manner. To asses overrepresentation of overlaps between BR-TF regulons, we selected a random group of TFs of the same

size as the BR-TF list and counted the number of significant regulon overlaps (adjusted p-value <0.05). This process was repeated 10,000 times to generate an empirical distribution of random regulon overlaps. We then compared the number of BR-TF overlaps to this distribution to calculate a p-value for BR-TF regulon overlap enrichment. The same approach was used to identify enrichment of PPIs between BR-TFs present in the AtTFIN-1 TF interactome dataset (Trigg et al., 2017). The complete networks and implementation of the NEST scoring metric (Jiang et al., 2015) used in this study are available in the R packages ‘wgn.athaliana` and `wgntools`. Networks were visualized using Cytoscape (Shannon et al., 2003) or Mango Graph Studio (Chang et al., 2016). GO enrichment for network gene lists was performed using gProfileR (version 0.6.6).

Large scale Y2H screening for TF PPIs

Full length BES1, BES1 NPS (amino acids 1-267, lacking C-terminal activation domain), PLATZ (AT4G17900) and ARID-HMG1 (AT1G76110) were cloned into pENTR-D-TOPO and recombined with pDEST32 via Gateway cloning to generate TF-GAL4-BD fusions for Y2H screening. The pDEST32 constructs were sequence verified, transformed in to yeast strain MaV203 (Vidal et al., 1996) by the PEG method and selected using SD -Leu medium. Similarly, *E.coli* glycerol stocks containing TF-GAL4-AD fusions in pDEST22 were obtained from the ABRC (Pruneda-Paz et al., 2014), plasmid DNA purified by miniprep, and transformed into yeast strain MaV103 in 96 well plates using the PEG method, followed by selection on SD -Trp medium. Individual copies of the pDEST22 TF library in MaV103 were aliquoted and stored in -80°C until use.

High-throughput Y2H screens were performed by mating the MaV203 yeast strains containing the BES1, PLATZ or ARID-HMG1 GAL4-BD fusions with the pDEST22 TF library in MaV103. After mating, the diploid cells were cultured in SD-Trp-Leu liquid medium for 2 days. Cells were resuspended by vortexing and the optical density (OD) at 600nm was determined using a multi-mode plate reader (Eppendorf AF2200, Hamburg, Germany) to estimate yeast growth. β-galactosidase activity was assessed using a commercially-available luminescent β-galactosidase substrate Beta-Glo (Promega, E4740), which is cleaved to release D-luciferin as a firefly luciferase (LUC) substrate (de Almeida et al., 2008). The LUC values were normalized to the OD600 values to account for differences in yeast growth. The ratio was then normalized to the value obtained from the control pDEST22 for each plate. A total of three independent screens were conducted for BES1/BES1-NPS and two screens were conducted for PLATZ and ARID-HMG1. Data from the independent screens were then combined to calculate mean reporter activity. TFs with a mean reporter activity of 1.5-fold above the pDEST22 negative control were considered putative interactors.

BRZ response assays

For BRZ response experiments we sterilized seeds for 2-4 hours in a Nalgene Acrylic Desiccator Cabinet (Fisher Scientific, 08-642-22) by mixing 200mL bleach (8.25% sodium hypochlorite) with 8mL concentrated hydrochloric acid to generate chlorine gas. Seeds were then resuspended using 0.1% agarose solution for plating. Control (BRZ0; DMSO solvent only) or BRZ250 treated (250nM BRZ) 1/2 LS plates supplemented with 1% (w/v) sucrose were prepared using an auto pipette to dispense 24mL of media into 100mm x 100mm square polystyrene petri dishes (Scientific,

FB0875711A). For TF OE experiments 10μM Beta-estradiol was added to the ½ LS medium. After seeds were plated, the plates were sealed with breathable tape (3M Micropore) and stored in the dark at 4°C for at least 5 days. Plates were then exposed to light for 6-8 hours and wrapped in foil for 7 days of growth. We ensured that the hypocotyls of the plants were touching the agar surface for accurate length measurements. Plates were imaged with an Epson Perfection V600 Flatbed Photo scanner at a resolution of 1200 DPI. A dark background was obtained during imaging by placing a black box over the open scanner. Hypocotyls were then measured either in ImageJ, or using MATLAB, which produced comparable results across several independent users and images.

BL response assays

BL response assays were conducted similar to the BRZ experiments described above expect that the plants were grown for 7 days at 22°C under continuous light and control (DMSO solvent only) or BL100 (100nM BL) treatments were used.

Greenhouse PCZ response experiments

We performed PCZ response experiments in a greenhouse setting in the spring of 2017 using 105 mutants along with WT, *bri1-301* and *bes1-D* controls. The complete list of mutants is provided along with the phenotypic data in Tables S18 and S19. 3 of the mutants were *bes1-D* second-site suppressors from a genetic screen and will be described in a separate publication. Seeds were sterilized and grown for 5 days on ½ LS plates and then transferred to soil with water only (control) or 50μM PCZ solution (PCZ treatment; Syngenta Banner Maxx II). Control or PCZ treatments continued to be

used to water the soil when it became dry through the duration of the experiment (typically about twice per week). A total of 1,764 plants were transferred to 98 trays each containing 18 individual ~9cm square pots. The 98 flats were arranged in 14 columns and 7 rows. A total of 7 blocks derived by dividing the 14 columns into 7 pairs were present in the experimental design. Each column within a block was randomly assigned as control or PCZ treated. Each flat consisted of 15 mutants along with the WT, *bri1-301* and *bes1-D* controls. All 105 mutants were present once in each column with the arrangement of all genotypes in the experiment determined by the alpha lattice method. Therefore, a total of 7 biological repeats of the 105 mutants were planted for each treatment. WT, *bri1-301* and *bes1-D* had a total of 49 biological repeats for each treatment. A single plant was transferred to each pot on 03-14-2017. Plastic domes were used to cover the flats and were removed on 03-17-2017. Imaging was started on 3-22-2017 once cameras were positioned. A long day photoperiod of ~16 hours was maintained during the experiment by turning on the lights when the ambient light level became low.

RGB images were acquired in JPEG format with Nikon Coolpix S3700 cameras at a resolution of 5152 x 3864. The cameras were controlled using Raspberry Pi microcomputers and programmed to capture images every 30 minutes during the daytime hours. Imaging continued until 04-21-2017. Since fluctuating light conditions in the greenhouse presented a challenge for image processing and segmentation we first selected a single image from each camera for each day between 03-24-2017 to 04-04-2017. We used a semi-automated image processing pipeline implemented in MATLAB to extract the area and solidity of the plants after segmentation.

Additionally, we allowed the plants to grow to maturity while maintaining the control or PCZ treatments. We tied up the inflorescence of each plant with a wooden stake. Once all plants had matured, we used a yard stick to manually measure the height from the base of the rosette to the tallest point of the inflorescence (plant height). Temperature and light conditions were monitored every 5 minutes throughout the experiment using 9 Onset HOBO® UA-002 Pendant Temperature Light Data Loggers (Cat #UA-002-64) and the whole room temperature and light data were collected using the built in Argus system.

Drought and PCZ response using RoAD system

A RoAD (robotic assay for drought) system was developed to maintain plants at given treatments targets and carry out the image acquisition. The system contains two tables which can hold up to 240 individual pots and a custom-built robot with magnetic guide sensors. The robot is an unmanned ground vehicle (Shah et al., 2016) carrying a Universal Robots UR10 manipulator (Universal Robots, Odense, Denmark), which can move to and park at a specific position with magnetic tape guidance. It is also instrumented with a bench scale (Avery Weigh-Tronix BSQ High Resolution Bench Base, Model BSQ-0912-001 with Model ZM401 Stainless Steel IP69 Weight Indicator, RMH systems, Iowa, USA), which serves as an automated weighing and watering station. Each pot is weighted when placed over the balance, and a specific amount of prescribed liquid can be applied using a pump to reach a target weight. The UR10 manipulator, carrying an RGB camera (exo249CU3, SVS-VISTEK GMBH, 1920 × 1200 pixels resolution) and gripper (Robotiq, Quebec, Canada), allows the robot to pick an

individual pot on the table and place it on the watering station, the top-view image of the pot is then captured by the camera and stored in the local disk for further analysis.

For experiments on the RoAD system, plants were grown on ½ LS plates for 7 days and then transferred to pots containing equal amounts of soil. The exact mass of dry soil was determined for each experiment. Control (3g water per g dry soil), PCZ (3g water with 100μM PCZ added/g dry soil) or Drought (0.75g water per g dry soil) conditions were imposed by weighing plants each day. If a plant fell below the calculated target weight, then the robot added the water or PCZ solution until the target weight was restored. The plant genotypes and treatments were determined according to a complete randomized block design with 8 biological replicates per genotype/treatment combination. A 12 hour light/dark cycle was used to delay flowering. Humidity was maintained below 50% relative humidity using a commercial dehumidifier.

An automatic image processing pipeline was developed for plant segmentation and trait extraction. To segment plant images, the Excess Green Index (ExG) was used to create a gray-scale image, image binarization was then performed using Otsu's method and small holes filled. The binary image was used to mask the original RGB image to isolate plant pixels. For the plants under water-limited conditions, the leaves turn dark purple and the output mask from ExG is always incomplete. To fully extract drought plants (which usually grew inside the pot due to decreased growth), the Hough transformation was implemented to detect the circle of the pot and the partial image inside the circle was segmented. The new image was converted to HSV (hue-saturation-value) color-space and the hue channel was isolated and binarized. Spurious components that do not belong to the plant were removed using morphological erosion

and dilation. The two binary images from ExG and hue channel were then joined together to acquire the final masked image.

The following phenotypic parameters were calculated to quantify the plant growth:

Area: the area of the plant canopy, expressed in square centimeters. The value is measured from the 2D image by counting the number of the pixels and scaled by the pixel size.

Convex Area (CA): the area of the convex hull. The convex hull of a rosette corresponds to the smallest convex set that enclose the rosette.

Bounding Box Area (BBA): the area of the bounding box. The bounding box refers to the smallest rectangular that envelopes the rosette.

Perimeter: the perimeter of the convex hull.

Solidity: the ratio between the area of the rosette and the area of the associated convex hull.

Aspect Ratio (AR): the ratio between the width of the bounding box and the length of the bounding box.

Rectangularity: the ratio between the area of a rosette and the area of its bounding box.

Water withholding drought assays

Drought survival assays were performed by withholding water for 2-3 weeks to impose drought stress followed by rewatering. 5-7 days after rewatering plants were scored for survival as judged by the presence of new green leaves. Equal water and soil amounts were assured in drought assays by weighing the amount of dry soil for each

pot and watering with equal amounts of water. Pots were randomized within trays to control for the effect of position on water loss.

Co-immunoprecipitation

For Co-IP experiments protoplasts were prepared from *Arabidopsis* rosette leaves (Wu et al., 2009; Yoo et al., 2007) and transformed with 10μg of 35S:BES1-FLAG plasmid along with 15μg of 35S:PLATZ-GFP, 35S:ARID-HMG1-GFP or 35S:GUS-GFP by the PEG method. 2 reactions for each combination were pooled and immunoprecipitated in IP buffer (10mM HEPES, pH 7.5, 100mM NaCl, 1mM EDTA, 10% Glycerol, 1mM PMSF and one pellet of Roche Complete protease inhibitor cocktail tablets per 10 mL of buffer) with 0.1% triton and 2% NP-40. Samples were vortexed and rotated end-over-end for 10 minutes at 4°C and then diluted 5-fold using IP buffer without detergent. Following centrifugation at 16,000g for 10 minutes at 4°C, the supernatant was incubated with GFP-trap beads for 6 hours at 4°C. The beads were washed 3 times with IP buffer + 0.1% Triton, and protein was eluted by boiling in 2X SDS sample buffer. Western blotting was performed with anti-GFP (Nolan et al., 2017c) or anti-FLAG antibodies (Sigma, Cat# F7425).

BN-PAGE

For BN-PAGE experiments to investigate BES1 nuclear complexes, nuclei were isolated from ~1g of 7-day old dark-grown *bes1-D* or *BES1-RNAi* seedlings as previously described (Guo et al., 2018). Tissue was ground to a fine powder under liquid nitrogen and resuspended in 15mL Nuclear Lysis Buffer (20mM Tris-HCl, pH 7.4, 25%

Glycerol, 20mM KCl, 2mM EDTA, 2.5mM $MgCl_2$, 250mM Sucrose, 1mM DTT and 1mM PMSF), filtered through miracloth, then a 45 micron filter and centrifuged for 10 min at 1500g at 4°C. The pellet was resuspended in nuclei resuspension buffer (20mM Tris-HCl pH 7.4, 25% Glycerol, 2.5mM $MgCl_2$) with 0.2% Triton and centrifuged for 10 min at 1500g at 4°C. After two more washes, the nuclei were resuspended in resuspension buffer without Triton and spun for 10 min at 1500g at 4°C. Nuclei were lysed using high-salt buffer (20mM HEPES, pH 7.4, 10mM KCl, 420mM NaCl, 1.5mM $MgCl_2$, 100mM EDTA, 1mM DTT, 1mM PMSF and 25% Glycerol) on ice for 30 minutes with vortexing. Commassie G-250 was added to a final concentration of 0.25% and samples were run on 4-16% NativePAGE Bis-Tris gels according to the manufacturer's protocol (ThermoFisher, BN1002BOX). NativeMark Unstained Protein Standard (ThermoFisher, LC0725) was run alongside the samples to allow for molecular weight estimation. Following semi-wet transfer to PVDF membrane, western blotting was performed with anti-BES1 antibodies.

BiFC Assays

BiFC assays were conducted using constructs for the N- or C-terminus of YFP as previously described (Nolan et al., 2017c; Wang et al., 2014; Yu et al., 2008). BES1, PLATZ or ARID-HMG1 fused to YFP fragments were transformed into *Agrobacterium tumefaciens* (strain GV3101). Agrobacterium cultures were grown overnight in LB medium containing 200mM acetosyringone, washed with infiltration medium (10 mM MgCl2, 10 mM MES, pH 5.7, 200 mM acetosyringone) and resuspended to an OD600 of 1.0. The Agrobacterium containing indicated constructs were mixed in equal ratios and infiltrated into the lower surface of *N. benthamiana* leaves. After 36-48 hours, YFP

signal was detected using a Leica SP5 X MP confocal microscope equipped with an HCS PL APO CS 20.030.70 oil objective. YFP was excited with a 514-nm laser line and detected from 530 to 560 nm. Images were acquired with LAS AF software (Leica Microsystems) using identical settings for samples and controls.

BES1 ChIP-seq

BES1-YPet constructs were generated through recombineering (Alonso and Stepanova, 2015) and transformed into WT Col-0 via floral dip (Clough and Bent, 1998). Plants were selected using BASTA resistance and homozygous lines carrying BES1-YPet were identified and used for ChIP-seq. 3-day old BES1-Ypet or WT controls grown in air were subjected to ChIP using anti-GFP antibodies, sequencing and data processing as previously described (Song et al., 2016a; Song et al., 2016b).

RNA-seq

Seeds for the indicated genotypes were sterilized with 70% EtOH + 0.1% Triton for 15 minutes, washed with 100% EtOH 3 times and plated on ½ LS plates with DMSO or 2uM BRZ. After 5 days stratification at 4°C the plates were put in the light for 6 hours and then wrapped in foil for 7 days growth in darkness. Plants were exposed to weak light for less than 30 seconds before tissue was frozen in liquid Nitrogen. Total RNA was extracted using Zymo DirecZol kit (Zymo Research). RNA concentrations and quality were analyzed using AATI Fragment Analyzer with Standard Sensitivity RNA Analysis Kit (DNF-489-0500). Approximately 500ng of RNA was used for library construction via the QuantSeq 3’ mRNA-Seq Library Prep FWD Kit for Illumina and sequenced on an Illumina HiSeq 2500 (50bp single end reads). FASTQ files for each sample were subject to quality control, trimming and mapped to the Arabidopsis TAIR10

genome using the BlueBee *A. thaliana* (TAIR10) Lexogen QuantSeq 2.2.2 FWD pipeline. For differential expression analysis, the R package 'DEseq2' (Love et al., 2014) was used to test the null hypothesis that expression of a given gene is not different between two genotypes. This null hypothesis was tested using a model with a negative binomial distribution. P-values of all statistical tests were converted to adjusted p-values (q-values) (Benjamini and Hochberg, 1995). A false discovery rate of 10% (q-value) was used to account for multiple testing.

Venny (http://bioinfogp.cnb.csic.es/tools/venny/index.html) was used to visualize overlapping gene lists and significance of gene list intersections were tested using Fisher's exact test implemented in the GeneOverlap R package (version 1.2.0). Gene clustering and heatmaps were visualized using ComplexHeatmap in R (Gu et al., 2016). Promoter analysis was conducted using DREME (Bailey, 2011) with 1kb upstream sequences downloaded from https://www.arabidopsis.org/tools/bulk/sequences/index.jsp. All TAIR10 promoters were used as background when determining enrichment in promoter analysis.

3.8 References

Agresti, A., and Bianchi, M.E. (2003). HMGB proteins and gene expression. Current Opinion in Genetics & Development *13*, 170-178.

Aibar, S., González-Blas, C.B., Moerman, T., Huynh-Thu, V.A., Imrichova, H., Hulselmans, G., Rambow, F., Marine, J.-C., Geurts, P., Aerts, J.*, et al.* (2017). SCENIC: single-cell regulatory network inference and clustering. Nature Methods *14*, 1083.

Albihlal, W.S., Obomighie, I., Blein, T., Persad, R., Chernukhin, I., Crespi, M., Bechtold, U., and Mullineaux, P.M. (2018). Arabidopsis HEAT SHOCK TRANSCRIPTION FACTORA1b regulates multiple developmental genes under benign and stress conditions. J Exp Bot *69*, 2847-2862.

Alonso, J.M., and Stepanova, A.N. (2015). A recombineering-based gene tagging system for Arabidopsis. Methods in molecular biology *1227*, 233-243.

Alonso, J.M., Stepanova, A.N., Leisse, T.J., Kim, C.J., Chen, H.M., Shinn, P., Stevenson, D.K., Zimmerman, J., Barajas, P., Cheuk, R.*, et al.* (2003). Genome-wide Insertional mutagenesis of Arabidopsis thaliana. Science *301*, 653-657.

Aluru, M., Zola, J., Nettleton, D., and Aluru, S. (2013). Reverse engineering and analysis of large genome-scale gene networks. Nucleic acids research *41*, e24.

Antosch, M., Mortensen, S.A., and Grasser, K.D. (2012). Plant proteins containing high mobility group box DNA-binding domains modulate different nuclear processes. Plant Physiol *159*, 875-883.

Asami, T., Min, Y.K., Nagata, N., Yamagishi, K., Takatsuto, S., Fujioka, S., Murofushi, N., Yamaguchi, I., and Yoshida, S. (2000). Characterization of brassinazole, a triazole-type brassinosteroid biosynthesis inhibitor. Plant Physiology *123*, 93-99.

Bai, M.-Y., Fan, M., Oh, E., and Wang, Z.-Y. (2012a). A Triple Helix-Loop-Helix/Basic Helix-Loop-Helix Cascade Controls Cell Elongation Downstream of Multiple Hormonal and Environmental Signaling Pathways in Arabidopsis. Plant Cell *24*, 4917-4929.

Bai, M.-Y., Shang, J.-X., Oh, E., Fan, M., Bai, Y., Zentella, R., Sun, T.-p., and Wang, Z.-Y. (2012b). Brassinosteroid, gibberellin and phytochrome impinge on a common transcription module in Arabidopsis. Nature Cell Biology *14*, 810-U878.

Bailey, T.L. (2011). DREME: motif discovery in transcription factor ChIP-seq data. Bioinformatics *27*, 1653-1659.

Bartlett, A., O'Malley, R.C., Huang, S.-s.C., Galli, M., Nery, J.R., Gallavotti, A., and Ecker, J.R. (2017). Mapping genome-wide transcription-factor binding sites using DAP-seq. Nature Protocols *12*, 1659.

Benjamini, Y., and Hochberg, Y. (1995). Controlling the False Discovery Rate - a Practical and Powerful Approach to Multiple Testing. J Roy Stat Soc B Met *57*, 289-300.

Bernardo-Garcia, S., de Lucas, M., Martinez, C., Espinosa-Ruiz, A., Daviere, J.M., and Prat, S. (2014). BR-dependent phosphorylation modulates PIF4 transcriptional activity and shapes diurnal hypocotyl growth. Genes Dev *28*, 1681-1694.

Breuer, C., Kawamura, A., Ichikawa, T., Tominaga-Wada, R., Wada, T., Kondou, Y., Muto, S., Matsui, M., and Sugimoto, K. (2009). The trihelix transcription factor GTL1 regulates ploidy-dependent cell growth in the Arabidopsis trichome. Plant Cell *21*, 2307-2322.

Bu, Q., Jiang, H., Li, C.B., Zhai, Q., Zhang, J., Wu, X., Sun, J., Xie, Q., and Li, C. (2008). Role of the Arabidopsis thaliana NAC transcription factors ANAC019 and

ANAC055 in regulating jasmonic acid-signaled defense responses. Cell Res *18*, 756-767.

Cano-Delgado, A., Yin, Y.H., Yu, C., Vafeados, D., Mora-Garcia, S., Cheng, J.C., Nam, K.H., Li, J.M., and Chory, J. (2004). BRL1 and BRL3 are novel brassinosteroid receptors that function in vascular differentiation in Arabidopsis. Development *131*, 5341-5351.

Carles, C.C., Choffnes-Inada, D., Reville, K., Lertpiriyapong, K., and Fletcher, J.C. (2005). ULTRAPETALA1 encodes a SAND domain putative transcriptional regulator that controls shoot and floral meristem activity in Arabidopsis. Development *132*, 897-911.

Carles, C.C., and Fletcher, J.C. (2009). The SAND domain protein ULTRAPETALA1 acts as a trithorax group factor to regulate cell fate in plants. Genes Dev *23*, 2723-2728.

Castro, M.A., de Santiago, I., Campbell, T.M., Vaughn, C., Hickey, T.E., Ross, E., Tilley, W.D., Markowetz, F., Ponder, B.A., and Meyer, K.B. (2016). Regulators of genetic risk of breast cancer identified by integrative network analysis. Nat Genet *48*, 12-21.

Chaiwanon, J., and Wang, Z.Y. (2015). Spatiotemporal Brassinosteroid Signaling and Antagonism with Auxin Pattern Stem Cell Dynamics in Arabidopsis Roots. Curr. Biol. *25*, 1031-1042.

Chang, J., Cho, H., and Chou, H.H. (2016). Mango: combining and analyzing heterogeneous biological networks. BioData mining *9*, 25.

Chen, J., Nolan, T., Ye, H., Zhang, M., Tong, H., Xin, P., Chu, J., Chu, C., Li, Z., and Yin, Y. (2017). Arabidopsis WRKY46, WRKY54 and WRKY70 Transcription Factors Are Involved in Brassinosteroid-Regulated Plant Growth and Drought Response. The Plant Cell, tpc.00364.02017.

Chockalingam, S., Aluru, M., and Aluru, S. (2016). Microarray Data Processing Techniques for Genome-Scale Network Inference from Large Public Repositories. Microarrays *5*, 23.

Chockalingam, S.P., Aluru, M., Guo, H., Yin, Y., and Aluru, S. (2017). Reverse Engineering Gene Networks: A Comparative Study at Genome-scale. In Proceedings of the 8th ACM International Conference on Bioinformatics, Computational Biology,and Health Informatics (Boston, Massachusetts, USA, ACM), pp. 480-490.

Chung, Y., Kwon, S.I., and Choe, S. (2014). Antagonistic Regulation of Arabidopsis Growth by Brassinosteroids and Abiotic Stresses. Mol Cells *37*, 795-803.

Clough, S.J., and Bent, A.F. (1998). Floral dip: a simplified method for Agrobacterium-mediated transformation of Arabidopsis thaliana. Plant Journal *16*, 735-743.

Clouse, S.D. (2011). Brassinosteroid Signal Transduction: From Receptor Kinase Activation to Transcriptional Networks Regulating Plant Development. Plant Cell *23*, 1219-1230.

Clouse, S.D. (2016). Brassinosteroid/Abscisic Acid Antagonism in Balancing Growth and Stress. Developmental cell *38*, 118-120.

Clouse, S.D., Langford, M., and McMorris, T.C. (1996). A brassinosteroid-insensitive mutant in Arabidopsis thaliana exhibits multiple defects in growth and development. Plant Physiology *111*, 671-678.

Coego, A., Brizuela, E., Castillejo, P., Ruiz, S., Koncz, C., del Pozo, J.C., Pineiro, M., Jarillo, J.A., Paz-Ares, J., Leon, J.*, et al.* (2014). The TRANSPLANTA collection of Arabidopsis lines: a resource for functional analysis of transcription factors based on their conditional overexpression. The Plant journal : for cell and molecular biology *77*, 944-953.

de Almeida, R.A., Burgess, D., Shema, R., Motlekar, N., Napper, A.D., Diamond, S.L., and Pavitt, G.D. (2008). A Saccharomyces cerevisiae cell-based quantitative beta-galactosidase assay compatible with robotic handling and high-throughput screening. Yeast (Chichester, England) *25*, 71-76.

De Grauwe, L., Vandenbussche, F., Tietz, O., Palme, K., and Van Der Straeten, D. (2005). Auxin, ethylene and brassinosteroids: tripartite control of growth in the Arabidopsis hypocotyl. Plant Cell Physiol *46*, 827-836.

de Zélicourt, A., Synek, L., Saad, M.M., Alzubaidy, H., Jalal, R., Xie, Y., Andrés-Barrao, C., Rolli, E., Guerard, F., Mariappan, K.G.*, et al.* (2018). Ethylene induced plant stress tolerance by Enterobacter sp. SA187 is mediated by 2-keto-4-methylthiobutyric acid production. PLoS genetics *14*, e1007273.

Eubel, H., Braun, H.-P., and Millar, A. (2005). Blue-native PAGE in plants: a tool in analysis of protein-protein interactions. Plant Methods *1*, 11.

Fan, M., Bai, M.-Y., Kim, J.-G., Wang, T., Oh, E., Chen, L., Park, C.H., Son, S.-H., Kim, S.-K., Mudgett, M.B.*, et al.* (2014). The bHLH Transcription Factor HBI1 Mediates the Trade-Off between Growth and Pathogen-Associated Molecular Pattern-Triggered Immunity in Arabidopsis. Plant Cell *26*, 828-841.

Fletcher, M.N., Castro, M.A., Wang, X., de Santiago, I., O'Reilly, M., Chin, S.F., Rueda, O.M., Caldas, C., Ponder, B.A., Markowetz, F.*, et al.* (2013). Master regulators of FGFR2 signalling and breast cancer risk. Nat Commun *4*, 2464.

Friedrichsen, D.M., Nemhauser, J., Muramitsu, T., Maloof, J.N., Alonso, J., Ecker, J.R., Furuya, M., and Chory, J. (2002). Three redundant brassinosteroid early response

genes encode putative bHLH transcription factors required for normal growth. Genetics *162*, 1445-1456.

Fujita, M., Fujita, Y., Maruyama, K., Seki, M., Hiratsu, K., Ohme-Takagi, M., Tran, L.S., Yamaguchi-Shinozaki, K., and Shinozaki, K. (2004). A dehydration-induced NAC protein, RD26, is involved in a novel ABA-dependent stress-signaling pathway. Plant J *39*, 863-876.

Gallego-Bartolome, J., Minguet, E.G., Grau-Enguix, F., Abbas, M., Locascio, A., Thomas, S.G., Alabadi, D., and Blazquez, M.A. (2012). Molecular mechanism for the interaction between gibberellin and brassinosteroid signaling pathways in Arabidopsis. Proceedings of the National Academy of Sciences of the United States of America *109*, 13446-13451.

Gendron, J.M., Haque, A., Gendron, N., Chang, T., Asami, T., and Wang, Z.-Y. (2008). Chemical genetic dissection of brassinosteroid-ethylene interaction. Molecular Plant *1*, 368-379.

Gomez-Mena, C., and Sablowski, R. (2008). ARABIDOPSIS THALIANA HOMEOBOX GENE1 establishes the basal boundaries of shoot organs and controls stem growth. Plant Cell *20*, 2059-2072.

Gonzalez-Grandio, E., Poza-Carrion, C., Sorzano, C.O., and Cubas, P. (2013). BRANCHED1 promotes axillary bud dormancy in response to shade in Arabidopsis. Plant Cell *25*, 834-850.

Gou, X.P., Yin, H.J., He, K., Du, J.B., Yi, J., Xu, S.B., Lin, H.H., Clouse, S.D., and Li, J. (2012). Genetic Evidence for an Indispensable Role of Somatic Embryogenesis Receptor Kinases in Brassinosteroid Signaling. PLoS genetics *8*.

Gu, Z., Eils, R., and Schlesner, M. (2016). Complex heatmaps reveal patterns and correlations in multidimensional genomic data. Bioinformatics *32*, 2847-2849.

Guan, Q., Yue, X., Zeng, H., and Zhu, J. (2014). The Protein Phosphatase RCF2 and Its Interacting Partner NAC019 Are Critical for Heat Stress–Responsive Gene Regulation and Thermotolerance in Arabidopsis. Plant Cell *In press.*

Gui, J., Zheng, S., Liu, C., Shen, J., Li, J., and Li, L. (2016). OsREM4.1 Interacts with OsSERK1 to Coordinate the Interlinking between Abscisic Acid and Brassinosteroid Signaling in Rice. Developmental cell *38*, 201-213.

Guo, H., Li, L., Aluru, M., Aluru, S., and Yin, Y. (2013). Mechanisms and networks for brassinosteroid regulated gene expression. Current Opinion in Plant Biology *16*, 545-553.

Guo, H., Li, L., Ye, H., Yu, X., Algreen, A., and Yin, Y. (2009). Three related receptor-like kinases are required for optimal cell elongation in Arabidopsis thaliana. Proceedings of the National Academy of Sciences of the United States of America *106*, 7648-7653.

Guo, H., Nolan, T.M., Song, G., Liu, S., Xie, Z., Chen, J., Schnable, P.S., Walley, J.W., and Yin, Y. (2018). FERONIA Receptor Kinase Contributes to Plant Immunity by Suppressing Jasmonic Acid Signaling in Arabidopsis thaliana. Current biology.

Hansen, F.T., Madsen, C.K., Nordland, A.M., Grasser, M., Merkle, T., and Grasser, K.D. (2008). A Novel Family of Plant DNA-Binding Proteins Containing both HMG-Box and AT-Rich Interaction Domains. Biochemistry *47*, 13207-13214.

Hartwig, T., Corvalan, C., Best, N.B., Budka, J.S., Zhu, J.Y., Choe, S., and Schulz, B. (2012). Propiconazole Is a Specific and Accessible Brassinosteroid (BR) Biosynthesis Inhibitor for Arabidopsis and Maize. PLoS One *7*.

He, J.X., Gendron, J.M., Sun, Y., Gampala, S.S.L., Gendron, N., Sun, C.Q., and Wang, Z.Y. (2005). BZR1 is a transcriptional repressor with dual roles in brassinosteroid homeostasis and growth responses. Science *307*, 1634-1638.

He, J.X., Gendron, J.M., Yang, Y.L., Li, J.M., and Wang, Z.Y. (2002). The GSK3-like kinase BIN2 phosphorylates and destabilizes BZR1, a positive regulator of the brassinosteroid signaling pathway in Arabidopsis. Proceedings of the National Academy of Sciences of the United States of America *99*, 10185-10190.

He, Y., Zhang, H., Sun, Z., Li, J., Hong, G., Zhu, Q., Zhou, X., MacFarlane, S., Yan, F., and Chen, J. (2017). Jasmonic acid-mediated defense suppresses brassinosteroid-mediated susceptibility to Rice black streaked dwarf virus infection in rice. The New phytologist *214*, 388-399.

Hickman, R., Van Verk, M.C., Van Dijken, A.J.H., Mendes, M.P., Vroegop-Vos, I.A., Caarls, L., Steenbergen, M., Van der Nagel, I., Wesselink, G.J., Jironkin, A.*, et al.* (2017). Architecture and Dynamics of the Jasmonic Acid Gene Regulatory Network. Plant Cell *29*, 2086-2105.

Hu, Y., and Yu, D. (2014). BRASSINOSTEROID INSENSITIVE2 interacts with ABSCISIC ACID INSENSITIVE5 to mediate the antagonism of brassinosteroids to abscisic acid during seed germination in Arabidopsis. Plant Cell *26*, 4394-4408.

Huynh-Thu, V.A., Irrthum, A., Wehenkel, L., and Geurts, P. (2010). Inferring Regulatory Networks from Expression Data Using Tree-Based Methods. PLoS One *5*, e12776.
Jiang, P., Wang, H.F., Li, W., Zang, C.Z., Li, B., Wong, Y.L.J., Meyer, C., Liu, J.S., Aster, J.C., and Liu, X.S. (2015). Network analysis of gene essentiality in functional genomics experiments. Genome Biology *16*.

Jiang, Y., and Deyholos, M.K. (2009). Functional characterization of Arabidopsis NaCl-inducible WRKY25 and WRKY33 transcription factors in abiotic stresses. Plant Molecular Biology *69*, 91-105.

Kawakatsu, T., Huang, S.C., Jupe, F., Sasaki, E., Schmitz, R.J., Urich, M.A., Castanon, R., Nery, J.R., Barragan, C., He, Y*., et al.* (2016). Epigenomic Diversity in a Global Collection of Arabidopsis thaliana Accessions. Cell *166*, 492-505.

Kim, T.-W., Guan, S., Sun, Y., Deng, Z., Tang, W., Shang, J.-X., Sun, Y., Burlingame, A.L., and Wang, Z.-Y. (2009). Brassinosteroid signal transduction from cell-surface receptor kinases to nuclear transcription factors. Nature Cell Biology *11*, 1254-U1233.

Kulkarni, S.R., Vaneechoutte, D., Van de Velde, J., and Vandepoele, K. (2017). TF2Network: predicting transcription factor regulators and gene regulatory networks in Arabidopsis using publicly available binding site information. Nucleic acids research.

Li, B., Gaudinier, A., Tang, M., Taylor-Teeples, M., Nham, N.T., Ghaffari, C., Benson, D.S., Steinmann, M., Gray, J.A., Brady, S.M*., et al.* (2014). Promoter-Based Integration in Plant Defense Regulation. *166*, 1803-1820.

Li, J., Nagpal, P., Vitart, V., McMorris, T.C., and Chory, J. (1996). A role for brassinosteroids in light-dependent development of *Arabidopsis*. Science *272*, 398-401.

Li, J., Wen, J.Q., Lease, K.A., Doke, J.T., Tax, F.E., and Walker, J.C. (2002). BAK1, an Arabidopsis LRR receptor-like protein kinase, interacts with BRI1 and modulates brassinosteroid signaling. Cell *110*, 213-222.

Li, J.M., and Chory, J. (1997). A putative leucine-rich repeat receptor kinase involved in brassinosteroid signal transduction. Cell *90*, 929-938.

Li, L., Ye, H., Guo, H., and Yin, Y. (2010). Arabidopsis IWS1 interacts with transcription factor BES1 and is involved in plant steroid hormone brassinosteroid regulated gene expression. Proceedings of the National Academy of Sciences of the United States of America *107*, 3918-3923.

Li, L., Yu, X., Thompson, A., Guo, M., Yoshida, S., Asami, T., Chory, J., and Yin, Y. (2009a). Arabidopsis MYB30 is a direct target of BES1 and cooperates with BES1 to regulate brassinosteroid-induced gene expression. Plant Journal *58*, 275-286.

Li, S., Fu, Q., Huang, W., and Yu, D. (2009b). Functional analysis of an Arabidopsis transcription factor WRKY25 in heat stress. Plant Cell Reports *28*, 683-693.

Love, M.I., Huber, W., and Anders, S. (2014). Moderated estimation of fold change and dispersion for RNA-seq data with DESeq2. Genome biology *15*, 550.

Lozano-Duran, R., Macho, A.P., Boutrot, F., Segonzac, C., Somssich, I.E., and Zipfel, C. (2013). The transcriptional regulator BZR1 mediates trade-off between plant innate immunity and growth. Elife *2*.

Lu, F., Cui, X., Zhang, S., Jenuwein, T., and Cao, X. (2011). Arabidopsis REF6 is a histone H3 lysine 27 demethylase. Nat Genet *43*, 715-719.

Malinovsky, F.G., Batoux, M., Schwessinger, B., Youn, J.H., Stransfeld, L., Win, J., Kim, S.K., and Zipfel, C. (2014). Antagonistic Regulation of Growth and Immunity by the Arabidopsis Basic Helix-Loop-Helix Transcription Factor HOMOLOG OF BRASSINOSTEROID ENHANCED EXPRESSION2 INTERACTING WITH INCREASED LEAF INCLINATION1 BINDING bHLH1. Plant Physiology *164*, 1443-1455.

Margolin, A.A., Wang, K., Lim, W.K., Kustagi, M., Nemenman, I., and Califano, A. (2006). Reverse engineering cellular networks. Nat Protoc *1*, 662-671.

Maruyama, K., Takeda, M., Kidokoro, S., Yamada, K., Sakuma, Y., Urano, K., Fujita, M., Yoshiwara, K., Matsukura, S., Morishita, Y.*, et al.* (2009). Metabolic Pathways Involved in Cold Acclimation Identified by Integrated Analysis of Metabolites and Transcripts Regulated by DREB1A and DREB2A. Plant Physiology *150*, 1972-1980.

Nagano, Y., Furuhashi, H., Inaba, T., and Sasaki, Y. (2001). A novel class of plant-specific zinc-dependent DNA-binding protein that binds to A/T-rich DNA sequences. Nucleic acids research *29*, 4097-4105.

Nakashima, K., Takasaki, H., Mizoi, J., Shinozaki, K., and Yamaguchi-Shinozaki, K. (2012). NAC transcription factors in plant abiotic stress responses. Biochim Biophys Acta *1819*, 97-103.

Nam, K.H., and Li, J.M. (2002). BRI1/BAK1, a receptor kinase pair mediating brassinosteroid signaling. Cell *110*, 203-212.

Niwa, M., Daimon, Y., Kurotani, K.-i., Higo, A., Pruneda-Paz, J.L., Breton, G., Mitsuda, N., Kay, S.A., Ohme-Takagi, M., Endo, M.*, et al.* (2013). BRANCHED1 Interacts with FLOWERING LOCUS T to Repress the Floral Transition of the Axillary Meristems in Arabidopsis. The Plant Cell *25*, 1228-1242.

Noguchi, T., Fujioka, S., Takatsuto, S., Sakurai, A., Yoshida, S., Li, J.M., and Chory, J. (1999). Arabidopsis det2 is defective in the conversion of (24R)-24-methylcholest-4-En-3-One to (24R)-24-methyl-5 alpha-cholestan-3-one in brassinosteroid biosynthesis. Plant Physiology *120*, 833-839.

Nolan, T., Chen, J., and Yin, Y. (2017a). Cross-talk of Brassinosteroid signaling in controlling growth and stress responses. Biochem J *474*, 2641-2661.

Nolan, T., Liu, S., Guo, H., Li, L., Schnable, P., and Yin, Y. (2017b). Identification of Brassinosteroid Target Genes by Chromatin Immunoprecipitation Followed by High-Throughput Sequencing (ChIP-seq) and RNA-Sequencing. In Brassinosteroids: Methods and Protocols, E. Russinova, and A.I. Caño-Delgado, eds. (New York, NY: Springer New York), pp. 63-79.

Nolan, T.M., Brennan, B., Yang, M., Chen, J., Zhang, M., Li, Z., Wang, X., Bassham, D.C., Walley, J., and Yin, Y. (2017c). Selective Autophagy of BES1 Mediated by DSK2 Balances Plant Growth and Survival. Developmental cell *41*, 33-46 e37.

O'Malley, R.C., Huang, S.S., Song, L., Lewsey, M.G., Bartlett, A., Nery, J.R., Galli, M., Gallavotti, A., and Ecker, J.R. (2016). Cistrome and Epicistrome Features Shape the Regulatory DNA Landscape. Cell *165*, 1280-1292.

Oh, E., Zhu, J.-Y., Bai, M.-Y., Arenhart, R.A., Sun, Y., and Wang, Z.-Y. (2014). Cell elongation is regulated through a central circuit of interacting transcription factors in the Arabidopsis hypocotyl. Elife *3*.

Oh, E., Zhu, J.-Y., and Wang, Z.-Y. (2012). Interaction between BZR1 and PIF4 integrates brassinosteroid and environmental responses. Nature Cell Biology *14*, 802-U864.

Park, S., Lee, C.-M., Doherty, C.J., Gilmour, S.J., Kim, Y., and Thomashow, M.F. (2015). Regulation of the Arabidopsis CBF regulon by a complex low-temperature regulatory network. The Plant Journal *82*, 193-207.

Pruneda-Paz, J.L., Breton, G., Nagel, D.H., Kang, S.E., Bonaldi, K., Doherty, C.J., Ravelo, S., Galli, M., Ecker, J.R., and Kay, S.A. (2014). A genome-scale resource for the functional characterization of Arabidopsis transcription factors. Cell Rep *8*, 622-632.

Pu, L., Liu, M.S., Kim, S.Y., Chen, L.F., Fletcher, J.C., and Sung, Z.R. (2013). EMBRYONIC FLOWER1 and ULTRAPETALA1 Act Antagonistically on Arabidopsis Development and Stress Response. Plant Physiol *162*, 812-830.

Rasheed, S., Bashir, K., Matsui, A., Tanaka, M., and Seki, M. (2016). Transcriptomic Analysis of Soil-Grown Arabidopsis thaliana Roots and Shoots in Response to a Drought Stress. Frontiers in Plant Science *7*, 180.

Schweizer, F., Fernandez-Calvo, P., Zander, M., Diez-Diaz, M., Fonseca, S., Glauser, G., Lewsey, M.G., Ecker, J.R., Solano, R., and Reymond, P. (2013). Arabidopsis basic helix-loop-helix transcription factors MYC2, MYC3, and MYC4 regulate glucosinolate biosynthesis, insect performance, and feeding behavior. Plant Cell *25*, 3117-3132.

Shah, D., Tang, L., Gai, J., and Putta-Venkata, R. (2016). Development of a Mobile Robotic Phenotyping System for Growth Chamber-based Studies of Genotype x Environment Interactions. IFAC-PapersOnLine *49*, 248-253.

Shahnejat-Bushehri, S., Tarkowska, D., Sakuraba, Y., and Balazadeh, S. (2016). Arabidopsis NAC transcription factor JUB1 regulates GA/BR metabolism and signalling. Nat Plants *2*, 16013.

Shani, E., Salehin, M., Zhang, Y., Sanchez, S.E., Doherty, C., Wang, R., Mangado, C.C., Song, L., Tal, I., Pisanty, O.*, et al.* (2017). Plant Stress Tolerance Requires Auxin-Sensitive Aux/IAA Transcriptional Repressors. Current biology : CB *27*, 437-444.

Shannon, P., Markiel, A., Ozier, O., Baliga, N.S., Wang, J.T., Ramage, D., Amin, N., Schwikowski, B., and Ideker, T. (2003). Cytoscape: a software environment for integrated models of biomolecular interaction networks. Genome Res *13*, 2498-2504.

Shibata, M., Breuer, C., Kawamura, A., Clark, N.M., Rymen, B., Braidwood, L., Morohashi, K., Busch, W., Benfey, P.N., Sozzani, R.*, et al.* (2018). GTL1 and DF1 regulate root hair growth through transcriptional repression of ROOT HAIR DEFECTIVE 6-LIKE 4 in Arabidopsis. Development *145*.

Shin, S.Y., Chung, H., Kim, S.Y., and Nam, K.H. (2016). BRI1-EMS-suppressor 1 gain-of-function mutant shows higher susceptibility to necrotrophic fungal infection. Biochemical and biophysical research communications *470*, 864-869.

Singh, A.P., and Savaldi-Goldstein, S. (2015). Growth control: brassinosteroid activity gets context. J. Exp. Bot. *66*, 1123-1132.

So, H.-A., Choi, S.J., Chung, E., and Lee, J.-H. (2015). Molecular characterization of stress-inducible PLATZ gene from soybean (Glycine max L.). Plant Omics *8*, 479-484.

Song, L., Huang, S.C., Wise, A., Castanon, R., Nery, J.R., Chen, H., Watanabe, M., Thomas, J., Bar-Joseph, Z., and Ecker, J.R. (2016a). A transcription factor hierarchy defines an environmental stress response network. Science *354*.

Song, L., Koga, Y., and Ecker, J.R. (2016b). Profiling of Transcription Factor Binding Events by Chromatin Immunoprecipitation Sequencing (ChIP-seq). In Current Protocols in Plant Biology (John Wiley & Sons, Inc.).

Sparks, E.E., Drapek, C., Gaudinier, A., Li, S., Ansariola, M., Shen, N., Hennacy, J.H., Zhang, J., Turco, G., Petricka, J.J.*, et al.* (2016). Establishment of Expression in the SHORTROOT-SCARECROW Transcriptional Cascade through Opposing Activities of Both Activators and Repressors. Developmental cell *39*, 585-596.

Sun, Y., Fan, X.-Y., Cao, D.-M., Tang, W., He, K., Zhu, J.-Y., He, J.-X., Bai, M.-Y., Zhu, S., Oh, E.*, et al.* (2010). Integration of Brassinosteroid Signal Transduction with the Transcription Network for Plant Growth Regulation in Arabidopsis. Developmental Cell *19*, 765-777.

Szekeres, M., Németh, K., Koncz-Kálmán, Z., Mathur, J., Kauschmann, A., Altmann, T., Rédei, G.P., Nagy, F., Schell, J., and Koncz, C. (1996). Brassinosteroids rescue the deficiency of CYP90, a cytochrome P450, controlling cell elongation and de-etiolation in *Arabidopsis*. Cell *85*, 171-182.

Tang, W., Yuan, M., Wang, R., Yang, Y., Wang, C., Oses-Prieto, J.A., Kim, T.-W., Zhou, H.-W., Deng, Z., Gampala, S.S.*, et al.* (2011). PP2A activates brassinosteroid-responsive gene expression and plant growth by dephosphorylating BZR1. Nature Cell Biology *13*, 124-U149.

Taylor-Teeples, M., Lin, L., de Lucas, M., Turco, G., Toal, T.W., Gaudinier, A., Young, N.F., Trabucco, G.M., Veling, M.T., Lamothe, R.*, et al.* (2015). An Arabidopsis gene regulatory network for secondary cell wall synthesis. Nature *517*, 571-575.

Tian, Y., Fan, M., Qin, Z., Lv, H., Wang, M., Zhang, Z., Zhou, W., Zhao, N., Li, X., Han, C.*, et al.* (2018). Hydrogen peroxide positively regulates brassinosteroid signaling through oxidation of the BRASSINAZOLE-RESISTANT1 transcription factor. Nat Commun *9*, 1063.

Tong, H.N., Xiao, Y.H., Liu, D.P., Gao, S.P., Liu, L.C., Yin, Y.H., Jin, Y., Qian, Q., and Chu, C.C. (2014). Brassinosteroid Regulates Cell Elongation by Modulating Gibberellin Metabolism in Rice. Plant Cell *26*, 4376-4393.

Tran, L.S., Nakashima, K., Sakuma, Y., Simpson, S.D., Fujita, Y., Maruyama, K., Fujita, M., Seki, M., Shinozaki, K., and Yamaguchi-Shinozaki, K. (2004). Isolation and functional analysis of Arabidopsis stress-inducible NAC transcription factors that bind to a drought-responsive cis-element in the early responsive to dehydration stress 1 promoter. Plant Cell *16*, 2481-2498.

Trigg, S.A., Garza, R.M., MacWilliams, A., Nery, J.R., Bartlett, A., Castanon, R., Goubil, A., Feeney, J., O'Malley, R., Huang, S.C.*, et al.* (2017). CrY2H-seq: a massively multiplexed assay for deep-coverage interactome mapping. Nat Methods *14*, 819-825.

Unterholzner, S.J., Rozhon, W., Papacek, M., Ciomas, J., Lange, T., Kugler, K.G., Mayer, K.F., Sieberer, T., and Poppenberger, B. (2015). Brassinosteroids Are Master Regulators of Gibberellin Biosynthesis in Arabidopsis. Plant Cell *27*, 2261-2272.

Vert, G., Walcher, C.L., Chory, J., and Nemhauser, J.L. (2008). Integration of auxin and brassinosteroid pathways by Auxin Response Factor 2. Proceedings of the National Academy of Sciences of the United States of America *105*, 9829-9834.

Vidal, M., Brachmann, R.K., Fattaey, A., Harlow, E., and Boeke, J.D. (1996). Reverse two-hybrid and one-hybrid systems to detect dissociation of protein-protein and DNA-protein interactions. Proc Natl Acad Sci U S A *93*, 10315-10320.

Vilarrasa-Blasi, J., González-García, M.-P., Frigola, D., Fàbregas-Vallvé, N., Alexiou, Konstantinos G., López-Bigas, N., Rivas, S., Jauneau, A., Lohmann, Jan U., Benfey, Philip N.*, et al.* (2015). Regulation of Plant Stem Cell Quiescence by a Brassinosteroid Signaling Module. Developmental cell *33*, 238.

Vilarrasa-Blasi, J., Gonzalez-Garcia, M.P., Frigola, D., Fabregas, N., Alexiou, K.G., Lopez-Bigas, N., Rivas, S., Jauneau, A., Lohmann, J.U., Benfey, P.N.*, et al.* (2014). Regulation of Plant Stem Cell Quiescence by a Brassinosteroid Signaling Module. Developmental cell *30*, 36-47.

Vragovic, K., Sela, A., Friedlander-Shani, L., Fridman, Y., Hacham, Y., Holland, N., Bartom, E., Mockler, T.C., and Savaldi-Goldstein, S. (2015). Translatome analyses capture of opposing tissue-specific brassinosteroid signals orchestrating root meristem differentiation. Proceedings of the National Academy of Sciences of the United States of America *112*, 923-928.

Wang, X.L., Chen, J.N., Xie, Z.L., Liu, S.Z., Nolan, T., Ye, H.X., Zhang, M.C., Guo, H.Q., Schnable, P.S., Li, Z.H.*, et al.* (2014). Histone Lysine Methyltransferase SDG8 Is Involved in Brassinosteroid-Regulated Gene Expression in Arabidopsis thaliana. Molecular Plant *7*, 1303-1315.

Wang, Y., Sun, S., Zhu, W., Jia, K., Yang, H., and Wang, X. (2013). Strigolactone/MAX2-induced degradation of brassinosteroid transcriptional effector BES1 regulates shoot branching. Developmental cell *27*, 681-688.

Wang, Z.Y., Nakano, T., Gendron, J., He, J.X., Chen, M., Vafeados, D., Yang, Y.L., Fujioka, S., Yoshida, S., Asami, T.*, et al.* (2002). Nuclear-localized BZR1 mediates brassinosteroid-induced growth and feedback suppression of brassinosteroid biosynthesis. Developmental cell *2*, 505-513.

Wu, F.-H., Shen, S.-C., Lee, L.-Y., Lee, S.-H., Chan, M.-T., and Lin, C.-S. (2009). Tape-Arabidopsis Sandwich - a simpler Arabidopsis protoplast isolation method. Plant Methods *5*.

Xie, M., Chen, H., Huang, L., O'Neil, R.C., Shokhirev, M.N., and Ecker, J.R. (2018). A B-ARR-mediated cytokinin transcriptional network directs hormone cross-regulation and shoot development. Nature Communications *9*, 1604.

Xu, W.H., Huang, J., Li, B.H., Li, J.Y., and Wang, Y.H. (2008). Is kinase activity essential for biological functions of BRI1? Cell Research *18*, 472-478.

Ye, H., Li, L., Guo, H., and Yin, Y. (2012). MYBL2 is a substrate of GSK3-like kinase BIN2 and acts as a corepressor of BES1 in brassinosteroid signaling pathway in Arabidopsis. Proceedings of the National Academy of Sciences of the United States of America *109*, 20142-20147.

Ye, H., Liu, S., Tang, B., Chen, J., Xie, Z., Nolan, T.M., Jiang, H., Guo, H., Lin, H.-Y., Li, L.*, et al.* (2017). RD26 mediates crosstalk between drought and brassinosteroid signalling pathways. Nature Communications *8*, 14573.

Yin, Y., Vafeados, D., Tao, Y., Yoshida, S., Asami, T., and Chory, J. (2005). A new class of transcription factors mediates brassinosteroid-regulated gene expression in Arabidopsis. Cell *120*, 249-259.

Yin, Y.H., Wang, Z.Y., Mora-Garcia, S., Li, J.M., Yoshida, S., Asami, T., and Chory, J. (2002). BES1 accumulates in the nucleus in response to brassinosteroids to regulate gene expression and promote stem elongation. Cell *109*, 181-191.

Yoo, C.Y., Pence, H.E., Jin, J.B., Miura, K., Gosney, M.J., Hasegawa, P.M., and Mickelbart, M.V. (2010). The Arabidopsis GTL1 transcription factor regulates water use efficiency and drought tolerance by modulating stomatal density via transrepression of SDD1. Plant Cell *22*, 4128-4141.

Yoo, S.D., Cho, Y.H., and Sheen, J. (2007). Arabidopsis mesophyll protoplasts: a versatile cell system for transient gene expression analysis. Nat Protoc *2*, 1565-1572.

Yu, X., Li, L., Li, L., Guo, M., Chory, J., and Yin, Y. (2008). Modulation of brassinosteroid-regulated gene expression by jumonji domain-containing proteins ELF6 and REF6 in Arabidopsis. Proceedings of the National Academy of Sciences of the United States of America *105*, 7618-7623.

Yu, X., Li, L., Zola, J., Aluru, M., Ye, H., Foudree, A., Guo, H., Anderson, S., Aluru, S., Liu, P.*, et al.* (2011). A brassinosteroid transcriptional network revealed by genome-wide identification of BESI target genes in Arabidopsis thaliana. Plant Journal *65*, 634-646.

Zhang, D., Ye, H., Guo, H., Johnson, A., Zhang, M., Lin, H., and Yin, Y. (2014). Transcription factor HAT1 is phosphorylated by BIN2 kinase and mediates brassinosteroid repressed gene expression in Arabidopsis. Plant Journal *77*, 59-70.

Zhang, F., Wang, L., Ko, E.E., Shao, K., and Qiao, H. (2018). Histone Deacetylases SRT1 and SRT2 Interact with ENAP1 to Mediate Ethylene-Induced Transcriptional Repression. Plant Cell *30*, 153-166.

Zhang, S., Cai, Z., and Wang, X. (2009). The primary signaling outputs of brassinosteroids are regulated by abscisic acid signaling. Proc Natl Acad Sci U S A *106*, 4543-4548.

Zheng, X.Y., Spivey, N.W., Zeng, W., Liu, P.P., Fu, Z.Q., Klessig, D.F., He, S.Y., and Dong, X. (2012). Coronatine promotes Pseudomonas syringae virulence in plants by activating a signaling cascade that inhibits salicylic acid accumulation. Cell Host Microbe *11*, 587-596.

Zheng, Z., Mosher, S.L., Fan, B., Klessig, D.F., and Chen, Z. (2007). Functional analysis of Arabidopsis WRKY25 transcription factor in plant defense against Pseudomonas syringae. BMC Plant Biology *7*, 2.

Zhou, X.Y., Song, L., and Xue, H.W. (2013). Brassinosteroids regulate the differential growth of Arabidopsis hypocotyls through auxin signaling components IAA19 and ARF7. Mol Plant *6*, 887-904.

3.9 Figures and Tables

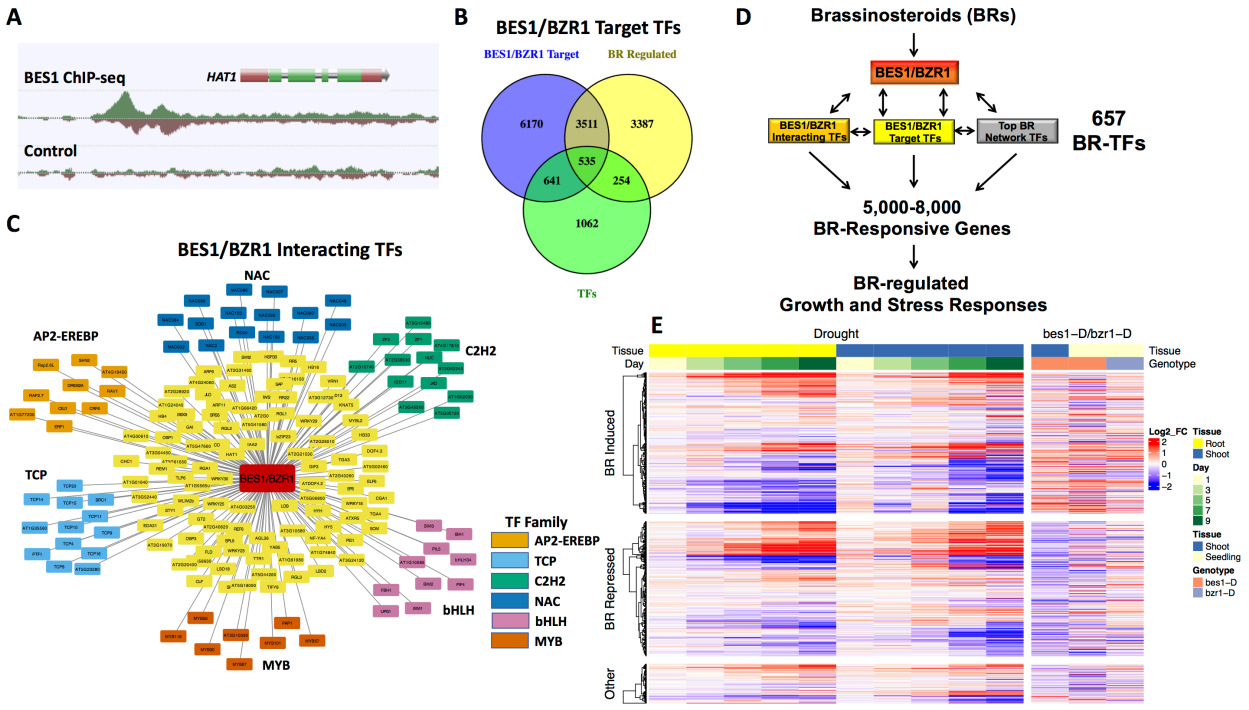

Figure 1: Identification of 657 BR-related transcription factors (BR-TFs)
(A) Example of BES1 binding to promoter region of a TF from ChIP-seq with BES1-YPet in 3-day-old dark grown seedlings.
(B) Comparison of BES1/BZR1 ChIP targets and BR regulated genes identifies 535 BES1/BZR1 Target TFs (BTFs).
(C) 169 putative BES1/BZR1 interacting TFs. Colors indicate select TF families. Other families are yellow.
(D) 657 BR-TFs likely function along with BES1/BZR1 to allow BRs to control 5000-8000 BR responsive genes. Top BR network TFs may also be regulated directly by BRs, rather than through BES1/BZR1 (not shown).
(E) Clustering analysis of *BR-TF* gene expression in response to drought or in *bes1-D* or *bzr1-D* mutants. The row dendrogram was obtained by hierarchical clustering of each indicated group of BR-TFs. Red/Blue color of the heatmap indicates log2 fold change (log2_FC). Day indicates the number of days drought treatment. Other colors are as indicated in the legend.

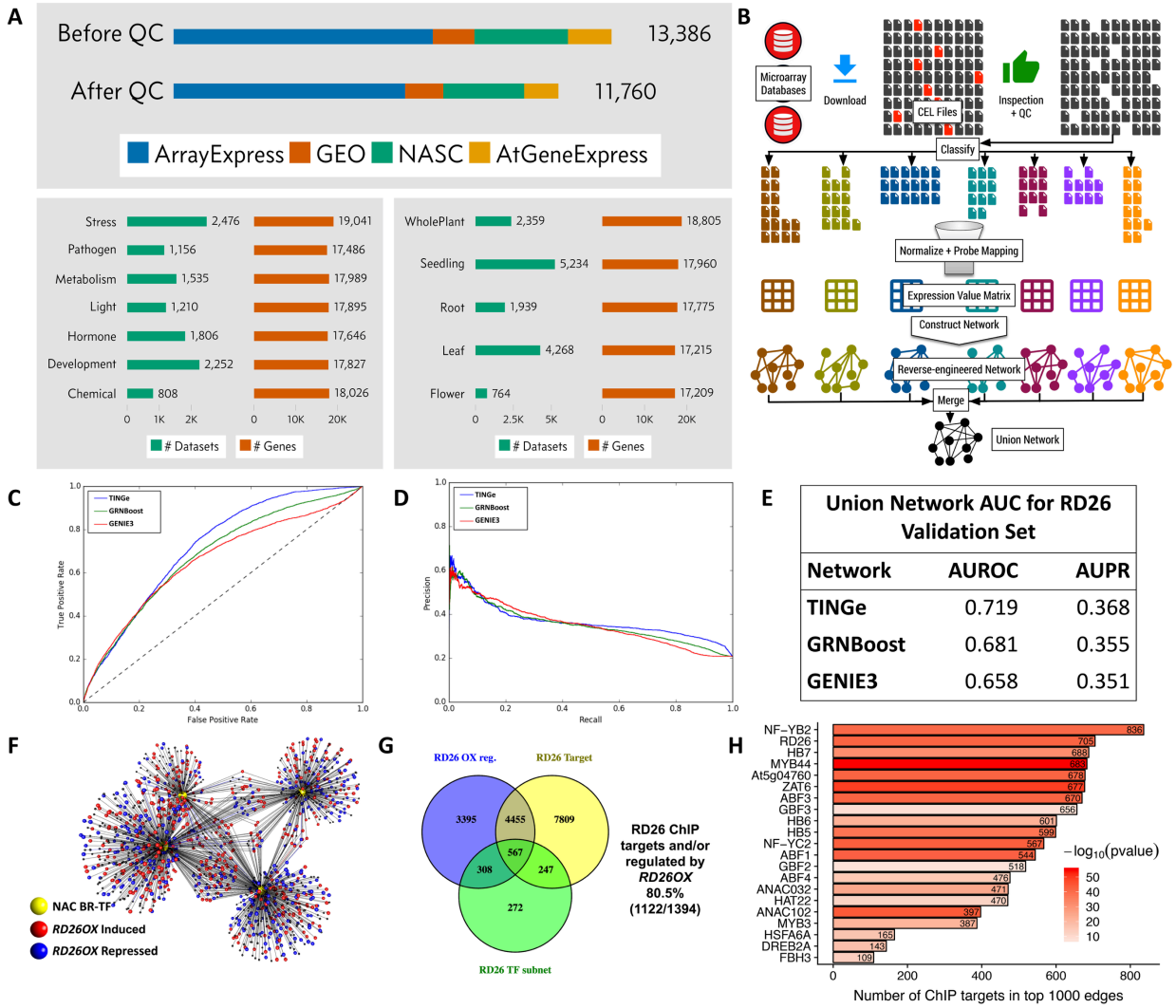

Figure 2: Construction and validation of GRNs from 11,760 transcriptome datasets

(A) Overview of transcriptome datasets used for GRN construction. Number of data sets before and after quality control (QC) are indicated. Datasets were categorized into seven process specific categories (lower left) or five tissue specific categories (lower right). The number of datasets and genes for each category is shown.

(B) Pipeline for GRN data processing and construction. Diagram reused from (Chockalingam et al., 2016) under Creative Commons Attribution License.

(C) AUROC traces for TINGe, GENIE3 or GRNBoost union networks using RD26 genes bound in ChIP-seq and regulated in RNA-seq as a benchmark.

(D) AUPR traces as described in (C).

(E) AUC values from (C) and (D) for the indicated networks.

(F) Subnetwork of RD26 and close homologs (NAC019, NAC055, NAC102) from TINGe union GRN. Legend indicates labeling of nodes based on *RD26 OX RNA-seq* regulation.

(G) Number of genes in RD26 subnetwork from (F) that are present in RD26 RNA-seq (left) or ChIP-seq (right) datasets. The total number of genes in the subnetwork that are present in RNA-seq or ChIP-seq datasets is indicated.

(H) Number of the top 1000 edges of TINGe union GRN experimentally validated from ChIP-seq data for each TF. Color indicates p-values from Fisher's exact test.

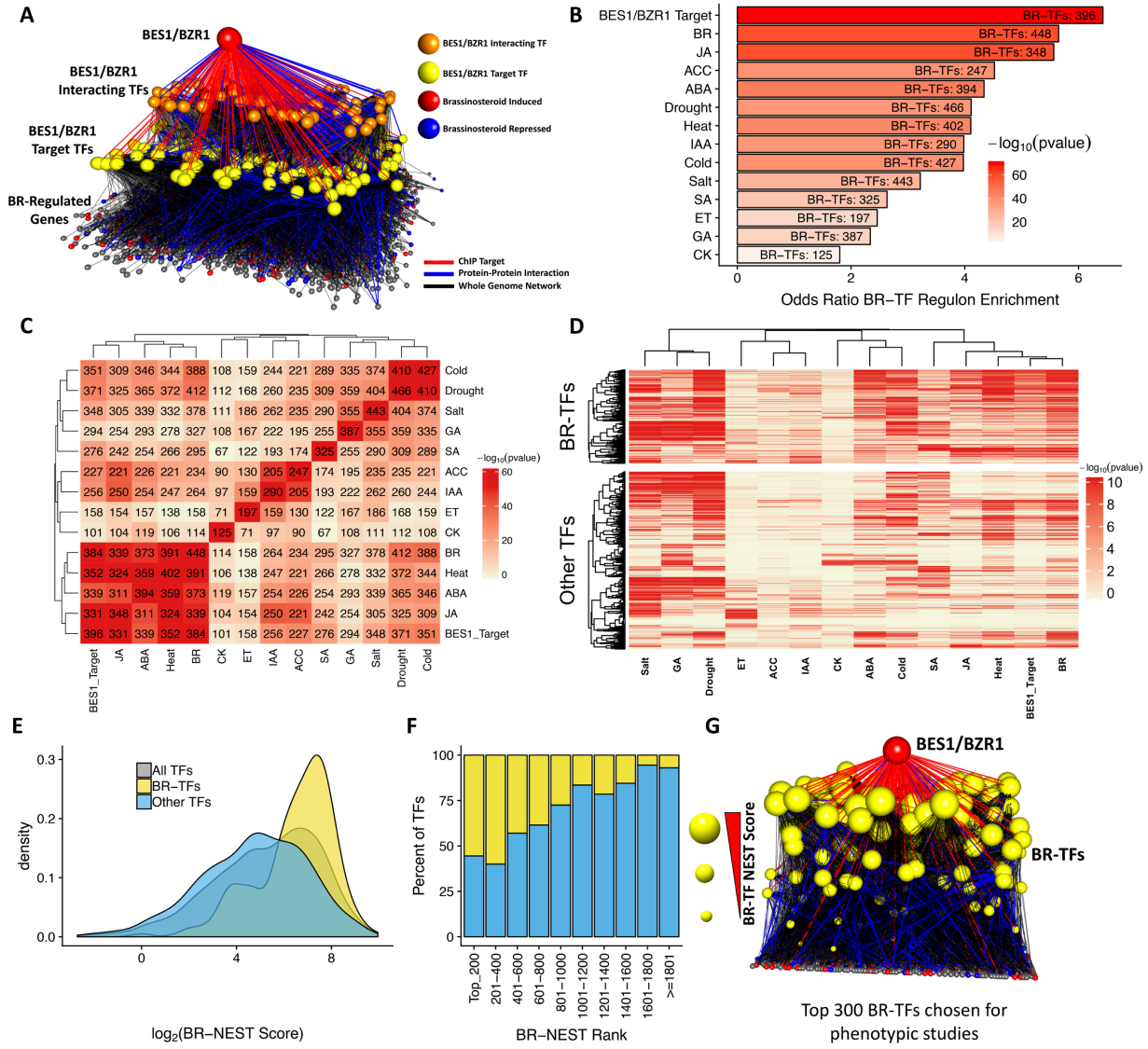

Figure 3: Analysis of BR-TF subnetworks

(A) BR-TF subnetwork showing BES1/BZR1 ChIP targets, TF PPIs and edges from TINGe union GRN. BES1 and BZR1 are labeled as BES1 for simplicity.
(B) Enrichment of BR-TFs for the indicated gene sets from Master Regulator Analysis (MRA). Numbers indicate how many BR-TFs have significant enrichment. p-values and odds ratios are from Fisher's exact test contrasting the number of significant BR-TFs vs. total significant TFs for each gene set.
(C) Intersection of significant BR-TFs from MRA. p-values are from Fisher's exact test for each intersection. Dendrogram was obtained by hierarchical clustering.
(D) Clustering of TFs from MRA. Each row represents a TF and each column a gene list assessed for enrichment in the MRA. MRA p-values for each TF are indicated by color.
(E) Distribution of BR-NEST scores among BR-TFs, other TFs (non-BR-TFs) and all TFs.
(F) Percentage of BR-TFs vs. other TFs based on BR-NEST rank. TFs are binned in groups of 200 according to BR-NEST.
(G) Subnetwork showing BES1/BZR1 and BR-TFs. Height and size of BR-TF nodes indicates BR-NEST scores used to prioritize BR-TFs for functional studies.

A

Line Type	Total Lines Tested	Number of Plants	Total TFs	BR Phenotype
Mutant BL response	316	28,211	300	80/300 TFs (26.7%)
Mutant BRZ response	311	19,640	296	93/296 TFs (31.4%)
Overexpression (OE) BRZ response	696	21,430	269	170/269 TFs (63.2%)

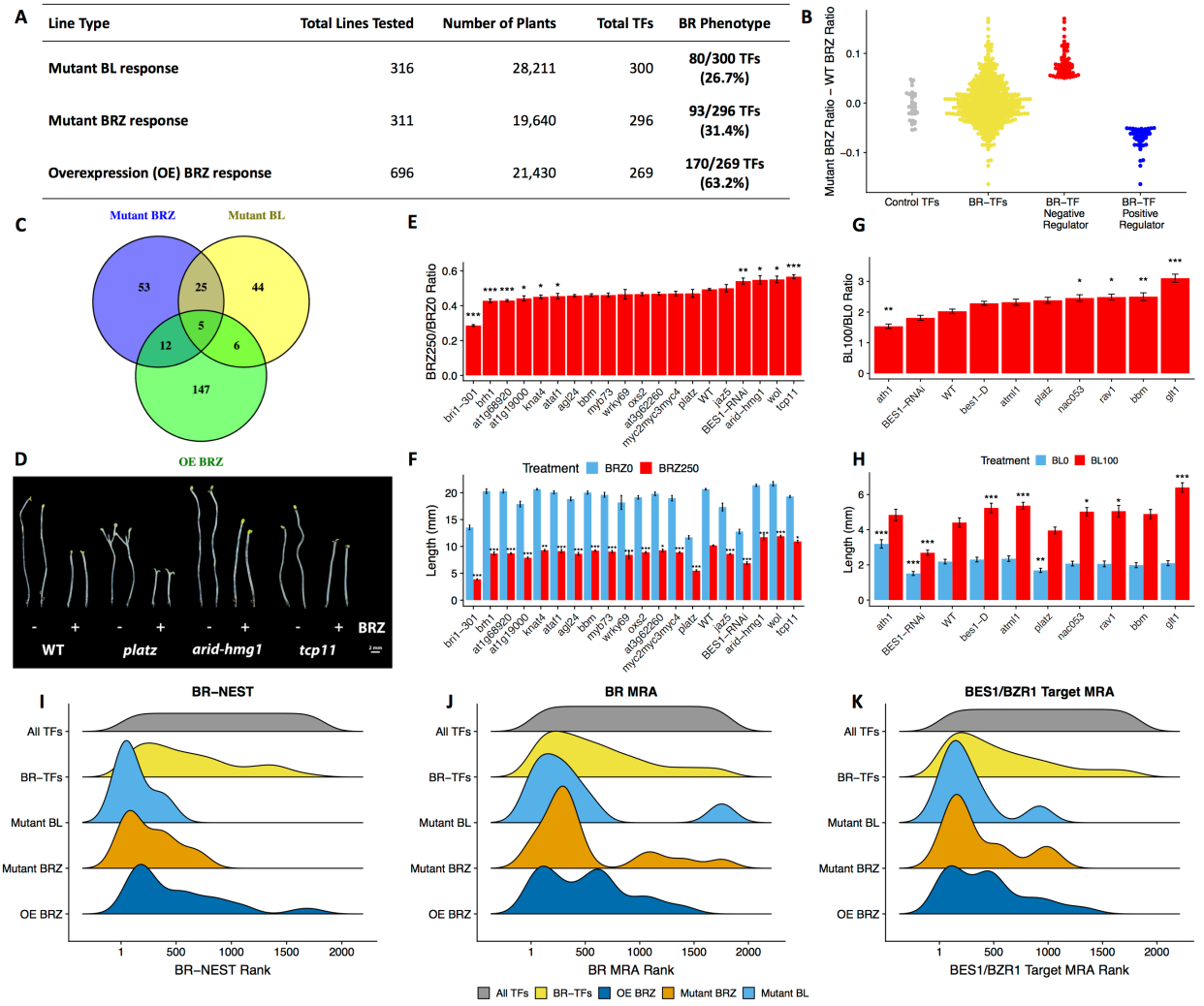

Figure 4: BL and BRZ phenomics reveals BR responses of BR-TFs

(A) Summary table of BL and BR responses. BR phenotypes are derived from KO or OE lines that showed a ratio differences from WT of at least 0.05 for BRZ assays or 0.25 for BL response assays. Each ratio is derived from a pair of 8-12 control and 8-12 treated plants.

(B) Comparison of BRZ ratios for indicated groups of TFs from BRZ response assays. Each data point represents a single biological replicate for a given TF mutant derived from a pair of 8-12 control and 8-12 treated plants. BR-TFs are separated into negative regulators with increased ratios or positive regulators with decreased ratios.

(C) Comparison of TFs with BRZ or BL phenotypes from (A).

(D) Representative phenotypes of WT and indicated mutants in BRZ response assays. BRZ0 indicates mock control. BRZ250 indicates 250nM BRZ treatment. Scale bars represent 1 mm.

(E) BRZ250/BRZ0 ratios from mutant BRZ confirmation experiments. Plants were grown for 7 days in dark conditions treated with either mock solvent (BRZ0) or 250nM BRZ (BRZ250). Data represent mean ± SEM of 4-8 independent replicates of 8-12 plants each. Labels indicate p-values compared to WT controls (* p-value <0.05, ** p-value <0.01 and *** p-value <0.001), Dunnett's method.

(F) Hypocotyl lengths from BRZ experiments in (E). Labels indicate p-values compared to WT controls from the same treatment group (* p-value <0.05, ** p-value <0.01 and *** p-value <0.001), Dunnett's method. Only differences between BRZ250 treated hypocotyl lengths were tested.

(G) BL100/BL0 ratios from mutant BL confirmation experiments. Plants were grown for 7 days in light and treated with either mock solvent (BL0) or 100nM BL (BL100). Data represent mean ± SEM of 4-8

independent replicates of 8-12 plants each. Labels indicate p-values compared to WT controls (* p-value <0.05, ** p-value <0.01 and *** p-value <0.001), Dunnett's method.
(H) Hypocotyl lengths from BL experiments in (G). Labels indicate p-values compared to WT controls from the same treatment group (* p-value <0.05, ** p-value <0.01 and *** p-value <0.001), Dunnett's method.
(I) Comparison of TF rankings based on BR-NEST among groups of confirmed mutant or OE lines from BL and BRZ response assays.
(J) Comparison of TF rankings based on enrichment of BR regulated genes (BR MRA) among groups of confirmed mutant or OE lines from BL and BRZ response assays.
(K) Comparison of TF rankings based on enrichment of BES1/BZR1 target genes (BES1/BZR1 Target MRA) among groups of confirmed mutant or OE lines from BL and BRZ response assays.

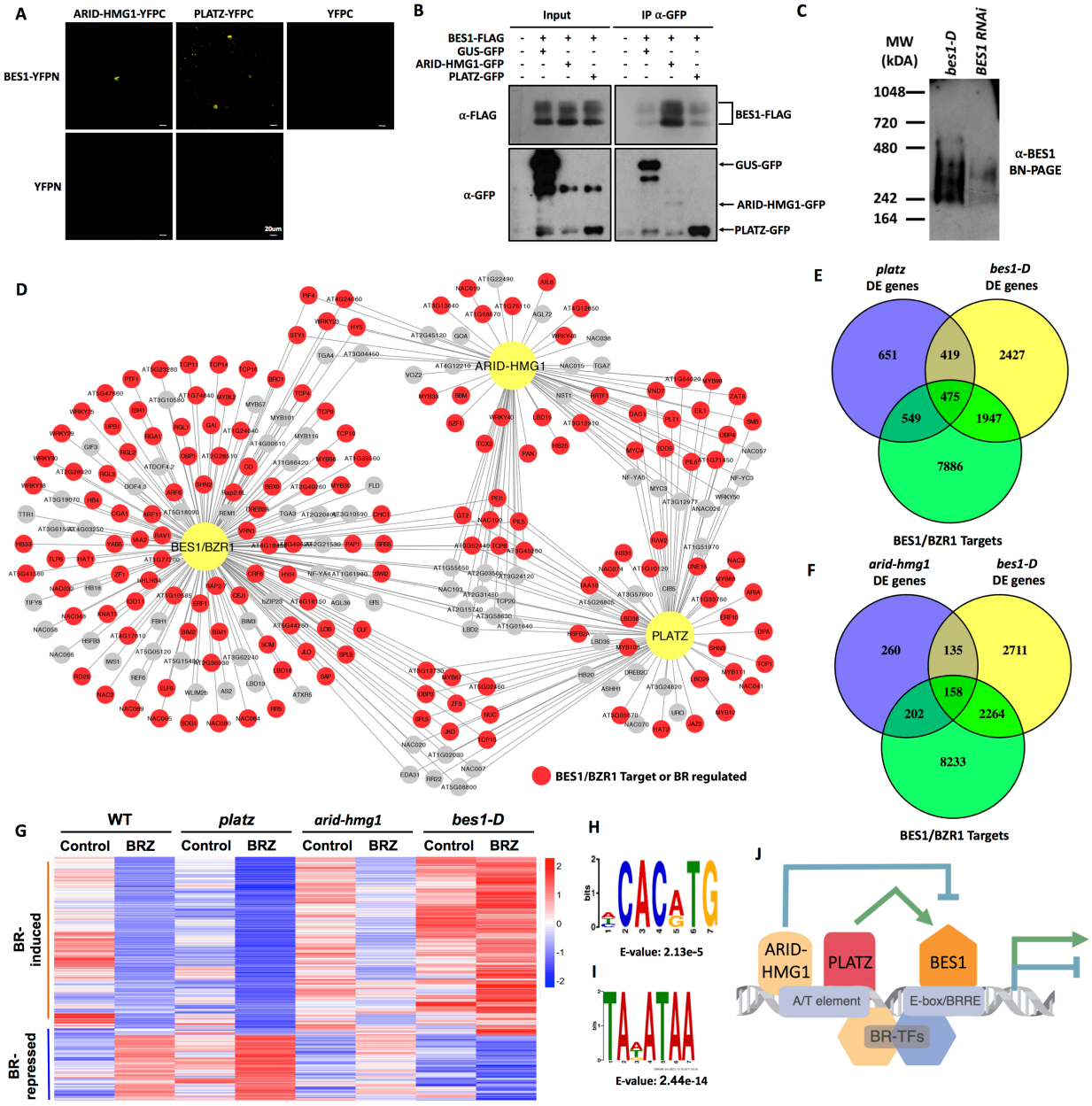

Figure 5: BES1, PLATZ and ARID-HMG1 interact with a common set of TFs and control BR-regulated gene expression

(A) Interaction between BES1 and PLATZ and BES1 and ARID-HMG1 in BiFC assays in *N. benthamiana*. Scale bar indicates 20 μm.

(B) Co-Immunoprecipitation of BES1 with PLATZ and ARID-HMG1. BES1-FLAG was coexpressed with GUS-GFP control, ARID-HMG1-GFP or PLATZ-GFP in Arabidopsis mesophyll protoplasts. GFP fusions were immunoprecipitated with GFP-Trap (IP α-GFP) followed by immunoblotting with indicated antibodies.

(C) Blue-Native Polyacrylamide Gel-Electrophoresis (BN-PAGE) followed by immunoblotting with anti-BES1 antibodies with nuclear extracts from etiolated *bes1-D* seedlings show that BES1 is present in several large complexes in the nucleus. *BES1 RNAi* was used as a negative control.

(D) Network showing putative PPIs between BES1/BZR1, PLATZ and ARID-HMG1 with other TFs. Red color indicates that an interacting TF is a BES1/BZR1 Target or regulated by BRs.

(E) Comparison of genes differentially expressed (DE) in *platz* or *bes1-D* with BES1/BZR1 Target genes. Data represent DE genes from whole transcriptome RNA-seq experiments using 7-day-old dark grown seedlings.
(F) Comparison of genes differentially expressed (DE) in *arid-hmg1* or *bes1-D* with BES1/BZR1 Target genes. Data represent DE genes from whole transcriptome RNA-seq experiments using 7-day-old dark grown seedlings.
(G) Clustering of 596 *bes1-D* regulated BES1/BZR1 targets with opposite patterns of regulation in *platz* and *arid-hmg1*. Color legend indicates row normalized gene expression values.
(H) A BES1 binding motif is enriched in the genes from (H).
(I) An A/T-rich binding motif is enriched in the genes from (H).
(J) Model for function of PLATZ and ARID-HMG1 in BR-regulated gene expression. PLATZ cooperates with BES1, whereas ARID-HMG1 antagonizes BES1. BES1, PLATZ and ARID-HMG1 interact with numerous other BR-TFs, possibly forming transcriptional complexes on BR-regulated gene promoters.

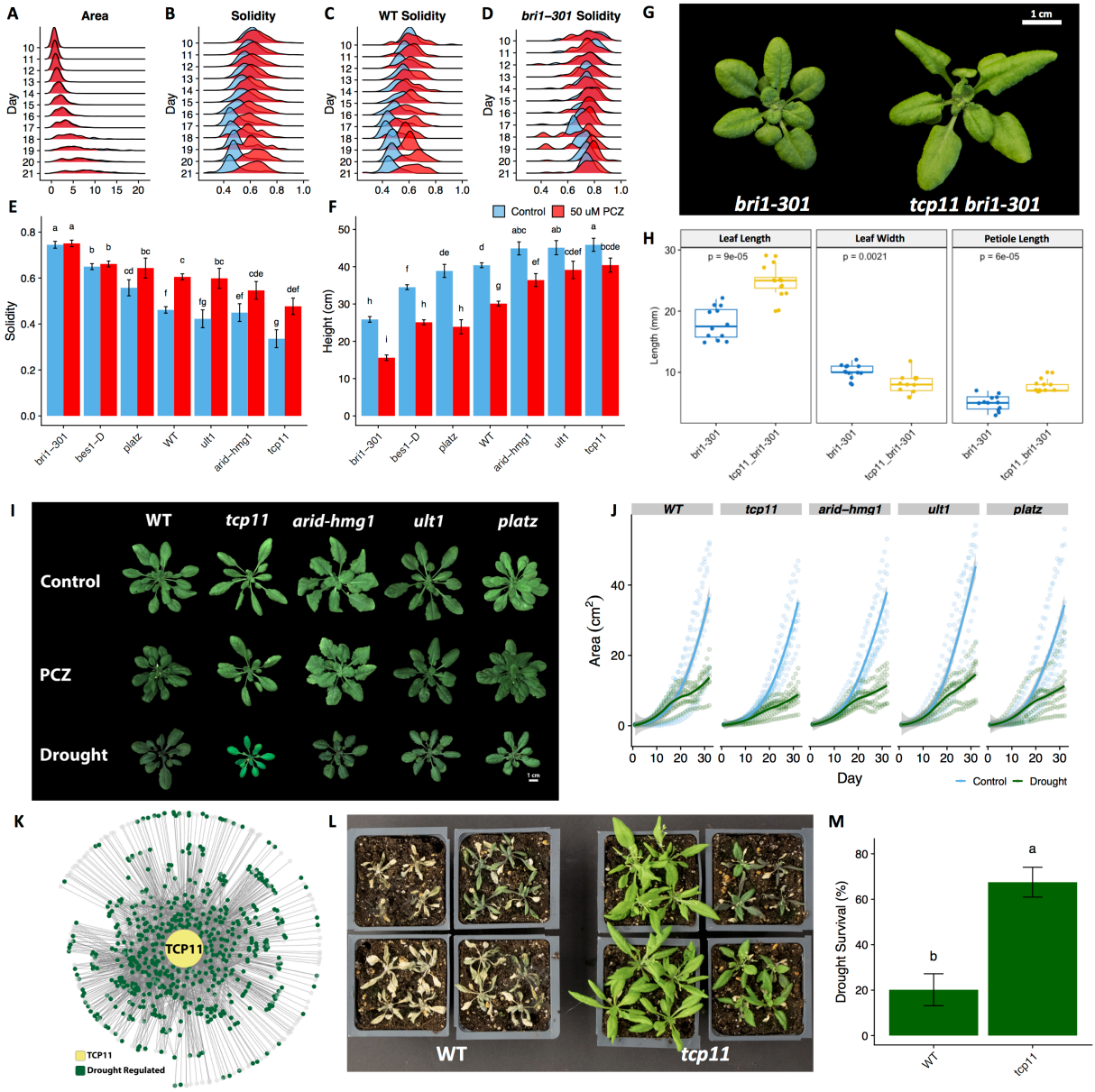

Figure 6: PCZ and drought responses of soil-grown BR-TF mutants

(A) Area (cm^2) of plants grown under control or 50μM PCZ in greenhouse conditions. Day indicates days after planting. Data represent density of all genotypes from the experiment.
(B) Solidity of plants grown under control or 50μM PCZ in greenhouse conditions. Day indicates days after planting. Data represent density of all genotypes from the experiment.
(C) Solidity of WT plants grown under control or 50μM PCZ in greenhouse conditions. Day indicates days after planting. Data represent density of all WT plants from the experiment.
(D) Solidity of *bri1-301* plants grown under control or 50μM PCZ in greenhouse conditions. Day indicates days after planting. Data represent density of all *bri1-301* plants from the experiment.
(E) Solidity of selected genotypes from greenhouse PCZ experiments described in (A-D) on the 21st day after planting. Data represent mean ± SEM from at least 40 biological repeats of WT, *bri1-301* and *bes1-D* and 3-7 biological repeats of other mutants. Different letters indicate a statistically significant difference $p < 0.05$, t-test.
(F) Final plant height of selected genotypes from greenhouse PCZ experiments. Plants were allowed to grow to maturity and the tallest point of the inflorescence was measured manually. Data represent mean

± SEM from at least 40 biological repeats of WT, *bri1-301* and *bes1-D* and 3-7 biological repeats of other mutants. Different letters indicate a statistically significant difference p <0.05, t-test.
(G) *tcp11* partially suppresses the growth phenotype of *bri1-301* in a *tcp11 bri1-301* double mutant. Plants are ~ 5 weeks old. Scale bar indicates 1cm.
(H) Leaf length, leaf width and leaf petiole length of *bri1-301* and *tcp11 bri1-301* double mutants from (G). p-values from t-tests are indicated, data represent 12 plants.
(I) Representative phenotypes of WT, *tcp11*, *arid-hmg1*, *ult1* and *platz* mutants under control, PCZ (100μM PCZ treatment) and drought (0.75g water per g dry soil) from RoAD system. Images are from day 28 of the experiment. Scale bar represents 1cm.
(J) Area of plants under control and drought treatments from the RoAD system described in (I). Individual data points are represented as circles along with a smoothed line for each genotype and treatment combination.
(K) The regulon of TCP11 is enriched from drought regulated genes in the GRN. Green color indicates drought regulation from transcriptome experiments.
(L) Representative photo of WT and *tcp11* mutants after water withholding drought stress assays. Water was withheld for approximately three weeks until plant wilting was observed. Plants were rewatered, allowed to recover for one week and photographed.
(M) Quantification of plant recovery after water withholding drought stress experiments described in (L). Plants that displayed new green leaves after the recovery period were scored as survivors. Data represent mean ± SEM from 11 biological replicates each consisting of at least 12 plants for each genotype. Different letters indicate a statistically significant difference p <0.05, t-test.

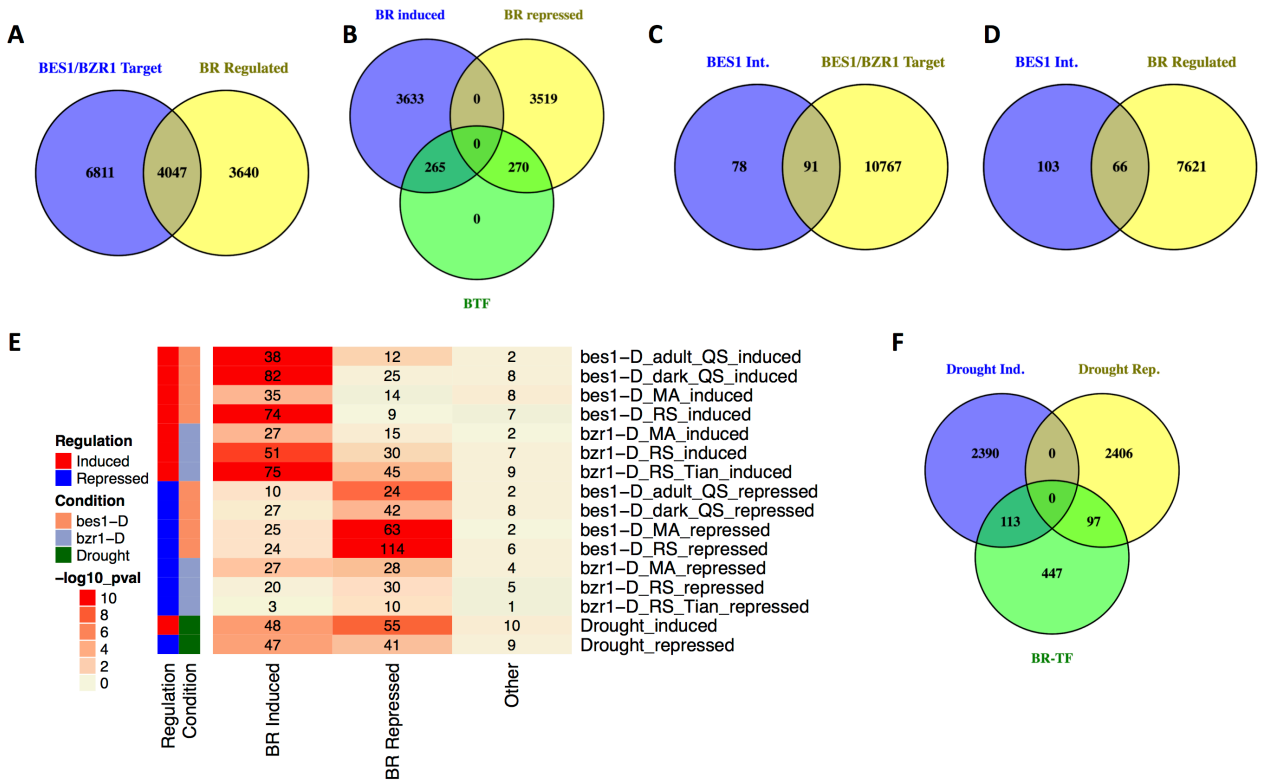

Figure S1: BES1/BZR1 target and BR-TF gene comparisons. Related to Figure 1.
(A) Overlap of combined BES1/BZR1 targets with BR regulated genes.
(B) Number of BR-induced and BR-repressed BR-TFs.
(C) Comparison of BES1/BZR1 interacting TFs (BES1 Int.) with BES1/BZR1 ChIP targets.
(D) Comparison of BES1/BZR1 interacting TFs (BES1 Int.) with BR-regulated genes.
(E) Intersection between BR-Induced BR-TFs, BR-Repressed BR-TFs or other BR-TFs and various BR or drought related gene lists. Red color indicates -log10 transformed p-value from Fisher's exact test. Gene lists are from the following sources: bes1-D adult QS and bes1-D dark QS (this study), bes1-D MA (Yu et al., 2011), bes-1D RS (Chen et al., 2017), bzr1-D MA (Sun et al., 2010) , bzr1-D RS (Bai et al., 2012b), bzr1-D RS Tian (Tian et al., 2018), Drought (Maruyama et al., 2009).
(F) Comparison between drought induced (Drought Ind.) or drought repressed (Drought Rep.) genes and BR-TFs.

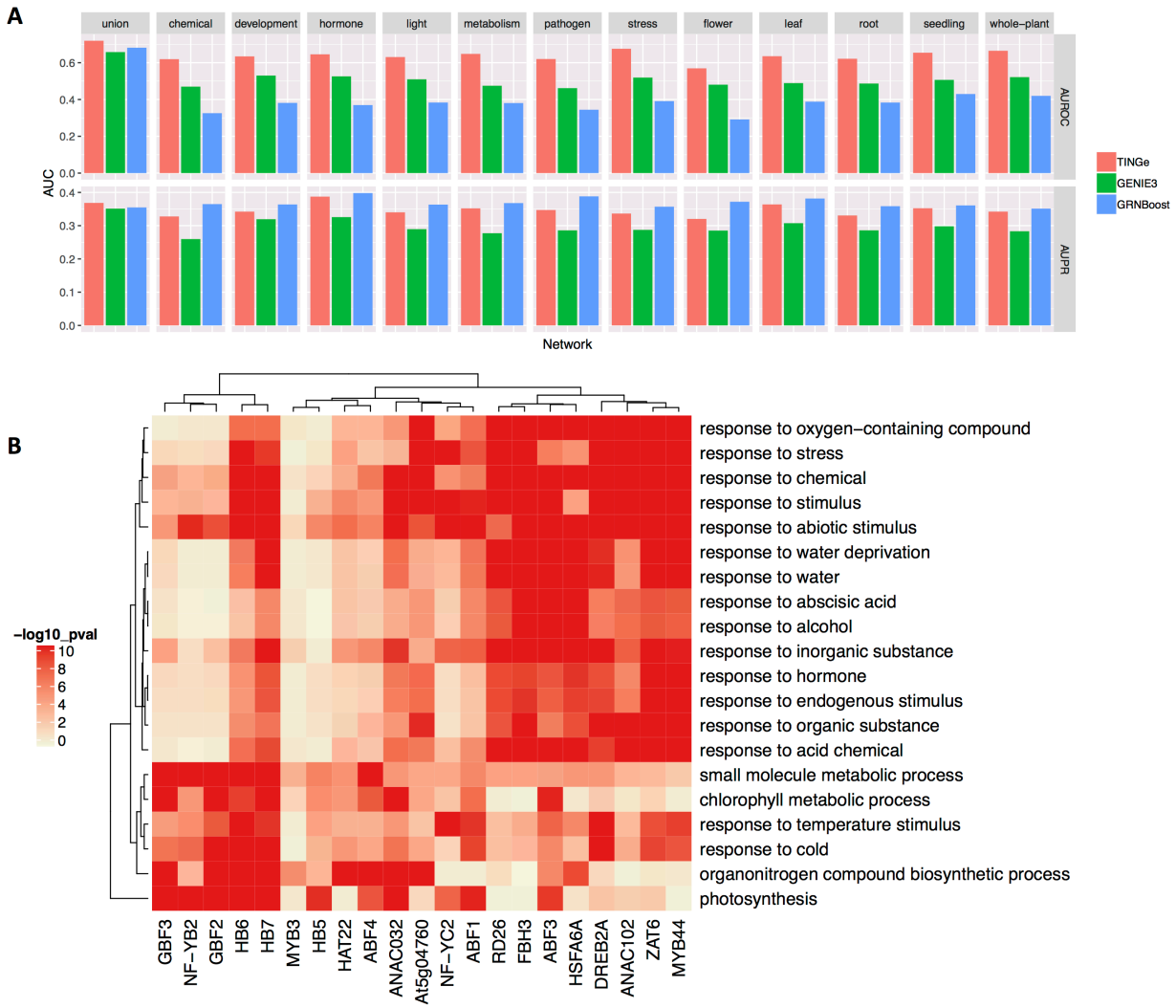

Figure S2: Additional GRN validation. Related to Figure 2.
(A) AUC values for the indicated networks produced by TINGe, GENIE3 or GRNBoost for the RD26 validation dataset.
(B) Gene ontology (GO) enrichment from the top 1000 edges for 21 ABA-related TFs from the TINGe union network. The median FDR corrected p-value across all 21 TFs was used to select 20 GO terms to plot. Color indicates -log10 transformed FDR corrected p-value. Hierarchical clustering was used to order rows and columns of the heatmap.

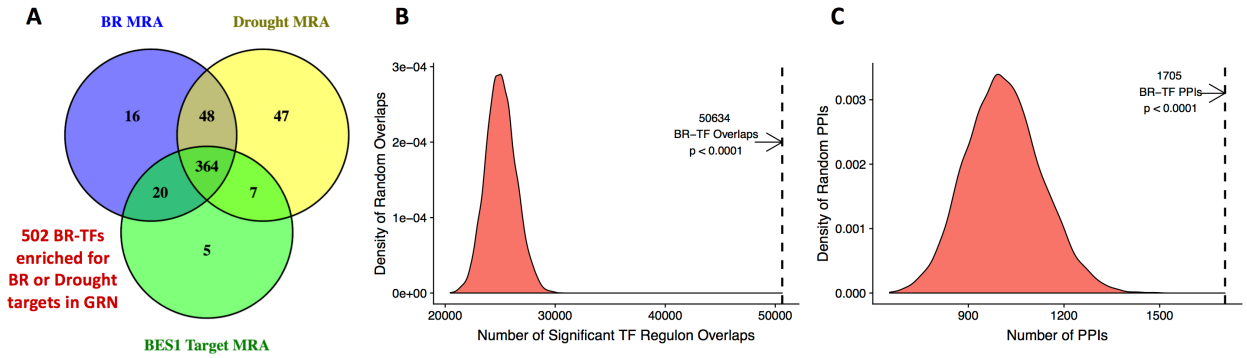

Figure S3: BR-TF overlap and PPIs in the GRN. Related to Figure 3.
(A) Number of BR-TFs with regulons enriched for BR regulated genes (BR MRA), drought regulated genes (Drought MRA) or BES1/BZR1 target genes (BES1 Target MRA). When combined, 502 BR-TFs are enriched for BR or Drought predicted targets in the GRN (left).
(B) Comparison of observed BR-TF regulon overlaps with an empirical distribution of overlaps from 10,000 permutations of randomly selected TF sets containing the same number of TFs as that contained in the BR-TF set.
(C) Comparison of observed BR-TF PPIs with an empirical distribution of PPIs from 10,000 permutations of randomly selected TF sets containing the same number of TFs as that contained in the BR-TF set.

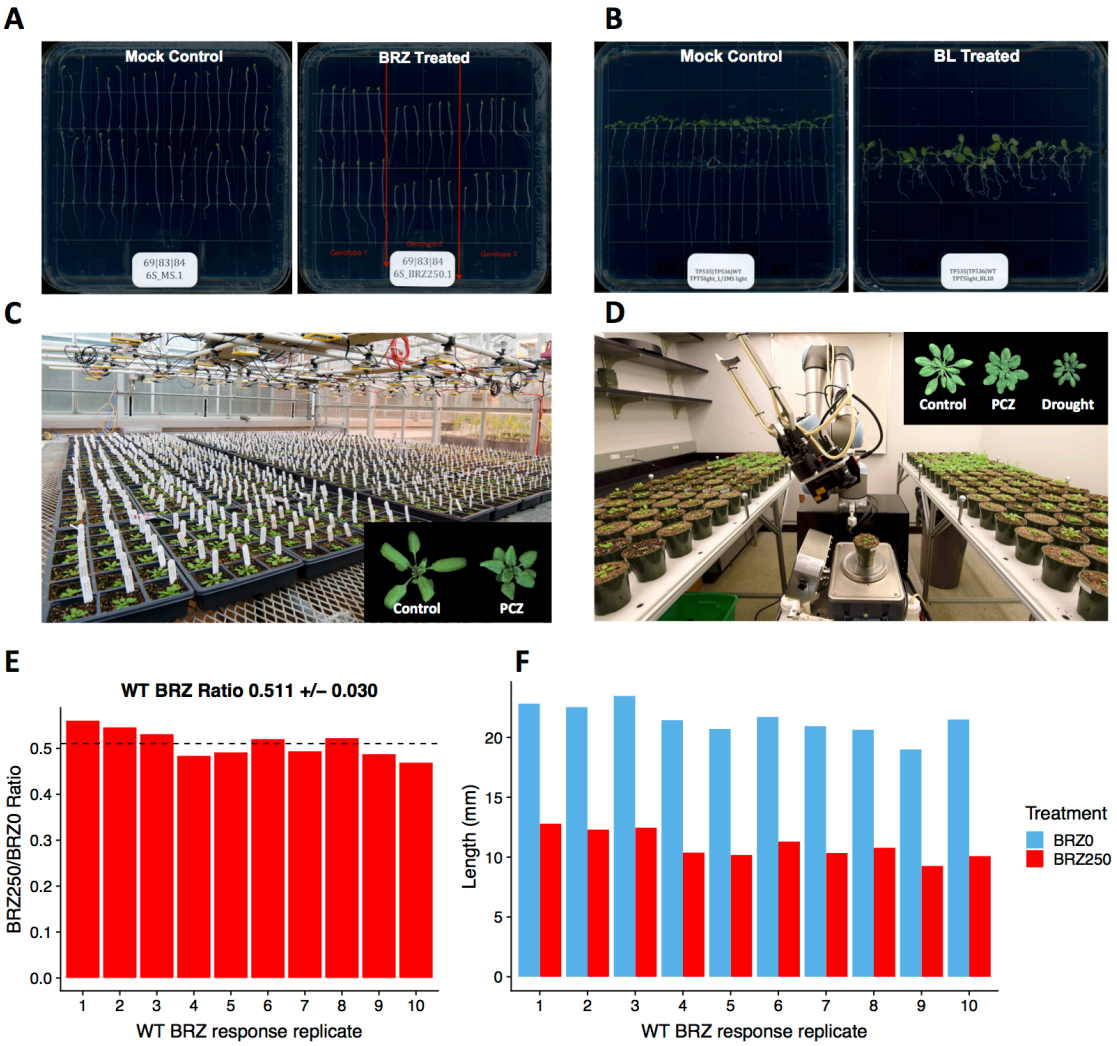

Figure S4: Functional studies of BR-TFs are enabled by high throughput phenotyping of BR-related phenotypes. Related to Figure 4.

(A) Response to Brassinosteroid biosynthesis inhibitor BRZ in 7-day old dark grown seedlings.
(B) Response to Brassinosteroid treatment with BL in 7-day old light grown seedlings.
(C) Response to Brassinosteroid biosynthesis inhibitor Propiconazole (Pcz) in soil grown plants.
(D) Robotic Assay for Drought (RoAD) for BR and drought experiments in soil.
(E) BRZ250/BRZ0 ratios from WT controls in BRZ experiments. Plants were grown for 7 days in dark conditions treated with either mock solvent (BRZ0) or 250nM BRZ (BRZ250). Each bar represents the mean of one replicate of 8-12 plants. The mean ± SD across 10 independent replicates is shown.
(F) Hypocotyl lengths from WT plants in BRZ experiments from (E)

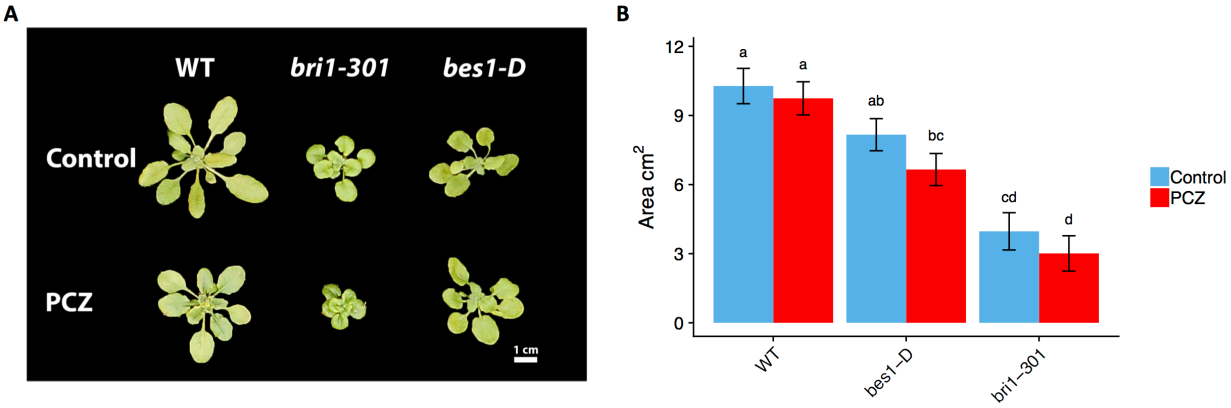

Figure S5: Phenotypes of WT, *bri1-301* and *bes1-D* in greenhouse PCZ experiments. Related to Figure 6.

(A) Phenotypes of WT, *bri1-301* and *bes1-D* under control and 50μM PCZ 21 days after planting from greenhouse PCZ experiments. Scale bar represents 1cm.

(B) Plant area from (A). Data represent mean ± SEM from at least 40 biological repeats. Different letters indicate a statistically significant difference $p < 0.05$, t-test

Table 1: Top AUROC score from each network validation dataset.
Refer to Table S4 for complete AUROC and AUPR dataset

Method	Network	Validation Dataset	AUROC
TINGe	union	RD26	0.719
TINGe	union	Song ChIP	0.662
GRNBoost	union	TF2N ChIP	0.604
TINGe	union	eQTL	0.567
TINGe	development	TF2N DE	0.655
TINGe	development	DAP-Seq	0.542
GENIE3	metabolism	Y1H	0.664

Table 2: Top 20 BR-TFs from BES1/BZR1 target master regulator analysis (MRA)

TF Name	ATID	Regulon Size	BES1/BZR1 Target Hits	BES1/BZR1 Target p-value	Reference
HAT1	AT4G17460	550	371	1.90E-41	Zhang et al., 2014
TCP11	AT5G08330	940	545	5.90E-33	
DREB26	AT1G21910	419	281	1.30E-30	
WRKY33	AT2G38470	464	300	1.50E-28	
MYB30	AT3G28910	475	300	4.50E-26	Li et al., 2009
IAA2	AT3G23030	279	197	9.30E-26	
RGL1	AT1G66350	669	393	3.60E-25	Bai et al., 2012
RD26	AT4G27410	507	313	6.70E-25	Ye et al., 2017
ULT1	AT4G28190	919	509	1.30E-24	
IAA19	AT3G15540	390	253	1.50E-24	Zhou et al., 2013
FBH3	AT1G51140	779	443	1.80E-24	
STZ	AT1G27730	221	162	3.80E-24	
LBD38	AT3G49940	580	346	7.10E-24	
BIM1	AT5G08130	388	250	1.10E-23	Yin et al., 2005
TCP15	AT1G69690	509	307	3.20E-22	
SHY2	AT1G04240	522	313	4.20E-22	
AT1G75710	AT1G75710	869	477	4.60E-22	
WRKY40	AT1G80840	343	223	6.10E-22	Lozano-Durán et al., 2013
WRKY47	AT4G01720	411	257	1.00E-21	
WRKY25	AT2G30250	1082	572	1.50E-21	

Table 3: Mutants with strong confirmed BRZ phenotypes

Name	GeneID	Mutant	BRZ0 Length (mm)	BRZ250 Length (mm)	BRZ250/ BRZ0 ratio	BR-NEST	BR-NEST RANK	BRZ ratio p-value	BRZ250 length p-value
WT	NA	NA	20.65	10.19	0.494	NA	NA	NA	NA
TCP11	AT5G08330	SALK_106694c	19.29	10.92	0.566	514.66	26	**<0.001**	**0.0131**
WRKY69	AT3G58710	SALK_130848c	18.19	8.42	0.465	503.41	28	0.6481	**<0.001**
PLATZ	AT4G17900	SALK_139889c	11.69	5.48	0.47	475.65	38	0.9919	**<0.001**
WOL	AT2G01830	SALK_048970c	21.65	11.9	0.55	387.87	62	**0.0214**	**<0.001**
KNAT4	AT5G11060	SALK_020216c	20.64	9.29	0.451	335.26	83	**0.0156**	**0.0038**
AT1G19000	AT1G19000	SALK_080218c	17.88	7.88	0.441	330.44	87	**0.044**	**<0.001**
BES1	AT1G19350	*BES1-RNAi*	12.77	6.89	0.541	311.27	95	**0.0017**	**<0.001**
ARID-HMG1	AT1G76110	SALK_076225c	21.38	11.71	0.548	290.97	108	**0.0281**	**<0.001**
BRH1	AT3G61460	SALK_101312c	20.29	8.68	0.428	225.74	189	**<0.001**	**<0.001**
BBM	AT5G17430	SALK_097021C	20.02	9.21	0.46	160.3	345	0.1112	**<0.001**
AT3G62260	AT3G62260	SALK_135177c	19.8	9.27	0.468	158.61	349	0.6559	**0.0285**
AGL24	AT4G24540	SALK_095007c	18.84	8.63	0.457	151.67	370	0.6867	**<0.001**
JAZ5	AT1G17380	SALK_053775c	17.34	8.6	0.5	150.73	375	1	**<0.001**
ATAF1	AT1G01720	SALK_057618c	20.08	9.12	0.454	128.74	447	**0.0244**	**<0.001**
MYC2	AT1G32640	*myc2myc3myc4*	18.98	8.88	0.47	101.67	574	0.8694	**<0.001**
MYB73	AT4G37260	SALK_023478c	19.61	9.02	0.461	80.91	682	0.1823	**<0.001**
OXS2	AT2G41900	SALK_126148C	19.13	8.91	0.466	75.47	720	0.6917	**<0.001**
BRI1	AT4G39400	*bri1-301*	13.53	3.87	0.286	NA	NA	**<0.001**	**<0.001**
AT1G68920	AT1G68920	SALK_135188C	20.28	8.7	0.429	NA	NA	**<0.001**	**<0.001**

Table 4: Mutants with strong confirmed BL phenotypes

Name	GeneID	Mutant	BL0 Length (mm)	BL100 Length (mm)	BL100 /BL0 ratio	BR-NEST	BR-NEST RANK	BL ratio p-value	BL100 p-value	BL0 p-value
WT	NA	NA	2.19	4.41	2.025	NA	NA	NA	NA	NA
NAC053	AT3G10500	SALK_022946c	2.07	5.03	2.458	782.05	7	**0.0260**	**0.0386**	1
ATML1	AT4G21750	SALK_131124C	2.35	5.37	2.321	607.84	15	0.3973	**<0.001**	0.9906
GTL1	AT1G33240	SALK_044308c	2.1	6.4	3.103	503.99	27	**<0.001**	**<0.001**	1
PLATZ	AT4G17900	SALK_139889c	1.69	3.96	2.384	475.65	38	0.1369	0.3457	0.0014
BES1	AT1G19350	*BES1-RNAi*	1.51	2.69	1.811	311.27	95	0.8954	**<0.001**	**<0.001**
ATH1	AT4G32980	SALK_113353C	3.19	4.84	1.537	295.98	107	**0.0055**	0.4201	**<0.001**
BBM	AT5G17430	SALK_097021C	1.99	4.89	2.503	160.3	345	**0.0074**	0.2453	0.8971
RAV1	AT1G13260	SALK_021865c	2.05	5.06	2.49	140.22	405	**0.0112**	**0.023**	0.9999
BES1	AT1G19350	*bes1-D*	2.3	5.24	2.286	311.27	95	0.7729	**0.001**	0.994

Table 5: OE lines with strong confirmed BRZ phenotypes

Name	GeneID	OE Line	BRZ0 Length (mm)	BRZ250 Length (mm)	BRZ250/ BRZ0 ratio	BR-NEST	BR-NEST RANK	BRZ Ratio p-value	BRZ250 p-value
WT	NA	WT	18.43	9.18	0.499	NA	NA	NA	NA
WRKY25	AT2G30250	TP379	17.42	7.11	0.41	496.99	32	0.9557	**0.0058**
AT4G17810	AT4G17810	TP1470	6.73	2.86	0.431	323.82	89	0.9983	**<0.001**
AT4G17810	AT4G17810	TP1471	15.28	7.37	0.482	323.82	89	1	**0.0166**
AT3G17100	AT3G17100	TP579	18.16	7.02	0.388	299.14	104	0.6065	**0.0029**
COL3	AT2G24790	TP364	15.73	6.93	0.445	297.54	105	1	**0.0014**
MYB34	AT5G60890	TP1089	10.73	4.91	0.457	279.74	120	1	**<0.001**
FBH3	AT1G51140	TP1192	14	5.81	0.416	268.03	136	0.9873	**<0.001**
MYB59	AT5G59780	TP1083	14.08	5.5	0.391	258.01	147	0.6874	**<0.001**
Rap2.6L	AT5G13330	TP929	15.38	6.94	0.455	249.06	159	1	**<0.001**
WRKY75	AT5G13080	TP927	16.05	6.94	0.433	248.13	162	0.9993	**<0.001**
AT2G44940	AT2G44940	TP453	7.25	2.75	0.381	237.84	174	0.5971	**<0.001**
tny	AT5G25810	TP981	12.06	5.36	0.435	218.89	200	1	**<0.001**
tny	AT5G25810	TP982	14.98	6.67	0.437	218.89	200	1	**<0.001**
PAP2	AT4G29080	TP805	16.11	7.17	0.442	214.11	210	1	**0.0093**
SCL13	AT4G17230	TP757	16.8	7.21	0.431	207.16	226	1	**0.0066**
OBP4	AT5G60850	TP1087	7.65	3.85	0.502	196.98	251	1	**<0.001**
ANT	AT4G37750	TP862	15.29	6.19	0.404	194.46	257	0.9178	**<0.001**
IAA13	AT2G33310	TP1280	16.53	5.92	0.351	189.08	269	0.0931	**<0.001**
RAV2	AT1G68840	TP222	13.88	3.72	0.273	171.34	314	**<0.001**	**<0.001**
AT2G28200	AT2G28200	TP1270	16.97	6.96	0.411	148.63	382	0.9697	**0.0024**
ANAC087	AT5G18270	TP954	14.62	6.09	0.417	136.99	417	0.9913	**<0.001**
ANAC087	AT5G18270	TP955	13.85	6.17	0.439	136.99	417	1	**<0.001**
MYC4	AT4G17880	TP1474	13.77	6.49	0.488	116.85	493	1	**<0.001**
IAA14	AT4G14550	TP748	18.02	7.45	0.415	106.09	548	0.9403	**0.0309**
PIL5	AT2G20180	TP335	5.04	3.06	0.621	103.01	563	0.9839	**<0.001**
ZAT11	AT2G37430	TP425	17.43	7.19	0.413	101.25	575	0.98	**0.0148**
RAP2.6	AT1G43160	TP121	16.35	6.91	0.422	100.13	582	0.998	**0.0015**
TMO6	AT5G60200	TP1085	15.53	7.16	0.463	76.72	705	1	**0.0014**
AT1G36060	AT1G36060	TP117	8.32	3.31	0.457	74.07	725	1	**<0.001**
AT1G36060	AT1G36060	TP118	2.07	2.22	1.074	74.07	725	**<0.001**	**<0.001**
SPL11	AT1G27360	TP1171	16.81	7.04	0.425	62.97	802	0.9148	**<0.001**
ORA47	AT1G74930	TP269	13.45	5.58	0.416	55.65	857	0.9547	**<0.001**
ORA47	AT1G74930	TP270	4.79	3.29	0.764	55.65	857	**<0.001**	**<0.001**
ERF4	AT3G15210	TP569	6.4	4.21	0.654	49.69	903	0.502	**<0.001**

CBF2	AT4G25470	TP791	17.84	7.5	0.421	43.73	952	0.9796	**0.0418**
MYB74	AT4G05100	TP713	15.91	7.26	0.459	30.54	1092	1	**0.0032**
AT3G10030	AT3G10030	TP1344	13.7	5.61	0.41	27.34	1129	0.6653	**<0.001**
NAC057	AT3G17730	TP1365	17.97	7.45	0.421	5.98	1612	0.8655	**0.0142**
DAZ1	AT2G17180	TP324	17.97	7.62	0.426	2.21	1756	0.9952	**0.0445**
BRC1	AT3G18550	TP1367	7.22	4.33	0.604	NA	NA	1	**<0.001**
BRC1	AT3G18550	TP1368	16.34	7.54	0.467	NA	NA	1	**0.0274**
AT1G50680	AT1G50680	TP143	10.58	3.9	0.369	NA	NA	0.1944	**<0.001**
CRF4	AT4G27950	TP1487	13.96	5	0.355	NA	NA	**0.0272**	**<0.001**
BBX26	AT1G60250	TP188	9.93	3.92	0.395	NA	NA	0.6393	**<0.001**
AT1G80400	AT1G80400	TP299	16.82	7.43	0.448	NA	NA	1	**0.011**

Table S1: 10,858 BES1/BZR1 Target genes
Table S2: 169 putative BES1 or BZR1 interacting TFs
Table S3: 657 Brassinosteroid-related TFs (BR-TFs)
Table S4: Network AUROC and AUPR scores from validation datasets
Table S5: GO enrichment for the top 1000 edges of the TINGe union network for 21 ABA TFs
Table S6: Combined BR-TF GRN from BES1/BZR1 targets, TF PPIs and TINGe union
Table S7: Master Regulatory Analysis (MRA) for hormone and stress responsive genes
Table S8: Arabidopsis 1001 genomes eQTL hits for BR-regulated genes
Table S9: BR-TF Regulon overlap analysis in TINGe GRN
Table S10: PPIs between BR-TFs in AtTFIN-1
Table S11: BR-NEST scores for TFs in the TINGe GRN
Table S12: Mutant BRZ phenotyping results
Table S13: OE BRZ phenotyping results
Table S14: Mutant BL phenotyping results
Table S15: Mutant BRZ phenotyping confirmation results
Table S16: Mutant BL phenotyping confirmation results
Table S17: OE BRZ phenotyping confirmation results
Table S18: Image traits from greenhouse PCZ experiments
Table S19: Plant height from greenhouse PCZ experiments
Table S20: Primers used for genotyping TF T-DNA mutant lines

CHAPTER 4

DISCUSSION AND FUTURE WORK

4.1 Dissertation Discussion

This dissertation summarizes my work on the mechanisms and networks of BES1 function in Brassinosteroid (BR)-mediated growth and stress responses. Two major questions were investigated: What are the processes controlling BES1 during stress conditions? And, how does BES1 direct a network of transcription factors (TF) that allow BRs to modulate the expression of thousands of genes? The research described herein illustrates multiple mechanisms that converge to inhibit BES1 when unfavorable conditions are encountered. First, stress leads to ubiquitination of BES1 by SINAT E3 ligases and degradation of BES1 by DSK2-mediated selective autophagy. Additionally, drought induces RD26, a TF that physically interacts with BES1 on BR-regulated target genes to shut down the transcriptional activity of BES1, promoting drought responses. On the other hand, BRs activate BES1 during favorable conditions. BES1 cooperates with WRKY46/54/70 and a large network of BR-related TFs (BR-TFs) to promote BR-regulated growth and inhibit stress responses.

BRs are a major family of plant hormones that function in a multitude of processes including growth (Chen et al., 2017; Clouse et al., 1996; Li et al., 1996; Noguchi et al., 1999; Nolan et al., 2017a; Nolan et al., 2017b; Szekeres et al., 1996; Ye et al., 2017). BR signaling leads to the activation of BES1 and BZR1 TFs that function as master regulators of BR-responses (He et al., 2005; Wang et al., 2002; Yin et al., 2005; Yin et al., 2002). Genetic screens identified *bes1-D* and *bzr1-D* as dominant gain-

of-function mutants in which BES1 or BZR1 proteins are dramatically stabilized (Wang et al., 2002; Yin et al., 2002). This early evidence pointed towards possible post-translational regulation of BES1 and BZR1. Consistent with this idea, BES1 and BZR1 can be targeted for ubiquitin mediated degradation by the proteasome (He et al., 2002; Wang et al., 2013) involving the Skp-CULLIN-F-box (SCF) E3 ubiquitin ligase MORE AXILLARY GROWTH LOCUS 2 (MAX2) (Wang et al., 2013), or the dark activated E3 ligase COP1 (Kim et al., 2014). These observations indicate that BES1/BZR1 can be degraded, but the downstream components and pathways involved remained to be fully defined.

In addition to the proteasome, ubiquitin-mediated protein degradation can occur through autophagy (Floyd et al., 2012; Kraft et al., 2010). A growing body of work is revealing that autophagy can be highly selective through the action of autophagy receptor proteins (Michaeli et al., 2016). These receptors connect cargos destined for degradation with the autophagy protein ATG8 (Marshall et al., 2015; Michaeli et al., 2016; Svenning et al., 2011; Zhou et al., 2013). DOMINANT SUPPRESSOR OF KAR2 (DSK2) is a ubiquitin-binding receptor implicated in protein degradation in yeast, animals and plants (Funakoshi et al., 2002; Lee et al., 2013; Lee and Brown, 2012; Lin et al., 2011). Homologs of DSK2 have been shown to interact with the autophagy protein LC3 (homologous to ATG8) (Lee et al., 2013), but the detailed functions and cargos of DSK2 had not been defined in plants. We found direct evidence linking the regulation and activity of DSK2 to BR signaling which leads to altered plant growth under drought and fixed-carbon starvation conditions.

Our studies show that BES1 is degraded by selective autophagy (Nolan et al., 2017b). DSK2 serves as an autophagy receptor for ubiquitinated BES1 by directly interacting with ATG8. This process is regulated by the GSK3-like kinase BIN2, which is repressed by BRs and activated by stresses (Wang et al., 2018; Youn and Kim, 2015; Zhang et al., 2009). BIN2 controls BES1 degradation through autophagy by phosphorylating DSK2 proximal to its ATG8-interacting motif (AIM). Phosphorylation of DSK2 by BIN2 promotes DSK2-ATG8 interaction, potentiating BES1 degradation through selective autophagy. Loss-of-function *DSK2 RNAi* plants have increased BES1 protein levels, altered global gene expression profiles and compromised survival during stresses. Our results thus revealed that plants coordinate growth and stress responses by targeting a central growth regulator to the selective autophagy pathway (Nolan et al., 2017b).

Our studies also uncovered a new function for *SINATs*, which encode E3 ubiquitin ligases that target the active unphosphorylated form of BES1 to influence BR-regulated growth in a light dependent manner (Yang et al., 2017). *SINATs* are induced by starvation stress and are involved in targeting BES1 for degradation under starvation conditions (Nolan et al., 2017b). This process likely occurs through interactions between SINAT2, DSK2 and BES1. Accordingly, loss-of-function *SINAT RNAi* plants displayed dramatically increased sensitivity to fixed-carbon starvation stress. *SINAT RNAi* plants have a more severe fixed-carbon starvation phenotype than *bes1-D,* but *bes1-D* has greater BES1 protein accumulation during starvation (Nolan et al., 2017b). These observations suggest that additional substrates of SINATs may exist and play important roles in survival during fixed-carbon starvation.

This work gives rise to several questions that remain to be investigated:

1) BES1 can be degraded by both the proteasome (He et al., 2002; Wang et al., 2013; Yang et al., 2017) and by selective autophagy (Nolan et al., 2017b). How do these pathways interact and what are the components and processes involved in targeting BES1 to one pathway versus the other?

2) What are the E3 ubiquitin ligases involved in BES1 degradation? Multiple families of E3s have been implicated in ubiquitinating BES1 or BZR1 (Kim et al., 2014; Nolan et al., 2017b; Wang et al., 2013; Yang et al., 2017), but loss-of-function mutants for these E3s do not recapitulate the strong BES1 protein accumulation observed in *bes1-D* mutants. Thus, additional E3s or other mechanisms for BES1 degradation are likely to exist. We and others have identified as many as 6 families of E3 ubiquitin ligases as potential BES1 interactors (data not shown). Therefore, an attractive hypothesis is that these E3s function redundantly to control BES1 stability. Future efforts should focus on understanding the relationship among BES1 interacting E3 ligases and characterize the role of these E3s in BES1 degradation.

3) The observation that BES1 can be degraded by DSK2 in an autophagy dependent manner suggests that autophagy can be highly selective and target important signaling components. It will be interesting to determine how widespread this phenomenon is. What other proteins are degraded by selective autophagy and what are the autophagy receptors involved? For example, we found that WRKY54 protein is degraded during drought stress in a similar manner to BES1 (Chen et al., 2017; Chen and Yin, 2017), indicating that WRKY54 may also be degraded through the autophagy

pathway. Future studies should test this hypothesis and work to identify the factors involved in WRKY54 degradation.

4) Our studies revealed that autophagy controls BR signaling during stress by degrading BES1 (Nolan et al., 2017b). In Wnt signaling, β-catenin is degraded by autophagy and also controls the expression of autophagy related genes including the autophagy receptor *p62* (Petherick et al., 2013). The BR and Wnt pathways share several common features (Yin et al., 2002), raising the possibility that BRs also regulate autophagy. Future exploration of BR-autophagy crosstalk will further our understanding of how plants control these important pathways for growth and stress responses.

The second major thrust of this dissertation was to define the transcriptional networks that allow BRs to mediate the expression of 5,000-8,000 genes. Gene expression programs such as those regulated by BRs are carried out through complex gene regulatory networks (GRNs). These GRNs are comprised of TF-target interactions that control gene expression. BES1 and BZR1 are the central transcriptional regulators in the BR pathway (He et al., 2005; Wang et al., 2002; Yin et al., 2005; Yin et al., 2002). A major step in understanding how BES1 and BZR1 control BR-regulated gene expression was to understand the target genes of these TFs. Genome-wide chromatin immunoprecipitation (ChIP) identified thousands of genes directly bound by BES1 and/or BZR1, including many BR-regulated genes and TFs (Sun et al., 2010; Yu et al., 2011). Subsequently, molecular and genetics studies aimed to characterize the functions of these TFs one or several at a time. These studies identified a number of important TFs in the BR pathway (Chen et al., 2017; Li et al., 2010; Li et al., 2009; Ye et

al., 2012; Ye et al., 2017; Yin et al., 2005; Zhang et al., 2014); however, a more complete understanding of how BRs control thousands of targets required a comprehensive systems biology approach.

To address this challenge, we took advantage of cutting-edge tools and techniques including computational modeling, genetics, genomics and high-throughput phenotyping. We used genome-wide chromatin immunoprecipitation (ChIP), transcriptome and TF interactome datasets to identify 657 BR-related Transcription Factors (BR-TFs) that are potentially involved in BR responses. We modeled BR GRNs using 11,760 publicly available microarray datasets and found several lines of evidence implicating BR-TFs in controlling BR- and drought-regulated genes. We leveraged these GRNs to prioritize BR-TFs for functional studies using metrics such as NEST (Network Essentiality Scoring Tool) (Jiang et al., 2015) and Master Regulator Analysis (MRA) (Fletcher et al., 2013; Margolin et al., 2006). Next, we tackled the challenge of scaling BR response assays to study hundreds of BR-TFs, establishing BR phenomics experiments in both petri plates and soil grown plants.

BR phenomics assays identified potential phenotypes for hundreds of BR-TFs and we characterized the detailed functions of two TFs identified in these experiments. These included PLATZ (PLANT A/T-RICH SEQUENCE AND ZINC-BINDING PROTEIN) (Nagano et al., 2001) and ARID-HMG1 (A/T-RICH INTERACTION DOMAIN HIGH MOBILITY GROUP1) (Hansen et al., 2008). Both of these TFs are implicated in binding to A/T-rich DNA elements (Antosch et al., 2012; Nagano et al., 2001), but they exhibit opposite phenotypes in terms of BR response. *platz* mutants display

characteristic BR loss-of-function phenotypes in the dark such as dwarfism and de-etiolation whereas *arid-hmg1* mutants are resistant to BRZ. PLATZ and ARID-HMG1 physically associate with BES1 in BiFC and Co-IP assays. Y2H interaction studies showed that BES1, PLATZ and ARID-HMG1 interact with a common set of BR-TFs. Furthermore, global gene expression studies indicated that *platz* and *arid-hmg1* mutants oppositely control BR-responsive gene expression. Together, these results indicate that PLATZ cooperates with BES1 and ARID-HMG1 antagonizes BES1. Since BES1, PLATZ and ARID-HMG1 interact with many other BR-TFs, an intriguing possibility is that these TFs form BR transcriptional complexes to control BR-regulated gene expression.

For many years, BR response assays have been performed on petri plates. To extend these experiments to a more realistic plant growth environment, we developed systems for BR response assays in soil-grown plants using an economical and widely available BR biosynthesis inhibitor called Propiconazole (PCZ) (Hartwig et al., 2012). We used time-lapse imaging to monitor BR response in PCZ experiments in a greenhouse setting, which allowed us to identify mutants such as *ultrapetala1* (*ult1*) that exhibited PCZ phenotypes but did not have obvious phenotypes in the seedling stage. Additionally, we developed the Robotic assay for Drought (RoAD) system. RoAD completely automates PCZ and drought experiments, allowing for daily weighing, watering and imaging of plants under control, PCZ or drought treatments. This phenomics platform established a system to study BR-drought crosstalk in soil-grown plants and identified the phenotypes of *tcp11* mutants. *tcp11* plants are resistant to PCZ, showing increased BR-regulated growth. Thus, we expected that *tcp11* mutants

would be susceptible to drought similar to other mutants that have increased BR response such as *bes1-D* (Chen et al., 2017; Nolan et al., 2017b; Ye et al., 2017). Surprisingly, we found that *tcp11* is resistant to drought stress, providing an opportunity to increase BR-regulated growth while maintaining drought stress resistance. Thus, systems approaches coupled with phenomics hold great promise in identifying factors that can improve plant growth and stress resilience.

Several areas for future exploration include:

1) The relationship between PLATZ and ARID-HMG1 on BR-regulated gene expression. PLATZ and ARID-HMG1 both bind to A/T-rich sequences. Do these factors compete for binding to the same sites to oppositely control BR-regulated genes? Future ChIP-seq, DNA-binding and promoter::luciferase reporter assays will begin to address this mechanism of regulation.

2) What components are present in BES1, PLATZ and ARID-HMG1 transcriptional complexes in plants? Our studies using Y2H approaches identified a large number of BR-TFs that interact with BES1, PLATZ and ARID-HMG1. Techniques such as affinity purification mass-spectrometry and proximity labeling should be used to clarify which of these BR-TFs associate with BES1, PLATZ and ARID-HMG1 *in vivo*.

3) We identified 657 BR-TFs implicated in controlling BR-regulated gene expression. What tissues do these BR-TFs function in? And, when are they regulated in response to BRs? Understanding the spatial and temporal regulation of BR-TFs is an important area that should be addressed in the future.

4) The GRNs investigated in this study were constructed using transcript levels as a proxy for TF abundance/activity. TFs are also subject to extensive regulation at the post-translational level including protein degradation and post-translational modifications. Incorporating these additional layers of regulation could allow for a more complete understanding of BR networks.

5) Finally, how does natural variation in the BR GRN shape BR responses? Fully sequenced genomes, methylomes and transcriptomes are available for 1,135 natural variants of Arabidopsis from around the world (Kawakatsu et al., 2016). We have already observed significant variation in BR responses among different Arabidopsis accessions (data not shown). Investigating the underlying genetic mechanisms, evolutionary forces and environmental interactions should yield additional insight into how BRs function in plant growth and stress pathways.

4.2 References

Antosch, M., Mortensen, S.A., and Grasser, K.D. (2012). Plant proteins containing high mobility group box DNA-binding domains modulate different nuclear processes. Plant Physiol *159*, 875-883.

Chen, J., Nolan, T., Ye, H., Zhang, M., Tong, H., Xin, P., Chu, J., Chu, C., Li, Z., and Yin, Y. (2017). Arabidopsis WRKY46, WRKY54 and WRKY70 Transcription Factors Are Involved in Brassinosteroid-Regulated Plant Growth and Drought Response. The Plant Cell, tpc.00364.02017.

Chen, J., and Yin, Y. (2017). WRKY transcription factors are involved in brassinosteroid signaling and mediate the crosstalk between plant growth and drought tolerance. Plant Signaling & Behavior, e1365212.

Clouse, S.D., Langford, M., and McMorris, T.C. (1996). A brassinosteroid-insensitive mutant in Arabidopsis thaliana exhibits multiple defects in growth and development. Plant Physiology *111*, 671-678.

Fletcher, M.N., Castro, M.A., Wang, X., de Santiago, I., O'Reilly, M., Chin, S.F., Rueda, O.M., Caldas, C., Ponder, B.A., Markowetz, F*., et al.* (2013). Master regulators of FGFR2 signalling and breast cancer risk. Nat Commun *4*, 2464.

Floyd, B.E., Morriss, S.C., MacIntosh, G.C., and Bassham, D.C. (2012). What to Eat: Evidence for Selective Autophagy in Plants. Journal of integrative plant biology *54*, 907-920.

Funakoshi, M., Sasaki, T., Nishimoto, T., and Kobayashi, H. (2002). Budding yeast Dsk2p is a polyubiquitin-binding protein that can interact with the proteasome. Proc Natl Acad Sci U S A *99*, 745-750.

Hansen, F.T., Madsen, C.K., Nordland, A.M., Grasser, M., Merkle, T., and Grasser, K.D. (2008). A Novel Family of Plant DNA-Binding Proteins Containing both HMG-Box and AT-Rich Interaction Domains. Biochemistry *47*, 13207-13214.

Hartwig, T., Corvalan, C., Best, N.B., Budka, J.S., Zhu, J.Y., Choe, S., and Schulz, B. (2012). Propiconazole Is a Specific and Accessible Brassinosteroid (BR) Biosynthesis Inhibitor for Arabidopsis and Maize. PLoS One *7*.

He, J.X., Gendron, J.M., Sun, Y., Gampala, S.S.L., Gendron, N., Sun, C.Q., and Wang, Z.Y. (2005). BZR1 is a transcriptional repressor with dual roles in brassinosteroid homeostasis and growth responses. Science *307*, 1634-1638.

He, J.X., Gendron, J.M., Yang, Y., Li, J., and Wang, Z.Y. (2002). The GSK3-like kinase BIN2 phosphorylates and destabilizes BZR1, a positive regulator of the brassinosteroid signaling pathway in Arabidopsis. Proc Natl Acad Sci U S A *99*, 10185-10190.

Jiang, P., Wang, H.F., Li, W., Zang, C.Z., Li, B., Wong, Y.L.J., Meyer, C., Liu, J.S., Aster, J.C., and Liu, X.S. (2015). Network analysis of gene essentiality in functional genomics experiments. Genome Biology *16*.

Kawakatsu, T., Huang, S.C., Jupe, F., Sasaki, E., Schmitz, R.J., Urich, M.A., Castanon, R., Nery, J.R., Barragan, C., He, Y*., et al.* (2016). Epigenomic Diversity in a Global Collection of Arabidopsis thaliana Accessions. Cell *166*, 492-505.

Kim, B., Jeong, Y.J., Corvalan, C., Fujioka, S., Cho, S., Park, T., and Choe, S. (2014). Darkness and gulliver2/phyB mutation decrease the abundance of phosphorylated BZR1 to activate brassinosteroid signaling in Arabidopsis. The Plant journal : for cell and molecular biology *77*, 737-747.

Kraft, C., Peter, M., and Hofmann, K. (2010). Selective autophagy: ubiquitin-mediated recognition and beyond. Nat Cell Biol *12*, 836-841.

Lee, D.Y., Arnott, D., and Brown, E.J. (2013). Ubiquilin4 is an adaptor protein that recruits Ubiquilin1 to the autophagy machinery. EMBO reports *14*, 373-381.

Lee, D.Y., and Brown, E.J. (2012). Ubiquilins in the crosstalk among proteolytic pathways. Biological chemistry *393*, 441-447.

Li, J., Nagpal, P., Vitart, V., McMorris, T.C., and Chory, J. (1996). A role for brassinosteroids in light-dependent development of *Arabidopsis*. Science *272*, 398-401.
Li, L., Ye, H., Guo, H., and Yin, Y. (2010). Arabidopsis IWS1 interacts with transcription factor BES1 and is involved in plant steroid hormone brassinosteroid regulated gene expression. Proceedings of the National Academy of Sciences of the United States of America *107*, 3918-3923.

Li, L., Yu, X., Thompson, A., Guo, M., Yoshida, S., Asami, T., Chory, J., and Yin, Y. (2009). Arabidopsis MYB30 is a direct target of BES1 and cooperates with BES1 to regulate brassinosteroid-induced gene expression. Plant Journal *58*, 275-286.

Lin, Y.L., Sung, S.C., Tsai, H.L., Yu, T.T., Radjacommare, R., Usharani, R., Fatimababy, A.S., Lin, H.Y., Wang, Y.Y., and Fu, H. (2011). The defective proteasome but not substrate recognition function is responsible for the null phenotypes of the Arabidopsis proteasome subunit RPN10. Plant Cell *23*, 2754-2773.

Margolin, A.A., Wang, K., Lim, W.K., Kustagi, M., Nemenman, I., and Califano, A. (2006). Reverse engineering cellular networks. Nat Protoc *1*, 662-671.

Marshall, R.S., Li, F., Gemperline, D.C., Book, A.J., and Vierstra, R.D. (2015). Autophagic Degradation of the 26S Proteasome Is Mediated by the Dual ATG8/Ubiquitin Receptor RPN10 in Arabidopsis. Molecular cell.

Michaeli, S., Galili, G., Genschik, P., Fernie, A.R., and Avin-Wittenberg, T. (2016). Autophagy in Plants--What's New on the Menu? Trends Plant Sci *21*, 134-144.

Nagano, Y., Furuhashi, H., Inaba, T., and Sasaki, Y. (2001). A novel class of plant-specific zinc-dependent DNA-binding protein that binds to A/T-rich DNA sequences. Nucleic acids research *29*, 4097-4105.

Noguchi, T., Fujioka, S., Takatsuto, S., Sakurai, A., Yoshida, S., Li, J.M., and Chory, J. (1999). Arabidopsis det2 is defective in the conversion of (24R)-24-methylcholest-4-En-3-One to (24R)-24-methyl-5 alpha-cholestan-3-one in brassinosteroid biosynthesis. Plant Physiology *120*, 833-839.

Nolan, T., Chen, J., and Yin, Y. (2017a). Cross-talk of Brassinosteroid signaling in controlling growth and stress responses. Biochem J *474*, 2641-2661.

Nolan, T.M., Brennan, B., Yang, M., Chen, J., Zhang, M., Li, Z., Wang, X., Bassham, D.C., Walley, J., and Yin, Y. (2017b). Selective Autophagy of BES1 Mediated by DSK2 Balances Plant Growth and Survival. Developmental cell *41*, 33-46 e37.

Petherick, K.J., Williams, A.C., Lane, J.D., Ordonez-Moran, P., Huelsken, J., Collard, T.J., Smartt, H.J., Batson, J., Malik, K., Paraskeva, C.*, et al.* (2013). Autolysosomal beta-catenin degradation regulates Wnt-autophagy-p62 crosstalk. EMBO J *32*, 1903-1916.

Sun, Y., Fan, X.-Y., Cao, D.-M., Tang, W., He, K., Zhu, J.-Y., He, J.-X., Bai, M.-Y., Zhu, S., Oh, E.*, et al.* (2010). Integration of Brassinosteroid Signal Transduction with the Transcription Network for Plant Growth Regulation in Arabidopsis. Developmental cell *19*, 765-777.

Svenning, S., Lamark, T., Krause, K., and Johansen, T. (2011). Plant NBR1 is a selective autophagy substrate and a functional hybrid of the mammalian autophagic adapters NBR1 and p62/SQSTM1. Autophagy *7*, 993-1010.

Szekeres, M., Németh, K., Koncz-Kálmán, Z., Mathur, J., Kauschmann, A., Altmann, T., Rédei, G.P., Nagy, F., Schell, J., and Koncz, C. (1996). Brassinosteroids rescue the deficiency of CYP90, a cytochrome P450, controlling cell elongation and de-etiolation in *Arabidopsis*. Cell *85*, 171-182.

Wang, H., Tang, J., Liu, J., Hu, J., Liu, J., Chen, Y., Cai, Z., and Wang, X. (2018). Abscisic Acid Signaling Inhibits Brassinosteroid Signaling through Dampening the Dephosphorylation of BIN2 by ABI1 and ABI2. Mol Plant *11*, 315-325.

Wang, Y., Sun, S., Zhu, W., Jia, K., Yang, H., and Wang, X. (2013). Strigolactone/MAX2-induced degradation of brassinosteroid transcriptional effector BES1 regulates shoot branching. Developmental cell *27*, 681-688.

Wang, Z.Y., Nakano, T., Gendron, J., He, J.X., Chen, M., Vafeados, D., Yang, Y.L., Fujioka, S., Yoshida, S., Asami, T.*, et al.* (2002). Nuclear-localized BZR1 mediates brassinosteroid-induced growth and feedback suppression of brassinosteroid biosynthesis. Developmental cell *2*, 505-513.

Yang, M., Li, C., Cai, Z., Hu, Y., Nolan, T., Yu, F., Yin, Y., Xie, Q., Tang, G., and Wang, X. (2017). SINAT E3 Ligases Control the Light-Mediated Stability of the Brassinosteroid-Activated Transcription Factor BES1 in Arabidopsis. Developmental cell *41*, 47-58 e44.

Ye, H., Li, L., Guo, H., and Yin, Y. (2012). MYBL2 is a substrate of GSK3-like kinase BIN2 and acts as a corepressor of BES1 in brassinosteroid signaling pathway in Arabidopsis. Proceedings of the National Academy of Sciences of the United States of America *109*, 20142-20147.

Ye, H., Liu, S., Tang, B., Chen, J., Xie, Z., Nolan, T.M., Jiang, H., Guo, H., Lin, H.-Y., Li, L.*, et al.* (2017). RD26 mediates crosstalk between drought and brassinosteroid signalling pathways. Nature Communications *8*, 14573.

Yin, Y., Vafeados, D., Tao, Y., Yoshida, S., Asami, T., and Chory, J. (2005). A new class of transcription factors mediates brassinosteroid-regulated gene expression in Arabidopsis. Cell *120*, 249-259.

Yin, Y.H., Wang, Z.Y., Mora-Garcia, S., Li, J.M., Yoshida, S., Asami, T., and Chory, J. (2002). BES1 accumulates in the nucleus in response to brassinosteroids to regulate gene expression and promote stem elongation. Cell *109*, 181-191.

Youn, J.H., and Kim, T.W. (2015). Functional Insights of Plant GSK3-like Kinases: Multi-Taskers in Diverse Cellular Signal Transduction Pathways. Molecular Plant *8*, 552-565.
Yu, X., Li, L., Zola, J., Aluru, M., Ye, H., Foudree, A., Guo, H., Anderson, S., Aluru, S., Liu, P.*, et al.* (2011). A brassinosteroid transcriptional network revealed by genome-wide identification of BESI target genes in Arabidopsis thaliana. Plant Journal *65*, 634-646.

Zhang, D., Ye, H., Guo, H., Johnson, A., Zhang, M., Lin, H., and Yin, Y. (2014). Transcription factor HAT1 is phosphorylated by BIN2 kinase and mediates brassinosteroid repressed gene expression in Arabidopsis. Plant Journal *77*, 59-70.

Zhang, S., Cai, Z., and Wang, X. (2009). The primary signaling outputs of brassinosteroids are regulated by abscisic acid signaling. Proc Natl Acad Sci U S A *106*, 4543-4548.

Zhou, J., Wang, J., Cheng, Y., Chi, Y.J., Fan, B., Yu, J.Q., and Chen, Z. (2013). NBR1-mediated selective autophagy targets insoluble ubiquitinated protein aggregates in plant stress responses. PLoS genetics *9*, e1003196.

APPENDIX A

RD26 MEDIATES CROSSTALK BETWEEN DROUGHT AND BRASSINOSTEROID SIGNALING PATHWAYS

Huaxun Ye[1]†, Sanzhen Liu[2‡], Buyun Tang[1#], Jiani Chen[1], Zhouli Xie[1], Trevor Nolan[1], Hao Jiang[1], Hongqing Guo[1], Hung-Ying Lin[2], Lei Li[3], Yanqun Wang[3], Hongning Tong[4], Mingcai Zhang[5], Chengcai Chu[4], Zhaohu Li[5], Maneesha Aluru[6], Srinivas Aluru[7], Patrick Schnable[2, 8] & Yanhai Yin[1*]

[1]Department of Genetics, Development and Cell Biology, Iowa State University, Ames, IA 50011, USA

[2]Department of Agronomy, Iowa State University, Ames, IA 50011, USA

[3]Department of Molecular Biology, Massachusetts General Hospital and Department of Genetics, Harvard Medical School, Boston, Massachusetts 02115, USA

[4]Institute of Genetics, Chinese Academy of Sciences, Beijing 100101, China

[5]State Key Laboratory of Plant Physiology and Biochemistry, Department of Agronomy, College of Agronomy and Biotechnology, China Agricultural University, Beijing 100193, China

[6] School of Biology, Georgia Institute of Technology, GA 30332, USA

[7]School of Computational Science and Engineering, Georgia Institute of Technology, GA 30332, USA

[8]Data2Bio LLC, Ames IA 50011-3650

†Current Address, Dupont Pioneer, Inc. Johnston, IA 50131

‡Current Address, Department of Plant Pathology, Kansas State University, Manhattan KS 66506-5502;

[#]Current Address: Department of Biochemistry and Molecular Biology, Indiana University School of Medicine, Indianapolis, IN 46202

* Corresponding Author: Department of Genetics, Development and Cell Biology
Iowa State University, Ames, Iowa 50011-3650
Tel: (515) 294-4816; Fax: (515) 294-5256

A.1 Abstract

Brassinosteroids (BRs) regulate plant growth and stress responses via the BES1/BZR1 family of transcription factors, which regulate the expression of thousands of downstream genes. BRs are involved in the response to drought, but the mechanistic basis of interactions between drought response and BR signaling remains to be established. Here we show that the NAC transcription factor RD26 mediates crosstalk between drought and BR signaling. *RD26* is a BES1 target gene and can inhibit BR-regulated growth when overexpressed. Global gene expression studies suggest that RD26 can act antagonistically to BR to regulate the expression of a subset of BES1-regulated genes thereby inhibiting BR function. We show that RD26 can interact with BES1 protein and antagonize BES1 transcriptional activity on BR-regulated genes and that BR signaling can also repress expression of *RD26* and its homologs and inhibit drought responses. Our results thus reveal a mechanism coordinating plant growth and drought tolerance.

A.2 Introduction

Brassinosteroids (BRs) are a group of plant steroid hormones regulating plant growth, development, and responses to biotic and abiotic stresses [1, 2]. Over the past two decades, the main components of the BR signaling pathway have been identified and characterized [3-22]. BR signaling leads to the accumulation of BES1/BZR1 (BRI1 EMS SUPPRESSOR 1/BRASSINAZOLE RESISTANT 1) family transcription factors in the nucleus to control the expression of target genes for BR responses [23-28].

Several studies indicated that treatment of exogenous BRs could enhance the tolerance of plants to drought [1, 29, 30]. However, BR-deficient mutants were reported to

have an enhanced tolerance to drought [31-33], suggesting an inhibitory effect of BRs on drought tolerance. These early studies imply complex relationships between BR-regulated growth and drought responses. Several transcription factors, including drought-induced transcription factor RD26 (RESPONSIVE TO DESICCATION 26) and several of its close homologs, have been identified as the direct targets of BES1 and BZR1 [23, 24], suggesting that these proteins may play important roles in interactions between BR and drought pathways.

RD26 belongs to the NAC (petunia NAM and *Arabidopsis* ATAF1, ATAF2 and CUC2) family of transcription factors, which are induced by drought, abscisic acid (ABA), NaCl and jasmonic acid (JA) [34-37]. Reporter gene expression studies showed that RD26 is expressed constitutively in both shoots and roots upon drought or salt stress treatments [41, 42]. RD26 and its homologs function to promote drought responsive gene expression and increase plant drought tolerance [35]. Recent studies showed that RD26 and its homologs, ANAC019 and ANAC055 are involved in plant bacterial pathogenesis, JA-mediated defense and thermotolerance[37-42].

In this study, we confirmed that *RD26* is a target gene of BES1 and negatively regulates the BR signaling pathway. RD26 affects BR-regulated gene expression when overexpressed globally by binding and antagonizing BES1 transcriptional activities. Loss-of-function mutants in the BR signaling pathway had higher drought tolerance, while gain-of-function mutants in the BR pathway exhibited lower drought tolerance compared to wild-type (WT). These results suggest that RD26 inhibits BR-regulated plant growth and BR pathway also negatively regulates drought tolerance, establishing

a mechanism for crosstalk between these two important pathways for plant growth and stress responses.

A.3 Results

RD26 is a negative regulator of the BR signaling pathway

Previous ChIP-chip studies indicated that *RD26* was a target of BES1 and BZR1 and its expression was repressed by BL (brassinolide, the most active BR), BES1 and BZR1 [23, 24]. Since, BES1 and BZR1 can bind to BRRE to repress gene expression, we examined the *RD26* gene promoter and found a BRRE site at nucleotide position -851 relative to the transcriptional start site. ChIP experiments showed that BES1 binds to the BRRE site *in vivo*, with more binding in *bes1-D* in which BES1 protein accumulates than in WT plants (Supplementary Figure 1a). *RD26* expression was reduced by BL in WT plants and was repressed in *bes1-D* (Fig. S1b). These results confirm that *RD26* is a target of BES1 and its expression is repressed by BL through BES1.

Our previous result indicated that the loss-of-function *rd26* mutant has a small increase in BR response [23], suggesting that RD26 functions with its homologs to inhibit BR response. To confirm this hypothesis, we generated *RD26* overexpression transgenic lines. *RD26* overexpressing plants (*RD26OX*) displayed a stunted growth phenotype, the severities of which correspond well with RD26 protein levels (Fig. 1a). Moreover, the *RD26OX* transgenic plants could suppress the phenotype of *bes1-D*, a gain-of-function mutant in the BR pathway (Fig. 1b). Western blotting indicated that BES1 protein levels and phosphorylation status did not change significantly in *bes1-D RD26OX* double mutant (Fig. 1c). These results suggest that RD26 functions downstream of BES1 to inhibit BR-mediated growth.

To confirm that *RD26OX* phenotype is related to reduced BR response, we determined its response to BL and to the BR biosynthesis inhibitor brassinazole (BRZ), which reduces endogenous BR levels [43]. RD26 overexpression plants have reduced response to BL in hypocotyl elongation assays (Fig. 1d). Likewise, *RD26OX* seedlings had shorter hypocotyls and were more sensitive to BRZ compared to Col-0 WT (Fig. 1e). Several RD26 homologs, *ANAC019*, *ANAC055* and *ANAC102*, are also BES1 and/or BZR1 direct targets, and are repressed by BRs likely functioning redundantly in BR responses [23, 24]. We generated quadruple mutant of *rd26 anac019 anac055 anac102.* The quadruple mutant has a BR response phenotype and showed increased response to BL (especially at 100 nM BL) compared to WT (Fig. 1d). The *rd26 anac019 anac055 anac102* quadruple mutant is less sensitive to BRZ, especially at higher concentrations (Fig. 1e and Fig. S1d). The genetic evidence demonstrates that RD26 and its close homologs play a negative role in the BR signaling pathway.

RD26 negatively regulates BR-responsive genes

To determine if the strong phenotype of *RD26OX* plants is indeed related to BR response, we examined several known BR-induced genes by qPCR (Fig. S2a). In general, many BR-induced genes we tested are down-regulated in *RD26OX*, including genes involved in BR-regulated cell elongation (TCH4 and EXPL2), supporting a role of RD26 in modulating BR-regulated gene expression and plant growth. To more fully understand how RD26 negatively regulates BR responses, we performed global gene expression studies with *RD26* mutants in the absence or presence of BRs by high throughput RNA-sequencing (RNA-seq). We used 4-week-old adult plants for gene expression studies because *RD26OX* plants display the most obvious growth

phenotype at this stage. In WT, 2678 genes were induced and 2376 genes were repressed by BL, among ~22,000 genes analyzed (Fig. 2, .Supplementary Data 1 & 2), as we previously reported [44]. The BR-regulated genes from our RNA-seq analysis in adult plants have significant overlaps (about 43%) with previous microarray analyses of BR-regulated genes in either seedlings or adult plants (Supplementary Data 3 & 4, and Fig. S2b) [24, 45-49]. Consistent with the strong phenotype of *RD26OX* plants, 3246 genes are up-regulated and 5479 genes are down-regulated in the transgenic plants, respectively (Fig. 2, Supplementary Data 5 & 6).

To explore how RD26 affects BR-regulated gene expression, we examined the overlaps between BR-regulated genes and genes affected in *RD26OX* plants by performing clustering analysis with specific gene groups. RD26 modulates BR-responsive genes in complex ways (Fig. 2, Fig. S3). Consistent with the negative role of RD26 in BR response, 43% (1141, Group 1) of BR-induced genes were down-regulated in *RD26OX* plants and their induction by BRs was reduced, but not abolished (Fig. 2a-b). In contrast, only 20% (539, Group 3) of BR-induced genes were up-regulated in *RD26OX* (Fig. 2a and Fig. S3a). These results suggest that RD26 negatively modulates a significant portion of BR-induced genes.

On the other hand, among 2376 BR-repressed genes, 595 (25%, Group 2) were up-regulated and 823 (35%, Group 4) were down-regulated in *RD26OX* plants (Fig. 2c-d and Fig. S3b). While Group 3 and Group 4 genes suggest positive role for RD26 in BR response (i.e. BR-induced genes are up-regulated and BR-repressed genes are down-regulated in *RD26OX*), Group 1 and Group 2 genes demonstrated a negative role of RD26 in BR response (BR-induced genes are down-regulated and BR-repressed genes

are up-regulated in *RD26OX*). In this study, we focus on the Group 1 and Group 2 genes to determine the mechanisms by which RD26 negatively regulates BR responses.

Consistent with the relatively weak BR-response phenotype of the *rd26 anac019 anac055 anac102* mutant, only 405 genes are up-regulated and 378 are down-regulated in *rd26 anac019 anac055 anac102* quadruple mutant (Fig. S4, Supplementary Data 7 & 8). We further compared BR-regulated genes and genes affected in *RD26OX* and the *rd26 anac019 anac055 anac102* mutant (Fig. S5a-b). Four subgroups are subjected to further clustering analysis: BR-induced genes that are down-regulated in *RD26OX* and up-regulated in the quadruple mutant (36, Fig. S5c); BR-induced genes that are up-regulated in *RD26OX* and down-regulated in the quadruple mutant (15, Fig. S5e); BR-repressed genes that are up-regulated in *RD26OX* and down-regulated in the quadruple mutant (44, Fig. S5d); and BR-repressed genes that are down-regulated in *RD26OX* and up-regulated in the quadruple mutant (19, Fig. S5f). Most of these genes are affected in opposite ways in the *rd26 anac019 anac055 anac102* mutant and *RD26OX*. These results support the conclusion that RD26 and its homologs function in a complex way to modulate BR regulated gene expression.

RD26 and BES1 differentially control BR-regulated genes

Previous studies indicated that both BES1 and BZR1 can bind to BRRE site or E-boxes to inhibit or activate gene expression, respectively[23, 24]. We examined the Group 1 and Group 2 gene promoters and found that BRRE elements are especially enriched in Group 2 gene promoters (Fig. S6a, Supplementary Table 1) and E-boxes (CANNTG,

especially a specific E-box CATGTG in BR-induced gene promoters [28]) are enriched in Group 1 gene promoters (Fig. S6b-c, Supplementary Table 1), within 500 base-pairs (bp) relative to the transcriptional start sites. The differential enrichments within -500 bp promoter regions are significant as most BES1 and BZR1 binding sites are located in the region as revealed by genome-wide ChIP-chip studies[23, 24]. We selected several gene promoters from Group 1 and Group 2 and fused with *luciferase* (*LUC*) gene, to generate reporter constructs. *BES1*, *RD26* or *BES1* plus *RD26* were co-expressed with the reporter constructs and the reporter gene expression was determined. While BES1 repressed and RD26 activated the expression of Group 2 genes, the reporter gene expression level was in between when *BES1* and *RD26* were co-expressed (Fig. 3a-c). In contrast, BES1 activated and RD26 repressed Group 1 reporter genes and the expression level fell in the middle when *RD26* and *BES1* were coexpressed (Fig. 3d-f). These results indicated that RD26 acts to antagonize BES1 actions on these BR-regulated genes.

To reveal the mechanisms by which RD26 inhibits the large number of BR-induced genes (Group 1, Fig. 2b) and up-regulates many BR-repressed genes (Group 2, Fig. 2d), we chose one gene representative of each group for further mechanistic studies. A BR-repressed gene, At4g18010, was chosen to represent Group 2 genes because it is up-regulated in *RD26OX* and its promoter contains a BRRE site at -405 bp relative to the transcription start site (Fig. S7a). Likewise, A BR-induced gene At4g00360 was chosen to represent Group 1 genes as its promoter contains a well-established BES1 binding site, CATGTG E-box, at nucleotide -470 (Fig. S7b).

To confirm the antagonistic effect of RD26 on BES1-mediated gene expression observed by LUC reporter gene assays, we examined the expression of these two genes in *bes1-D*, *RD26OX* and *bes1-D RD26OX* plants, in which BES1, RD26 or both are increased. As shown in Fig. 3g, the expression of At4g18010 was down-regulated in *bes1-D* and up-regulated in *RD26OX*, but the expression level was in between in *bes1-D RD26OX* double mutant. In contrast, the expression of At4g00360 was much higher in *bes1-D* compared to *bes1-D RD26OX*, while its expression was significantly repressed in *RD26OX* (Fig. 3h).

RD26 and BES1 bind to DNA-binding sites simultaneously

Previous DNA binding experiments showed that NAC transcription factors including RD26 (ANAC072) and ANC019 could bind to DNA sequences with two motifs: CATGT(G) and a CACG core spaced by varying numbers of nucleotides [35, 39, 40]. The NAC binding sites are very similar to E-box (CANNTG) or conserved core sequence of BRRE site (CGTGT/CG), well established binding sites for BES1/BZR1 [23, 24]. These results suggest that RD26 and BES1 could potentially bind to the same site to modulate BR-regulated gene expression.

We first used yeast one-hybrid assays to test if BES1 and RD26 can target to the same promoter fragments (Fig. 4). We fused several fragments of At4g18010 promoter (-P1, -P2 and -P3, with BRRE located in P3) and At4g00360 promoter (-P1, -P2 and -P3, with CACGTG E-box located in P3) to pLacZi reporter (Clontech, Inc) and integrated them into the yeast genome (Fig. 4a). Mutants were also generated in which At4g18010-P3 BRRE and At4g00360-P3 E-box were mutated to unrelated sequences

(see Fig. 5a). BES1 (with pGBKT7 vector), RD26 (with pGADT7 vector) or both BES1 and RD26 were expressed in each of the reporter yeast strain and the LacZ expression was determined. As shown in Fig. 4b, while neither BES1 nor RD26 significantly changed the gene expression from At4g18010-P3, co-expression of BES1 and RD26 activated the reporter gene expression. It's worth noting that the fusion of GAL4 activation domain in pGADT7 to RD26 apparently changed RD26 property in yeast to become an activator in combination with BES1 (compared with the result from plants in Fig. 3), which is necessary to detect BES1/RD26 interaction in yeast. Moreover, mutation of the BRRE in At4g18010-P3 completely abolished the activation (Fig. 4b). The results demonstrated that BES1 and RD26 act through BRRE site in At4g18010-P3 promoter fragment. Similarly, co-expression of BES1 and RD26 activated At4g00360-P3 reporter, which is much reduced when the CATGTG E-box is mutated, indicating that BES1 and RD26 act through the CATGTG E-box in At4g00360-P3 (Fig. 4c) to regulate gene expression.

We also performed ChIP assays with WT and *RD26OX* transgenic plants, with BES1 antibody [23] or RD26 antibodies we generated (Fig. S8). While BES1 itself binds to At4g18010 promoter (P3) in WT plants, such binding is enhanced in *RD26OX* plants (Fig. 4d, columns 3-4), suggesting that BES1 and RD26 together enhance binding to the promoter region. Consistent with the result that RD26 antibody detects RD26 in *RD26OX* but not in WT plants (Fig. S8a-b), RD26 binding to the At4g18010 promoter (P3) in *RD26OX* was strongly apparent but barely detectable in WT (Fig. 4d, columns 5-6). In contract, such cooperative binding is not detected in the more upstream promoter region (Fig. 4d, columns 9-12).

To confirm that BES1 and RD26 can bind to the same promoter regions at the same time, we also performed ChIP-reChIP with chromatin prepared from *RD26OX, rd26 anac019 anac055 anac102 (rdQ) or BES1RNAi* plants in which BES1 level is reduced [27] (Fig. S9). When the first ChIP was performed with anti-BES1 antibody and eluted chromatin samples were then immunoprecipitated with anti-RD26 or IgG control, significant enrichment of BES1/RD26 binding was detected in *RD26OX* plants, which is clearly reduced in *rdQ* mutant, and moderately reduced in *BES1RNAi* plants with two pairs of independent qPCR primers (Fig.S9 a-b). Similar results were obtained when the first ChIP was performed with anti-RD26 antibody and reChIP with anti-BES1 (Fig. S9c). These results suggest that BES1 and RD26 can simultaneously bind to the At4g18010 gene promoter in *vivo*.

To further reveal the biochemical mechanisms by which RD26 antagonizes BES1 actions, Electrophoretic Mobility Shift Assay (EMSA) experiments were performed with recombinant BES1 and RD26 proteins using DNA probes containing BRRE (from At4g18010) or CATGTG E-box (from At4g00360) (Fig. 5a and Fig. S10). While BES1 binds to BRRE (CGTGTG) from At4g18010 quite strongly, RD26 binds to the probe more weakly; and both bindings were abolished with mutant probe in which BRRE is mutated (Fig. 5b). Interestingly, BES1 and RD26 together can bind to the BRRE probe more strongly, and the binding is also abolished when the BRRE site is mutated (Fig. 5b). Similar results were obtained with probe containing CATGTG E-box from At4g00360. While RD26 and BES1 can each bind to E-box site separately, RD26 and BES1 synergistically bind to WT but not mutated E-box probe (Fig. 5c). Since BES1 (335 aa) and RD26 (298 aa) are similar in predicted protein sizes, the strong bands

when both proteins are present more likely represent heterodimer of the two proteins, while each of them likely bind to the probe as homodimer. Taken together, the DNA binding and gene expression results suggest that RD26 interacts with BES1 on BRRE site to inhibit BES1's repression function (Fig. 5d) and on E-box to inhibit BES1's activation function (Fig. 5e).

The yeast one-hybrid and DNA binding experiments described above suggest that BES1 and RD26 may be able to interact with each other. To test this hypothesis, we expressed full-length or truncated BES1 with MBP, and RD26 and truncations with GST (Glutathione S-transferase) tag, respectively (Fig. 6a). GST pull-down assays indicated that full-length RD26 could interact with full-length BES1 protein (Fig. 6b). The domains involved in DNA binding/dimerization of BES1 (aa 1-89) and RD26 (aa1-140) are sufficient for the interaction (Fig. 6c). Split Luciferase (Luc) assay was used to test if RD26 and BES1 interact in plants [50]. RD26 was fused with amino-part of Luc (NLuc) and BES1 was fused with carboxyl-part of Luc (CLuc), respectively (Fig. 6d). Co-expression of RD26-NLuc and CLuc-BES1 in tobacco leaves led to increased Luc activity, while co-expression of controls (RD26-NLuc with CLuc or CLuc-BES1 with N-Luc) only produced background level activities (Fig. 6e).

We further confirmed that BES1 and RD26 interaction in vivo by co-immunoprecipitation and by BiFC experiments. GFP antibody (tagged to BES1) can specifically pull-down RD26-MYC co-expressed in tobacco leaves (Fig. 6f). In BiFC assays, co-expression of BES1-YFPN and RD26 YFPC lead to complementation of YFP in the nucleus (Fig. 6g-h), but not from BES1-YFPN/YFPC or YFPN/RD26 YFPC controls (Fig. 6i-l). Taken together, these results indicated that BES1 and RD26 can

interact with each other through corresponding DNA binding/dimerization domains and inhibit each other's functions on Group 1 and Group 2 genes.

BR signaling pathway inhibits drought response

Since BRs function through BES1/BZR1 to repress the expression of RD26 and its homologs, we tested whether the BR pathway affects plant drought response. Previous data showed that the expression of RD26 was induced by drought [29, 30, 35, 41]. Drought induces 2503 and represses 2862 genes (combination of 2-day and 3-day drought treatment data, Supplementary Data 9&10) [51]. Analysis of gene expression affected in *RD26OX* and drought-regulated genes revealed that RD26 up-regulated 38% (963) of drought-induced genes, but only 12% (346) of drought-repressed genes; similarly, RD26 down-regulated 45% (1299) of drought-repressed genes, but only 19% (488) of drought-induced genes (Fig. S11). The results suggest that RD26 plays a major role in plant drought responses.

We also compared BR-regulated genes and drought-regulated genes and found that about 38% of BR-regulated genes are modulated by drought (Fig. S12). If BR signaling indeed inhibits drought response, we expect that loss-of-function BR mutants have increased, and gain-of-function mutants have decreased, drought tolerance. BR loss-of-function mutant, *bri1-5*, a weak BR receptor mutant [52], was exposed to drought stress. After drought stress and recovery, 50% of *bri1-5* mutant plants survived, compared to 16% for WT (Fig. 7a, top panel). On the other hand, a gain-of-function mutant in the BR pathway, *bes1-D*, showed less drought tolerance. Only 22% of *bes1-D* mutants survived, but all of WT controls survived in the drought stress experiment (Fig.

7a bottom panel). The drought response phenotypes were also confirmed in *bes1-D* in Col-0 background [53] with the same trend (Fig. S13).

To test our hypothesis that BR signaling pathway inhibits drought response by repressing *RD26* and its homologs, the expression of several drought-induced or drought-related genes were examined in *bri1-5* mutant and *bes1-D* mutant. Transgenic plants overexpressing *RD26/ANAC072, ANAC019 or ANAC055* could enhance the tolerance to drought stress, suggesting that RD26 and its homologs ANAC019 and ANAC055 are involved in drought response[19]. RT-qPCR results showed that the expression of all three genes plus *ANAC102* are increased in *bri1-5* mutant and decreased in *bes1-D* mutant (Fig. 7b). We also examined 5 other genes involved in drought tolerance [54]. All 5 genes are up-regulated in *bri1-5* and down-regulated in *bes1-D* (Fig. 7b). The results demonstrated that drought response genes are constitutively expressed in loss-of-function BR mutants and repressed in gain-of-function BR mutants, confirming that BR signaling pathway inhibits drought response, likely by repressing the expression of *RD26* and its homologs.

We examined the double mutant *bes1-D RD26OX* and found that RD26 overexpression can clearly rescue the *bes1-D* phenotype in drought response (Fig. S14a). Consistent with the facts that RD26OX suppress *bes1-D* phenotypes, several *bes1-D* induced genes are down-regulated in *RD26OX* plants (Fig. S14b). The expression of these genes is also reduced in *bes1-D RD26OX* double mutant compared to *bes1-D* (Fig. S14b). The gene expression studies support the idea that *RD26* suppresses *bes1-D* phenotypes.

To further understand the relationships among BES1 and RD26/its close homologs, we constructed a GRN (Gene Regulatory Network) based on gene expression correlations using *BES1, RD26, ANAC019, ANAC 055* and *ANAC 102* as seed genes [55]. The GRN showed that *RD26* and three of its close homologs have extensive expression correlations, directly or through other genes (Fig. 7c). Interestingly, *BES1* has relatively fewer connections to other genes; and the "RD26/homolog cluster" and "BES1 cluster" are connected through only one gene, *BOS1*, which was implicated in plant responses to drought, high salinity and fungal pathogens[54, 56].

To validate the GRN, we compared the genes in the network with genes affected in *RD26OX*, as well as drought- and BR-regulated genes (Fig. S15). Interestingly, 82% of the 103 genes in the GRN are affected in *RD26OX*, although only about 1/3 of total detected genes are affected in *RD26 OX* plants. Similarly, 72% and 52% of the genes in the GRN are either regulated by drought or BRs, despite the fact that only about ¼ of total genes are regulated by drought or BRs. The computationally generated GRN and its validation by RNA-seq data support the conclusions that (1): there are close interactions between BES1-mediated BR pathway and drought pathway represented by RD26 and its homologs; (2) Although the interactions between BES1 and RD26 can happen at transcriptional level (i.e. through BOS1), post-transcriptional regulations such as protein-protein interaction between RD26 and BES1 likely play a major role.

A.4 Discussion

In this study, we found that the drought-responsive transcription factor *RD26* is a target of BES1 and functions to inhibit BR responses. Gene expression studies revealed that RD26 and BES1 act antagonistically in the regulation of many BR response genes. The

antagonistic interactions happen at multiple levels. While BES1/BZR1 function to repress the expression of *RD26* at transcription level, RD26 protein interacts with BES1 and inhibits its transcriptional activity. Our results thus establish a molecular link and mechanism of interaction between BR and drought response pathways (Fig. 8).

Our genetic, genomic, molecular and biochemical results demonstrated that RD26 functions to inhibit the BR pathway (Fig. 8). RD26 is induced by drought, promotes drought regulated gene expression and confers drought tolerance when overexpressed [35, 36]. Our genetic studies demonstrate that RD26 is a negative regulator of the BR pathway as overexpression of *RD26* leads to reduced plant growth and BR response and knockout of *RD26* and three of its homologs leads to increased BR response. The relatively weak growth phenotype of *rd26 anac019 anac055 anac102* mutant may be explained by additional family members, which possibly function redundantly in the inhibition of BR response. The fact that a smaller number of genes affected in *rd26 anac019 anac055 anac102* mutant compared to RD26OX transgenic plants is consistent this hypothesis. RD26 and its homologs appear to function as part of a highly redundant and complex network to confer drought tolerance and to inhibit plant growth during drought stress.

Global gene expression studies revealed that RD26 functions to modulate BR responsive gene expression in a complex manner, i.e. RD26 can either activate or repress both BR-induced and BR-repressed genes. However, a large number of BR-induced genes (1141 or 43% of BR-induced genes identified in this study) are significantly down-regulated in *RD26 OX* (Group 1, Fig. 2). Our molecular and biochemical studies suggest that RD26 affects Group 1 gene expression by binding to

the BES1 target site (E-box) and neutralizing BES1 activation activity, potentially by forming an inactive heterodimer (Figs. 3-5). Likewise, 595 (or 25%) BR-repressed genes are up-regulated in *RD26OX*, suggesting that BR and RD26 have opposite function on these genes (Group 2, Fig. 2). Indeed, the molecular and biochemical evidence suggests that while BES1 binds to BRRE to repress gene expression, RD26 can antagonize BES1-mediated gene repression (Fig. 3). We also provided evidence that BES1 and RD26 protein can interact with each other *in vitro* and *in vivo* (Fig. 6). While many protein-protein interactions between transcription factors synergistically activate or repress transcription, our results suggest that BES1 and RD26 interact and antagonize each other's transcriptional activities on Group 1 and Group 2 gene promoters. Our findings thus reveal a previously unknown mechanism that two signaling pathways converge on the same promoter element through two interacting transcription factors to coordinate plant growth and stress responses. Consistent with our conclusion, recent ChIP-seq studies showed that RD26 target gene promoters under abscisic acid treatment are enriched in G-box sequence (CACGTG, a specialized E-box)[57], very similar to BES1 target sites derived from ChIP-chip study[23].

We also observed an inhibitory effect of the BR pathway on drought response as a loss-of-function BR mutant is resistant to drought and a gain-of-function mutant of the BR pathway had compromised drought response. The transcriptional repression of RD26 and its homolog genes by BRs likely play a major role in the observed inhibition of drought response by the BR pathway as the expression of *RD26* and its homologs (including *ANAC019, ANAC 055* and *ANAC102*) are significantly increased in *bri1* and decreased in *bes1-D* (Fig. 7b). While we have provided experimental evidence that

RD26 antagonizes BES1-mediated gene expression on the BES1 target sites, it remains to be determined if BES1 inhibits RD26 mediated gene expression on RD26-related drought target genes.

We propose that the antagonistic interaction between BES1 and RD26 likely ensures that plant growth is reduced when plants are under drought stress, under which *RD26* and its homologs are up-regulated to inhibit BR-induced growth, thus allowing more resources to deal with the drought stress. On the other hand, under normal growth conditions when there is no drought stress, BR signaling represses the drought pathway by repressing the expression of *RD26* and its homologs.

It is worth noting that RD26 and BES1 don't seem to act antagonistically at all times. For example, 539 BR-induced genes (20%, Group 3) are up-regulated, and 823 BR-repressed genes (35%, Group 4) are down-regulated in *RD26OX* (Fig. S3), indicating that RD26 and BES1 act in a similar fashion on these two group of genes. It is possible that RD26 and BES1 target different promoter elements to achieve the positive interactions between RD26 and BES1. It has been suggested that at least under some conditions, exogenously applied BR can improve plant drought tolerance [58]. It is possible that under these circumstances, the Group 2 and Group 4 genes play more dominant roles than Group 1 and Group 2 genes, which can potentially allow BR to activate some drought-induced genes and repress BR-repressed genes and thus promote drought tolerance. More investigation is needed to better understand the interaction between RD26 and BES1 on Group 3 and Group 4 genes.

In summary, we have identified RD26 as a molecular link that coordinates BR and drought responses. We further found that while BES1 functions to repress RD26 gene

expression, RD26 interacts with BES1 and inhibits BES1 transcriptional activity. This reciprocal inhibitory mechanism not only ensures that BR-induced growth is inhibited under drought conditions, but also prevents unnecessary activation of drought response when plants undergo BR-induced growth.

A.5 Methods

Plant materials and growth condition

T-DNA insertion mutants, *rd26* (At4g27410, SALK_063576), *anac019* (At1g52890, SALK_096295), *anac055* (At3g15500, SALK_014331), and *anac102* (At5g63790, SALK_030702) were obtained from ABRC (*Arabidopsis* Biological Resource Center). All plants were grown on 1/2MS plates and/or in soil under long day conditions (16h light/ 8h dark) at 22°C. BRZ and BL response experiments were carried out as previous described [59]. Briefly, seeds were sterilized with 70% ethanol and 0.1% Triton X-100 for 15 min and washed with 100% ethanol 3 times and dried in filter papers in a sterile hood. The seeds were sprinkled onto ½ Linsmaier and Skoog (LS) medium (Caisson Lab) with 0.7% Phytoblend agar (Caisson Lab) and various concentrations of BRZ (provided by Prof. Tadao Asami) or BL (Wako Biochemical). Both BRZ and BL (1 mM stock in DMSO) were added to medium after autoclave and the plates with seeds were placed at 4°C for 3 days. After exposing to light for 8 hours, the plates were wrapped with 3 layers of Aluminum foil and incubated in the dark at 25 °C for 5 days for BRZ response and in the constant light for 7 days for BL response experiments. Hypocotyls were scanned and measured using Image J (https://imagej.nih.gov/ij/). Ten to fifteen hypocotyls were measured and averages and s.d. were calculated and plotted.

Plasmid constructs

For MYC-tagged transgenic plants, RD26 genomic sequence including its 5' UTR was cloned from wild type and fused with MYC tag and CaMV 35S promoter into pZP211 vector [60]. For recombinant protein purification, full-length or fragments of *RD26* and *BES1* [48] coding regions were cloned into pETMALc-H vector [61] or pET-42a (Novagen).

Generation and analysis of transgenic plants

The construct of RD26-MYC driven by 35S promoter was transformed into Agrobacterium tumefaciens (stain GV3101) which were used to transform plants by the floral dip method [62]. Transgenic lines were selected on 1/2 MS medium plus 60μg/ml gentamycin. Transgene expression was analyzed by western blotting with 2μg anti-cMYC (Sigma, C3956) antibody or HERK1 antibody as control. HERK1 kinase domain[49] and full-length RD26 recombinant proteins were expressed from pETMALc-H and used to generate polyclonal antibody at Iowa State University Hybridoma Facility (http://www.biotech.iastate.edu/biotechnology-service-facilities/hybridoma-facility/). About 2 μg of affinity purified antibody was used in each Western blotting in 10 ml.

Gene expression analysis

For *RD26*, At4g00360 and At4g18010 gene expression, total RNA was extracted and purified from 2-week-old plants of different genotypes using RNeasy Mini Kit (Qiagen). Mx4000 multiplex quantitative PCR system (Stratagene) and SYBR GREEN PCR Master Mix (Applied Biosystems) were used in quantitative real-time PCR

analysis. For transient expression, promoters for At4g00360 (1552) and At4g18010 (1515bp), At1g22400 (1922bp), At5g17860 (1119bp), At4g14365 (430bp) and At3g19720 (411bp) were cloned and used to drive luciferase reporter gene expression. BES1 coding region driven by CaMV 35S promoter was cloned into pZP211 vector, while RD26-MYC construct used in transgenic plant generation was also used in transient experiment. Tobacco leaf transient assay [63] was used to examine the effect of RD26 and BES1 on reporter gene expression either with individual protein or with combination of BES1 and RD26. Equal amount of Agrobacterium cells (measured by $O.D_{600}$, adjusted to the same with vector-containing strain) were injected into the leaves of tobacco. The activities of the luciferase were measured in total protein extracts from triplicate samples (collected with a 5mm leaf puncher with same number of leaf discs in each sample) using Berthold Centro LB960 luminometer with luciferase assay system following the manufacturer's instruction (Promega). The relative level of luciferase activity was normalized by the total amount protein for each sample.

For global gene expression, total RNA was extracted and purified from 4-week-old plants of different genotypes using RNeasy Mini Kit (Qiagen). Duplicated RNA samples were subjected to RNA-seq using HiSeq2000 50 bp single-end sequencing in the DNA facility at Iowa State University. Raw RNA-seq reads were subjected to quality checking and trimming and then aligned to the *Arabidopsis* reference genome (TAIR10) using an intron-aware aligner, Genomic Short-read Nucleotide Alignment Program (GSNAP) [64]. The alignment coordinates of uniquely aligned reads for each sample were used to independently calculate the read depth of each annotated gene. Genes with an average of at least one uniquely mapped read across samples were tested for differential

expression using QuasiSeq (http://cran.r-project.org/web/packages/QuasiSeq). The generalized linear model Quasi-likelihood spline method assuming negative binomial distribution of read counts implemented in the QuasiSeq package was used to compute a p-value for each gene. The 0.75 quantile of reads from each sample was used as the normalization factor [65]. A multiple test controlling approach was used to convert p-values to q-values for controlling false discovery rate (FDR) [66]. For most of the comparisons, q-values no larger than 0.05 were considered to be differentially expressed. Due to the strong growth phenotype of *RD26OX* transgenic lines, more stringent ($q<0.003$) condition was used to determine differentially expressed genes. For heatmap plotting, average reads per million (RPM) for each gene were used and RPM data were scaled to the same level between genes. The overlapped genes were identified and displayed using Venny$^{2.0}$ program (http://bioinfogp.cnb.csic.es/tools/venny/).

Chromatin Immunoprecipitation

Chromatin immunoprecipitation was performed as previously described [23] with modifications [67]. Briefly, 5 g of 4-week-old plants were fixed in 1% formaldehyde and used to isolate nuclei and chromatin. The chromatin was sheared with Diagenode Bioruptor sonication system with 30 cycles of 30-second on and 30-second off in icy water-bath. Twenty ug of affinity purified BES1[23], RD26 antibodies (see “Generation and analysis of transgenic plants” section) or IgG (Sigma, I5006) were used to immunoprecipitate chromatin, which was collected with 20ul Dynabeads protein A (Invotrogen). Three qPCR technical repeats were used to calculate enrichment folds compared to ubiquitin control (UBQ5). The enrichment of specific transcription factors

was examined by qPCR with primers from indicated regions. The averages and standard errors were derived from 4 biological repeats.

For ChIP-reChIP, chromatin was prepared from 15g *RD26OX, BES1RNAi or rdQ* mutant plants with a modified protocol in which the crosslinking with formaldehyde was performed after tissue grinding in liquid nitrogen and all the buffer volumes were scaled up by 15-folds compared to the published protocol [68]. The sonication and immunoprecipitation were performed as described above with BES1 or RD26 antibody. Each first immunoprecipitated chromatin sample was eluted with 75 ul 10 mM Tris-HCl (pH 8.0), 1 mM EDTA, 2% SDS and 15 mM DTT and diluted 20 folds for second immunoprecipitation with corresponding antibody (RD26 or BES1) or IgG control. The enrichment at specific regions was determined by qPCR with indicated primers as described above. The averages and standard errors were derived from 3 biological repeats.

Other Bioinformatics analysis:

For promoter motif analysis, we downloaded Group 1 & 2 genes upstream 3kb sequence from TAIR database (https://www.Arabidopsis.org/tools/bulk/sequences/index.jsp). Based on these sequence information, we coded in-house Perl scripts to match possible E-box and BRRE motif in upstream 3,000 bp region by searching conserved sequence “CANNTG” for general E-box or CATGTG for specific E-box and conserved sequence “CGTG(T/C)G” for BRRE site. All the statistical analysis was done by R language (http://www.R-project.org/). We fitted a negative binominal model for fitting the

frequency of E-box and BRRE domain in “glm.nb” function then calculate P-value for each comparison. The density was plots were generated by R language “plot” function.

For re-analysis of previous published microarray data[24, 45-49], we downloaded the microarray raw CEL data from Riken and analyzed the arrays using "Robust Multi-array Average (RMA) method [69] to obtain gene expression data. To analyze gene expression and compare expression between the wild type and hormone treatments, we used the linear model for microarray (limma) package from the Bioconductor project (http://www.bioconductor.org). When estimating statistical significance for log2 transformed fold change replicates were combined, analogous to the classical pooled two-sample t-test. To account for multiple testing we used the Benjamini-Hochberg method and significance level for detection is at 5%. The differential expressed genes were combined with published gene lists to obtain the BR-regulated genes by microarrays and listed in Supplementary Data 3 and 4.

Protein-protein interaction experiments

The Split Luciferase Complementation Assays were performed as described [50]. The coding region of RD26 and BES1 were cloned into pCAMBIA1300-nLUC construct and pCAMBIA1300-cLUC construct, respectively. Tobacco leaf transient assay was used to examine luciferase activity in the presence or absence of RD26 and/or BES1. Equal amount of Agrobacterium cells (measured by OD_{600}, adjusted to same with vector containing strain) were injected to tobacco leaves. The luciferase activities were measured from protein extracts from triplicate samples as described above. For the IP experiments, tobacco leaves were homogenized in protein lysis buffer (1 mM EDTA,

10% glycerol, 75 mM NaCl, 0.05% SDS, 100 mM Tris-HCl, pH 7.4, 0.1% Triton X-100 and 1 × complete cocktail protease inhibitors). After protein extraction, anti-GFP antibody (10 ul, Life Technologies-Molecular Probes, A21311) was added to total proteins. After incubation with gentle mixing for 1 h at 4℃, 200 uL fresh 50% slurry of protein A beads (Trisacryl Immobilized Protein A-20338, Thermo Sci) were added, and incubation was continued for 1h. Protein A beads were pelleted by centrifugation at 2000 rpm for 1 min, and the supernatant was removed. The precipitated beads were washed at least 4 times with the protein extraction buffer and then eluted by 2 × SDS protein loading buffer with boiling for 5 minutes. The IP products were used for Western blotting with 2ug of anti-BES1 antibody or MYC antibody (Sigma, C3956). BiFC experiments were performed as recently described [44]. BES1 and RD26 cDNAs were cloned into N- or C-terminus of EYFP vectors [70]. Sequencing-confirmed constructs were transformed into *Agrobacterium tumefaciens* strain GV3101. Agrobacteria were grown in LB medium containing 0.2M acetosyringone and washed with ½ LS medium, pH 5.6 and resuspended to OD_{600} 0.5 with ½ LS medium containing 0.2M acetosyringone. Combinations of Agrobacterium were infiltrated into *Nicotiana benthamiana* leaves and examined for YFP signals three days after infiltration. A Leica SP5 X MP confocal microscope equipped with an HCS PL APO CS 20.0×0.70 oil objective was used to detect reconstituted YFP, was excited with a 514-nm laser line and detected from 530 to 560 nm. The LAS AF software (Leica Microsystems) were used to obtain images with same settings.

EMSA experiments

EMSA experiments were carried out as described previously [25]. After annealing, oligonucleotide probes were labeled with P32-γ-ATP using T4 polynucleotide kinase. About 0.2 ng probe and indicated amount of proteins purified from E. coli were mixed in 20μl binding buffer (25 mM HEPES-KOH [pH 8.0], 1 mM DTT, 50 mM KCL, and 10% glycerol). After 40min incubation on ice, the reactions were resolved by 5% native polyacrylamide gels with 1× TGE buffer (6.6 g/l Tris, 28.6g/l glycine, 0.78 g/l EDTA [pH 8.7]).

Drought stress tolerance of BR signaling mutants

Drought stress tolerance experiments were carried out as described previously [35] with minor modifications: different genotype plants were grown on 1/2 MS medium for 2 weeks, then transferred to soil, and grown for one more week in growth chamber (22C, 60% relative humidity, long day conditions) before exposure to drought stress. Drought stress was imposed by withholding water until the lethal effect of dehydration was observed on wild-type control or *bes1-D* plants. The numbers of plants that survived and continued to grow were counted after watering for 7 days.

Generation of the *Arabidopsis* RD26-BES1 subnetwork

We first constructed a whole genome network of *Arabidopsis* using the TINGe software[55]. To construct the *Arabidopsis* network, microarray data was collected from a total of 3546 non-redundant Affymetrix ATH1 expression profiles. The data was subjected to statistical normalization and filtering, following which 15,495 genes

remained for network construction. The RD26-BES1 subnetwork was then extracted from the whole genome network using a subnetwork analysis tool, GeNA[55]. GeNA ranks each gene in the whole genome network with respect to its relevance to a given set of seed genes and extracts a subnetwork containing the seed genes and genes of highest ranks with respect to the seed genes.

Yeast One Hybrid Assays

Matchmaker One-hybrid system (Clontech) was used to test the binding of BES1/RD26 to At4g18010 and At4g00360 gene promoters following the manufacture's instructions (http://download.bioon.com.cn/upload/month_0907/20090707_dab6285a579af1fb2ccd87zow1gx859t.attach.pdf). Briefly, promoter fragments were cloned into pLacZi (Kpn I and SalI sites) and integrated into the genome of yeast strain YM4271 to generate reporter lines. Mutant reporter lines were also generated with promoter fragments in which BES1/RD26 binding sites were mutated. BES1 and RD26 were expressed in the reporter strains with pGBKT7 and pGADT7, respectively. The LacZ expression in each strain was determined by filter assays.

Data availability: The raw RNA-seq reads are deposited to NCBI SRA with accession number PRJNA223275. All other data supporting the findings of this study are available within the manuscript and its supplementary files or are available from the corresponding author upon request.

A.6 Figures

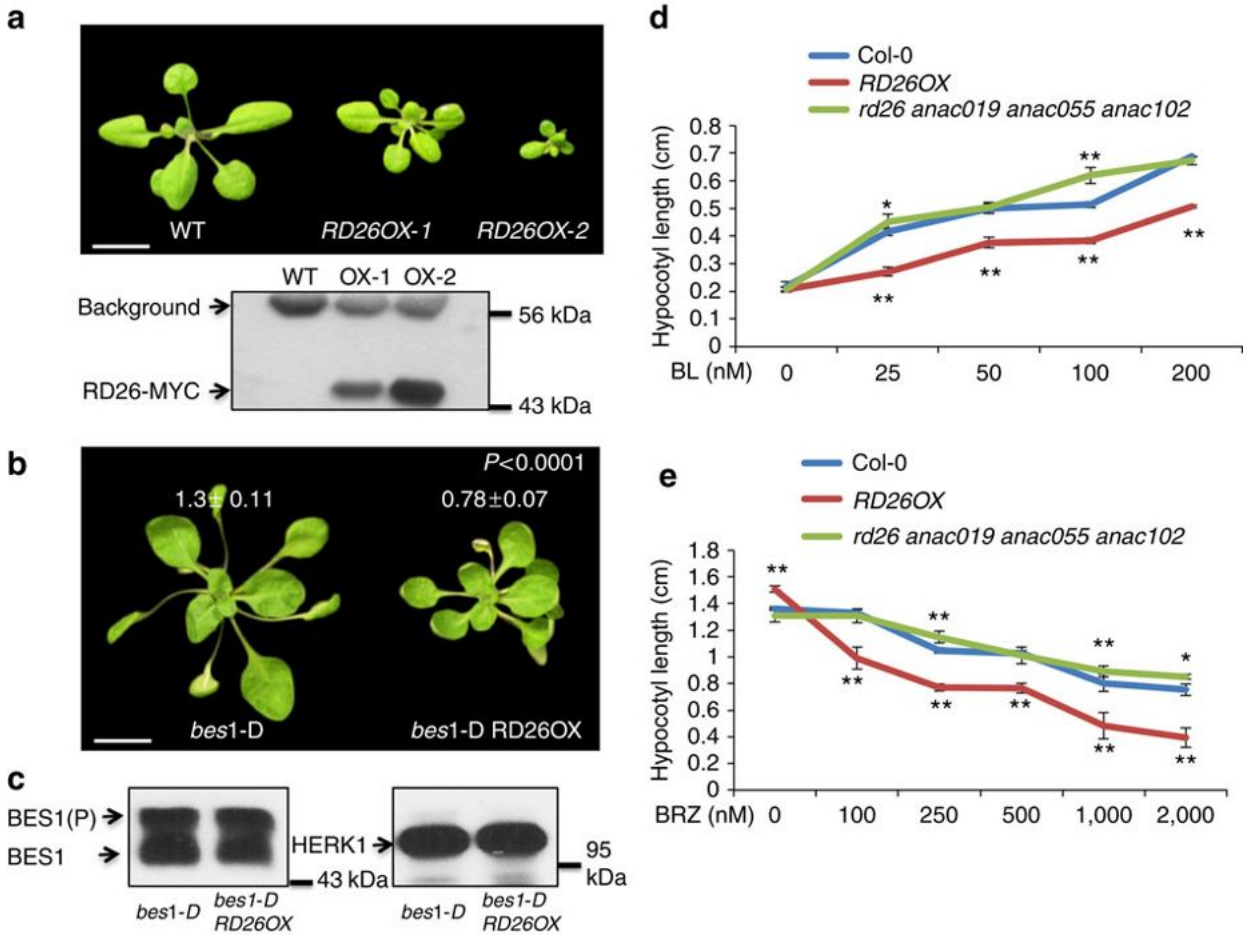

Fig. 1: RD26 functions as a negative regulator in BR signaling pathway.
(a) The phenotype of 4-week-old *RD26* overexpression (*RD26OX*) plants. The stunted growth phenotype of *RD26OX* plant (upper) is correlated with the protein level of *RD26* transgene (lower panel) examined by Western blotting. T3 homozygous plants were used in the experiments and the phenotypes have been stable for many generations after T3. The bar represents 1 cm.
(b) *RD26OX* suppressed *bes1-D* phenotype. 4-week-old plants of *bes1-D* and *bes1-D RD26OX* double mutants are shown. The bar represents 1 cm. The average petiole length of the sixth leaves and s.d. are indicated (n=10).
(c) BES1 protein levels and phosphorylation status did not change in *bes1-D RD26OX* (right lane) compared to *RD26OX* (left lane) as shown by a Western blot (left panel). A loading control with HERK1 is also shown (right panel).
(d) The hypocotyl lengths of 10-day-old light-grown seedlings in the absence or presence of different concentrations of BL. Averages and s.d. were calculated (n=5-10). The experiments were repeated twice with similar results.
(e) The hypocotyl lengths of 5-day-old dark-grown seedlings in the absence or presence of different concentrations of BRZ. Averages and s.d. were calculated (n=10-15). The experiments were repeated three times with similar results. Significant differences were based on Student's t-test (**p<0.01; *p<0.05), which is applied to all other experiments in this study. Also see Fig. S1c.

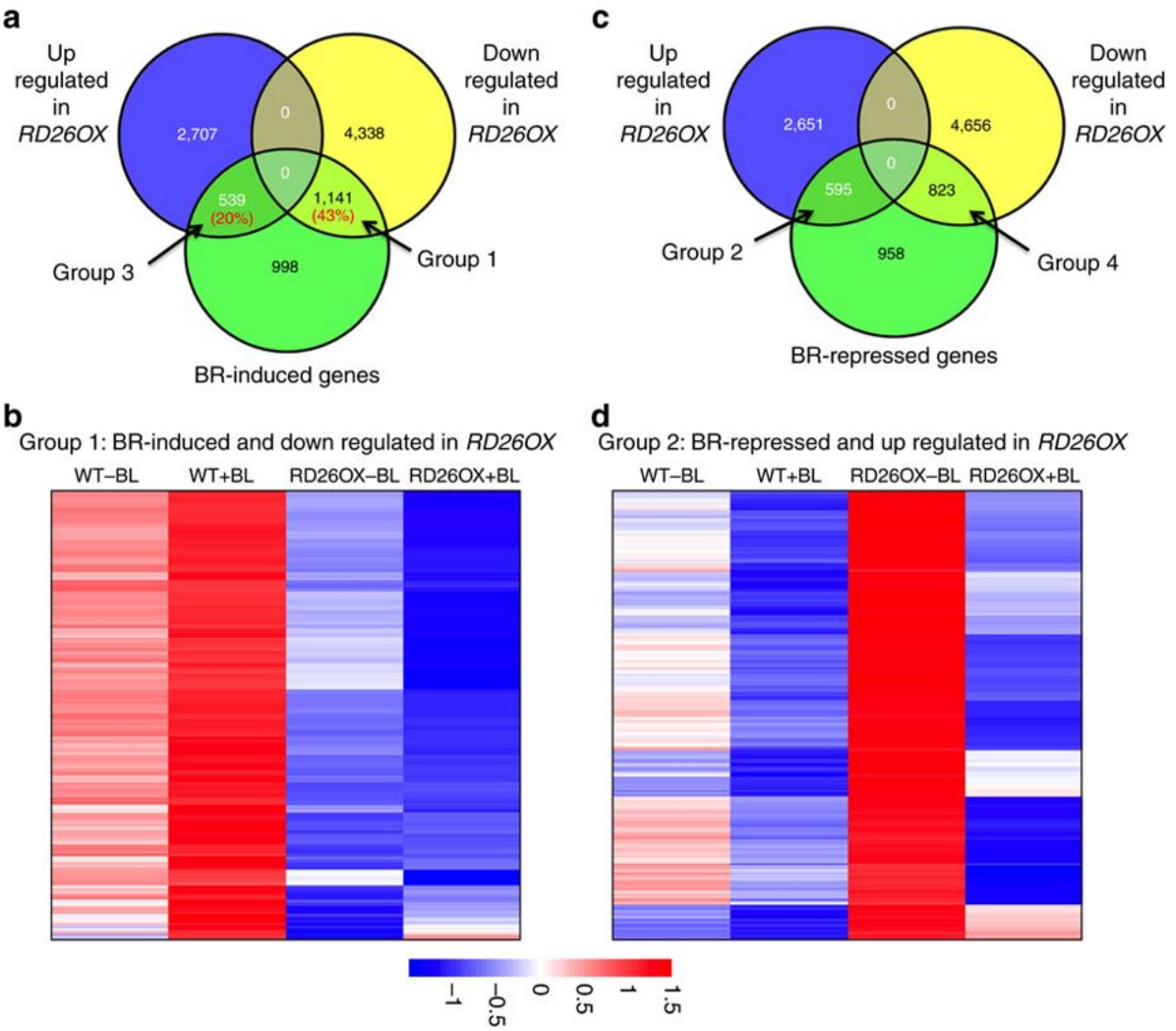

Fig. 2: RD26 negatively regulates the expression of some BR-responsive genes.
(a) Venn diagram shows the overlap between BR-induced genes and *RD26OX*-regulated genes.
(b) Clustering analysis of Group 1 genes. 1141 BR-induced genes are down-regulated in *RD26OX* plants.
(c) Venn diagram shows the overlap between BR-repressed genes and genes affected in *RD26OX*.
(d) Clustering analysis of Group 2 genes. 595 BR-repressed genes are up-regulated in *RD26OX* plants.

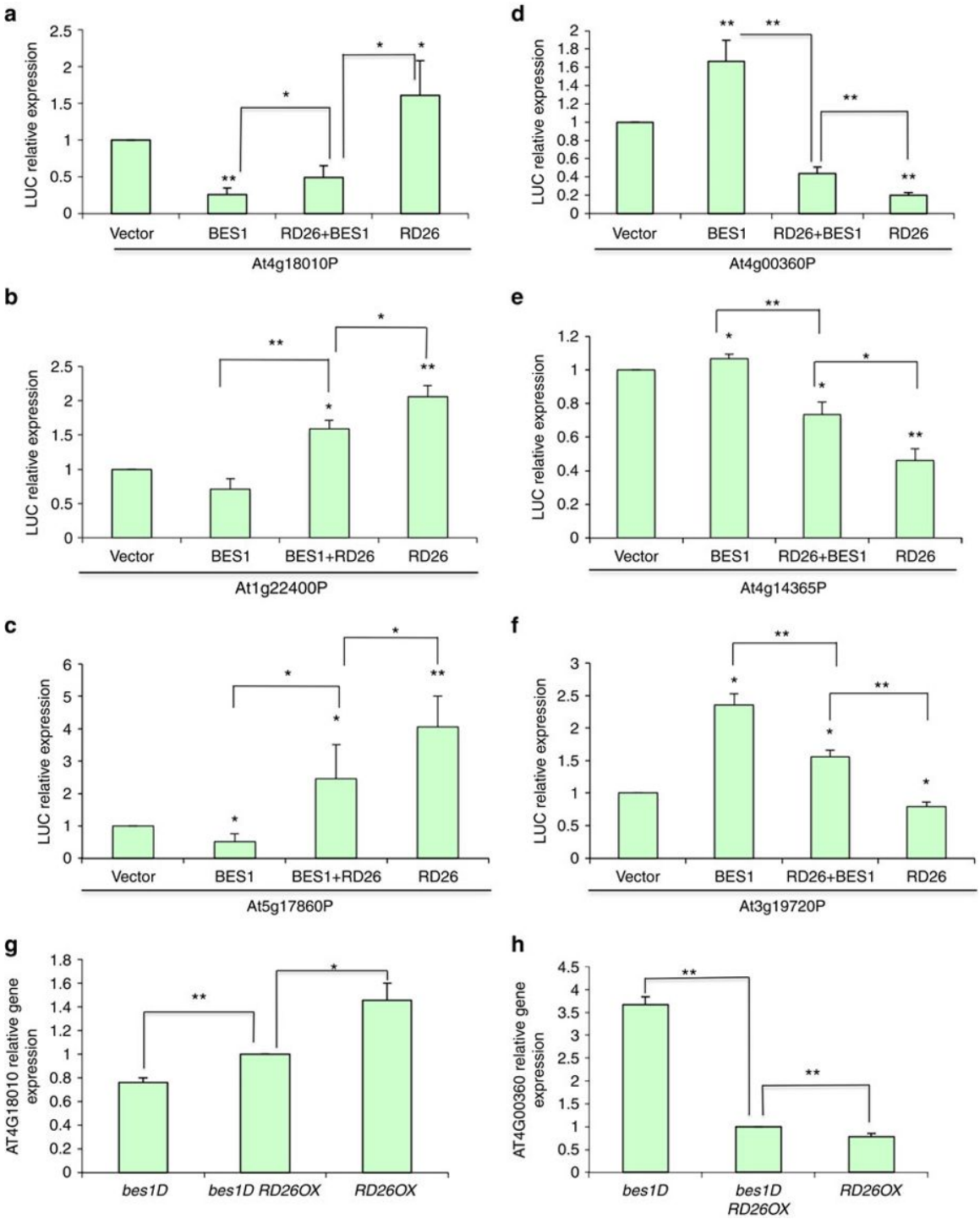

Fig 3: RD26 inhibits BES1 transcriptional activity.

(a-f) Transient gene expression assays were performed in tobacco leaves with *indicated gene promoters-LUC* reporter genes co-transfected with *BES1* and/or *RD26* via Agrobacterium. The relative expression levels of luciferase were normalized with total protein. The average and s.d. were from three to five biological repeats (n=3-5).

(g-h) The expression of *At4g00360* and *At4g18010* were examined in *bes1-D*, *bes1-D RD26OX* double mutant and *RD26OX*, by qPCR. The average and s.d. were from three biological repeats (n=3).

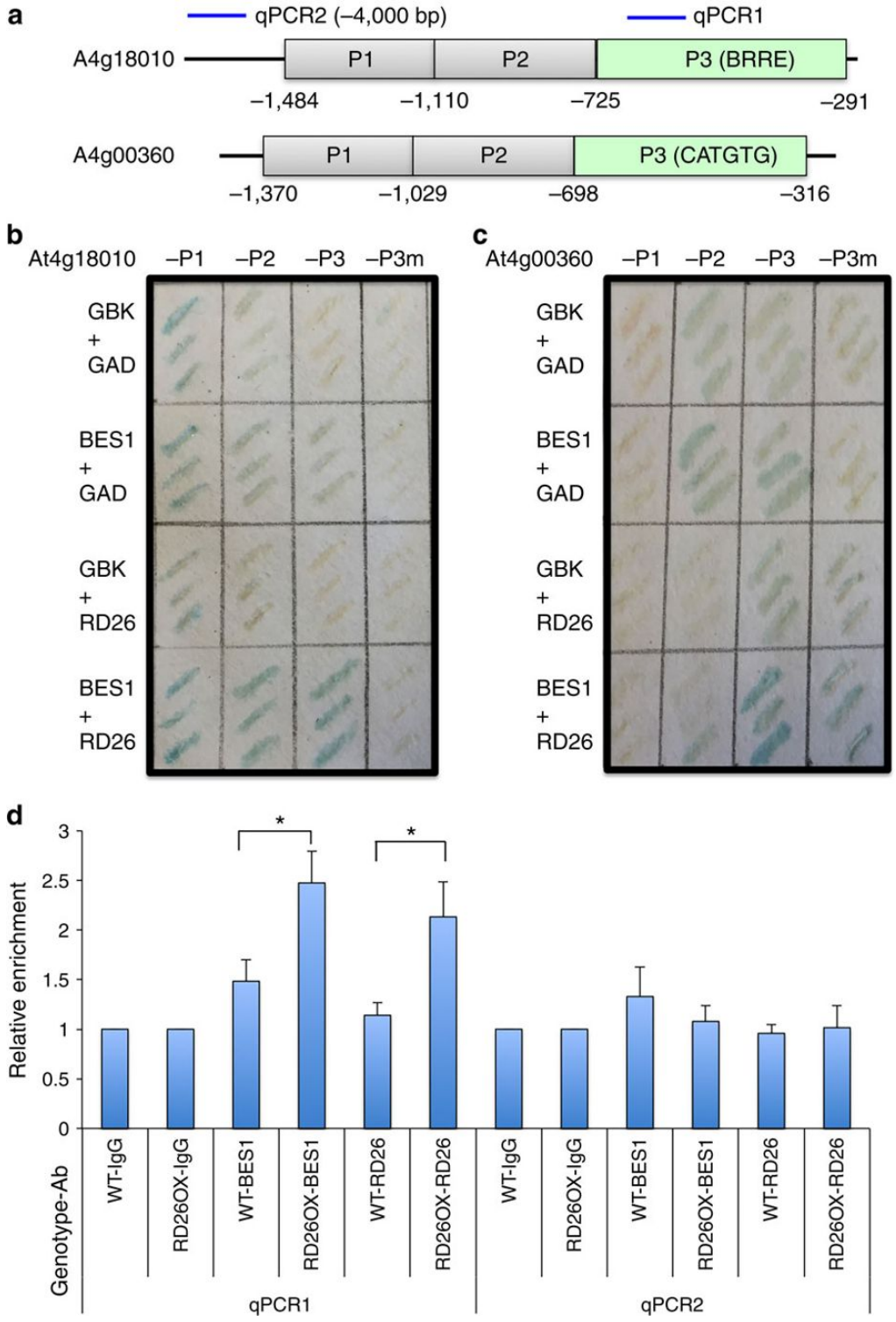

Fig. 4: BES1 and RD26 act together through E-box or BRRE sites in target gene promoters.

(a) At4g18010 and At4g00360 promoters were divided into three fragments based on known BRRE site and CATGTG E-box present in P3 fragments. Mutant P3 fragments (P3m) in which BRRE and CATGTG

E-box was mutated (see Fig 5a), were also generated. Each fragment was cloned into in yeast one-hybrid vector pLacZi (Clontech, Inc.) and integrated into yeast strain YM4271.
(b) BES1 (in pGBKT7, TRP marker), RD26 (in pGADT7, LEU marker), BES1+RD26 were transformed into yeast reporter strains described in (a) with control plasmids and selected in media lacking LEU and TRP. The yeast colonies were grown on filter paper for LacZ assays. BES1 and RD26 seem to be able to function through At4g18010-P2, although there are no known BES1 or RD26 binding sites in this fragment (Fig. S7).
(c) At4g00360-P3 reporter was activated when both BES1 and RD26 are expressed in yeast, but not activated when either BES1 or RD26 are expressed.
(d) BES1 binding to At4g18010 promoter is enhanced in *RD26OX* plants as revealed by ChIP assays. WT and *RD26-MYC* overexpression plants (*RD26OX*) were used to prepare chromatin and ChIP with antibodies (Ab) against BES1, RD26 or IgG control. The ChIP products were used to detect At4g18010 using primers for qPCR1 (within P3 fragment, see a) and qPCR2 (about -4,000bp upstream of the transcriptional start site). The average and standard errors are derived from four biological repeats (n=4). The significance of enrichment was determined by student's t-test (*$p<0.05$)

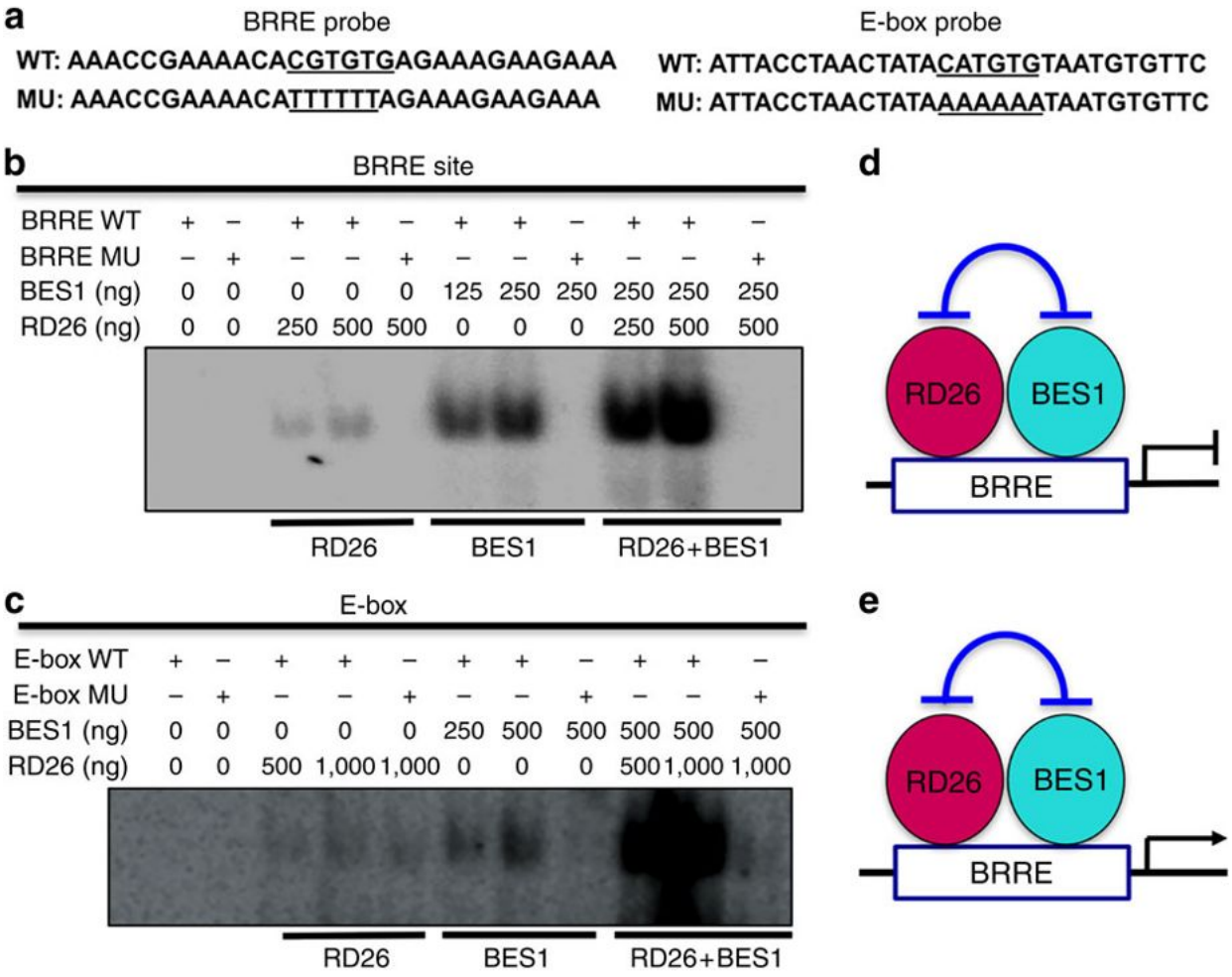

Fig. 5: BES1 and RD26 synergistically bind to BRRE or E-box sequence of BR-responsive genes.

(a) DNA sequences used for binding assays. Wild-type (WT) and mutant (MU) forms of BRRE- and E-box containing probes are shown.

(b) BES1 and RD26 bind to BRRE element. The DNA sequences containing WT or mutated form of BRRE (CGTGTG) from At4g18010 used as probes for DNA binding are shown. WT or mutant (MU) probes were labeled with ^{32}P-ATP and used in binding reactions with indicated amount (ng) of recombinant proteins.

(c) BES1 and RD26 bind to E-box. The DNA sequences containing WT or mutated form of E-box (CATGTG) from At4g00360 used as probes for DNA binding are shown.

(d) A model of RD26 and BES1 binding to BRRE shows that RD26 and BES1 inhibit each other's transcriptional activities.

(e) A model of RD26 and BES1 binding to E-box shows that that RD26 and BES1 inhibit each other's transcriptional activities.

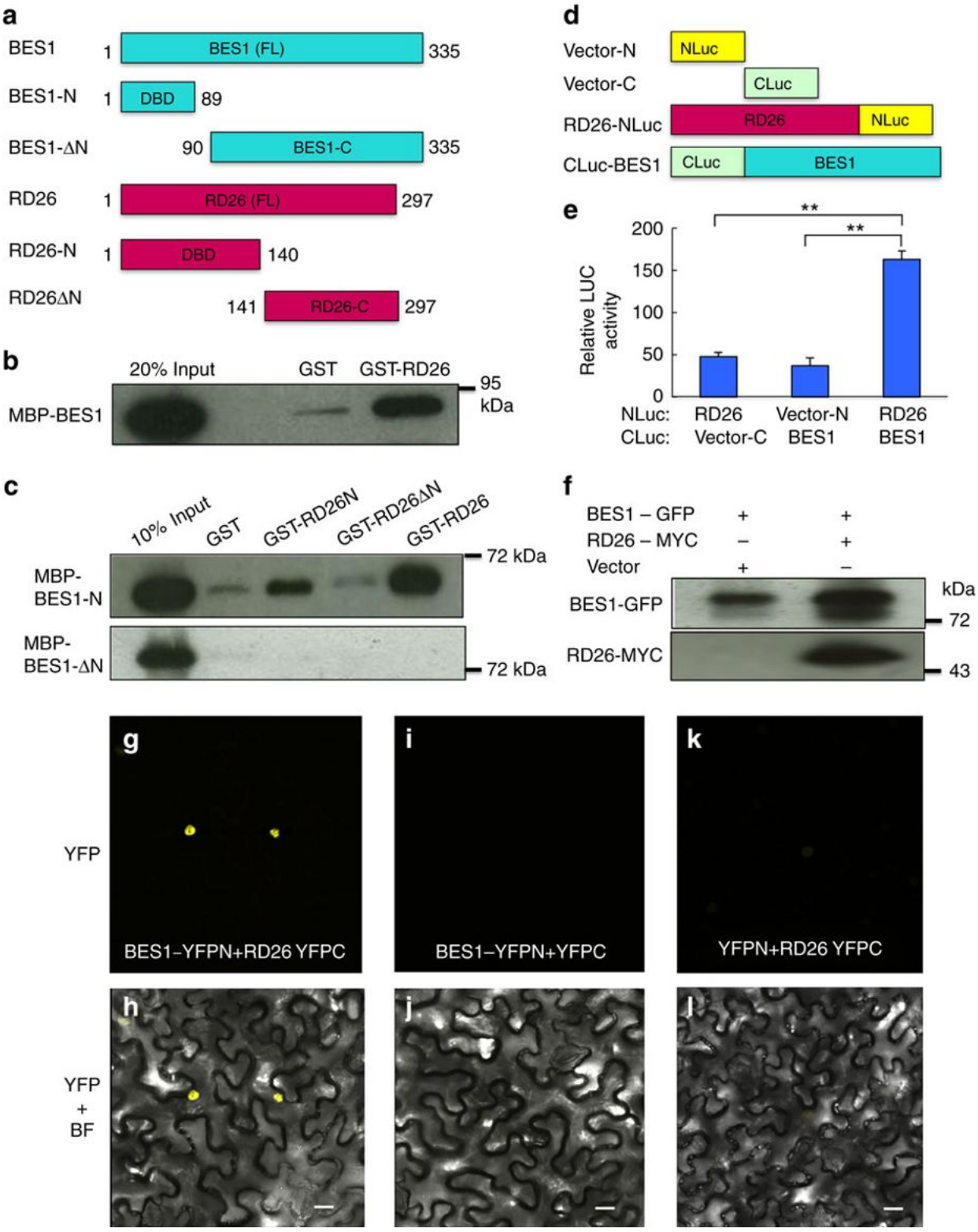

Fig. 6: RD26 interacts with BES1 *in vitro* and *in vivo*.

(a) Schematic representation of BES1 and RD26 proteins. Full-length (FL) or domains involved DNA binding/dimerization for BES1 (aa 1-89) or RD26 (aa 1-140) are shown.

(b) BES1 interacts with RD26 in GST pull-down assays. GST-RD26, but not GST, pulled down BES1. MBP-BES1 was detected by ant-MBP antibody. 20% MBP-BES1 input is shown.
(c) The DNA binding and dimerization domains of BES1 (1-89) and RD26 (1-140) interacts with each other.
(d) Schematic representation of constructs used for split-LUC assays. Amino or carboxyl parts of Luciferase (NLuc and CLuc) were fused with RD26 or BES1, respectively.
(e) RD26 and BES1 interact with each other in vivo. RD26-NLuc and CLuc-BES1 as well as indicated controls were co-expressed in tobacco leaves and Luc activities were measured and normalized against total protein. The averages and s.d. of relative luciferase activities were derived from 6 biological repeats (independent leaves). All the experiments were repeated three times with similar results.
(f) BES1 interacts with BES1 through co-immunoprecipitation assay. BES1-GFP and RD26-MYC were co-expressed in tobacco leaves and protein extract was immunopreciitated with anti-GFP antibody and detected with anti-BES1 (top panel) or anti-MYC (bottom panel) antibodies.
(g-l) BES1 interacts with RD26 in BiFC assays. Co-expression of 35S:BES1-YFPN with 35S:RD26-YFPC in tobacco leaves led to reconstitution of YFP signal in the nucleus. No positive signal was observed in control samples co-expressing 35S:BES1-YFPN and 35S:YFPC or 35S:YFPN and 35S:RD26-YFPC. For each panel YFP as well as YFP and bright field (BF) merged images (YFP + BF) from confocal microscopy are shown. Scale bars indicate 20 μM. The experiments were repeated three times, with similar results.

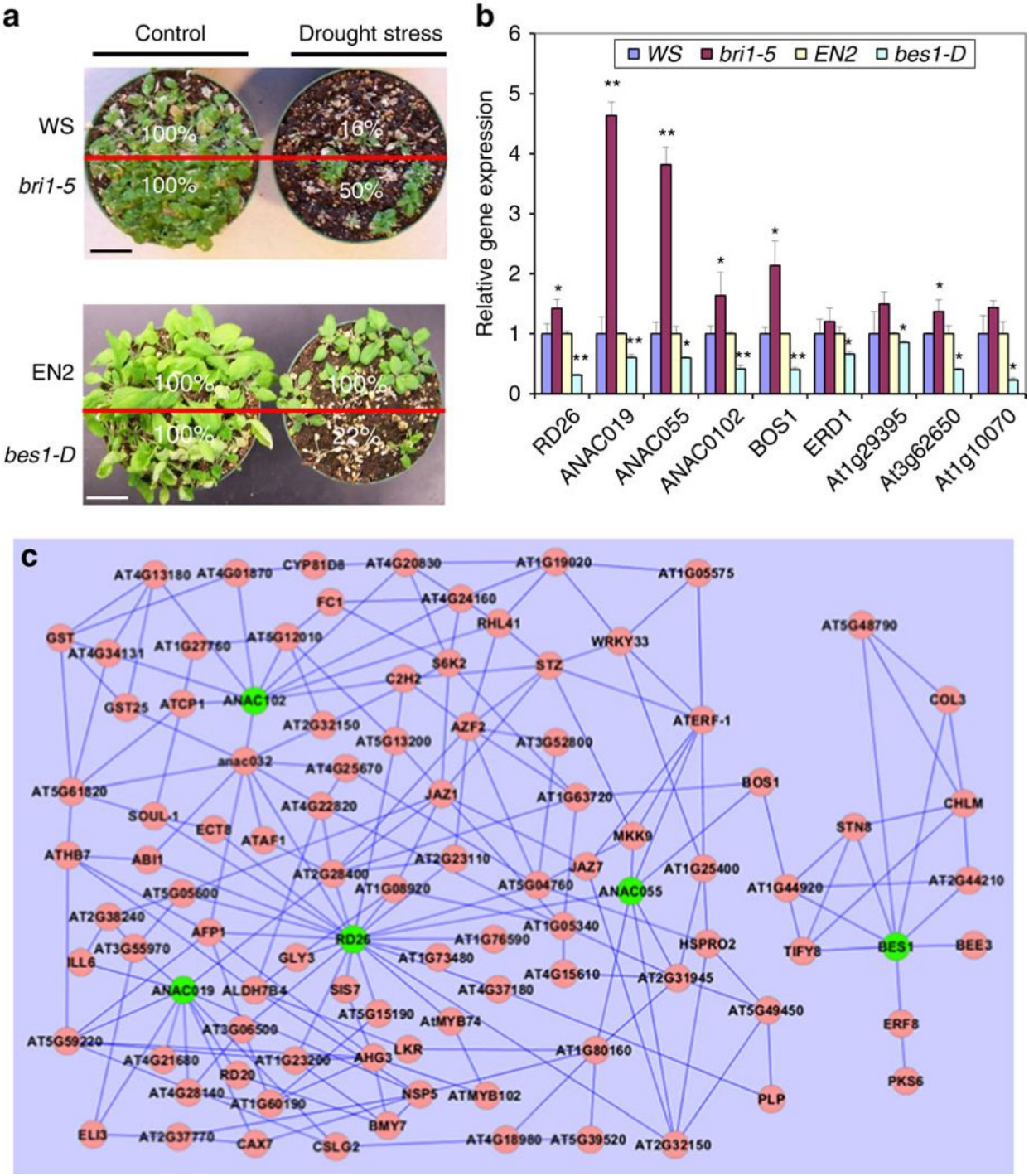

Fig. 7: BR signaling pathway inhibits drought response.

(a) BR loss-of-function mutant plants (*bri1-5*) have increased and gain-of-function BR mutants (*bes1-D*) have decreased drought tolerance. Survival rates of WS (wild-type), *bri1-5* mutant, *EN2* (wild-type) and *bes1-D* mutant plants after withholding water for 14-20 days (drought stress) and rehydration for 7 days (rehydration). The survival rate is indicated in the picture. The bars represent 3 cm. This experiment was repeated three times with similar results.

(b) Drought responsive genes are up-regulated in *bri1-5* and down-regulated in *bes1-D* mutants. The expression levels of drought-induced genes were examined by qPCR using RNA prepared from *bri1* and *bes1-D* mutants. The difference was significant based on Student's t-Test (*$p<0.05$, **$p<0.01$, n=3).
(c) RD26-BES1 Gene Regulatory Network (GRN). A 103-gene subnetwork extracted from the *Arabidopsis* whole genome network[55] using the subnetwork analysis tool, GeNA. Seed genes (ANAC019, RD26, ANAC055, ANAC102, and BES1,) are shown in green. The network topology is displayed using Cytoscape.

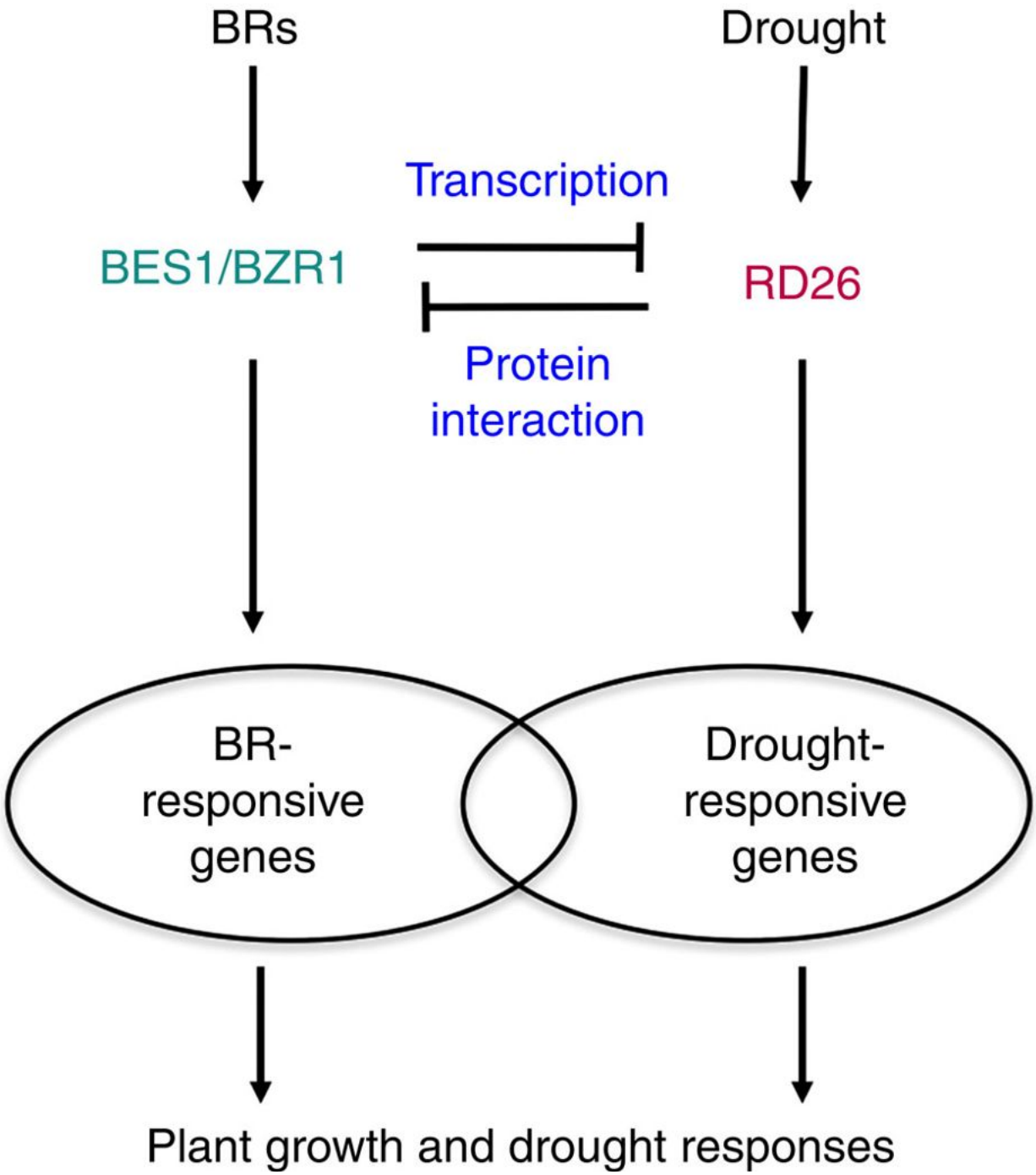

Fig. 8: A model of crosstalk between BR and drought response pathways.
Drought stress induces the expression of *RD26* to mediate the response of plants to drought. Upon the increased expression, RD26 not only inhibits the expression of BES1 at the mRNA level, but also binds to E-box and BRRE site to inhibit BES1's functions in mediating BR-regulated gene expression (Group I and II genes), which results in the inhibition of BR regulated growth. On the other hand, BR signaling represses the expression of *RD26* through BES1 and also directly inhibits the expression of other drought-related genes to inhibit drought response.

A.7 Supplementary Figures and Tables

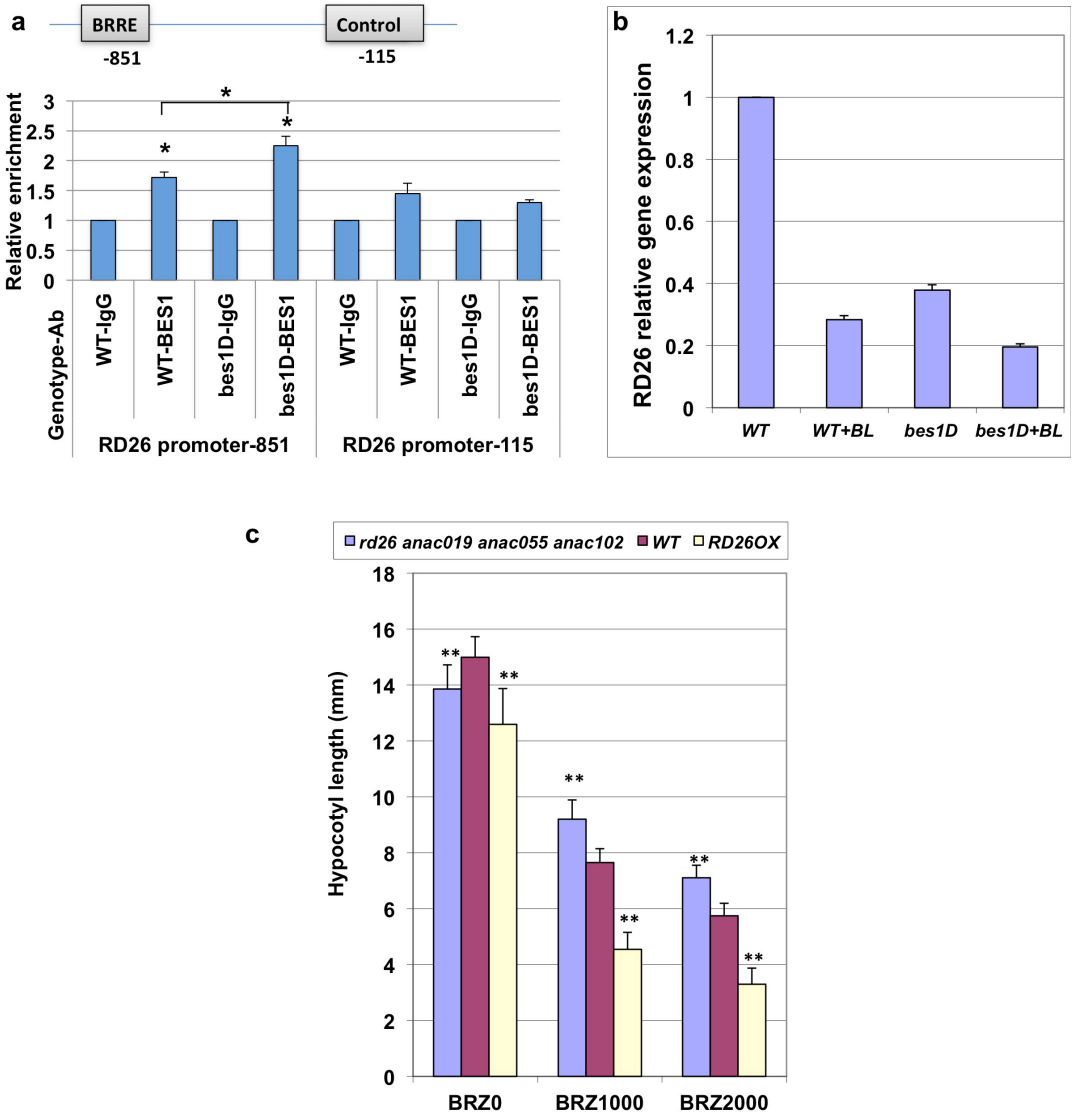

Fig. S1: *RD26* is a target of BES1 and functions as a negative regulator in the BR pathway.

(a) BES1 targets the BRRE site on RD26 promoter. ChIP was performed with anti-BES1 antibodies in WT and *bes1-D* adult plants. The binding of BES1 at the BRRE site (-851) and control site (-115) of the *RD26* gene promoter were examined by qPCR.

(b) The expression of *RD26* was examined by quantitative qPCR in WT and *bes1-D* plants with or without 1,000 nM BL treatment for 2.5 hr.

(c) BRZ responses of RD26 overexpression (*RD26OX*) and *rd26 anac019 anac055 anac102* quadruple mutants. The hypocotyl lengths of 5-day-old dark-grown seedlings in the absence or presence of different concentrations of BRZ. Error bars indicate s.d. (n=15-20). The difference was significant based on Student's t-Test (*p<0.05; **p<0.01).

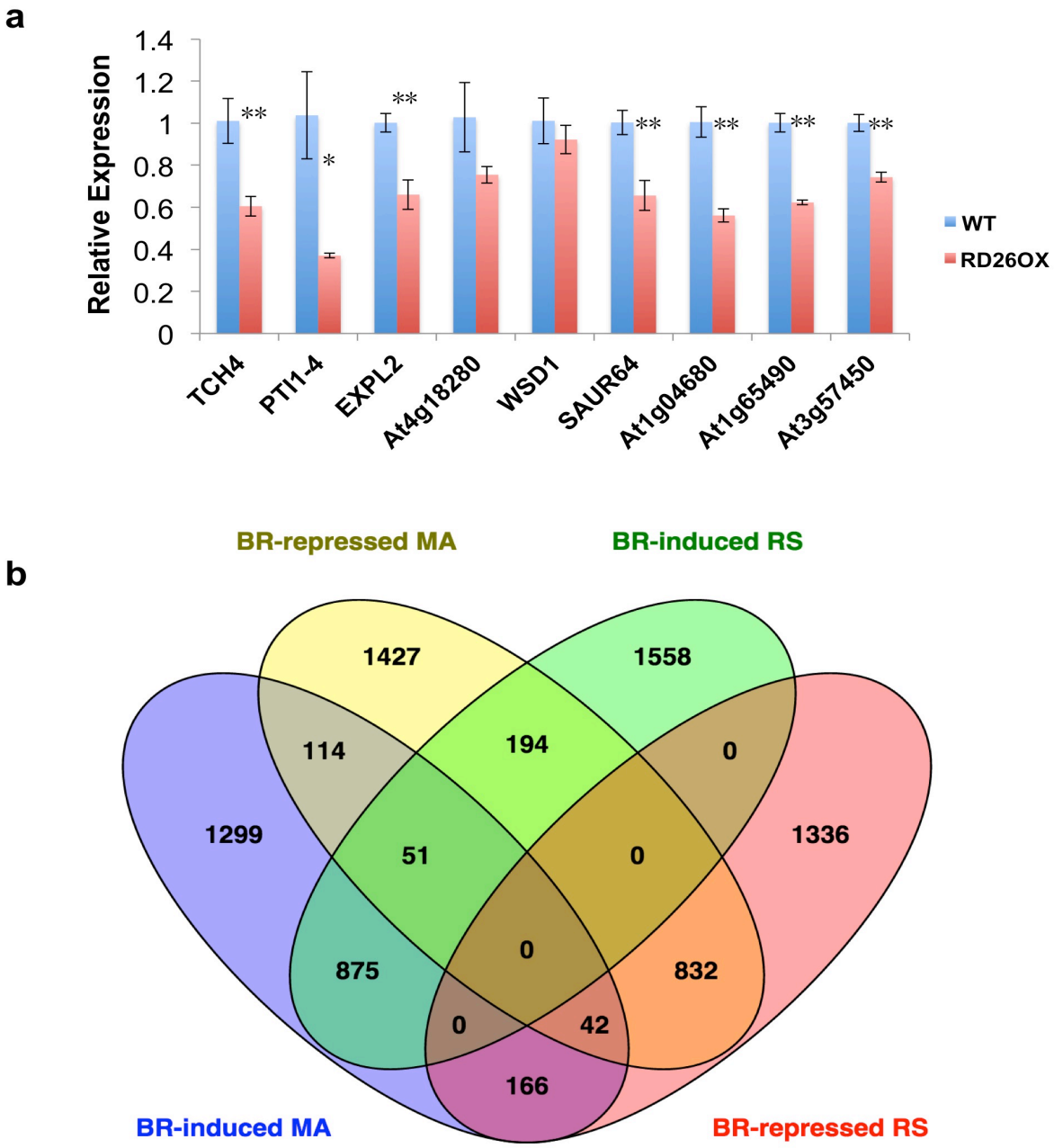

Fig. S2 Comparison of BR responsive gene sets

(a) The expression of BR-response genes in *RD26OX Arabidopsis* plants.
The expression of the selected genes was examined by qPCR using RNA prepared from corresponding 5 week-old plants. Error bars represent s.d. (n=3). Differences are significant based on Student's t-test (*p<0.05, **p<0.01).

(b) Overlap between BR-regulated genes identified by RNA-seq (RS, this study) and previously published by Microarrays (MA). Venn diagram shows that about 43% of genes overlap between those identified by RNA-seq with adult plants and those identified by microarrays from seedlings or adult plants [24, 45-49]. Note that a small portion of genes can be either induced or repressed, likely depending on physiological conditions of BR treatments.

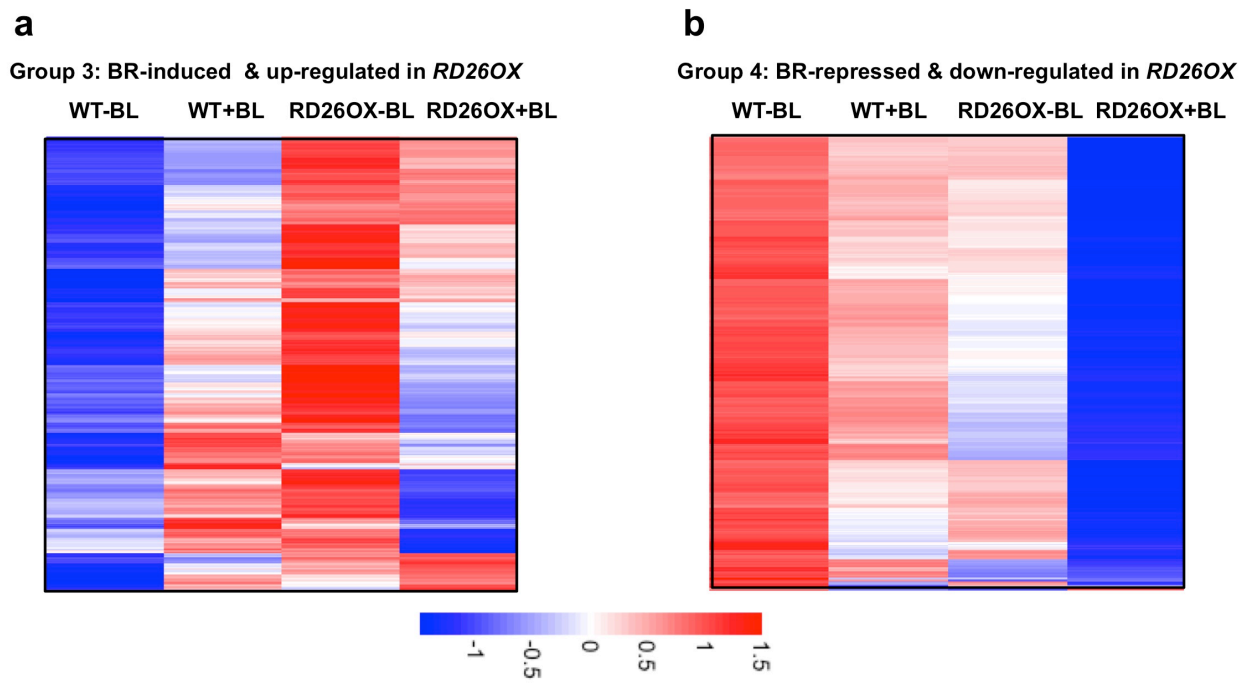

Fig. S3: **Clustering analysis of Group 3 and Group 4 genes.**
(a) Group 3 gene expression in WT with or without BL treatment (lane 1 and lane 2) and in *RD26OX* transgenic plant with or without BL treatment (lane 3 and lane 4).
(b) Group 4 gene expression in WT with or without BL treatment (lane1 and lane 2) and in *RD26OX* transgenic plant with or without BL treatment (lane 3 and lane 4).

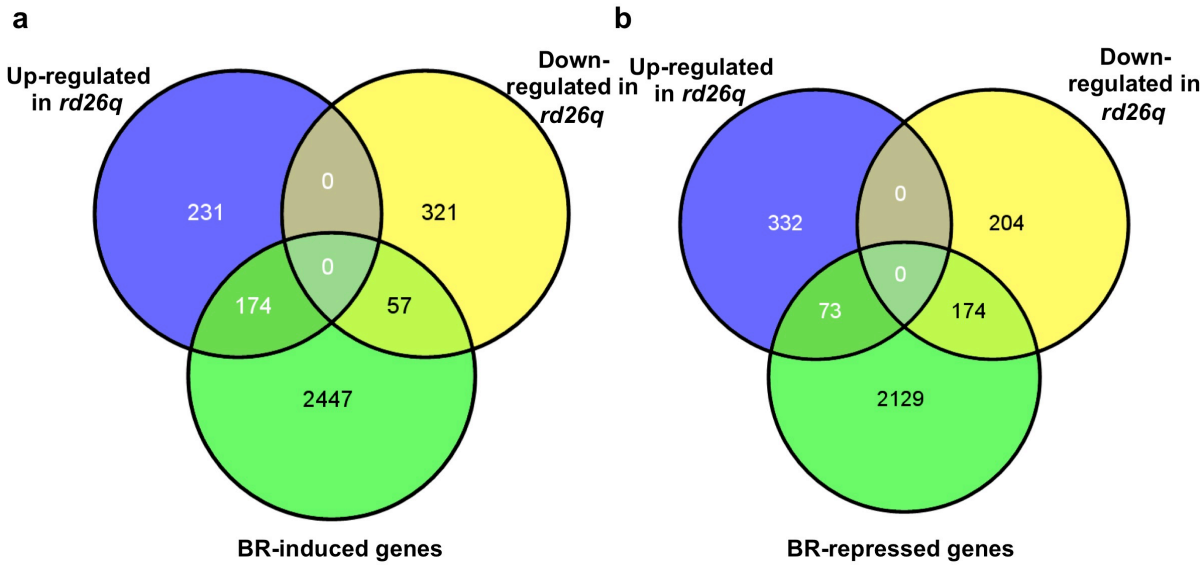

Fig. S4: Overlap between BR-regulated genes and genes affected in *rd26 anac019 anac055 anac102* quadruple mutant.

Venn diagrams show the overlaping genes between BR-induced (a) or BR-repressed (b) genes affected in *rd26 anac019 anac055 anac102* quadruple (*rd26q*) mutant-regulated genes.

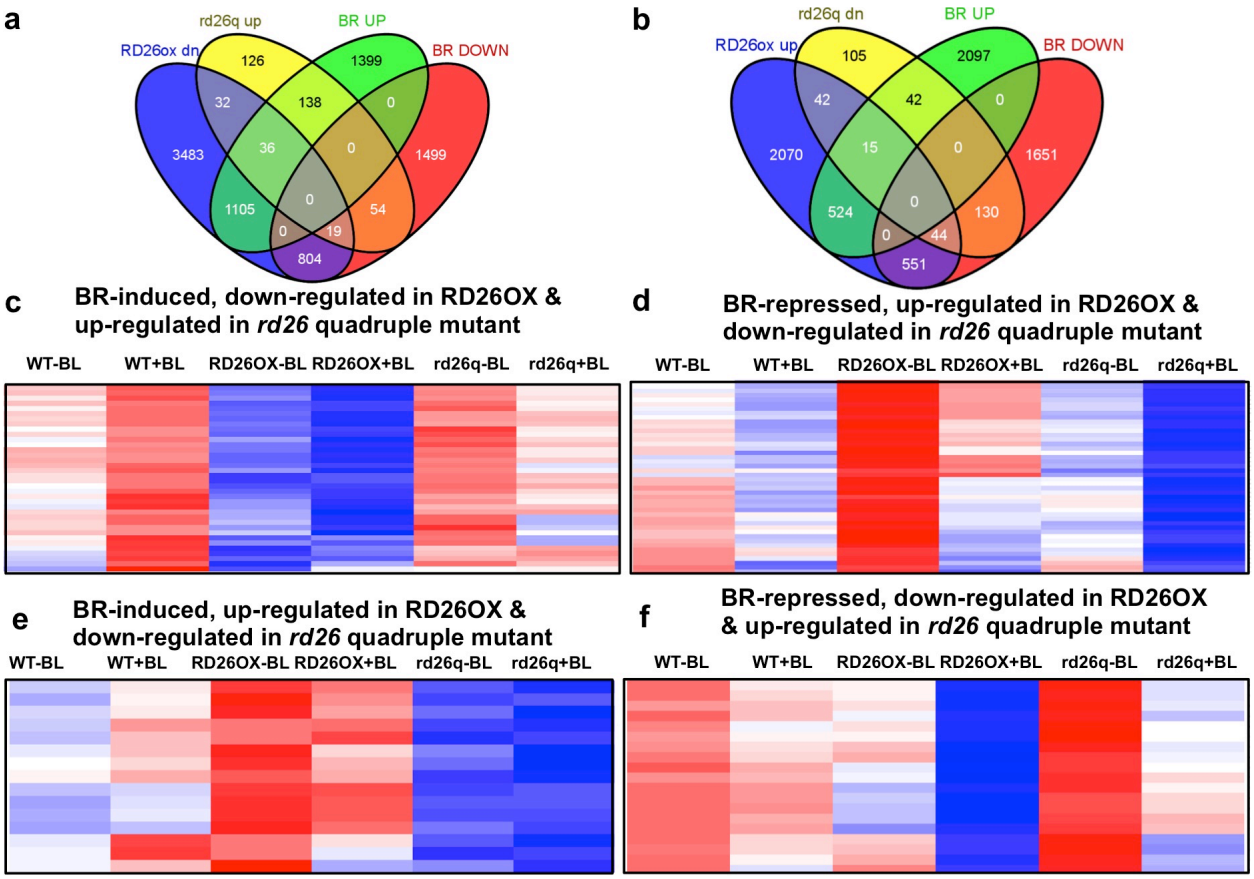

Fig. S5: Overlap between BR-regulated genes and genes differentially affected in RD26OX and in *rd26 anac019 anac055 anac102* quadruple mutant.

Venn diagrams show the overlap genes between genes up-regulated in *rd26q* and down-regulated in *RD26OX* with BR-regulated genes (a), genes down-regulated in *rd26q* and up-regulated in *RD26OX* with BR-regulated genes (b).

(c-f) Clustering analysis of BR-regulated genes affected in opposite ways in *RD26OX* and *rd26q* quadruple mutant.

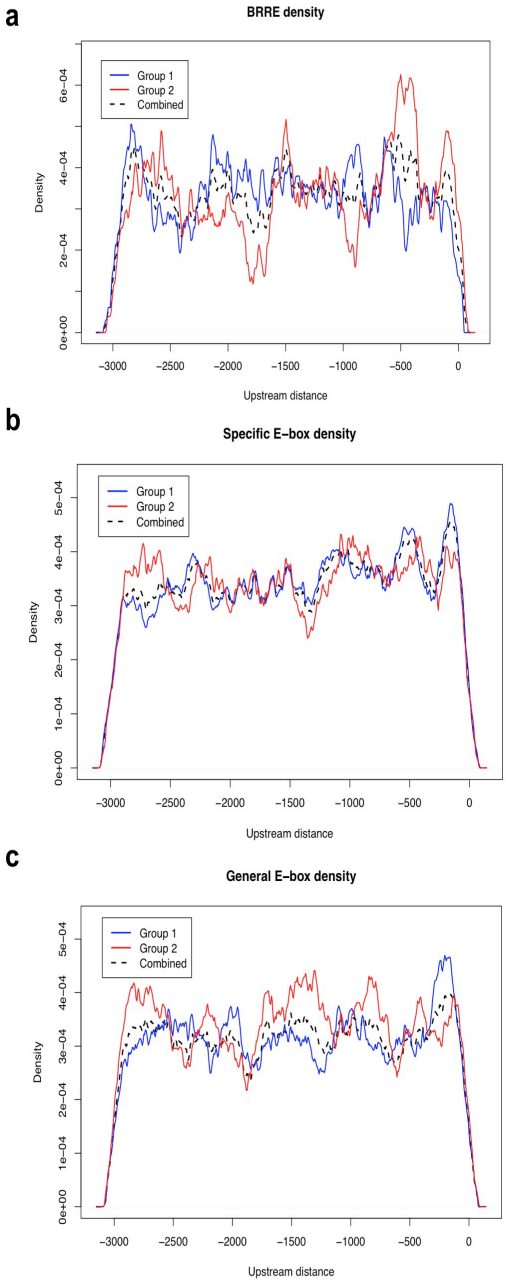

Fig. S6: Different BES1 binding sites are differentially enriched in Group 1 and Group 2 BR-regulated genes.

(a) BRRE sites (CGTGT/CG) are enriched in Group 2 genes, especially in the -500 bp promoter regions relative to the transcriptional start sites.

(b) A specific E-box, CATGTG, which is often found in BR-induced genes, are enriched in Group 1 BR-regulated genes in the -500 bp promoter regions.

(c) The general E-box (CANNTG) are also enriched in Group 1 BR-regulated genes within -500 bp promoter regions. Although the general E-boxes are also enriched in Group 2 genes between 1,000-3,000 bp of their promoter regions, the functions of these E-boxes are not clear as BES1 and BZR1 mostly bind to -500 bp promoter regions to regulate gene expression [23, 24].

a At4g18010 Promoter Sequence

P1
ttgtgaatcaaactaatttatttaagtagctttggtcaaccgaaactttcctaatgaccttcgttacgtcctctatccgc
aaattgcattgcatgggcgtcagttttttttccttttttcttaataacgcgtcaatttatttttatgatgatgattatgtttagttga
aataatcttcagttattaattagatatttcttggtaaatatttttttacaaatatgctgtcagaaattcaaagttatgtatttcca
taccatattggactccatactttatatcttctcagttgagtatccttcaaattcacctgttttggaaattggaaatataattta
gttttagaaatgttttaagttaaaacataacagttaacaaagaaaagatatagacaatttttaagactttttaaatgtg
agggattctcactttttcgttgttttctaatggttccaattcatagttatcgtataatattatttaacgaaacattagtcaaa

P2
taaataatctatctattcgccgactgtatggctgaaaatattagctggagctagactcgtattgaaaaaattaatccat
atatttgttgcctaggagagtgacattttgacctttttaataacataccaaaaaggccgtttatttaatatattatccagat
agcagcgttgaatcggattttggttggttttggtttatgtgttttagatttttggttaaagcaaaccactaacttaagtcagg
tcaaagtatttcagcaaaactaattctcaaataatcacttttactccgcaaaactgcttgtcaaaatatagtttttg
acttccaacgagccatttttttgctaattcagtttaactagtatacgcaaaaaaaaaaaaatgtttagataaattaaaattt

P3
cggttaacttttataaaaaagtttcagtctgtctgtttgattcggtttactttaactaaatgccactatcttaaaagatgaa
gtaaacatttataataattcggtatggtcggtacaatcagtctagtaaaaccgaattgagaaaaccaggtcggttcg
aatatatccaaaaaccgaaaacacgtgtgagaaagaagaaatcagggaattaaatctgacagtctttatagttt
tctttaatatgtcttccccaaaaaatcaaattatgaataaaaaaagtggatcgcaagttgcagttggttctttacgg
gcaacgaaggctgttaaataacagccatagcttttcttcgaaacgaacccaaaaaataatatcagagaattttcat
cattacacctttttttttctttgcctttgccttgccttcacacgtcttcttgtttgtactctccacttttttttctttgtgtccttttctt
tgttcttgctctagttcgtgtctcttctttaactctctgtcactattataaatatcaaactctgacattttcttctgttcaaattctc
ctcgaaactcccccaaa

b At4g00360 Promoter Sequence

P1
tctcttgatacaatgcatatagaaactgacaaataatcgaagaaattgtacttgagcccattacgactattgaa
aattctgattttggatgaattcagcggaaactacaaatttaagagtactttatgtgtataatatgaagcctatatatat
agaattactaatgtaataaaataagaaccggtgaaaaggggacaagatcacaaggttttcgcattcagtgcct
ttacagagttatatatttgatgatgttattgcttacttgcctaatagtactatactactatatatatctaaggtaacacatg
tatatatatgtcacatagacattactagtatat1028attatgtacttctatcatatatttatgatattgcagttgca
gcgtacacaagtcagctccttttgacttttacatctcatgaatgcattgccatgacatctaatcttactcgagatttgt
gcatgcacattattcacttttgtctttgcaatttttgttattgtaaaaaaaggaaaaacaaatgtaaaagagagaga

P2
gaccagaaaggtctaactaaacctaaagagtcaatgaaatgtgtttctttcttgtgggattaatcaattcactcttta
acacttctttataccattgaagaaattagatgaaagagtcacgagttgcttaccaaatccctcacaagaattga
gaactgataaaccaaattgagaagattaaatatcacgtctccttttgatctctattataattaatcgaaaataaaa
ataagagttttcaacaaaacgtgatcattggtttacgatcacttgcaaagtcaaacctaaaacgtagcattagtac

P3
actaaccttaaatactaattatatcatgcaaaccctaatgtcattacctaactatacatgtgtaatgtgttcaaca
gatcttcttaacccacattagatcaatattaaacaataaaaagattcttatatattctactacttacttcttcttattccca
tccatatttttctgtgccttaggttctcaactaatctcatttaatttagctagcacacagagaaacacacacgtat
ataaataatatgataacacacaaaaagactcatatatataaataattagagtcattaaatgtggattcatcattaa
atgaaacaactcttcttctctgtacaatttctcttcacaccttcaccaaattctttgacttcaaaaatcttataaaatttat
atatctccaaaaccataaaaccaaaacgagttttcacaaataaattacttagttgaaatttcaaatctcattcaatta
gggtacactctctcaacaatccacattaatgaggttgctgcttctgatggcta

Fig. S7: Promoter sequences of At4g18010 (a) and At4g00360 (b) used in the study.

The DNA sequences from 5'-3' are shown. Three promoter fragments (P1, P2 and P3) used in yeast one-hybrid assays are indicated and color-coded. The primers used to clone each promoter fragments are also indicated. BRRE site (CGTGTG) in At4g18010-P3 (a) and CATGTG E-box in At4g00360-P3 (b) are indicated in red.

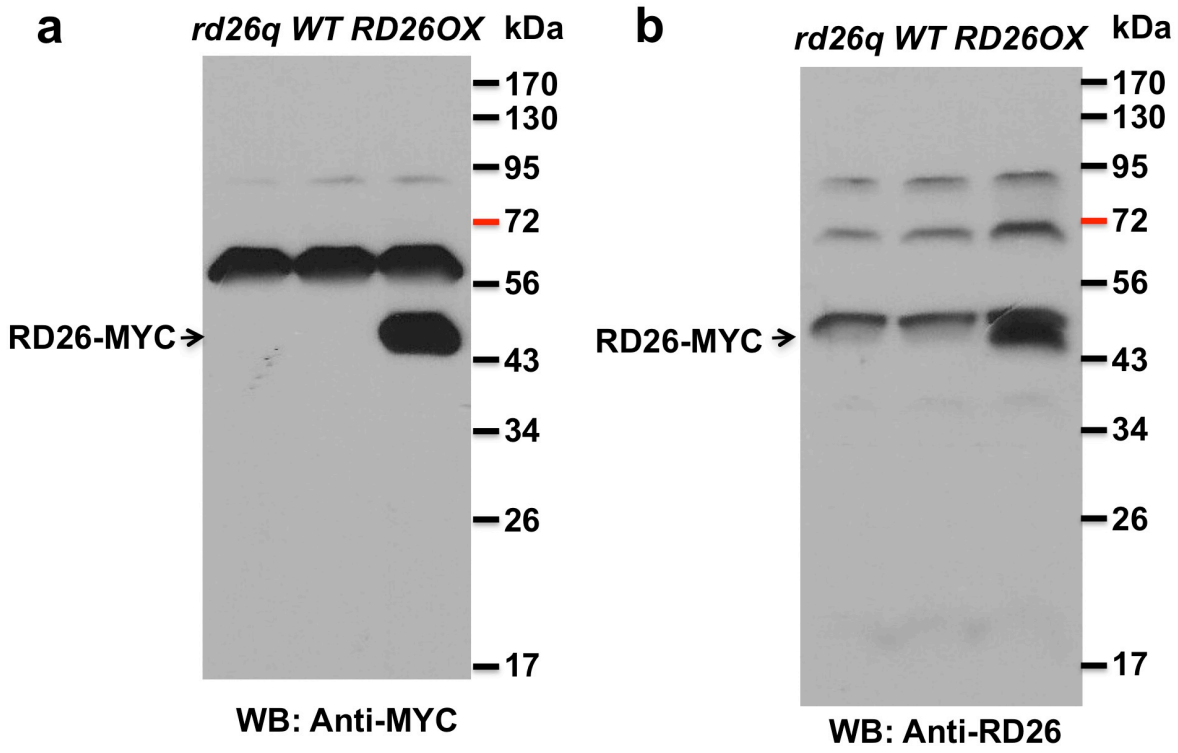

Fig. S8: Validation of anti-RD26 antibody.

(a) A Western blot of protein prepared from *rd26q* quadruple mutant, WT and *RD26OX* plants with anti-c-Myc antibody (Sigma, CS3956).

(b) A Western blot of protein prepared from *rd26q* quadruple mutant, WT and *RD26OX* plants with anti-RD26 antibody. The RD26 antibody detects overexpressed RD26-MYC in the transgenic lines, but not in *rd26q* quadruple mutant or in WT plants likely due to the fact that *RD26* expression is induced by drought stress.

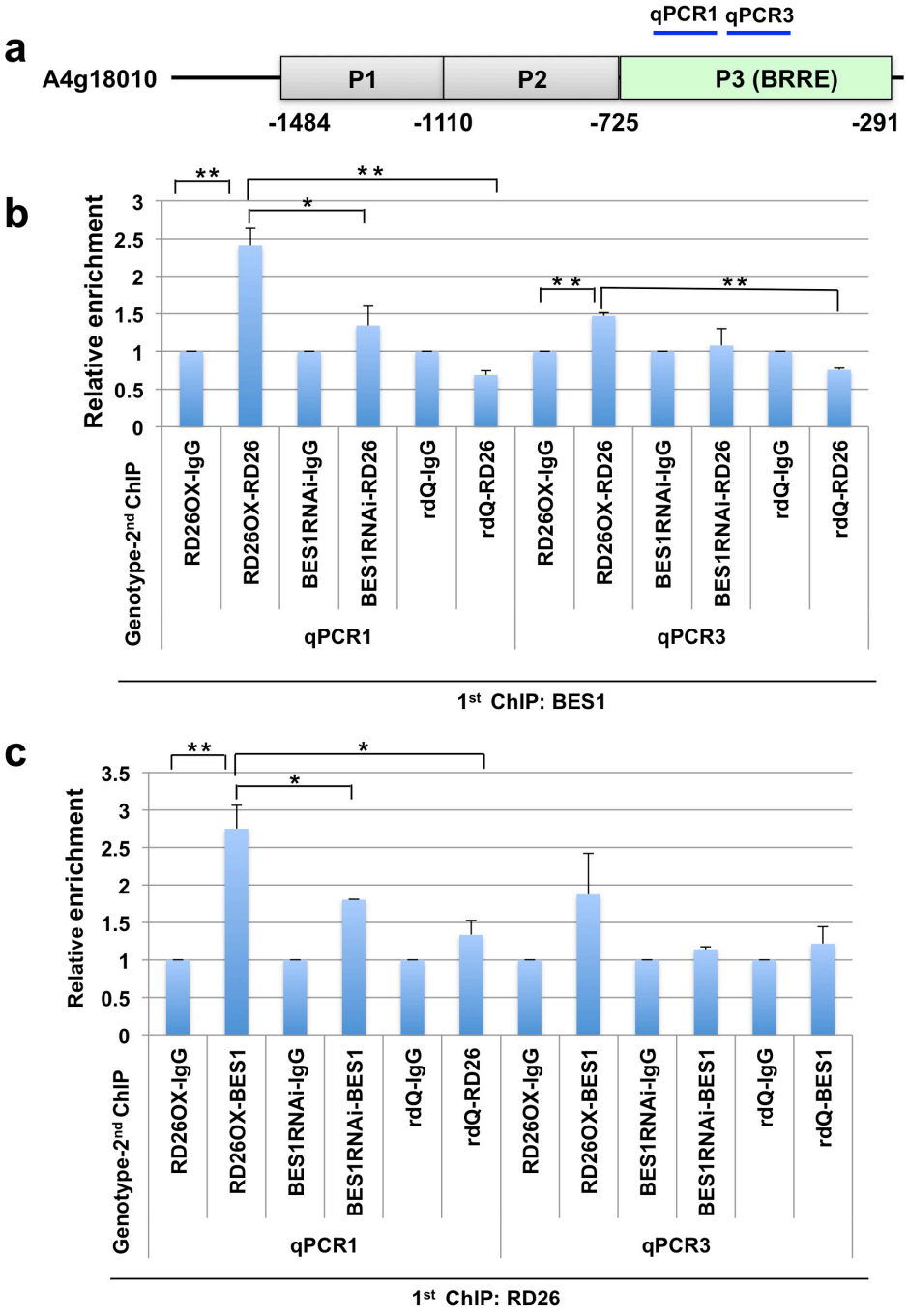

Fig. S9: BES1 and RD26 bind to target gene promoter as revealed by ChIP-reChIP.
(a) At4g18010 promoter structure shows two qPCR primer-pairs (qPCR1 and qPCR3) used. (b-c) RD26 and BES1 can bind to At4g18010 simultaneously as revealed by ChIP-reChIP. Chromatin prepared from *RD26OX*, *rdQ* and *BES1 RNAi* plants was firstly immunoprecipitated with BES1(b) or RD26 (c) antibody. The first ChIP products were immunoprecipitated for 2nd ChIP with either RD26 (b) or BES1 (c) antibody as well as IgG and detected using qPCR primers. The qPCR1 primers appear to work more effectively than qPCR3 primers. Error bars indicate s.e.m. (n=3).

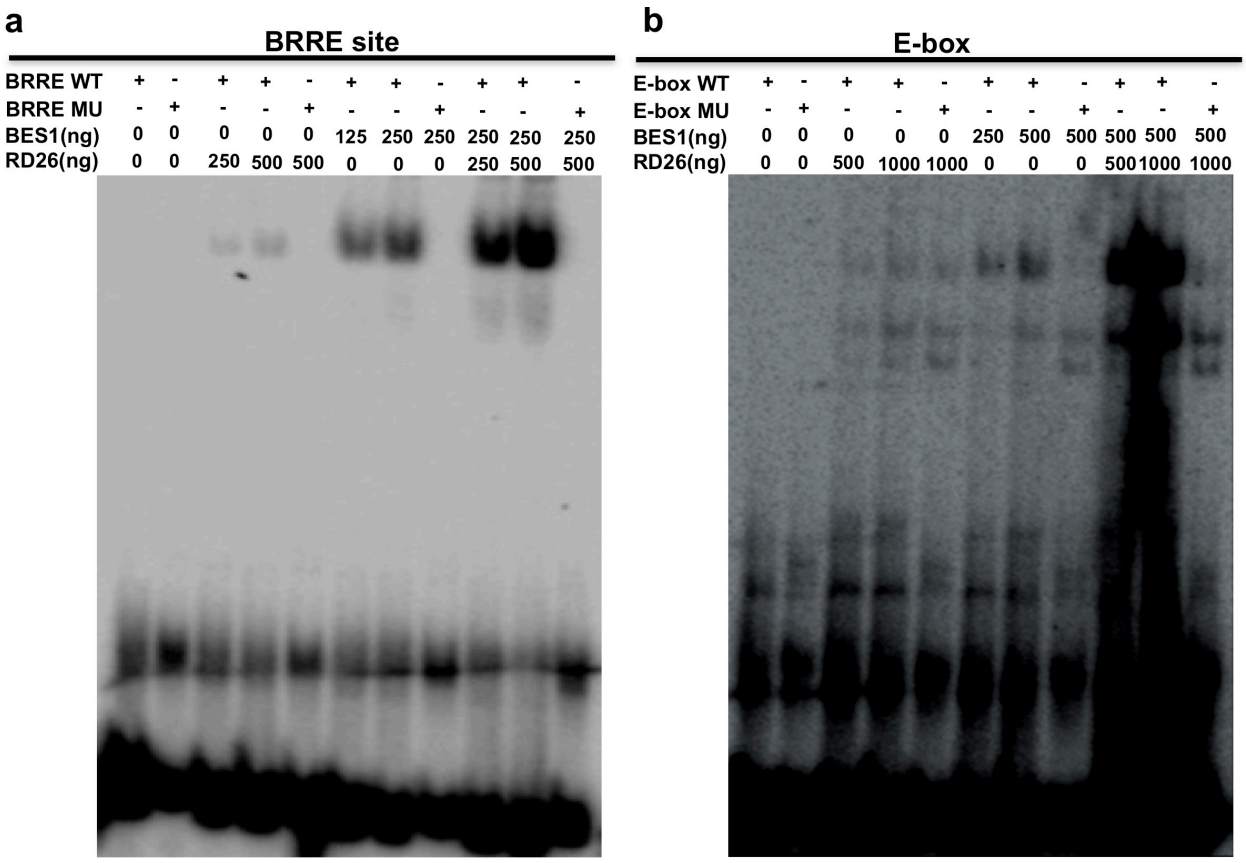

Fig. S10: BES1 and RD26 individually bind to E-box or BRRE site, but they together displayed strong synergistic binding on both sites. The full images for Fig. 5b and Fig. 5c are shown.

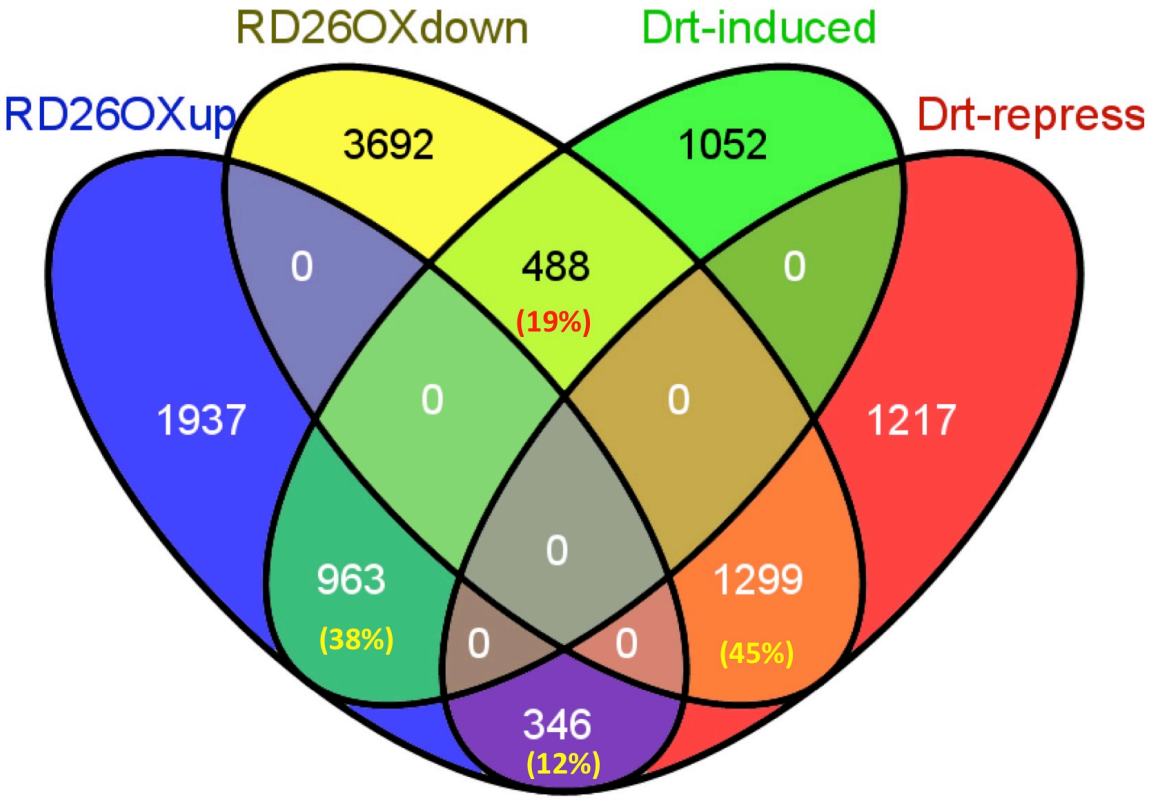

Fig. S11: RD26 mediates the expression of a large portion of drought-responsive genes.

Venn diagram shows the overlap genes between genes either up- or down-regulated in RD26OX as well as drought (Drt)-induced or drought-repressed genes. The drought-regulated genes are derived from [51].

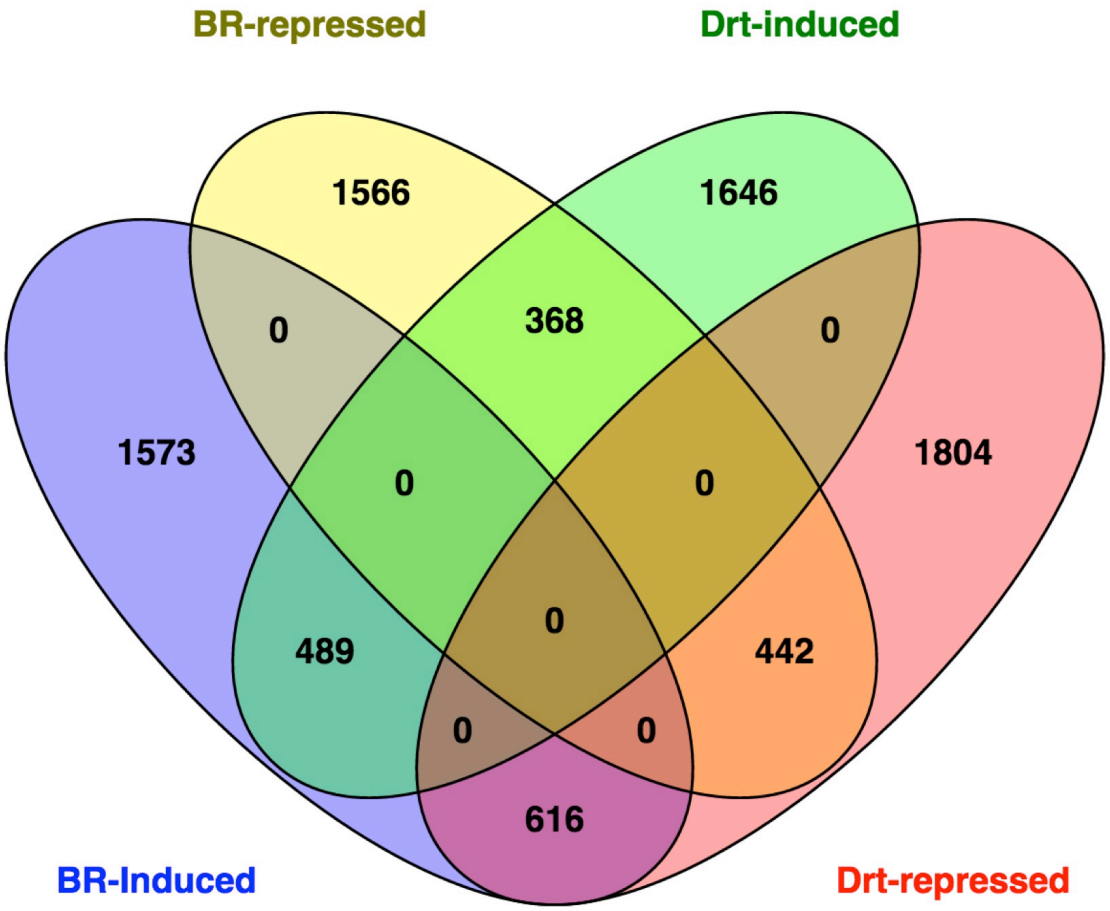

Fig. S12: Overlaps between BR-regulated and drought-responsive genes.
Venn diagram shows the overlap genes between genes either BR-induced or BR-repressed as well as drought (Drt)-induced or drought-repressed genes. The drought-regulated genes are derived from [51].

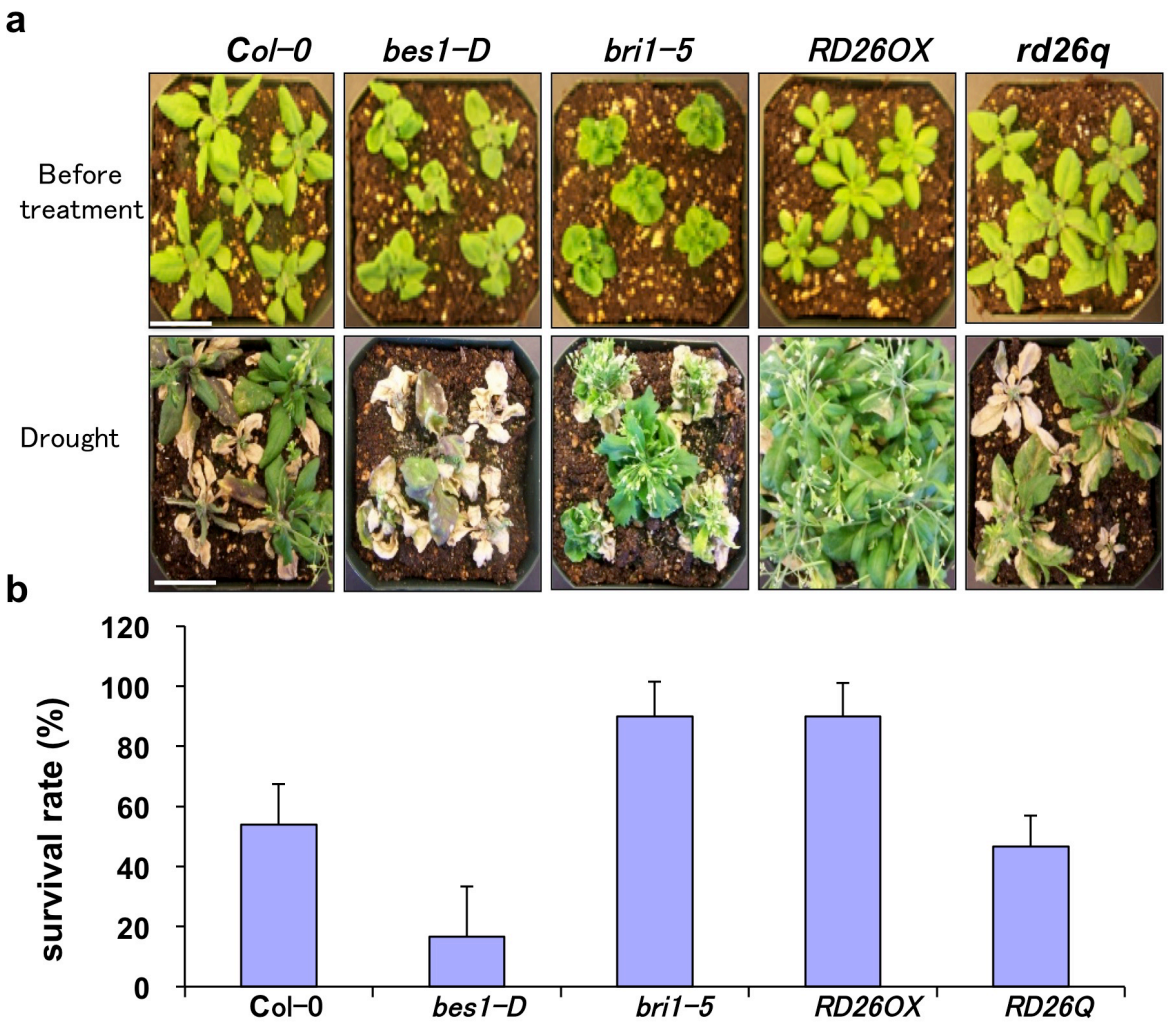

Fig. S13: The drought response phenotypes of BR and *RD26* mutants.

(a) Drought assay (4 week-old plants were withheld water for 2 weeks, and then re-watered for 3 days.) for *Col-0, bes1-D, bri1-5, RD26OX* or *rd26 anac019 anac055 anac102* quadruple mutant *(rd26q)* plants. For each line, 20 plants were tested. Selected pots with plants before drought treatments and after drought treatments are shown. The survival rate for two biological repeats are shown. Scale bars represent 2.5 cm. (b). The experiments were repeated three times with same trend.

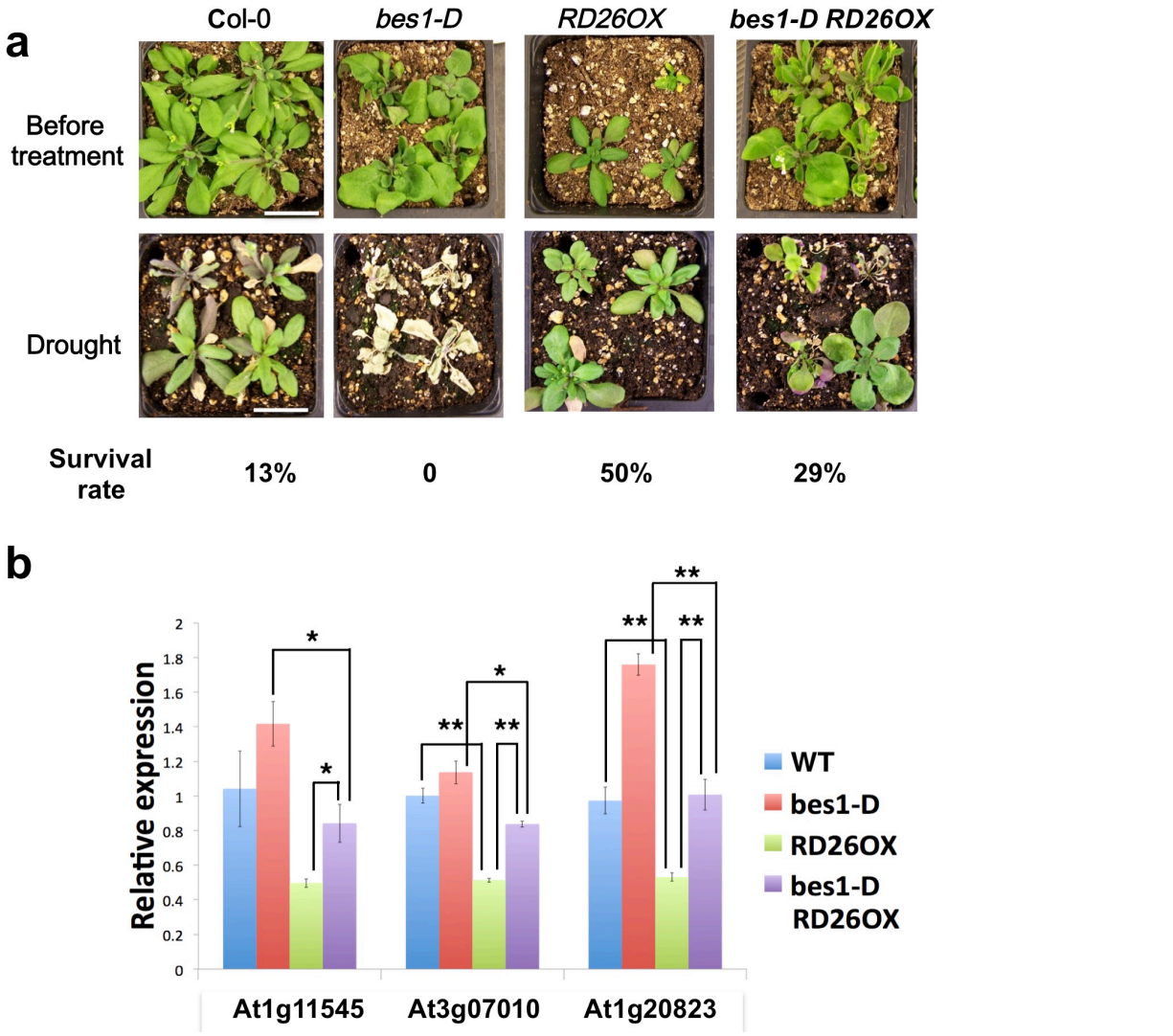

Fig. S14: *RD26* overexpression suppresses *bes1-D* phenotype in drought response.

(a) Drought assay (4 week-old plants were withheld water for 2 weeks, and then re-watered for 3 days.) for *Col-0, bes1-D, RD26OX, or bes1-D RD26OX plants.* For each line, 32-40 plants were tested. Selected pots with plants before drought treatments and after drought treatments are shown. Scale bars represent 2 cm. The experiments were repeated three times with same trend.

(b) The expression of several BES1 and RD26 regulated genes in *Col-0, bes1-D, RD26OX, or bes1-D RD26OX plants.* The expression of those genes were examined by qPCR using RNA prepared from corresponding 5 week-old plants. Error bars indicate s.d. (n=3).

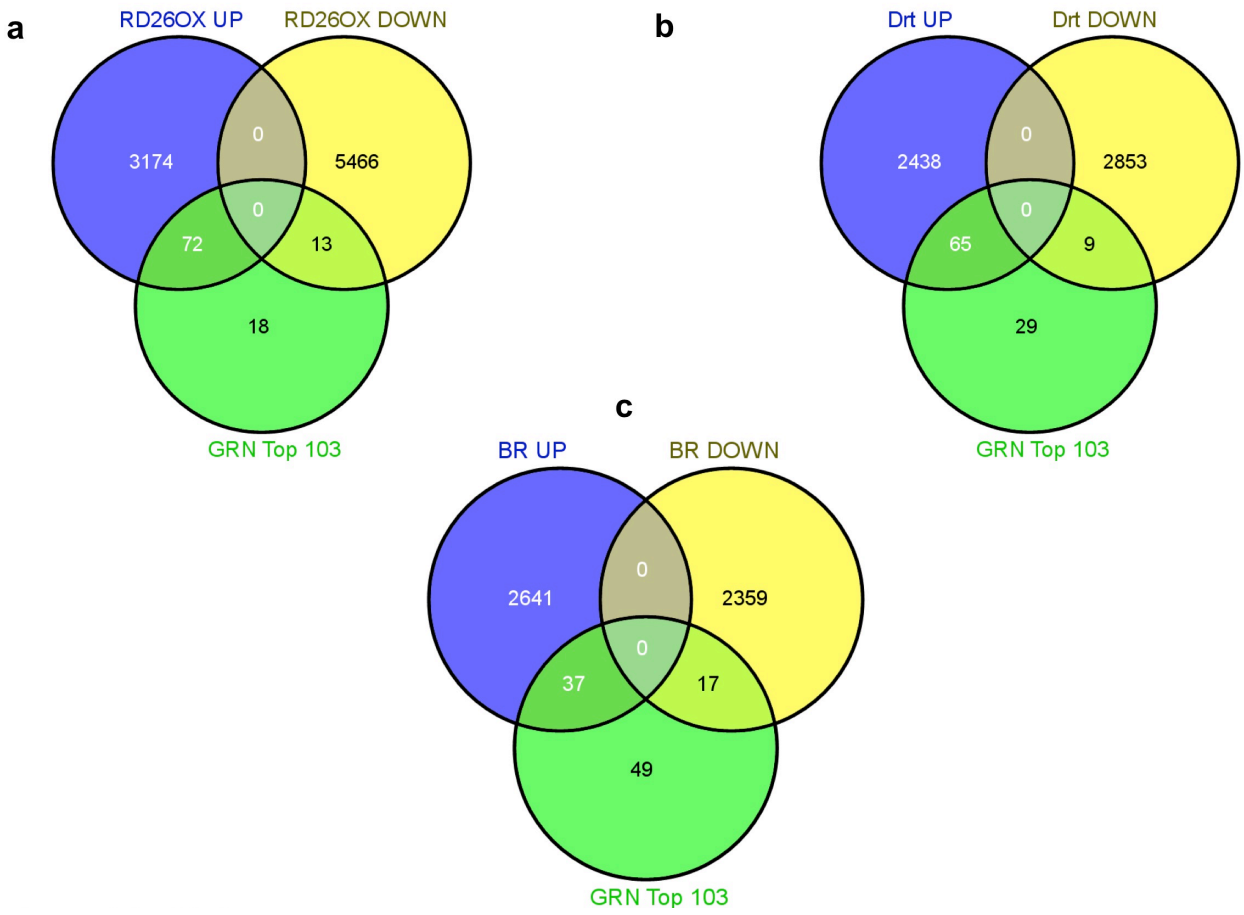

Fig. S15. Validation of GRN by differential gene expression in RD26OX, and by drought or BR- regulated genes.

Venn diagram shows the overlap genes between genes in the top 103 of the derived GRN (GRN top 103) and genes either up- or down-regulated in RD26OX (a), genes regulated by drought (b), or genes regulated by BRs (c).

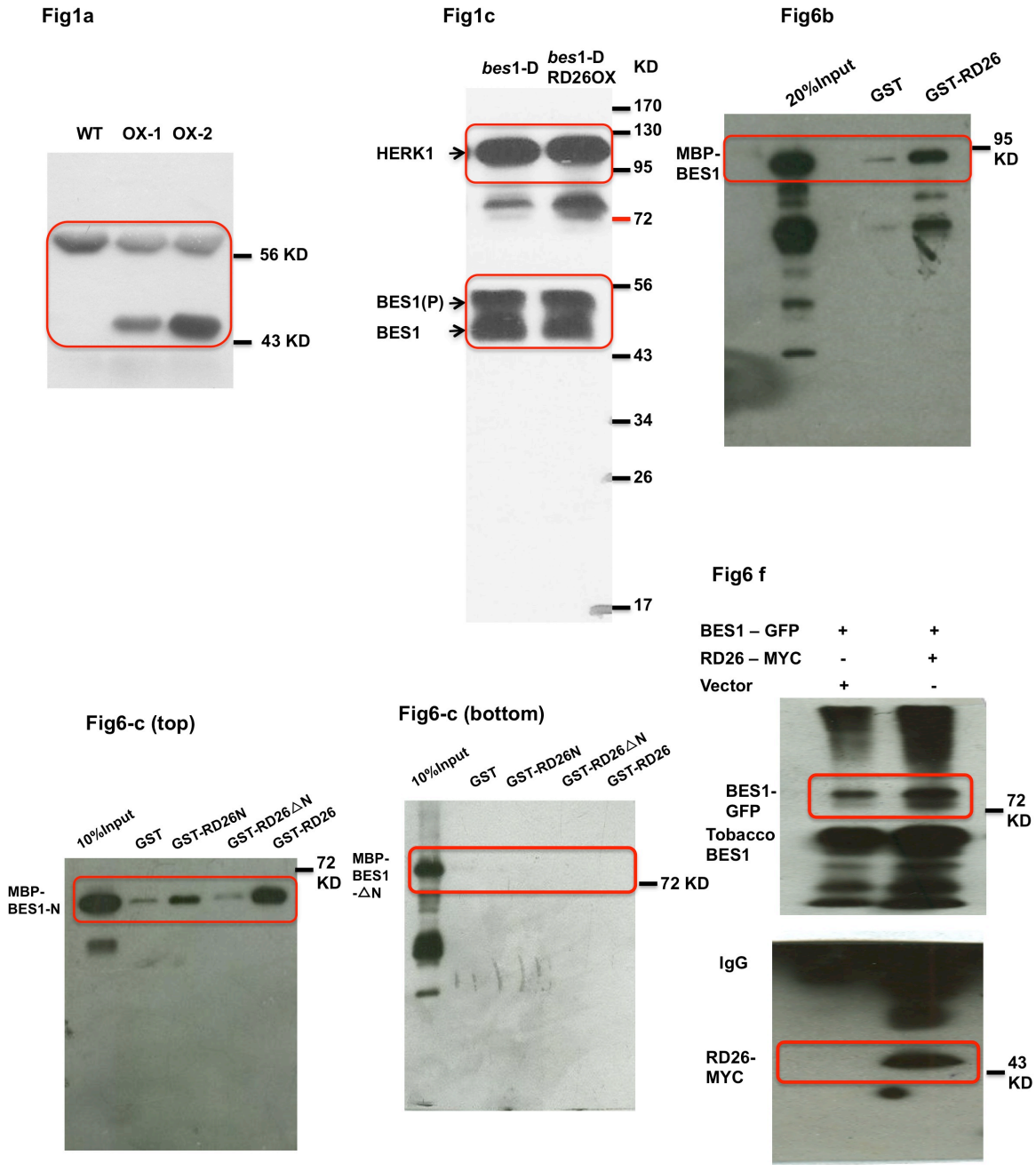

Fig. S16. Uncropped images of Western blots present in this study.

Table S1. Frequencies of specific promoter elements presented in Group 1 and Group 2 gene promoters

	Specific E-box (CATGTG)	General E-box (CAXXTG)	BRRE (CGTGT/CG)
Group 1	0.17*	1.73	0.05
Group 2	0.13	1.67	0.12*
Control	0.12	1.65	0.07

The sequences in 500 bp upstream of the selected promoters were used to search for indicated promoter elements. The frequency of indicated promoter element in each one promoter is indicated. The control used 1000 randomly selected genes that are not in Group 1 or Group 2. The significance of enrichment compared to control was calculated by fitting negative binomial model and indicated (* $p<0.05$).

Table S2. The DNA primers used in this study

RD26LP	AGTGATCGAGTGCTTCAGGAC	GENOTYPING
RD26RP	ACTCGTGCATAATCCAGTTGG	
ANAC019LP	TCAATGAACTCAAGGGATTGC	
ANAC019RP	ATGCGGTTTGGGTTAGAAAAC	
ANAC055LP	TAAACGATGAGCGATAGCGAG	
ANAC055RP	AAAGGAACCAAAACCAATTGG	
ANAC102LP	TAATCGTATGACCCGACTTGG	
ANAC102RP	TCTATCTTTGCCGGAGATGTG	
RD26BamHI	CGCGGATCCATGGGTGTTAGAGAGAAAGATCCGTTAG	PROTEIN EXPRESSION
RD26SacI	GCCGAGCTCTCATTGCCTAAACTCGAATGTTTGACCCG	
RD26SalI	GCCGTCGACTCATTGCCTAAACTCGAATGTTTGACCCG	
RD26NSalI	CGGGTCGACTATTAAGCGATACTCGTGCATAATCC	
RD26△NBamHI	GCGGGATCCGAACATTCTCGTAGCCATGGAAGC	
gRD26NAsp718	CGCGGTACCATCTCTCTGTGAACAAGAATTCTCCACGTTCAC	TRANSGENIC PLANT
gRD26CSal1	CGCGTCGACTTGCCTAAACTCGAATGTTTGACCCGAAACACC	
RD26CHIP1F	TCCCAACACGTGTACAATTCA	BES1 ChIP
RD26CHIP1R	AAAACAAATGGCACTAAGACGTT	
RD26CHIPCF	TTGTCCAAAAGATCGACGAA	
RD26CHIPCR	CTTCGATTCCTCAGCAACCA	
RD26RTF	GGCACTAAAACCAACTGGATTATGCACGAG	GENE EXPRESSION
RD26RTR	GGAGTAACAGCTTGTCTCTGAGATCCAG	
ANACO19RTF	GCTCCTAAAGGTACTAAAACCAATTGGATC	
ANAC019RTR	CCATTATCGTAAACTTGTTTTTGTGCAC	
ANAC055RTF	TTGGATTATGCATGAGTACCGTCTCATCG	
ANAC055RTR	CCATTGTTGCTGTATTCACGACCACTCG	
ANAC102RTF	CGAGTATCGTCTCGCTAATGTCGATCGATC	
ANAC102RTR	ACGTACTCATCTTTTCCGTCGGTTTCTCAG	
BOS1RTF	TTCATGAATTACGACTACAACAACAA	
BOS1RTR	AGAACCAGAATTCTTCATCAGTTTCT	
ERD1RTF	ATTGATCATAATGACCTCTAATGTCG	
ERD1RTR	ATCTTCAACAATCTCTGTGACAGTTC	
AT1G29395RTF	CAGAAACCATTCCTCTCTCTTAAACT	
AT1G29395RTR	ATACACCATACTCTCCCTTAATCCAG	
AT3G62650RTF	GGAGAGGATACGAGAAGCTTGAT	
AT3G62650RTR	CACCATCAGTATCGACTTGTAAATCT	
AT1G10070RTF	GTCTATGCATCTCCAGTTGGTAACTA	
AT1G10070RTR	GCCTTCTCTACTACCTGATAACCTTG	
AT1G20823F	TGTTGCCAGGTGTCACAAGT	
AT1G35230F	CTCCCTCAGCTCCTACCACT	
AT5G52760F	CATGACCGCAAAGAACGCTG	
AT1G20823R	CTTCGCCTTGCTTGATTCGG	
AT1G35230R	GGAGAGCCACTTAGGGGAGA	
AT5G52760R	TCGAGAAACGGTGACAAGCG	

AT4G01870F	CATGTGAGTTTCAATAAAGATGGTG	
AT4G01870R	CGTCTAATTTCACAACGTACAAATC	
AT1g11545F	AATCGGGAGATGCGACATTC	
AT1g11545R	CGTGTAGCCCAATCGTCAGC	
AT3G07010F	CTAAGGAGGTGACTAAGAGAGAGTAC	
AT3G07010R	CGACGAGTGAGGATGATTTG	
AT1G22400F	GCGGATCAACGCTGGAGATA	
AT1G22400R	AACTCTCATCTTTTAGCGGACA	
AT5G17860F	CCGCCTGGTTGTTTGTTCTG	
AT5G17860R	TGCCAAGAGAGAGAAGCGTG	
AT1G65490F	ACGCAACGAAGAACGAAATGG	
AT1G65490R	GGATTTCCCCAAAACGCAAGT	
AT1G04680F	TAAAGAGGTGACGAAGAGAGTGG	
AT1G04680R	GTGGTGGGGTAGTAACTATGAGG	
AT3G57450F	GAAATACACGGAGATGTTGGAC	
AT3G57450R	TACACTTGAGAAGATTTGATACCG	
TCH4F	GGTTCCCTCAAGGTCTTCCTA	
TCH4R	AAAAGCACATTGTAACAAAGAGAATA	
PTI1-4F	AGTCACATGGGCTACACCTAAAC	
PTI1-4R	CTTCCCCTGGAGCTACGGC	
EXPL2F	TGTCGATATTGAATACAGGAGAGTTC	
EXPL2R	CATTTTGCCGTCGTAGCCTG	
WSD1-F	TGGCGAAGGGTTCAAAGTGT	
WSD1-R	AGCTTCTACTGCCTTTCCTCC	
SAUR64-F	AGTGCTACTAGCTCAACCGC	
SAUR64-R	TAGGTCCACCAGTTGGGAGG	
AT1G20823F	TGTTGCCAGGTGTCACAAGT	
AT1G35230F	CTCCCTCAGCTCCTACCACT	
AT5G52760F	CATGACCGCAAAGAACGCTG	
AT1G20823R	CTTCGCCTTGCTTGATTCGG	
AT1G35230R	GGAGAGCCACTTAGGGGAGA	
AT5G52760R	TCGAGAAACGGTGACAAGCG	
AT4G01870F	CATGTGAGTTTCAATAAAGATGGTG	
AT4G01870R	CGTCTAATTTCACAACGTACAAATC	
AT1g11545F	AATCGGGAGATGCGACATTC	
AT1g11545R	CGTGTAGCCCAATCGTCAGC	
AT3G07010F	CTAAGGAGGTGACTAAGAGAGAGTAC	
AT3G07010R	CGACGAGTGAGGATGATTTG	
AT1G22400F	GCGGATCAACGCTGGAGATA	
AT1G22400R	AACTCTCATCTTTTAGCGGACA	
AT4G18010FBH1	CGCGGATCCTTGTGAATCAAACTAATTTATTTAAGTAGC	TRANSIENT EXPRESSION
AT4G18010RHD3	CGCAAGCTTCTTCTTAGATCTCAGAAAAAGATTTTGTTTC	
AT4G00360FBH1	CGCGGATCCTCTCTTGATACAATGCATATAGAAACTGAC	
AT4G00360RHD3	CGCAAGCTTATCAATGAATATGAAATGATACTAAAATGG	
AT1G22400F	CGCGGATCCGGTGTTTCAATGGGGGTGCTC	
AT1G22400R	CCCAAGCTTCAAATGTGAGTTTTGGTTTGCCTTTG	

AT5G17860F	CGCGGATCCCGGTTACGTTGCATAAATATTTATCTG	
AT5G17860R	CCCAAGCTTGTGGAACAATAATGAGGTGTGTTAG	
AT4G14365F	CGCGGATCCGATCCACGTACGATTTTCTTAGG	
AT4G14365R	CCCAAGCTTGAAGGAATATCAAATGAATTGAACTTAG	
AT3G19720F	CGCGGATCCCACAAGAGAGACCTTTAAGAAATG	
AT3G19720R	CCCAAGCTTGTCTCTTACGAAAATGAGCAAGAG	
4G18010BDF	AAACCGAAAACACGTGTGAGAAAGAAGAAA	EMSA EXPERIMENT
4G18010BDR	TTTCTTCTTTCTCACACGTGTTTTCGGTTT	
4G18010BDMF	AAACCGAAAACATTTTTTAGAAAGAAGAAA	
4G18010BDMR	TTTCTTCTTTCTAAAAAATGTTTTCGGTTT	
4G00360BDF	ATTACCTAACTATACATGTGTAATGTGTTC	
4G00360BDR	GAACACATTACACATGTATAGTTAGGTAAT	
4G00360BDMF	ATTACCTAACTATAAAAAAATAATGTGTTC	
4G00360BDMR	GAACACATTATTTTTTTATAGTTAGGTAAT	
AT4g18010qPCR1F	GTATGGTCGGTACAATCAGTC	RD26 and BES1 ChIP and reChIP
AT4g18010qPCR1R	AACTGCAACTTGCGATCCAC	
AT4g18010qPCR2F	GGTATGTTTGGCAAATTCAGC	
AT4g18010qPCR2R	TAAGATGGTGTAGACTGTAGG	
AT4g18010qPCR3F	GTATGGTCGGTACAATCAGTC	
AT4g18010qPCR3F	AACTGCAACTTGCGATCCAC	
UBQ5F	AAGATCCAAGACAAGGAAGG	
UBQ5R	GAAGAACAGCGAGCTTAACC	
At4g18010P1 F	CGGGGTACCTTGTGAATCAAACTAATTTATTTAAGTAGC	Yeast One-hybrid assays
At4g18010P1 R	CGCGTCGACAAAGTGAGAATCCCTCACATTTAAAAG	
At4g18010P2 F	CGGGGTACCCAAAGAAAAGATATAGACAATTTTAAGACT	
At4g18010P2 R	CGCGTCGACAACTATATTTTGACAAGCAGTTTTGCG	
At4g18010P3 F	CGGGGTACCACTAATTCTCAAATAATCACTTTTACTCCG	
At4g18010P3 R	CGCGTCGACCTGCAACTTGCGATCCACT	
At4g00360P1 F	CGGGGTACCTCTCTTGATACAATGCATATAGAAACTGAC	
At4g00360P1 R	CGCGTCGACTGACTTGTGTACGCTGCAACT	
At4g00360P2 F	CGGGGTACCATTATGTACTTCTATCATATATTTATGATATTGC	
At4g00360P2 R	CGCGTCGACTGATATTTAATCTTCTCAATTTGGTTTATC	
At4g00360P3 F	CGGGGTACCAAATCCCTCACAAGAATTGAGAACTG	
At4g00360P3 R	CGCGTCGACAGCTAAATTAAATGAGATTAGTTGAGAACC	
RD26 GAD F EcoRI	CGCGAATTCATGGGTGTTAGAGAGAAAGATC	
RD26 GAD R XhoI	CCCCTCGAGTCATTGCCTAAACTCGAATGTTTGACC	

Supplementary Data 1-10

Supplementary Data 1: List of BR-induced genes by RNA-seq.

The BR-induced genes were identified in this study by RNA-seq with 4-week-old adult plants treated with or without 1 uM BL (Fig. 2).

Supplementary Data 2: List of BR-repressed genes by RNA-seq.

The BR-induced genes were identified in this study by RNA-seq with 4-week-old adult plants treated with or without 1 uM BL (Fig. 2).

Supplementary Data 3: List of BR-induced genes by microarrays.

The BR-induced genes in seedling or adult plants derived from previous microarray studies [24, 45-49]. The original data were also reanalyzed as described in Methods section.

Supplementary Data 4: List of BR-repressed genes by microarrays.

The BR-repressed genes in seedling or adult plants derived from previous microarray studies[24, 45-49] . The original data were also reanalyzed as described in Methods section.

Supplementary Data 5: List of genes up-regulated in *RD26OX* transgenic plants.

The genes up-regulated in *RD26OX* plants compared to WT were identified in this study by RNA-seq with 4-week-old adult plants without BL treatment (Fig. 2).

Supplementary Data 6: List of genes down-regulated in *RD26OX* transgenic plants.

The genes down-regulated in *RD26OX* plants compared to WT were identified in this study by RNA-seq with 4-week-old adult plants without BL treatment (Fig. 2).

Supplementary Data 7: List of genes up-regulated in *rd26 anac019 anac055 anac102* quadruple mutants.

The genes up-regulated in *rd26 anac019 anac055 anac102* quadruple mutant plants compared to WT were identified in this study by RNA-seq with 4-week-old adult plants without BL treatment (Fig. S4).

Supplementary Data 8: List of genes down-regulated in *rd26 anac019 anac055 anac102* quadruple mutants.

The genes down-regulated in *rd26 anac019 anac055 anac102* quadruple mutant plants compared to WT were identified in this study by RNA-seq with 4-week-old adult plants without BL treatment (Fig. S4).

Supplementary Data 9: List of genes up-regulated by drought stress.

Drought induced genes (combination of 2-day and 3-day dehydration treatment data) were from previous study by microarray analysis [51].

Supplementary Data 10: List of genes down-regulated by drought stress.

Drought induced genes (combination of 2-day and 3-day dehydration treatment data) were from previous study by microarray analysis [51].

A.8 References

1. Krishna, P. Brassinosteroid-Mediated Stress Responses. *J Plant Growth Regul* **22**, 289-297 (2003).
2. Clouse, S.D. Molecular genetic studies confirm the role of brassinosteroids in plant growth and development. *Plant J* **10**, 1-8 (1996).
3. Wang, Z.Y., Bai, M.Y., Oh, E. & Zhu, J.Y. Brassinosteroid signaling network and regulation of photomorphogenesis. *Annu Rev Genet* **46**, 701-724 (2012).
4. Clouse, S.D. Brassinosteroid signal transduction: from receptor kinase activation to transcriptional networks regulating plant development. *Plant Cell* **23**, 1219-1230 (2011).
5. Li, J. Regulation of the nuclear activities of brassinosteroid signaling. *Curr Opin Plant Biol* **13**, 540-547 (2010).

6. She, J. *et al.* Structural insight into brassinosteroid perception by BRI1. *Nature* **474**, 472-476 (2011).
7. Hothorn, M. *et al.* Structural basis of steroid hormone perception by the receptor kinase BRI1. *Nature* **474**, 467-471 (2011).
8. Li, J. & Chory, J. A putative leucine-rich repeat receptor kinase involved in brassinosteroid signal transduction. *Cell* **90**, 929-938 (1997).
9. Wang, H. *et al.* Dual role of BKI1 and 14-3-3 s in brassinosteroid signaling to link receptor with transcription factors. *Dev Cell* **21**, 825-834 (2011).
10. Jaillais, Y. *et al.* Tyrosine phosphorylation controls brassinosteroid receptor activation by triggering membrane release of its kinase inhibitor. *Genes Dev* **25**, 232-237 (2011).
11. Wang, X. & Chory, J. Brassinosteroids regulate dissociation of BKI1, a negative regulator of BRI1 signaling, from the plasma membrane. *Science* **313**, 1118-1122 (2006).
12. Gou, X. *et al.* Genetic evidence for an indispensable role of somatic embryogenesis receptor kinases in brassinosteroid signaling. *Plos Genet* **8**, e1002452 (2012).
13. Oh, M.H. *et al.* Tyrosine phosphorylation of the BRI1 receptor kinase emerges as a component of brassinosteroid signaling in *Arabidopsis*. *Proc Natl Acad Sci U S A* **106**, 658-663 (2009).
14. Wang, X. *et al.* Sequential transphosphorylation of the BRI1/BAK1 receptor kinase complex impacts early events in brassinosteroid signaling. *Dev Cell* **15**, 220-235 (2008).
15. Nam, K.H. & Li, J. BRI1/BAK1, a receptor kinase pair mediating brassinosteroid signaling. *Cell* **110**, 203-212 (2002).
16. Li, J. *et al.* BAK1, an *Arabidopsis* LRR receptor-like protein kinase, interacts with BRI1 and modulates brassinosteroid signaling. *Cell* **110**, 213-222 (2002).
17. Tang, W. *et al.* PP2A activates brassinosteroid-responsive gene expression and plant growth by dephosphorylating BZR1. *Nat Cell Biol* **13**, 124-131 (2011).
18. Kim, T.W., Guan, S., Burlingame, A.L. & Wang, Z.Y. The CDG1 kinase mediates brassinosteroid signal transduction from BRI1 receptor kinase to BSU1 phosphatase and GSK3-like kinase BIN2. *Mol Cell* **43**, 561-571 (2011).
19. Yan, Z., Zhao, J., Peng, P., Chihara, R.K. & Li, J. BIN2 functions redundantly with other *Arabidopsis* GSK3-like kinases to regulate brassinosteroid signaling. *Plant Physiol* **150**, 710-721 (2009).
20. Mora-Garcia, S. *et al.* Nuclear protein phosphatases with Kelch-repeat domains modulate the response to brassinosteroids in *Arabidopsis*. *Genes Dev* **18**, 448-460 (2004).
21. Li, J. & Nam, K.H. Regulation of brassinosteroid signaling by a GSK3/SHAGGY-like kinase. *Science* **295**, 1299-1301 (2002).
22. Tang, W. *et al.* BSKs mediate signal transduction from the receptor kinase BRI1 in *Arabidopsis*. *Science* **321**, 557-560 (2008).
23. Yu, X. *et al.* A brassinosteroid transcriptional network revealed by genome-wide identification of BESI target genes in *Arabidopsis* thaliana. *Plant J* **65**, 634-646 (2011).

24. Sun, Y. *et al.* Integration of brassinosteroid signal transduction with the transcription network for plant growth regulation in *Arabidopsis*. *Dev Cell* **19**, 765-777 (2010).
25. Yin, Y. *et al.* A new class of transcription factors mediate brassinosteroid-regulated gene expression in *Arabidopsis*. *Cell* **120**, 249-259. (2005).
26. He, J.X. *et al.* BZR1 is a transcriptional repressor with dual roles in brassinosteroid homeostasis and growth responses. *Science* **307**, 1634-1638 (2005).
27. Yin, Y. *et al.* BES1 accumulates in the nucleus in response to brassinosteroids to regulate gene expression and promote stem elongation. *Cell* **109**, 181-191 (2002).
28. Wang, Z.Y. *et al.* Nuclear-localized BZR1 mediates brassinosteroid-induced growth and feedback suppression of brassinosteroid biosynthesis. *Dev Cell* **2**, 505-513 (2002).
29. Kagale, S., Divi, U.K., Krochko, J.E., Keller, W.A. & Krishna, P. Brassinosteroid confers tolerance in *Arabidopsis* thaliana and Brassica napus to a range of abiotic stresses. *Planta* **225**, 353-364 (2007).
30. Sairam, R. Brassinosteroid confers tolerance in *Arabidopsis* thaliana and Brassica napus to a range of abiotic stresses. *Planta* **225**, 353-364. (1994).
31. Beste, L. *et al.* Synthesis of hydroxylated sterols in transgenic *Arabidopsis* plants alters growth and steroid metabolism. *Plant Physiol* **157**, 426-440 (2011).
32. Noguchi, T. *et al. Arabidopsis* det2 is defective in the conversion of (24R)-24-methylcholest-4-En-3-one to (24R)-24-methyl-5alpha-cholestan-3-one in brassinosteroid biosynthesis. *Plant Physiol* **120**, 833-840 (1999).
33. Feng, Y., Yin, Y.H. & Fei, S.Z. Down-regulation of BdBRI1, a putative brassinosteroid receptor gene produces a dwarf phenotype with enhanced drought tolerance in Brachypodium distachyon. *Plant Sci* **234**, 163-173 (2015).
34. Nakashima, K., Takasaki, H., Mizoi, J., Shinozaki, K. & Yamaguchi-Shinozaki, K. NAC transcription factors in plant abiotic stress responses. *Biochim Biophys Acta* **1819**, 97-103 (2012).
35. Tran, L.S. *et al.* Isolation and functional analysis of *Arabidopsis* stress-inducible NAC transcription factors that bind to a drought-responsive cis-element in the early responsive to dehydration stress 1 promoter. *Plant Cell* **16**, 2481-2498 (2004).
36. Fujita, M. *et al.* A dehydration-induced NAC protein, RD26, is involved in a novel ABA-dependent stress-signaling pathway. *Plant J* **39**, 863-876 (2004).
37. Chung, Y., Kwon, S.I. & Choe, S. Antagonistic Regulation of *Arabidopsis* Growth by Brassinosteroids and Abiotic Stresses. *Mol Cells* **37**, 795-803 (2014).
38. Takasaki, H. *et al.* SNAC-As, stress-responsive NAC transcription factors, mediate ABA-inducible leaf senescence. *Plant J* **84**, 1114-1123 (2015).
39. Guan, Q., Yue, X., Zeng, H. & Zhu, J. The Protein Phosphatase RCF2 and Its Interacting Partner NAC019 Are Critical for Heat Stress–Responsive Gene Regulation and Thermotolerance in *Arabidopsis*. *Plant Cell* **In press.** (2014).
40. Bu, Q. *et al.* Role of the *Arabidopsis* thaliana NAC transcription factors ANAC019 and ANAC055 in regulating jasmonic acid-signaled defense responses. *Cell Res* **18**, 756-767 (2008).

41. Li, S. *et al.* The role of ANAC072 in the regulation of chlorophyll degradation during age- and dark-induced leaf senescence. *Plant Cell Rep* **35**, 1729-1741 (2016).
42. Zheng, X.Y. *et al.* Coronatine Promotes Pseudomonas syringae Virulence in Plants by Activating a Signaling Cascade that Inhibits Salicylic Acid Accumulation. *Cell Host Microbe* **11**, 587-596 (2012).
43. Asami, T. *et al.* Characterization of brassinazole, a triazole-type brassinosteroid biosynthesis inhibitor. *Plant Physiol* **123**, 93-100 (2000).
44. Wang, X.L. *et al.* Histone Lysine Methyltransferase SDG8 Is Involved in Brassinosteroid-Regulated Gene Expression in *Arabidopsis* thaliana. *Mol Plant* **7**, 1303-1315 (2014).
45. Goda, H. *et al.* The AtGenExpress hormone and chemical treatment data set: experimental design, data evaluation, model data analysis and data access. *Plant J* **55**, 526-542 (2008).
46. Goda, H. *et al.* Comprehensive comparison brassinosteroid-regulated of auxin-regulated and brassinosteroid-regulated genes in *Arabidopsis*. *Plant Physiol* **134**, 1555-1573 (2004).
47. Nemhauser, J.L., Mockler, T.C. & Chory, J. Interdependency of brassinosteroid and auxin signaling in *Arabidopsis*. *PLoS Biol* **2**, E258 (2004).
48. Li, L., Ye, H., Guo, H. & Yin, Y. *Arabidopsis* IWS1 interacts with transcription factor BES1 and is involved in plant steroid hormone brassinosteroid regulated gene expression. *Proc Natl Acad Sci U S A* **107**, 3918-3923 (2010).
49. Guo, H.Q. *et al.* Three related receptor-like kinases are required for optimal cell elongation in *Arabidopsis* thaliana. *P Natl Acad Sci USA* **106**, 7648-7653 (2009).
50. Chen, H. *et al.* Firefly luciferase complementation imaging assay for protein-protein interactions in plants. *Plant Physiol* **146**, 368-376 (2008).
51. Maruyama, K. *et al.* Metabolic pathways involved in cold acclimation identified by integrated analysis of metabolites and transcripts regulated by DREB1A and DREB2A. *Plant Physiol* **150**, 1972-1980 (2009).
52. Noguchi, T. *et al.* Brassinosteroid-insensitive dwarf mutants of *Arabidopsis* accumulate brassinosteroids. *Plant Physiol* **121**, 743-752 (1999).
53. Vilarrasa-Blasi, J. *et al.* Regulation of Plant Stem Cell Quiescence by a Brassinosteroid Signaling Module (vol 30, pg 36, 2014). *Dev Cell* **33**, 238-238 (2015).
54. Mengiste, T., Chen, X., Salmeron, J. & Dietrich, R. The BOTRYTIS SUSCEPTIBLE1 gene encodes an R2R3MYB transcription factor protein that is required for biotic and abiotic stress responses in *Arabidopsis*. *Plant Cell* **15**, 2551-2565 (2003).
55. Aluru, M., Zola, J., Nettleton, D. & Aluru, S. Reverse engineering and analysis of large genome-scale gene networks. *Nucleic Acids Research* **In press** (2012).
56. Cui, F., Brosche, M., Sipari, N., Tang, S. & Overmyer, K. Regulation of ABA dependent wound induced spreading cell death by MYB108. *New Phytol* **200**, 634-640 (2013).
57. Song, L. *et al.* A transcription factor hierarchy defines an environmental stress response network. *Science* **354**, 598-+ (2016).

58. Divi, U.K., Rahman, T. & Krishna, P. Brassinosteroid-mediated stress tolerance in *Arabidopsis* shows interactions with abscisic acid, ethylene and salicylic acid pathways. *Bmc Plant Biol* **10**, 151 (2010).
59. Li, L. *et al. Arabidopsis* MYB30 is a direct target of BES1 and cooperates with BES1 to regulate brassinosteroid-induced gene expression. *Plant J* **58**, 275-286 (2009).
60. Hajdukiewicz, P., Svab, Z. & Maliga, P. The small, versatile pPZP family of Agrobacterium binary vectors for plant transformation. *Plant Mol Biol* **25**, 989-994. (1994).
61. Pryor, K.D. & Leiting, B. High-level expression of soluble protein in Escherichia coli using a His(6)-tag and maltose-binding-protein double-affinity fusion system. *Protein Expres Purif* **10**, 309-319 (1997).
62. Clough, S.J. & Bent, A.F. Floral dip: a simplified method for Agrobacterium-mediated transformation of *Arabidopsis* thaliana. *Plant J* **16**, 735-743. (1998).
63. Antony, G. *et al.* Rice xa13 recessive resistance to bacterial blight is defeated by induction of the disease susceptibility gene Os-11N3. *Plant Cell* **22**, 3864-3876 (2010).
64. Wu, T.D. & Nacu, S. Fast and SNP-tolerant detection of complex variants and splicing in short reads. *Bioinformatics* **26**, 873-881 (2010).
65. Bullard, J.H., Purdom, E., Hansen, K.D. & Dudoit, S. Evaluation of statistical methods for normalization and differential expression in mRNA-Seq experiments. *Bmc Bioinformatics* **11**, 94 (2010).
66. Benjamini, Y. & Hochberg, Y. Controlling the false discovery rate: a practical and powerful approach to multiple testing. *J. Roy. Statist. Soc. Ser. B* **57**, 289-300 (1995).
67. Nolan, T. *et al.* Identification of Brassinosteroid Target Genes by Chromatin Immunoprecipitation Followed by High-throughput Sequencing (ChIP-seq) and RNA-seq. *Methods in Molecular Biology* **Brassinosteroids: Methods and Protocols (Russinova E. and Caño-Delgado, A.I. Eds)**, In press. (2017).
68. Zhang, B.L., Wang, L., Zeng, L.P., Zhang, C. & Ma, H. *Arabidopsis* TOE proteins convey a photoperiodic signal to antagonize CONSTANS and regulate flowering time. *Gene Dev* **29**, 975-987 (2015).
69. Irizarry, R.A. *et al.* Exploration, normalization, and summaries of high density oligonucleotide array probe level data. *Biostatistics* **4**, 249-264 (2003).
70. Yu, X., Li, L., Guo, M., Chory, J. & Yin, Y. Modulation of brassinosteroid-regulated gene expression by Jumonji domain-containing proteins ELF6 and REF6 in *Arabidopsis*. *Proc Natl Acad Sci U S A* **105**, 7618-7623 (2008).

A.9 Acknowledgements

We thank Dr. Eddy Yeh for help with RNA-seq analysis, Weijia Su for helping with BR and BRZ response experiments and Tadao Asami (University of Tokyo) for providing

BRZ. The work is supported by grant from NSF (IOS-1257631) and by Plant Science Institute at Iowa State University.

A.10 Author Contributions

HY and YY originally conceived the project. HY, BT, JC, ZX, HJ performed genetic, physiological, biochemical and gene expression studies. TN performed BiFC and gene clustering analyses. SL, HYL, LL, YW, MZ, ZL and PS are involved in RNA-seq and bioinformatics analyses. HT and CC are involved in yeast one-hybrid assays. HG and YY performed ChIP and Re-ChIP experiments. MA and SA performed computational modeling. HY and YY wrote the paper with contributions from most coauthors.

APPENDIX B

ARABIDOPSIS WRKY46, WRKY54 AND WRKY70 TRANSCRIPTION FACTORS ARE INVOLVED IN BRASSINOSTEROID-REGULATED PLANT GROWTH AND DROUGHT RESPONSE

A paper published in *The Plant Cell*

Jiani Chen[a], Trevor Nolan[a], Huaxun Ye[a1], Mingcai Zhang[a,b], Hongning Tong[c], Peiyong Xin[d], Jinfang Chu[d], Chengcai Chu[c], Zhaohu Li[b], & Yanhai Yin[a2]

[a] Department of Genetics, Development and Cell Biology, Iowa State University, 1111 WOI Road, Ames, IA 50011, USA

[b] State Key Laboratory of Plant Physiology and Biochemistry, Department of Agronomy, College of Agronomy and Biotechnology, China Agricultural University, Beijing 100193, China

[c] State Key Laboratory of Plant Genomics and [d] National Centre for Plant Gene Research, Institute of Genetics and Developmental Biology, Chinese Academy of Sciences, Beijing, 100101, China

[1]Current Address, Dupont Pioneer, Inc. Johnston, IA 50131

[2]Corresponding Author: Department of Genetics, Development and Cell Biology, Iowa State University, 1111 WOI Road, Ames, IA 50011, USA. Tel: (515) 294-4816; yin@iastate.edu

B.1 Abstract

Plant steroid hormones, Brassinosteroids (BRs), play important roles in growth and development. BR signaling controls the activities of BES1/BZR1 transcription factors. Besides the role in promoting growth, BRs are also implicated in plant responses to drought stress. However, the molecular mechanisms through which BRs regulate drought response have just begun to be revealed. On the other hand, the functions of WRKY transcription factors in BR-regulated plant growth have not been established, although their roles in stress responses are well documented. Here we found that three group III WRKY transcription factors, WRKY46, WRKY54 and WRKY70, are involved in both BR-regulated plant growth and drought response as the *wrky46 wrky54 wrky70* triple mutant has defects in BR-regulated growth and is more tolerant to drought stress. RNA-seq analysis revealed global roles of WRKY46, WRKY54 and WRKY70 in promoting BR mediated gene expression and inhibiting drought responsive genes. WRKY54 directly interacts with BES1 to cooperatively regulate the expression of target genes. In addition, WRKY54 is phosphorylated and destabilized by GSK3-like kinase BIN2, a negative regulator in the BR pathway. Our results therefore establish WRKY46/54/70 as important signaling components that are positively involved in BR-regulated growth and negatively involved in drought responses.

B.2 Introduction

Plant steroid hormones, Brassinosteroids (BRs), modulate multiple plant growth and developmental processes, including cell elongation and division, vascular differentiation, senescence, photomorphogenes and response to biotic and abiotic

stresses (Li et al., 1996; Szekeres et al., 1996; Li and Chory, 1997). Over the past decades, extensive genetic and molecular studies have revealed the BR signaling pathway. BRs are perceived by the plasma membrane-localized receptor kinase BRI1 and co-receptor BAK1; and the signal is transduced through various intermediates including the negative acting GSK3-like kinase BIN2 to downstream BES1/BZR1 family transcription factors (TFs), which regulate the expression of thousands of genes for BR response (Clouse et al., 1996; Li and Chory, 1997; Li et al., 2001; He et al., 2002; Li and Nam, 2002; Li et al., 2002; Nam and Li, 2002; Wang et al., 2002; Yin et al., 2002; Zhao et al., 2002; Clouse, 2011; Guo et al., 2013).

BRs interact extensively with gibberellic acid (GA) in the regulation of plant growth (Bai et al., 2012; Gallego-Bartolome et al., 2012; Li et al., 2012; Tong et al., 2014; Unterholzner et al., 2015; Shahnejat-Bushehri et al., 2016). In addition to the critical role in the plant growth and development, BRs are also involved in a wide range of stress responses, such as cold stress, drought, oxidative stress, high salt, high temperature, heavy metal and pathogen attack (Krishna, 2003; Hao et al., 2013; Rajewska et al., 2016). Earlier studies suggested positive roles of BRs in drought tolerance in wheat, *Arabidopsis thaliana* and *Brassica napus* (Sairam, 1994; Kagale et al., 2007). For example, overexpression of *Arabidopsis* BR biosynthetic gene *AtDWF4* in *Brassica napus* resulted in enhanced tolerance to drought (Sahni et al., 2016). However, genetic studies also indicated a negative role of BRs or BR signaling in drought responses. Loss-of-function BR mutants showed increased tolerance to drought (Beste et al., 2011; Northey et al., 2016; Nolan et al., 2017; Ye et al., 2017), and RNAi knockdown of *BRI1* in *Brachypodium distachyon* led to enhanced drought tolerance and

elevated expression of drought-regulated genes (Feng et al., 2015). Recent studies have started to reveal mechanisms of BR-abiotic stress signaling. BIN2 phosphorylates and positively regulates SnRK2.2 and 2.3 as well as ABI5 involved in drought/ABA signaling (Cai et al., 2014; Hu and Yu, 2014). ABA induces the expression of OsREM4.1, a membrane anchored protein that inhibits BR signaling by inhibiting BRI1-BAK1 complex formation (Clouse, 2016; Gui, 2016). More recently, it was found that RD26, a NAC transcription factor, mediates crosstalk between BR and drought pathways through reciprocal inhibition between RD26 and BES1 transcriptional activities (Ye et al., 2017). Under drought or starvation conditions, BES1 is targeted to selective autophagy through the actions of SINAT E3 ubiquitin ligase and ubiquitin receptor protein DSK2, thereby balancing plant growth and stress responses (Nolan et al., 2017; Yang et al., 2017).

The WRKY family TFs are only found in higher plants and are composed of over 70 members in *Arabidopsis* (Ulker and Somssich, 2004). This family of TFs contains a well conserved WRKY domain, which binds to the W-box ((T)TGACC/T) in the target gene promoters (Eulgem and Somssich, 2007), and a zinc finger motif at its C-terminus either $CX_{4-5}CX_{22-23}HXH$ (CCHH, X denotes any amino acid, 4-5/22-23 indicate the number of amino acids) or $CX_7CX_{23}HXC$ (CCHC) (Eulgem, 2000). The WRKY family is categorized into three groups according to the number of WRKY domains and the structure of zinc finger (Rushton et al., 2010). WRKY46, WRKY54, WRKY70 belong to the group III with one WRKY domain and CCHC zinc finger motif (Eulgem, 2000). Many studies have indicated that WRKY TFs play crucial roles in plant innate immunity as well as abiotic responses (Eulgem, 2000; Li et al., 2006; Eulgem and Somssich, 2007;

Murray, 2007; Ulker et al., 2007; Higashi et al., 2008; Ren et al., 2010; Rushton et al., 2010; Chen et al., 2012; Hu et al., 2012; Li et al., 2013; Chujo et al., 2014). It is known that WRKY TFs can control multiple plant responses via transcriptional reprogramming (Rushton et al., 2010). For instance, WRKY46 participated in basal defense against bacteria *Pseudomonas syringae* since gain-of-function *WRK46* plants were more resistant to the bacteria (Hu et al., 2012). In addition, WRKY46 was found to have dual roles in regulating plant responses to drought and salt stress as the overexpression of *WRKY46* resulted in hypersensitivity to drought and salt stress with a higher rate of water loss (Ding et al., 2014b). Microarray analysis showed that WRKY46 regulates a number of genes in cellular osmoprotection and redox homeostasis under dehydration stress (Ding et al., 2014b). Similarly, a *wrky54 wrky70* double mutant showed increased tolerance to osmotic stress, which was accompanied by enhanced stomatal closure and improved water retention, suggesting that WRKY54 and WRKY70 cooperate as negative regulators of osmotic stress in *Arabidopsis* (Li et al., 2013). Although the role of WRKY family TFs in stress responses is well established, their role in hormone-regulated plant growth remains to be investigated.

In this study, we found that *Arabidopsis WRKY46, WRKY54* and *WRKY70* were induced by BRs and play positive roles in BR-regulated plant growth. Moreover, we showed that *WRKY46, WRKY54* and *WRKY70* negatively regulate drought tolerance, consistent with their previously described role in stress response. RNA-seq analysis indicated that WRKY46, WRKY54 and WRKY70 negatively regulate dehydration-responsive gene expression while promoting BR regulated gene expression. Further, we demonstrated that WRKY54 interacts with BES1 to control the expression of BR-

regulated and dehydration-responsive genes. Our results thus revealed the dual roles of WRKY46/54/70 in plant growth and drought responses by cooperating with BR-regulated transcription factor BES1.

B.3 Results

WRKY46, WRKY54 and WRKY70 are positive regulators in BR pathway

Our previously published microarray data showed that the expression levels of *WRKY46*, *WRKY54* and *WRKY70* were induced by BRs in wild-type (Emsley and Cowtan) seedlings and also increased in *bes1-D* mutants treated with or without brassinolide (BL), the most active BR (Noguchi et al., 2000; Li et al., 2010). To confirm this result, *WRKY46*, *WRKY54* and *WRKY70* mRNA levels were determined in 4-week-old WT and *bes1-D* mutants with or without BL treatment by quantitative real-time PCR (qPCR). Consistent with previous microarray data, *WRKY46/54/70* transcript levels were increased by 1.5 to 6 fold in adult WT and/or *bes1-D* plants after BL treatment (Figure 1A). These results indicate that BRs promote the expression of *WRKY46/54/70.*

To determine the biological functions of WRKY46/54/70 in the BR pathway, we obtained T-DNA insertion lines for these genes (Supplemental Figure 1A). Single knockout mutants for *wrky46*, *wrky54* or *wrky70* did not show any obvious growth phenotype compared to WT (Figure 1B). Since WRKY46, WRKY54 and WRKY70 have high similarities in protein sequences (Supplemental Figure 1B) and might function redundantly, we generated *wrky46 wrky54*, *wrky46 wrky70* and *wrky54 wrky70* double mutants to determine their role in plant growth. The double mutants showed a slightly reduced-growth phenotype than WT or the single mutants (Supplemental Figure 2A). We then generated *wrky46 wrky54 wrky70* triple mutants (*w54t*), which displayed a

stronger reduction in growth with shorter blade lengths, blade widths and petiole lengths (Figure 1B and 1C). Moreover, *w54t* has a dwarf phenotype at the flowering stage (Supplemental Figure 2B). Genetic complementation experiments were performed to confirm that the *w54t* mutant phenotype is caused by loss-of-function of these genes. Expression of *WRKY54* in *w54t* mutant rescued the mutant phenotype, as 123 out of 227 transgenic plant showed a clear WT-like phenotype, whereas none of the 143 *w54t* plant lines transformed with control vector showed rescued phenotype (Figure 1D; Supplemental Figure 2C). To further determine if other Class III members (WRKY30, WRKY41 and WRKY53) contribute to plant growth, we constructed a sextuple mutant *wrky46 wrky54 wrky70 wrky30 wrky41 wrky53* (*wrkyS*) and found that the sextuple mutants have a slightly stronger growth phenotype than *w54t* triple mutants (Supplemental Figure 3A to 3C), suggesting that WRKY30, WRKY41 and WRKY53 play some role in vegetative growth. Taken together, these genetic results indicate that WRKY46/54/70 together with other group III WRKY TFs function redundantly and play a positive role in plant growth.

We then monitored BES1 protein levels, a well-established marker for the BR pathway. BES1 levels, particularly the dephosphorylated form, were decreased significantly in 4 week-old *w54t* plants compared to WT, whereas the single mutants had only slightly reduced BES1 levels (Figure 1B, middle and lower panels) (Yin et al., 2002; Yin et al., 2005). The reduction of BES1 protein might be due to reduced BR biosynthesis or signaling. To elucidate the mechanism underlying the altered BES1 protein levels, the expression of BR biosynthesis genes, *DWF4*, *DET2* and *CPD,* was determined in the *w54t* mutants (Kim et al., 2005). The mRNA level of *DWF4*, *DET2* and

CPD decreased 1 to 5-fold in the triple mutant compared to WT (Supplemental Figure 4A). The reduction of BR biosynthesis genes in *w54t* prompted us to determine the endogenous levels of BRs in WT and *w54t* plants (Xin et al., 2013). The amount of BL was below detectable levels in adult leaves, but the level of castasterone (CS), a precursor of BL, was slightly reduced by 10% in *w54t* compared to WT (Supplemental Figure 4B). The sextuple mutant *wrkyS* showed a 20% decrease in CS levels accompanied by a stronger reduction in growth (Supplemental Figure 4B). The levels of 6-deoxoCS, the precursor of CS, which is about 50-100 times more abundant than CS, does not seem to significantly change in the mutants (Supplemental Figure 4C and 4D).

We also examined the BES1 protein phosphorylation status and level in *w54t* mutant in response to BL. Application of exogenous BL restored the BES1 protein level in *w54t* to the WT level after 0.5 hour BL treatment (Figure 1E). However, when grown in the presence of different concentrations of BL, the *w54t* mutant showed decreased sensitivity to BL compared to WT with shorter hypocotyls, although BL could restore the BES1 protein in *w54t* to the WT level (Figure 1F; Supplemental Figure 5A). We also determined mutant responses to other plant hormones and found that the *w54t* as well as single mutants have normal response to auxin and ethylene in hypocotyl elongation assays (Supplemental Figure 5B) (Smalle J., 1997). It appears that *w54t* mutants also have reduced hypocotyl elongation in response to gibberellic acid (GA), consistent with recent findings that BRs can function upstream of GA to regulate cell elongation (Supplemental Figure 5B) (Tong et al., 2014; Unterholzner et al., 2015). The fact that BES1 levels could be restored by BL treatment yet the *w54t* mutant still displayed

decreased BL response suggests that WRKY46/54/70 might play a pivotal role in BR signaling.

WRKY46/54/70 is required for the regulation of BR/BES1 target genes

BES1/BZR1 interact with other transcription factors, such as MYB30, PIF4 and HAT1 to control BR-regulated gene expression (Li et al., 2009; Li et al., 2012; Oh et al., 2012; Zhang et al., 2014). We hypothesized that WRKY46/54/70 might also function as cofactors of BES1 to regulate BR target genes. To test this idea, we first performed RNA-sequencing analysis with 4-week-old adult plants of *w54t*, and analyzed the overlap of the genes differentially expressed in the triple mutant with those affected in *bes1-D,* a gain-of-function mutant in *BES1*, to determine if WRKY46/54/70 regulate the expression of BR/BES1 target genes. A significant portion of genes up- or –down-regulated in the *w54t* mutant are down- or up-regulated in *bes1-D*, respectively (Figure 2B and 2C; Supplemental Table 1 and Table 2). The results suggest that WRKY46/54/70 positively participate in BES1-regulated gene expression. Similar results were observed in the *wrkyS* mutant (Supplemental Figure 6A and 6B).

To confirm the effect of WRKY46/54/70 on the transcriptional regulation on BR targets, we used qPCR to examine the expression of several genes differentially expressed in *w54t* that are also regulated by BRs as reported in our previous global gene expression analysis (Supplemental Table 5) (Yu et al., 2011; Wang et al., 2014). All three of the BR-induced genes tested have compromised induction by BL in *w54t* (Figure 2C). Similarly, three of the BR-repressed genes that were examined are up-regulated in *w54t* (Figure 2D). The results indicate that WRKY46/54/70 are required for

the expression of BR-regulated gene expression, confirming that WRKY46/54/70 function positively in BR signaling.

BES1 cooperates with WRKY54 to regulate the transcription of BR target genes

Next, given the strong effect of *w54t* mutants on BR regulated gene expression, we tested if WRKY46/54/70 interact with BES1 to cooperatively regulate BR regulated gene expression. We first chose WRKY54 as a representative TF of the WRKY46/54/70 family to investigate the interaction between WRKYs and BES1. Yeast-two hybrid assays demonstrated an interaction between BES1 and WRKY54 (Supplemental Figure 7A) which was confirmed by GST pull-down using maltose binding protein (MBP)-tagged BES1 protein and glutathione S-transferase (GST)-tagged WRKY54 (Supplemental Figure 7B).

We next tested the interaction between BES1 and WRKY54 *in vivo* by biomolecular fluorescence (BiFC) assay with BES1 fused to the N-terminal of YFP (YFPN) and WRKY54 fused to the C-terminal of YFP (YFPC). When co-expressed in *N. benthamiana*, BES1-YFPN and WRKY54-YFPC resulted in reconstituted YFP signal (Figure 3A). However, no fluorescence signal was observed in negative controls where WRKY54-YFPC was co-expressed with YFPN or BES1-YFPN was expressed with YFPC (Figure 3A; Supplemental Figure 7F). These results confirm that WRKY54 interacts with BES1 *in vivo*. Similar results were obtained for WRKY46 and WRKY70 in BiFC assays, indicating that these TFs also interact with BES1 (Figure 3A).

To test our hypothesis that WRKY54 and BES1 cooperate in the regulation of BR target genes, two BR-repressed genes (*At2g45210* and *At1g43910*) were used to generate promoter-luciferase (LUC) reporter constructs for transient gene expression

analysis in *N. benthamiana*. BES1 or WRKY54 alone repressed reporter activity to about 50% of the control level and the reporter activity was further reduced to about 20% when both BES1 and WRKY54 were co-expressed (Figure 3B and 3C). Taken together, our results indicate that BES1 and WRKY54 interact with each other and cooperate to regulate the expression of BR target genes.

WRKY46, WRKY54 and WRKY70 play negative roles in drought response

WRKY54 and WRKY70 were previously identified as negative regulators of osmotic stress tolerance in *Arabidopsis* (Li et al., 2013). To test whether WRKY46/54/70 regulate drought tolerance, WT, *wrky46, wrky54* and *wrky70* single mutants, *wrky46 wrky54*, *wrky46 wrky70* and *wrky54 wrky70* double mutants and *w54t* triple mutants were subjected to drought survival assays. After drought and re-watering, *w54t* mutants exhibited significantly higher survival rates than WT, the single mutants or the double mutants (Figure 4A and 4B; Supplemental Figure 8). The results indicate that WRKY46/54/70 negatively regulate drought stress response.

WRKY46/54/70 repress dehydration-inducible gene expression

To reveal the mechanism of WRKY46/54/70 in drought response, we performed global gene expression studies using 4-week old WT and *w54t* plants under control and dehydration conditions by RNA-seq. After 4-hour dehydration, 310 genes were induced and 244 genes were repressed in WT plants (Figure 4C, Supplemental Table 3). Consistent with their strong phenotype in growth and drought response, 4,600 genes were up-regulated and 4,530 genes were down-regulated in *w54t* mutants (Figure 2B; Supplemental Table 2). Many of the genes differentially expressed in *w54t* mutants are involved in response to various stresses and cellular processes (Supplemental Figure

10). Among these, 156 of dehydration-repressed genes were constitutively down-regulated and 164 of the dehydration-induced genes were constitutively up-regulated in *w54t* mutant without dehydration treatments (Figure 4D and 4E). These results were consistent with our observation that *w54t* was more tolerant to drought stress. We compared the genes differentially regulated in *w54t* under dehydration condition (143 genes down-regulated in *w54t* upon dehydration and 235 genes up-regulated in *w54t* upon dehydration) with those differentially expressed in *bes1-D* and found that the,mre were significant overlaps between these two datasets (Supplemental Figure 8D). 55.2% of genes down-regulated in *w54t* under dehydration condition were up-regulated in *bes1-D*, but only 3% of the genes were down-regulated in *bes1-D*. Similarly, one quarter of genes up-regulated in *w54t* under dehydration condition were down-regulated in *bes1-D*, whereas about 14% were up-regulated in *bes1-D*. The results suggest that WRKY46/54/70 indeed play important roles in BR-regulated drought tolerance.

To confirm our RNA-seq data, three dehydration-induced genes, *ABI5*, *GLYI7* and *RD20* were chosen for qPCR validation (Fujita et al., 2005; Yuan et al., 2014; Pinedo et al., 2015). The expression of these genes increased significantly in *w54t* mutants with or without dehydration (Figure 5A). Next, we investigated if BES1 and WRKY54 cooperate in the regulation of dehydration-induced genes using LUC reporter assays with the *GLY17* promoter. BES1 or WRKY54 individually resulted in about 2-fold reduction in reporter activity, and co-expression of BES1 and WRKY54 led to a further reduction, showing a 4-fold reduction in reporter activity (Figure 5C). The W-box ((T)TGACC/T) and G-box (CACGTG) were previously shown to be conserved binding motifs for WRKY TFs and BES1, respectively (Eulgem and Somssich, 2007; Yu et al.,

2011). To test if the repression effect of WRKY54 and BES1 on the dehydration-inducible gene is through binding to the W-box and G-box, *GLYI7* promoter containing mutated W-box, G-box or both were fused with LUC and coexpressed with BES1 or WRKY54 alone or together (Figure 5B). The results showed that W-box mutation disrupted WRKY54-mediated repression of the *GLYI7* promoter (Figure 5C). Similarly, mutation of the G-box abrogated the effect of BES1 on *GLY17* promoter activity. The simultaneous mutation of W-box and G-box completely reversed the repressive effect of both BES1 and WRKY54 on *GLYI7* expression (Figure 5C). Taken together, these results indicate that WRKY46/54/70 negatively modulate drought tolerance and likely cooperate with BES1 to repress drought-inducible genes by binding to the W-box and G-box, respectively.

WRKY54 is phosphorylated and destabilized by BIN2 kinase

BIN2, a glycogen synthase kinase-3 like kinase, is a negative regulator in the BR pathway. Substrates of BIN2 share a consensus motif S/TXXXS/T, where S/T denotes serine or threonine and X can be any amino acid (Zhao et al., 2002). WRKY54 protein has 29 putative BIN2 phosphorylation sites, suggesting that it might be a substrate of BIN2 (Supplemental Figure 7C). Yeast two-hybrid assays indicated that BIN2 and WRKY54 indeed interacted with each other (Supplemental Figure 7D). GST pull-down assay showed that GST-WRKY54, but not GST alone, pulled down a significant amount of MBP-BIN2 (Supplemental Figure 7E). BiFC assays further indicated the direct interaction between WRKY54/WRKY46/WRKY70 and BIN2 (Figure 6A). These results suggest that WRKY54 and its homologs directly interact with BIN2.

To test if WRKY46/54/70 are substrates of BIN2, we then carried out *in vitro*

kinase assays with ^{32}P labeled ATP. MBP-tagged WRKY54 could be phosphorylated by GST-BIN2 kinase; and the phosphorylation of WRKY54 and BIN2 auto-phosphorylation was inhibited by bikinin, an inhibitor of BIN2 kinase (Figure 6B and 6C) (De Rybel et al., 2009). These results indicate that WRKY54 is a substrate of BIN2. Similar results were obtained for WRKY46 and WRKY70, indicating that these TFs are also phosphorylated by BIN2 kinase (Figure 6B; Supplemental Figure 7G).

Several previous reports indicated that BIN2 phosphorylation can lead to protein destabilization *in vivo* (Youn and Kim, 2015). In order to determine the biological function of BIN2 phosphorylation on WRKY54 *in vivo*, the stability of WRKY54 in *BIN2* gain-of-function (*bin2-1*) and loss-of-function (*bin2-3 bil1 bil2*) mutants was examined by immunoblotting with a WRKY54 antibody we developed (Supplemental Figure 9A and 9B). As shown in Fig. 6D, WRKY54 protein was increased by more than 3-fold in *bin2-3 bil1 bil2* triple mutants and reduced by half in *bin2-1* compared to WT (Figure 6D). These results suggest that WRKY54 stability is negatively correlated with BIN2 abundance *in vivo*. To confirm these results, we examined WRKY54 accumulation in WT plants after 1 μM BL treatment, which inhibits BIN2 kinase activity. WRKY54 protein accumulated to about 2.2 fold after 4 hours of BL treatment (Figure 6E). These results illustrate that WRKY54 is involved in the BR pathway and can be regulated by BRs at both transcriptional and post-transcriptional levels.

The roles of WRKY and BES1 in the crosstalk of plant growth and stress response prompted us to examine the protein level of WRKY54 and BES1 in response to drought stress. Water was withheld from 4-week-old WT plants; and control or drought-treated samples were collected 8-10 days after withholding water. As shown in

Figure 7A, the protein levels of WRKY54 and BES1 started to decrease 9-days after drought treatment and WRKY54 protein was almost undetectable at the 10-day time point (Figure 7A). These results suggest that WRKY54 plays a vital role in the coordination of plant growth and drought stress response.

B.4 Discussion

WRKY transcription factors, found exclusively in the plant kingdom, integrate various signaling pathways to modulate numerous processes including stress responses, nutrient deprivation, senescence, seed and trichome development and embryogenesis (Hinderhofer and Zentgraf, 2001; Johnson, 2002; Miao, 2004; Ulker et al., 2007; Zhou, 2011; Besseau et al., 2012; Ding et al., 2014a). Many *Arabidopsis WRKY* genes are regulated by bacterial pathogen or salicylic acid treatment (Dong, 2003), and genetic studies have indicated that WRKY transcription factors can regulate plant defense either positively or negatively (Pandey and Somssich, 2009). WRKY TFs also regulate abiotic stress responses including drought, salinity, radiation, and cold (Banerjee and Roychoudhury, 2015). However, to the best of our knowledge, a role of WRKYs in BR regulation of plant growth has not been previously reported.

Here, we found that Group III WRKY transcription factors play an important role in BR-regulated plant growth as *w54t* triple mutants displayed a dwarf phenotype and compromised BR responses. Our results suggest that WRKY46/54/70 play positive roles in plant growth mainly by regulating BR signaling with a smaller effect on BR biosynthesis. The role of WRKY46/54/70 in BR signaling is supported by its reduced response in hypocotyl elongation (Figure 1) and significant overlaps between genes differentially expressed in *w54t* mutant and in *bes1-D* (Figure 2). Moreover, WRKY54

affects BR-regulated genes by interacting and cooperating with BES1 (Figure 3). Our results therefore establish that WRKY46/54/70 promote BR signaling and are required for optimal plant growth.

The regulation of WRKY54 by BIN2 kinase, a negative regulator in the BR pathway, provides further support for its involvement in BR signaling. BIN2, a GSK3-like kinase, plays diverse roles in cellular processes including BR signaling by phosphorylating an array of substrates, leading to functional consequences such as altered protein stability (Youn and Kim, 2015). Here, we identified WRKY54 as a substrate of BIN2 kinase and BIN2 phosphorylation led to destabilization of the WRKY54 protein (Figure 6). It is possible that BIN2 phosphorylation of WRKY54 functions to release the inhibitory effect of WRKY54 on the transcription of drought-responsive genes during drought stress (Zhang, 2009).

Our global gene expression studies revealed the molecular basis for the function of WRKY46/54/70 in drought responses. WRKY54 and WRKY70 were reported to act as negative regulators in osmotic stress tolerance in *Arabidopsis* (Li et al., 2013). WRKY46 is induced by drought stress and was found to regulate osmotic stress responses (Ding et al., 2014b). Consistent with these reports, we found that *wrky46 wrky54 wrky70* triple mutants were more tolerant to drought stress, suggesting that they negatively regulate the drought response (Figure 4). Consistent with the mutant phenotype, we found that about 53% dehydration-induced genes are up-regulated and 64% of dehydration–repressed genes are down-regulated in *w54t* mutants (Figure 4). Our results therefore establish WRKY46/54/70 as important negative regulators for drought tolerance that at least partially mediate BR-repression of drought responses.

Interestingly, WRKY54 cooperates with BES1 in the regulation of both BR- and dehydration regulated genes (Figure 3; Figure 5). Previous studies revealed that WRKY responds to various environmental signals or plant developmental processes through physical interaction with a wide range of proteins related to signaling, transcription and chromatin remodeling (Chi et al., 2013). Likewise, BES1/BZR1 interact with multiple cofactors to control BR-regulated plant growth and development (Guo et al., 2013). This study established that BES1-WRKY54 interactions play important roles in BR-regulated plant growth and drought responses (Figure 7).

In summary, we demonstrated that WRKY46, WRKY54 and WRKY70 are involved in BR-regulated plant growth by regulating BR signaling. In addition, WRKY46, WRKY54 and WRKY70 negatively regulate drought tolerance by inhibiting dehydration-inducible gene expression. Future identification of WRKY54 interacting partners and target genes can further our understanding of the mechanisms by which WRKY regulates BR-regulated growth and drought responses.

B.5 Methods

Plant Materials, Growth Conditions and Hormone Responses

Arabidopsis thaliana ecotype *Columbia* (*Col-0*) was used as the wild type. T-DNA insertion lines, *wrky46* (SALK_134310), *wrky54* (CS873142) and *wrky70* (SALK_025198), were obtained from Arabidopsis Biological Resource Center (ABRC). Seeds were sterilized by 70% (v/v) ethanol and 0.1% (v/v) Triton X-100. All of the plants were grown on ½ MS plates with 1% sucrose under long day condition (16h light/8h dark) at 22°C. BL (10nM, 100nM) were added to the ½ MS agar plates. The average hypocotyl lengths were measured using 15 samples and repeated 3 times. 14-day-old

seedlings were transferred to soil and grown under the same condition in growth chambers.

Drought Stress Treatment

For drought treatment, soil was weighed in each pot before transferring the seedlings to make sure each pot has the same amount of the soil and same volume of water in the flat. Seedlings was grown on ½ MS medium for two weeks and then transferred into the weighted soil. Plants were watered once 1 week after transferring into soil and then water was withheld for 2 weeks. The survival rates are scored based upon plants that were surviving 2 days after re-watering from three biological replicates. Each biological repeat has four or five pots for each genotype. All of the pots were randomly distributed in the flat and were rotated frequently during drought stress to minimize the effect from growth environment (Shi et al., 2015). Similar results were obtained for at least three repeats at different times. Three biological replicates were performed each time with three technical replicates (one pot/technical replicate).

Plasmid Construction and Protein-Protein Interaction Assays

The DNA primer sequences used for this study are listed in Table S4. For the yeast two-hybrid assays, *WRKY54* was cloned into both GAL4 bait and prey vectors. *BES1* and *BIN2* were cloned into GAL4 bait and prey vectors, respectively (Clontech). The constructs were transformed into yeast strain Y187 and the lacZ reporter assay was measured using X-gal according to the manufacturer's protocol (Clontech). For GST pull-down assay, WRKY54 fused to GST tag was cloned into both pET42a and purified with glutathione agarose beads (Sigma). BIN2 and BES1 were fused with MBP and purified with amylose resin (NEB). GST pull-down assays were performed as

described (Yin et al., 2002). For Biomolecular fluorescence complementation (BiFC) assay, the N-terminus (amino acids 1-174) or C-terminus (amino acids 175-239) of YFP vectors were described in (Yu et al., 2008). The full-length coding region of WRKY54 and BES1 were cloned into YFPC and YFPN and then transformed into *Agrobacterium tumefaciens* strains GV3101. BiFC assay were performed as described (Wang et al., 2014).

***In vitro* Kinase Assay**

For the *in vitro* kinase assay, MBP and MBP-WRKY54 were incubated with GST-BIN2 kinase in 20ul of kinase buffer (20 mM Tris [pH 7.5], 100 mM NaCl, and 12 mM MgCl2 and 10 μCi ^{32}P-γATP (Yin et al., 2002). After incubation at 37°C for 1 hour, 20 μl 2XSDS buffer were added to stop the reaction and then the samples were boiled for 5 minutes. Proteins were resolved by SDS-PAGE gel and phosphorylation signal was detected by Typhoon/Image Quant TL.

Gene Expression Analysis and Luciferase (LUC) Assay

For the gene expression analysis, 1000nM BL was sprayed on four-week-old *bes1-D*, *wrky46 wrky54 wrky70* and WT. DMSO was used as control. Plant tissues were collected after 2.5 hours' treatment and total RNA was extracted using TRIzol Reagent (Thermo Fisher) and RNeasy Mini Kt (Qiagen). SYBR Green PCR Master Mix (Applied Biosystems) was used in qPCR analysis and qPCR samples were run on Mx4000 multiplex quantitative PCR (qPCR) system (Stratagene) with three technical replicates. UBQ5 was used as the internal control. Similar result was obtained from three biological replicates.

For the transient expression of BR-regulated genes, *At2g45210* and *At1g43910* promoter were fused with luciferase (LUC) reporter gene. *WRKY54* and *BES1* coding regions were cloned into pZP211 vector and transformed into *Agrobacterium*. Equal amount of *Agrobacterium* cells transformed with BES1 or WRKY54 or BES1 and WRKY54 was injected into tobacco leaves. The luciferase activities were measured with the luciferase assay system from Promega and Berthold Centro LB960 luminometer. The luciferase data were normalized by the total protein content.

For the transient expression of dehydration-inducible genes, *GLYI7* promoter driven firefly LUC and CaMV35S driven REN was constructed in the same plasmid and transformed into *Arabidopsis* protoplast with WRKY54 or BES1 alone or together. Protoplasts were prepared based on the protocol from Yoo *et al.* (Yoo et al., 2007). After 16h incubation, protoplasts were collected and the dual-luciferase assay system from Promega was used to measure the activity of firefly luciferase (LUC) and renilla luciferase (REN) sequentially using a Berthold Centro LB960 luminometer. The ratio of LUC/REN was calculated and relative ratio was used as the final measurement.

Determination of Endogenous BRs Levels

The quantification of endogenous BRs levels was performed based on the method reported previously with some simplifications in sample pretreatment (Xin et al., 2013). The harvested plant materials were first ground to a fine powder with a MM-400 mixer milling (Retsch). One hundred milligrams of the powder was extracted with 1 mL of 90% aqueous methanol (MeOH) in ultrasonic bath for 1 hour. Simultaneously D3-BL, D3-CS and D3-6-deoxo-CS were added to the extract as internal standards for BRs content measurement. After the MCX cartridge (3 mL, 60 mg, Waters) was activated

and equilibrated with 2 mL of MeOH, water and 40% MeOH in sequence, the crude extracts reconstructed in 40% MeOH were loaded onto the cartridge. Then the MCX cartridge was washed with 2 mL of 10% MeOH, 40% MeOH in sequence. At last BRs were eluted with MeOH. After dried with N2 stream, the eluent was redissolved with ACN to be derivatized with DMAPBA prior to UPLC-MS/MS analysis. BRs analysis was performed on a quadrupole linear ion trap hybrid MS (QTRAP 5500, AB SCIEX) equipped with an electrospray ionization source coupled with a UPLC (Waters). The UPLC inlet method, ESI source parameters, MRM transitions and the related compound-dependent parameters were set as described in the previous report (Xin et al., 2013). As for 6-deoxo-CS or D3-6-deoxo-CS, the MRM transition 580.4>176.1 or 583.4>176.1 was used for quantification and 580.4>190.1 or 583.4>190.1 for qualification. The collision energies were set as 60 V and 50 V for the transitions respectively.

Phylogenetic Analysis

The Phylogenetic Tree of six WRKY genes was generated using Clustal Omega (Sievers et al., 2011).

Quantitative PCR (qPCR) Measurement

PCR was performed in a 20ul reaction containing SYBR Green PCR Master Mix (Applied Biosystems), cDNA and primers (listed in S4 Table) and measured with Stratagene Mx4000 qPCR machine.

WRKY54 Antibody Generation and Purification

Serum was generated from rabbit after multiple injection of MBP-WRKY54 (full-length) protein as the antigen. WRKY54 antibody was then purified from the serum with

CNBr-activated sepharose. The beads were incubated with 2mg MBP-WRKY54 protein in 5ml coupling buffer (0.125M phosphate, pH8.3) overnight at 4^{o}C. Then beads were transferred to a 2.5cm column and equilibrate with 10ml PBS. Rabbit serum (10 ml) is diluted 3 volumes PBS and applied to the column. The beads in the column were washed with 30 ml PBS buffer. The bound antibody was eluted with 225ul glycine•Cl (pH2.0) directly into the tube with 25ul neutralizing buffer (1M Tris 8.0).

Dehydration RNAseq and Data Analysis

Three biological replicates of 4-week-old *wrky46 wrky54 wrky70* and WT plants were grown in soil under long day conditions (16 hours' light, 8 hours' dark). The whole rosette leaves were cut and placed in empty petri dish (150X15mm) as dehydration treatment or in petri dish with moistened kimwipes as mock control. Each petri dish consisted 3 or 4 plants and was considered as one biological replicate. The petri dish was sealed with parafilm and left for 4 hours. Tissue was then collected and processed for RNA extraction using Trizol and RNeasy Mini Kit (Qiagen) with on-column DNase digestion and cleaned up with column, following the manufacturer's instructions.

Library preparation and RNA sequencing were performed by BGI Americas using an Illumina HiSeq 2000 with 50bp single-end reads and ~30 million reads per sample. Raw RNA-Seq reads were subjected to quality checking and trimming. The trimmed reads of each sample were aligned to the public available reference genome of Arabidopsis (TAIR10) using GSNAP. The alignment coordinates of uniquely aligned reads to the reference genome were used for lookup and read count tallies were computed for each annotated gene. Finally, RNA-Seq reads were used to identify

differentially expressed genes (DEGs) with R package DESeq2 for comparison between *wrky46 wrky54 wrky70* and WT that were subjected for control or dehydration treatment. Normalization was conducted by DESeq2 automatically that corrects for biases introduced by differences in the total numbers of uniquely mapped reads in each sample. Normalized read counts were used to calculate fold-changes (FC) and statistical significance (*Data2Bio LLC*). Clustering was performed using the 'aheatmap' function of the NMF package in R and log2 reads per million (RPM) mapped reads values were used for clustering analysis. Gene Ontology (GO) analysis was performed using BiNGO software.

B.6 Acknowledgements

We thank Data2Bio, Inc. (Ames, Iowa) and Sanzhen Liu (Kansas State University) for help with RNA-seq analysis, and Tadao Asami (University of Tokyo) for providing BRZ. The work is supported by grant from NSF (IOS-1257631) and by Plant Sciences Institute at Iowa State University. PX and J Chu are supported by National Natural Science Foundation of China Grant 31470433. J Chen was partially supported by fellowship from China Scholar Council.

B.7 Author Contributions

JC performed most of the experiments unless indicated as follows. JC and TN conducted RNAseq experiment together and analyzed RNAseq data with MZ and ZL. HY was involved in generating the mutants. TN performed the confocal microscopy in BiFC assays. HT, CC, PX and J Chu conducted the BR measurements and analyzed the data. JC and YY wrote the paper with input from other co-authors.

B.8 References

Bai, M.Y., Shang, J.X., Oh, E., Fan, M., Bai, Y., Zentella, R., Sun, T.P., and Wang, Z.Y. (2012). Brassinosteroid, gibberellin and phytochrome impinge on a common transcription module in Arabidopsis. Nat Cell Biol **14,** 810-817.

Banerjee, A., and Roychoudhury, A. (2015). WRKY proteins: signaling and regulation of expression during abiotic stress responses. ScientificWorldJournal **2015,** 807560.

Besseau, S., Li, J., and Palva, E.T. (2012). WRKY54 and WRKY70 co-operate as negative regulators of leaf senescence in Arabidopsis thaliana. J Exp Bot **63,** 2667-2679.

Beste, L., Nahar, N., Dalman, K., Fujioka, S., Jonsson, L., Dutta, P.C., and Sitbon, F. (2011). Synthesis of hydroxylated sterols in transgenic Arabidopsis plants alters growth and steroid metabolism. Plant Physiol **157,** 426-440.

Cai, Z., Liu, J., Wang, H., Yang, C., Chen, Y., Li, Y., Pan, S., Dong, R., Tang, G., Barajas-Lopez Jde, D., Fujii, H., and Wang, X. (2014). GSK3-like kinases positively modulate abscisic acid signaling through phosphorylating subgroup III SnRK2s in Arabidopsis. Proc Natl Acad Sci U S A **111,** 9651-9656.

Chen, L., Song, Y., Li, S., Zhang, L., Zou, C., and Yu, D. (2012). The role of WRKY transcription factors in plant abiotic stresses. Biochim Biophys Acta **1819,** 120-128.

Chi, Y., Yang, Y., Zhou, Y., Zhou, J., Fan, B., Yu, J.Q., and Chen, Z. (2013). Protein-protein interactions in the regulation of WRKY transcription factors. Mol Plant **6,** 287-300.

Chujo, T., Miyamoto, K., Ogawa, S., Masuda, Y., Shimizu, T., Kishi-Kaboshi, M., Takahashi, A., Nishizawa, Y., Minami, E., Nojiri, H., Yamane, H., and Okada, K. (2014). Overexpression of phosphomimic mutated OsWRKY53 leads to enhanced blast resistance in rice. PLoS One **9,** e98737.

Clouse, S. (2016). Brassinosteroid/Abscisic Acid Antagonism in Balancing Growth and Stress. . Dev Cell **38,** 118-120.

Clouse, S.D. (2011). Brassinosteroid signal transduction: from receptor kinase activation to transcriptional networks regulating plant development. Plant Cell **23,** 1219-1230.

Clouse, S.D., Langford, M., and McMorris, T.C. (1996). A brassinosteroid-insensitive mutant in Arabidopsis thaliana exhibits multiple defects in growth and development. Plant Physiol **111,** 671-678.

De Rybel, B., Audenaert, D., Vert, G., Rozhon, W., Mayerhofer, J., Peelman, F., Coutuer, S., Denayer, T., Jansen, L., Nguyen, L., Vanhoutte, I., Beemster, G.T., Vleminckx, K., Jonak, C., Chory, J., Inze, D., Russinova, E., and Beeckman, T. (2009). Chemical inhibition of a subset of Arabidopsis thaliana GSK3-like kinases activates brassinosteroid signaling. Chem Biol **16,** 594-604.

Ding, Z.J., Yan, J.Y., Li, G.X., Wu, Z.C., Zhang, S.Q., and Zheng, S.J. (2014a). WRKY41 controls Arabidopsis seed dormancy via direct regulation of ABI3 transcript levels not downstream of ABA. Plant J **79,** 810-823.

Ding, Z.J., Yan, J.Y., Xu, X.Y., Yu, D.Q., Li, G.X., Zhang, S.Q., and Zheng, S.J. (2014b). Transcription factor WRKY46 regulates osmotic stress responses and stomatal movement independently in Arabidopsis. Plant J **79,** 13-27.

Dong, J.C., C.; Chen, Z. (2003). Expression profiles of the Arabidopsis WRKY gene superfamily during plant defense response. Plant Mol Biol **51,** 21-37.

Emsley, P., and Cowtan, K. (2004). Coot: model-building tools for molecular graphics. . Acta Crystal **D60,** 2126.

Eulgem, T., and Somssich, I.E. (2007). Networks of WRKY transcription factors in defense signaling. Curr Opin Plant Biol **10,** 366-371.

Eulgem, T., Rushton, P. J., Robatzek, S., Somssich, I. E. (2000). The WRKY superfamily of plant transcription factors. Trends Plant Sci **5,** 199-206.

Feng, Y., Yin, Y.H., and Fei, S.Z. (2015). Down-regulation of BdBRI1, a putative brassinosteroid receptor gene produces a dwarf phenotype with enhanced drought tolerance in Brachypodium distachyon. Plant Science **234,** 163-173.

Fujita, Y., Fujita, M., Satoh, R., Maruyama, K., Parvez, M.M., Seki, M., Hiratsu, K., Ohme-Takagi, M., Shinozaki, K., and Yamaguchi-Shinozaki, K. (2005). AREB1 is a transcription activator of novel ABRE-dependent ABA signaling that enhances drought stress tolerance in Arabidopsis. Plant Cell **17,** 3470-3488.

Gallego-Bartolome, J., Minguet, E.G., Grau-Enguix, F., Abbas, M., Locascio, A., Thomas, S.G., Alabadi, D., and Blazquez, M.A. (2012). Molecular mechanism for the interaction between gibberellin and brassinosteroid signaling pathways in Arabidopsis. Proc Natl Acad Sci U S A **109,** 13446-13451.

Gui, J., Zheng, S., Liu, C., Shen, J., Li, J., and Li, L. . (2016). OsREM4.1 Interacts with OsSERK1 to Coordinate the Interlinking between Abscisic Acid and Brassinosteroid Signaling in Rice. . Dev Cell **38,** 201-213.

Guo, H., Li, L., Aluru, M., Aluru, S., and Yin, Y. (2013). Mechanisms and networks for brassinosteroid regulated gene expression. Curr Opin Plant Biol **16,** 545-553.

Hao, J., Yin, Y., and Fei, S.Z. (2013). Brassinosteroid signaling network: implications on yield and stress tolerance. Plant Cell Rep **32,** 1017-1030.

He, J.X., Gendron, J.M., Yang, Y., Li, J., and Wang, Z.Y. (2002). The GSK3-like kinase BIN2 phosphorylates and destabilizes BZR1, a positive regulator of the brassinosteroid signaling pathway in Arabidopsis. Proc Natl Acad Sci U S A **99,** 10185-10190.

Higashi, K., Ishiga, Y., Inagaki, Y., Toyoda, K., Shiraishi, T., and Ichinose, Y. (2008). Modulation of defense signal transduction by flagellin-induced WRKY41 transcription factor in Arabidopsis thaliana. Mol Genet Genomics **279,** 303-312.

Hinderhofer, K., and Zentgraf, U. (2001). Identification of a transcription factor specifically expressed at the onset of leaf senescence. Planta **213,** 469-473.

Hu, Y., Dong, Q., and Yu, D. (2012). Arabidopsis WRKY46 coordinates with WRKY70 and WRKY53 in basal resistance against pathogen Pseudomonas syringae. Plant Sci **185-186,** 288-297.

Hu, Y.R., and Yu, D.Q. (2014). BRASSINOSTEROID INSENSITIVE2 Interacts with ABSCISIC ACID INSENSITIVE5 to Mediate the Antagonism of Brassinosteroids to Abscisic Acid during Seed Germination in Arabidopsis. Plant Cell **26,** 4394-4408.

Johnson, C.S. (2002). TRANSPARENT TESTA GLABRA2, a Trichome and Seed Coat Development Gene of Arabidopsis, Encodes a WRKY Transcription Factor. The Plant Cell Online **14,** 1359-1375.

Kagale, S., Divi, U.K., Krochko, J.E., Keller, W.A., and Krishna, P. (2007). Brassinosteroid confers tolerance in Arabidopsis thaliana and Brassica napus to a range of abiotic stresses. Planta **225,** 353-364.

Kim, T.W., Hwang, J.Y., Kim, Y.S., Joo, S.H., Chang, S.C., Lee, J.S., Takatsuto, S., and Kim, S.K. (2005). Arabidopsis CYP85A2, a cytochrome P450, mediates the Baeyer-Villiger oxidation of castasterone to brassinolide in brassinosteroid biosynthesis. Plant Cell **17,** 2397-2412.

Krishna, P. (2003). Brassinosteroid-Mediated Stress Responses. J Plant Growth Regul **22,** 289-297.

Li, J., and Chory, J. (1997). A putative leucine-rich repeat receptor kinase involved in brassinosteroid signal transduction. Cell **90,** 929-938.

Li, J., and Nam, K.H. (2002). Regulation of brassinosteroid signaling by a GSK3/SHAGGY-like kinase. Science **295,** 1299-1301.

Li, J., Nam, K.H., Vafeados, D., and Chory, J. (2001). BIN2, a new brassinosteroid-insensitive locus in Arabidopsis. Plant Physiol **127,** 14-22.

Li, J., Brader, G., Kariola, T., and Palva, E.T. (2006). WRKY70 modulates the selection of signaling pathways in plant defense. Plant J **46,** 477-491.

Li, J., Wen, J., Lease, K.A., Doke, J.T., Tax, F.E., and Walker, J.C. (2002). BAK1, an Arabidopsis LRR receptor-like protein kinase, interacts with BRI1 and modulates brassinosteroid signaling. Cell **110,** 213-222.

Li, J., Besseau, S., Toronen, P., Sipari, N., Kollist, H., Holm, L., and Palva, E.T. (2013). Defense-related transcription factors WRKY70 and WRKY54 modulate osmotic stress tolerance by regulating stomatal aperture in Arabidopsis. New Phytol **200,** 457-472.

Li, J.M., Nagpal, P., Vitart, V., McMorris, T.C., and Chory, J. (1996). A role for brassinosteroids in light-dependent development of Arabidopsis. Science **272,** 398-401.

Li, L., Ye, H., Guo, H., and Yin, Y. (2010). Arabidopsis IWS1 interacts with transcription factor BES1 and is involved in plant steroid hormone brassinosteroid regulated gene expression. Proc Natl Acad Sci U S A **107,** 3918-3923.

Li, L., Yu, X., Thompson, A., Guo, M., Yoshida, S., Asami, T., Chory, J., and Yin, Y. (2009). Arabidopsis MYB30 is a direct target of BES1 and cooperates with BES1 to regulate brassinosteroid-induced gene expression. Plant J **58,** 275-286.

Li, Q.F., Wang, C., Jiang, L., Li, S., Sun, S.S., and He, J.X. (2012). An interaction between BZR1 and DELLAs mediates direct signaling crosstalk between brassinosteroids and gibberellins in Arabidopsis. Sci Signal **5,** ra72.

Miao, Y.L., T.; Zimmermann, P.; Zentgraf, U. (2004). Targets of the WRKY53 transcription factor and its role during leaf senescence in Arabidopsis. Plant Mol Biol **55,** 853-867.

Murray, S.I., RA.; Petersen, LN.; Denby, KJ. (2007). Basal Resistance Against Pseudomonas syringae in Arabidopsis Involves WRKY53 and a Protein with Homology to a Nematode Resistance Protein. MPMI **20,** 1431-1438.

Nam, K.H., and Li, J. (2002). BRI1/BAK1, a receptor kinase pair mediating brassinosteroid signaling. Cell **110,** 203-212.

Noguchi, T., Fujioka, S., Choe, S., Takatsuto, S., Tax, F.E., Yoshida, S., and Feldmann, K.A. (2000). Biosynthetic pathways of brassinolide in Arabidopsis. Plant Physiology **124,** 201-209.

Nolan, T.M., Brennan, B., Yang, M., Chen, J., Zhang, M., Li, Z., Wang, X., Bassham, D.C., Walley, J., and Yin, Y. (2017). Selective Autophagy of BES1 Mediated by DSK2 Balances Plant Growth and Survival. Dev Cell **41,** 33-46 e37.

Northey, J.G., Liang, S., Jamshed, M., Deb, S., Foo, E., Reid, J.B., McCourt, P., and Samuel, M.A. (2016). Farnesylation mediates brassinosteroid biosynthesis to regulate abscisic acid responses. Nat Plants **2,** 16114.

Oh, E., Zhu, J.Y., and Wang, Z.Y. (2012). Interaction between BZR1 and PIF4 integrates brassinosteroid and environmental responses. Nat Cell Biol **14,** 802-809.

Pandey, S.P., and Somssich, I.E. (2009). The role of WRKY transcription factors in plant immunity. Plant Physiol **150,** 1648-1655.

Pinedo, I., Ledger, T., Greve, M., and Poupin, M.J. (2015). Burkholderia phytofirmans PsJN induces long-term metabolic and transcriptional changes involved in Arabidopsis thaliana salt tolerance. Front Plant Sci **6,** 466.

Rajewska, I., Talarek, M., and Bajguz, A. (2016). Brassinosteroids and Response of Plants to Heavy Metals Action. Front Plant Sci **7**.

Ren, X., Chen, Z., Liu, Y., Zhang, H., Zhang, M., Liu, Q., Hong, X., Zhu, J.K., and Gong, Z. (2010). ABO3, a WRKY transcription factor, mediates plant responses to abscisic acid and drought tolerance in Arabidopsis. Plant J **63,** 417-429.

Rushton, P.J., Somssich, I.E., Ringler, P., and Shen, Q.J. (2010). WRKY transcription factors. Trends Plant Sci **15,** 247-258.

Sahni, S., Prasad, B.D., Liu, Q., Grbic, V., Sharpe, A., Singh, S.P., and Krishna, P. (2016). Overexpression of the brassinosteroid biosynthetic gene DWF4 in Brassica napus simultaneously increases seed yield and stress tolerance. Sci Rep **6,** 28298.

Sairam, R.K. (1994). Effects of homobrassinolide application on plant metabolism and grain yield under irrigated and moisture-stress conditions of two wheat varieties. Plant Growth Regul **14,** 173-181.

Shahnejat-Bushehri, S., Tarkowska, D., Sakuraba, Y., and Balazadeh, S. (2016). Arabidopsis NAC transcription factor JUB1 regulates GA/BR metabolism and signalling. Nat Plants **2,** 16013.

Shi, H.T., Chen, Y.H., Qian, Y.Q., and Chan, Z.L. (2015). Low Temperature-Induced 30 (LTI30) positively regulates drought stress resistance in Arabidopsis: effect on abscisic acid sensitivity and hydrogen peroxide accumulation. Front Plant Sci **6**.

Sievers, F., Wilm, A., Dineen, D., Gibson, T.J., Karplus, K., Li, W., Lopez, R., McWilliam, H., Remmert, M., Soding, J., Thompson, J.D., and Higgins, D.G. (2011). Fast, scalable generation of high-quality protein multiple sequence alignments using Clustal Omega. Mol Syst Biol **7,** 539.

Smalle J., H.M., Kurepa J., Van Montagu M., Straeten D. V. (1997). Ethylene can stimulate Arabidopsis hypocotyl elongation in the light. Proc Natl Acad Sci U S A **94,** 2756-2761.

Szekeres, M., Nemeth, K., Koncz-Kalman, Z., Mathur, J., Kauschmann, A., Altmann, T., Redei, G.P., Nagy, F., Schell, J., and Koncz, C. (1996). Brassinosteroids rescue the deficiency of CYP90, a cytochrome P450, controlling cell elongation and de-etiolation in Arabidopsis. Cell **85,** 171-182.

Tong, H., Xiao, Y., Liu, D., Gao, S., Liu, L., Yin, Y., Jin, Y., Qian, Q., and Chu, C. (2014). Brassinosteroid regulates cell elongation by modulating gibberellin metabolism in rice. Plant Cell **26,** 4376-4393.

Ulker, B., and Somssich, I.E. (2004). WRKY transcription factors: from DNA binding towards biological function. Curr Opin Plant Biol **7,** 491-498.

Ulker, B., Shahid Mukhtar, M., and Somssich, I.E. (2007). The WRKY70 transcription factor of Arabidopsis influences both the plant senescence and defense signaling pathways. Planta **226,** 125-137.

Unterholzner, S.J., Rozhon, W., Papacek, M., Ciomas, J., Lange, T., Kugler, K.G., Mayer, K.F., Sieberer, T., and Poppenberger, B. (2015). Brassinosteroids Are Master Regulators of Gibberellin Biosynthesis in Arabidopsis. Plant Cell **27,** 2261-2272.

Wang, X.L., Chen, J.N., Xie, Z.L., Liu, S.Z., Nolan, T., Ye, H.X., Zhang, M.C., Guo, H.Q., Schnable, P.S., Li, Z.H., and Yin, Y.H. (2014). Histone Lysine Methyltransferase SDG8 Is Involved in Brassinosteroid-Regulated Gene Expression in Arabidopsis thaliana. Molecular Plant **7,** 1303-1315.

Wang, Z.Y., Nakano, T., Gendron, J., He, J., Chen, M., Vafeados, D., Yang, Y., Fujioka, S., Yoshida, S., Asami, T., and Chory, J. (2002). Nuclear-localized BZR1 mediates brassinosteroid-induced growth and feedback suppression of brassinosteroid biosynthesis. Dev Cell **2,** 505-513.

Xin, P.Y., Yan, J.J., Fan, J.S., Chu, J.F., and Yan, C.Y. (2013). An Improved Simplified High-Sensitivity Quantification Method for Determining Brassinosteroids in Different Tissues of Rice and Arabidopsis. Plant Physiology **162,** 2056-2066.

Yang, M., Li, C., Cai, Z., Hu, Y., Nolan, T., Yu, F., Yin, Y., Xie, Q., Tang, G., and Wang, X. (2017). SINAT E3 Ligases Control the Light-Mediated Stability of the Brassinosteroid-Activated Transcription Factor BES1 in Arabidopsis. Dev Cell **41,** 47-58 e44.

Ye, H., Liu, S., Tang, B., Chen, J., Xie, Z., Nolan, T.M., Jiang, H., Guo, H., Lin, H.Y., Li, L., Wang, Y., Tong, H., Zhang, M., Chu, C., Li, Z., Aluru, M., Aluru, S., Schnable, P.S., and Yin, Y. (2017). RD26 mediates crosstalk between drought and brassinosteroid signalling pathways. Nat Commun **8,** 14573.

Yin, Y., Vafeados, D., Tao, Y., Yoshida, S., Asami, T., and Chory, J. (2005). A new class of transcription factors mediates brassinosteroid-regulated gene expression in Arabidopsis. Cell **120,** 249-259.

Yin, Y., Wang, Z.Y., Mora-Garcia, S., Li, J., Yoshida, S., Asami, T., and Chory, J. (2002). BES1 accumulates in the nucleus in response to brassinosteroids to regulate gene expression and promote stem elongation. Cell **109,** 181-191.

Yoo, S.D., Cho, Y.H., and Sheen, J. (2007). Arabidopsis mesophyll protoplasts: a versatile cell system for transient gene expression analysis. Nat Protoc **2,** 1565-1572.

Youn, J.H., and Kim, T.W. (2015). Functional Insights of Plant GSK3-like Kinases: Multi-Taskers in Diverse Cellular Signal Transduction Pathways. Molecular Plant **8,** 552-565.

Yu, X., Li, L., Guo, M., Chory, J., and Yin, Y. (2008). Modulation of brassinosteroid-regulated gene expression by Jumonji domain-containing proteins ELF6 and REF6 in Arabidopsis. Proc Natl Acad Sci U S A **105,** 7618-7623.

Yu, X., Li, L., Zola, J., Aluru, M., Ye, H., Foudree, A., Guo, H., Anderson, S., Aluru, S., Liu, P., Rodermel, S., and Yin, Y. (2011). A brassinosteroid transcriptional network revealed by genome-wide identification of BESI target genes in Arabidopsis thaliana. Plant J **65,** 634-646.

Yuan, X., Li, Y., Liu, S., Xia, F., Li, X., and Qi, B. (2014). Accumulation of eicosapolyenoic acids enhances sensitivity to abscisic acid and mitigates the effects of drought in transgenic Arabidopsis thaliana. J Exp Bot **65,** 1637-1649.

Zhang, D.W., Ye, H.X., Guo, H.Q., Johnson, A., Zhang, M.S., Lin, H.H., and Yin, Y.H. (2014). Transcription factor HAT1 is phosphorylated by BIN2 kinase and mediates brassinosteroid repressed gene expression in Arabidopsis. Plant Journal **77,** 59-70.

Zhang, S.C., Z.; Wang, X. (2009). The primary signaling outputs of brassinosteroids are regulated by abscisic acid signaling
. Proc Natl Acad Sci U S A **106,** 4543-4548.

Zhao, J., Peng, P., Schmitz, R.J., Decker, A.D., Tax, F.E., and Li, J. (2002). Two putative BIN2 substrates are nuclear components of brassinosteroid signaling. Plant Physiol **130,** 1221-1229.

Zhou, X.J., Y., Yu, D. (2011). WRKY22 transcription factor mediates dark-induced leaf senescence in Arabidopsis. Mol Cell **31,** 303-313.

B.9 Figures

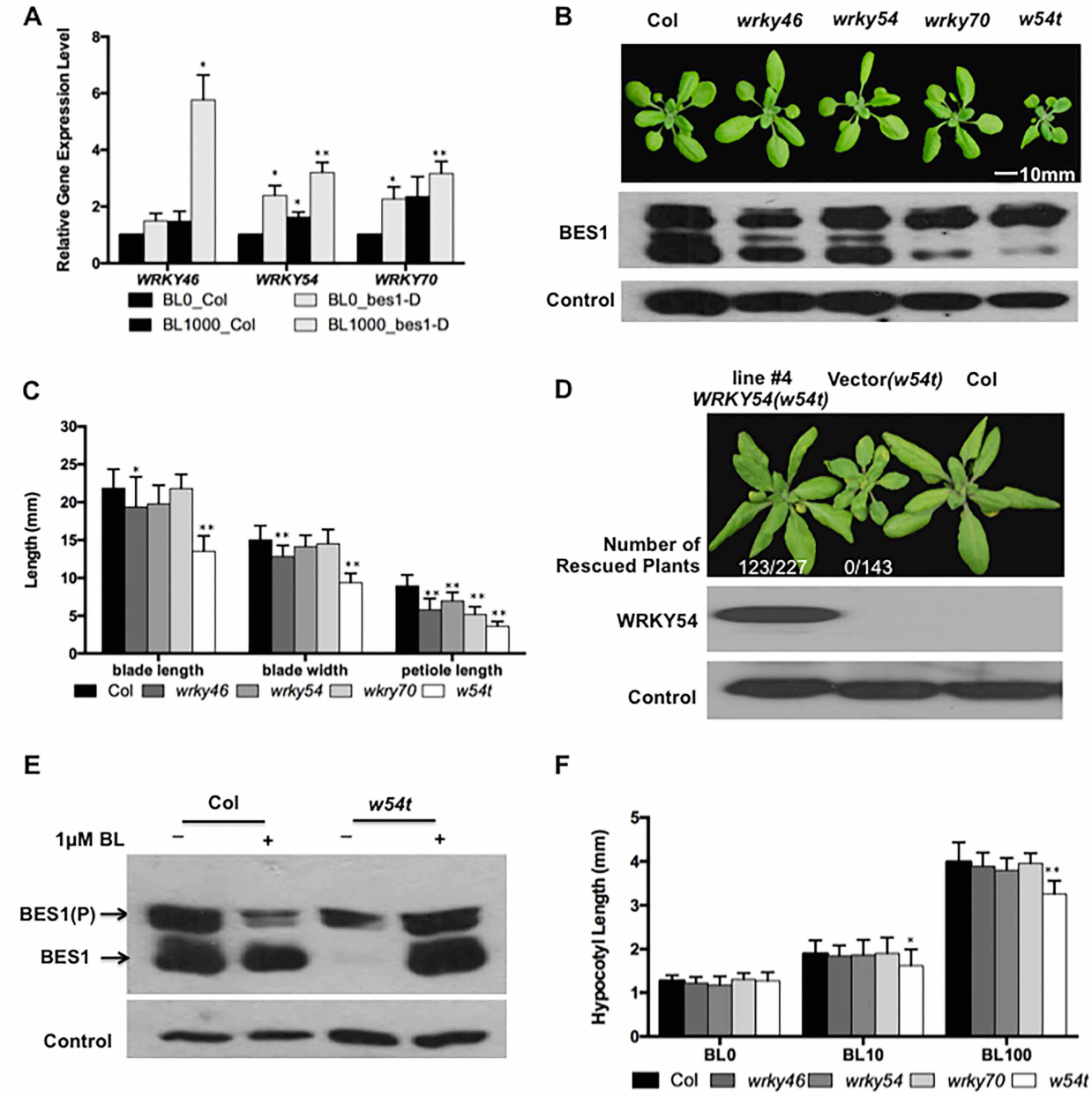

Figure 1. WRKY46, WRKY54 and WRKY70 function redundantly and play positive roles in the BR pathway. (A) *WRKY46*, *WRKY54* and *WRKY70* mRNA levels were determined in *WT* and *bes1-D* treated with 1μm BL or mock control for 2.5h. The averages and SD were derived from three biological replicates. (B) Top: The growth phenotype of three-week-old *WT, wrky46, wrky54, wrky70* and *wrky46 wrky54 wrky70 triple mutant* (abbreviated as *w54t* in all Figures). Bottom: BES1 protein levels were determined by immunoblot and a loading control was shown at the bottom. (C) The measurement of blade lengths, blade widths and petiole lengths of the sixth leaves.

Error bars indicate SD, n = 13 (* P < 0.05, ** P < 0.01; Student's t test). (D) Transgenic complementation of *w54t* mutant with P_{WRKY54}:*WRKY54-FLAG* fusion gene and empty vector as the control. Top: Four-week-old WT, transgenic plants with vector (*w54t*) or *WRKY54* (*w54t*) are shown. Bottom: WRKY54 protein accumulation was detected in the transgenic plants by immunoblot with anti-FLAG antibody and HERK1 loading control was shown at the bottom. (E) BES1 protein accumulation was determined in four-week-old *w54t* leaves soaked in ½ liquid MS medium with 1μm BL or DMSO for 30 minutes. (F) Hypocotyl lengths of 5-day-old seedlings grown on ½ MS medium with 0, 10 and 100 nM BL. Mean was calculated and the SD was also presented. Error bars indicate standard deviation (* P < 0.05, ** P < 0.01; Student's t test).

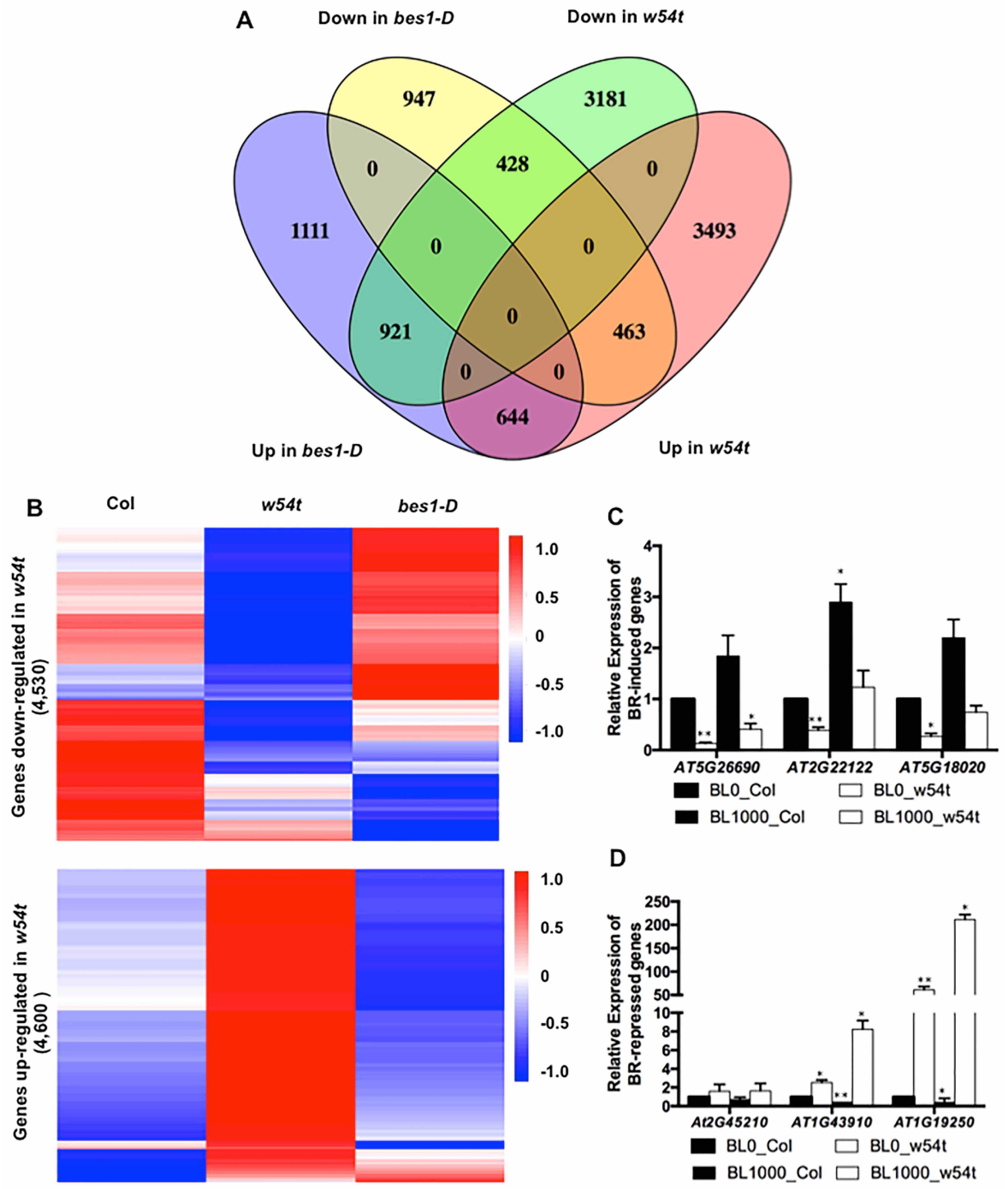

Figure 2. WRKY46, WRKY54 and WRKY70 regulate the expression of BR targets genes. (A) Venn diagram showing overlaps among genes up- or down-regulated in *w54t* with those differentially expressed in *bes1-D*. (B) Clustering analysis of genes differentially expressed in *w54t* under control conditions within WT, *w54t* and *bes1-D*. Values indicate normalized expression levels. (C) The expression of genes down-regulated in *w54t* was examined using four-week-old plants treated with or without 1μm BL. The averages and SD are derived from three biological replicates. (D) The expression of genes up-regulated in *w54t* was examined as described in (C).

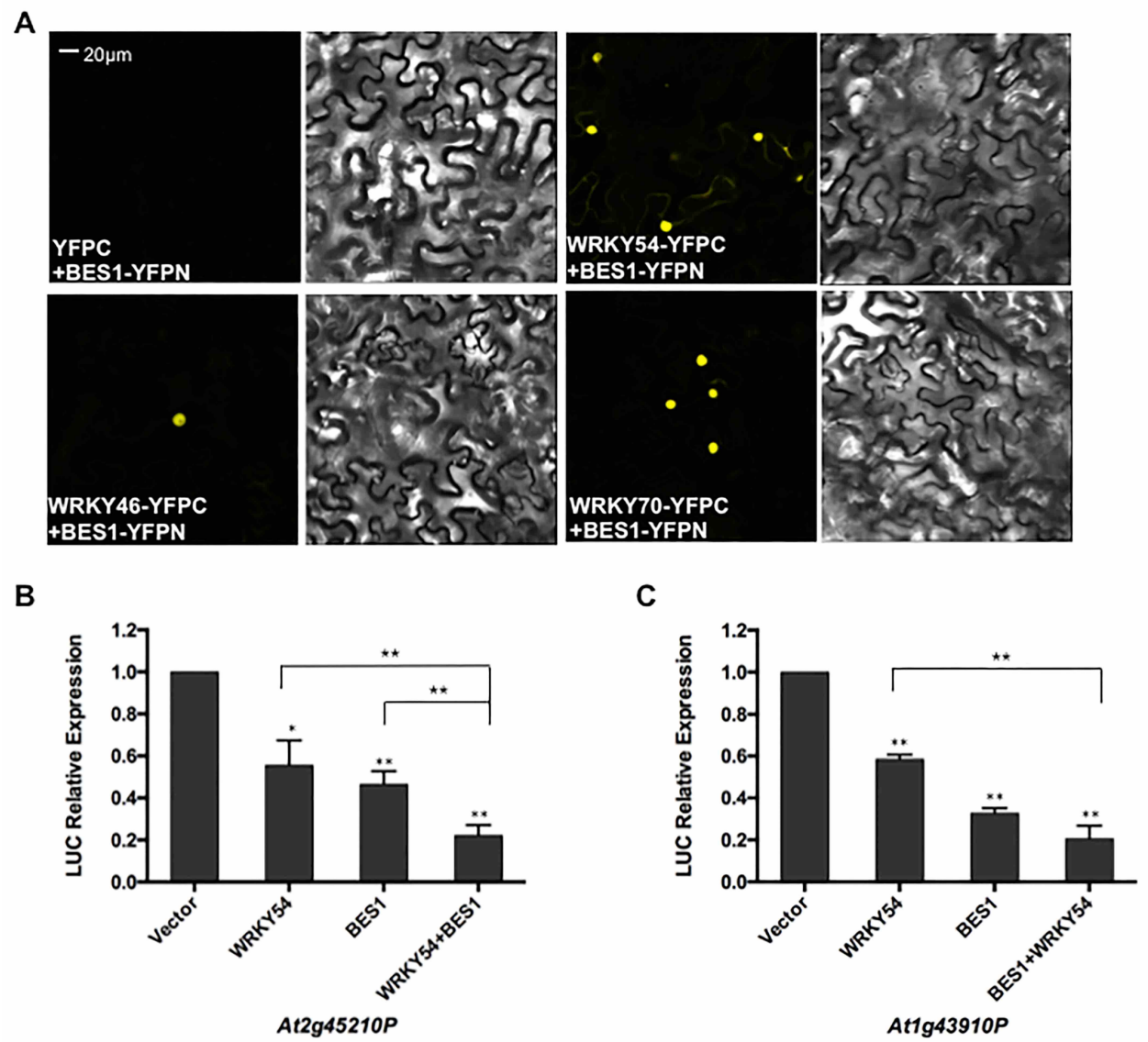

Figure 3. WRKY46, WRKY54 and WRKY70 directly interact with BES1 both *in vivo* and *in vitro*. (A) WRKY46/54/70 interact with BES1 by BiFC assay in vivo. Co-transformation of WRKY46/54/70-YFPC and BES1-YFPN led to the expression of YFP signal, whereas no signal was detected when BES1-YFPN and YFPC or WRKY46/54/70-YFPC and YFPN were co-expressed (see Figure S7F). The experiments were performed twice with similar results. (B) – (C) Transient expression of luciferase (LUC) driven by the BR-regulated gene promoters of *At2g45210* (B) and *At1g43910* (C). The mean and SD were derived from three biological repeats.

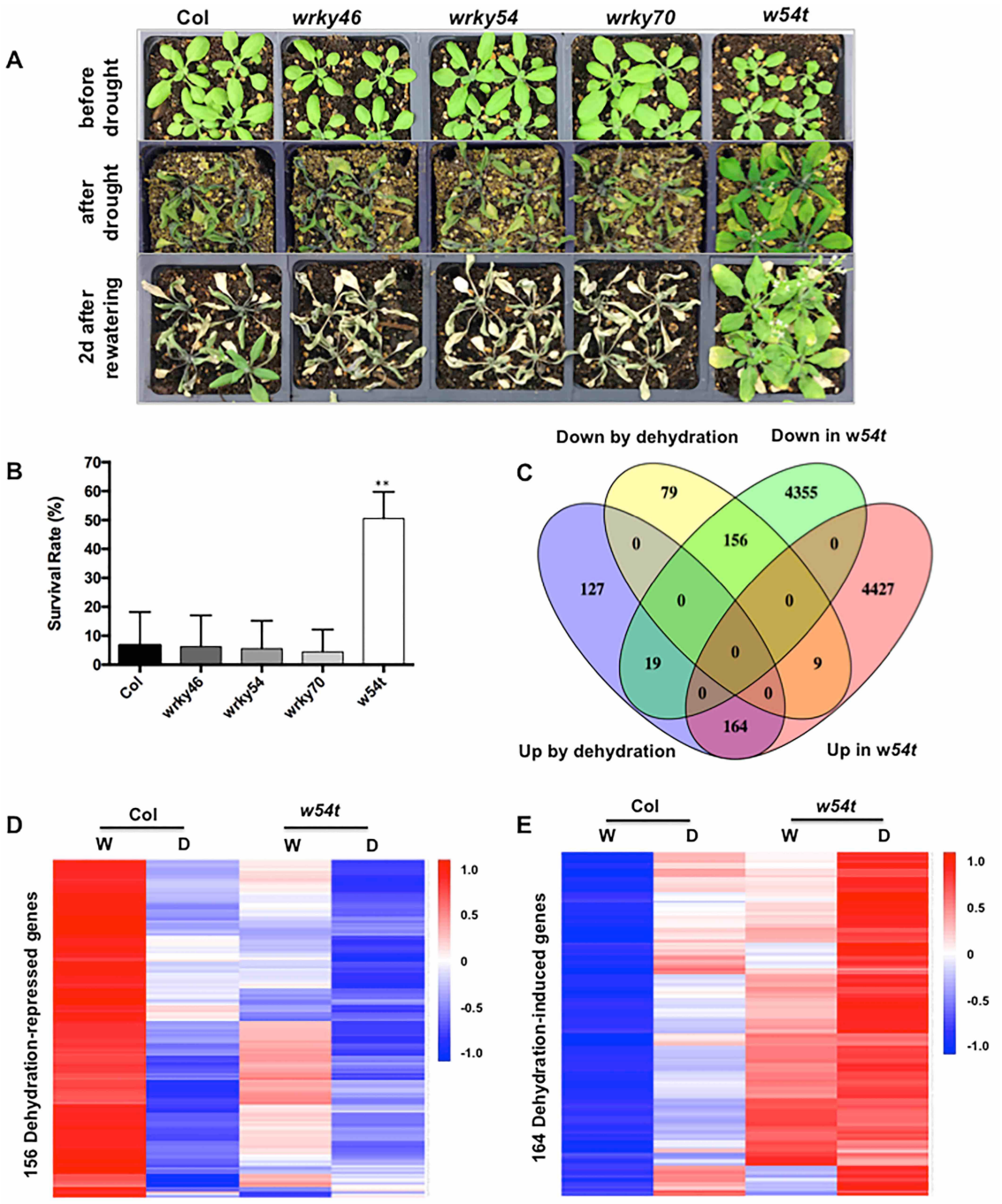

Figure 4. WRKY46, WRKY54 and WRKY 70 play negative roles in drought response. (A) Phenotype of WT, *wrky46, wrky54, wrky70* and *w54t* plants before drought (top), after drought (middle) and two days after rewatering (bottom). (B) The survival rate after recovery was determined. The mean and SD were from three biological repeats. (C) Venn diagram showing comparisons among genes differentially expressed in *w54t* and genes up- or down-regulated by dehydration in WT. (D) Clustering of dehydration down-regulated genes in WT and *w54t* mutants under control condition (W) or dehydration (D). (E) Clustering of dehydration up-regulated genes in

WT and *w54t* mutants under control condition (W) or dehydration (D). Values indicate normalized expression levels.

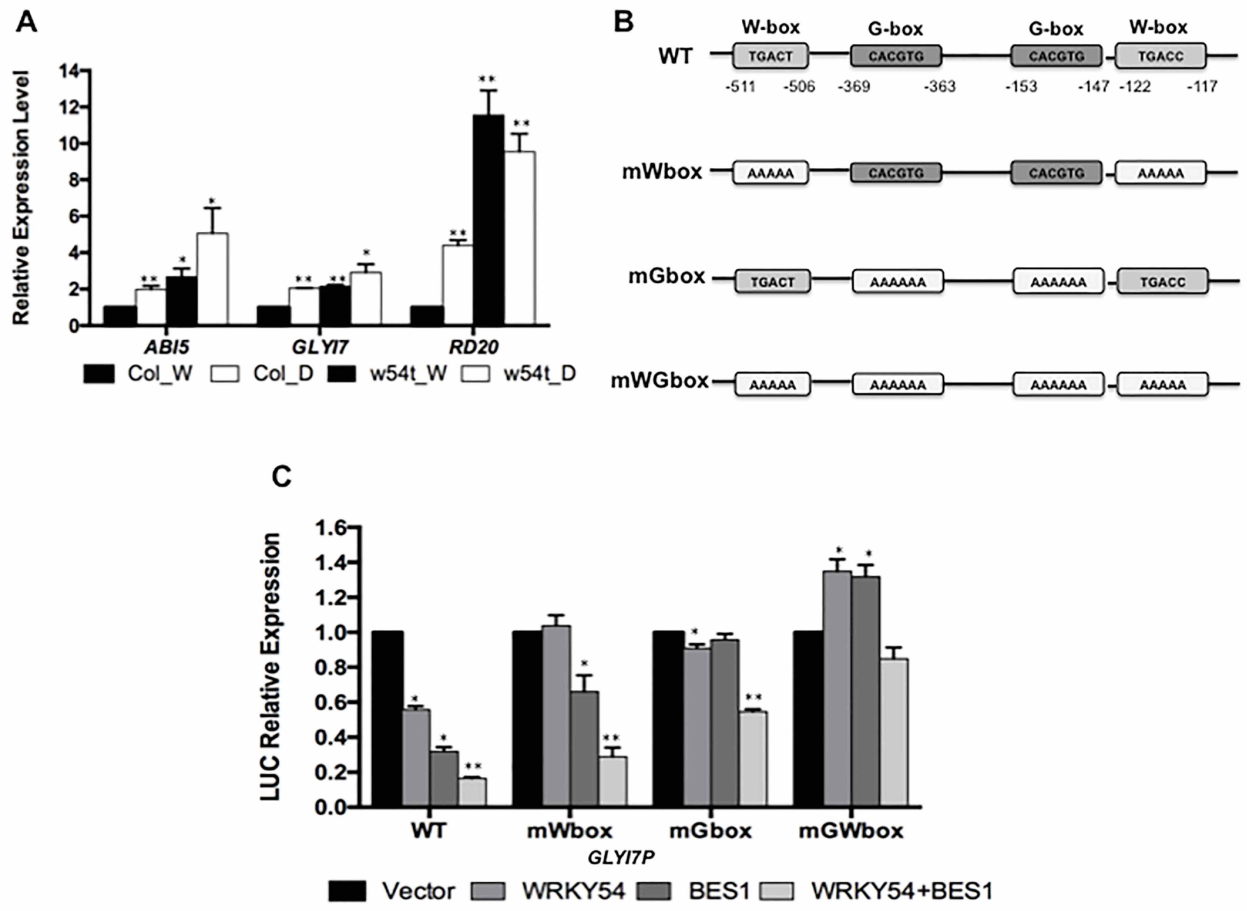

Figure 5. WRKY54 and BES1 cooperate to negatively regulate dehydration-induced genes. (A) The expression of dehydration-inducible genes, *ABI5*, *GLYI7* and *RD20* was determined in WT and *w54t* by qPCR. Error bars indicate standard deviation. (B) Schematic diagram of the promoter region of *GLYI7*. Red box indicates W-box and green box represents G-box. Yellow box is W-box or G-box after mutation. mWbox: the mutation of W-box; mGbox: the mutation of G-box; mGWbox: the mutation of both G-box and W-box. (C) Transient expression of *GLYI7P*-fLUC and mutated W-box or G-box or both of *GLYI7P*-fLUC was determined in the presence of WRKY54 and/or BES1 in protoplasts. Error bars indicate standard deviation (* $P < 0.05$, ** $P < 0.01$; Student's t test).

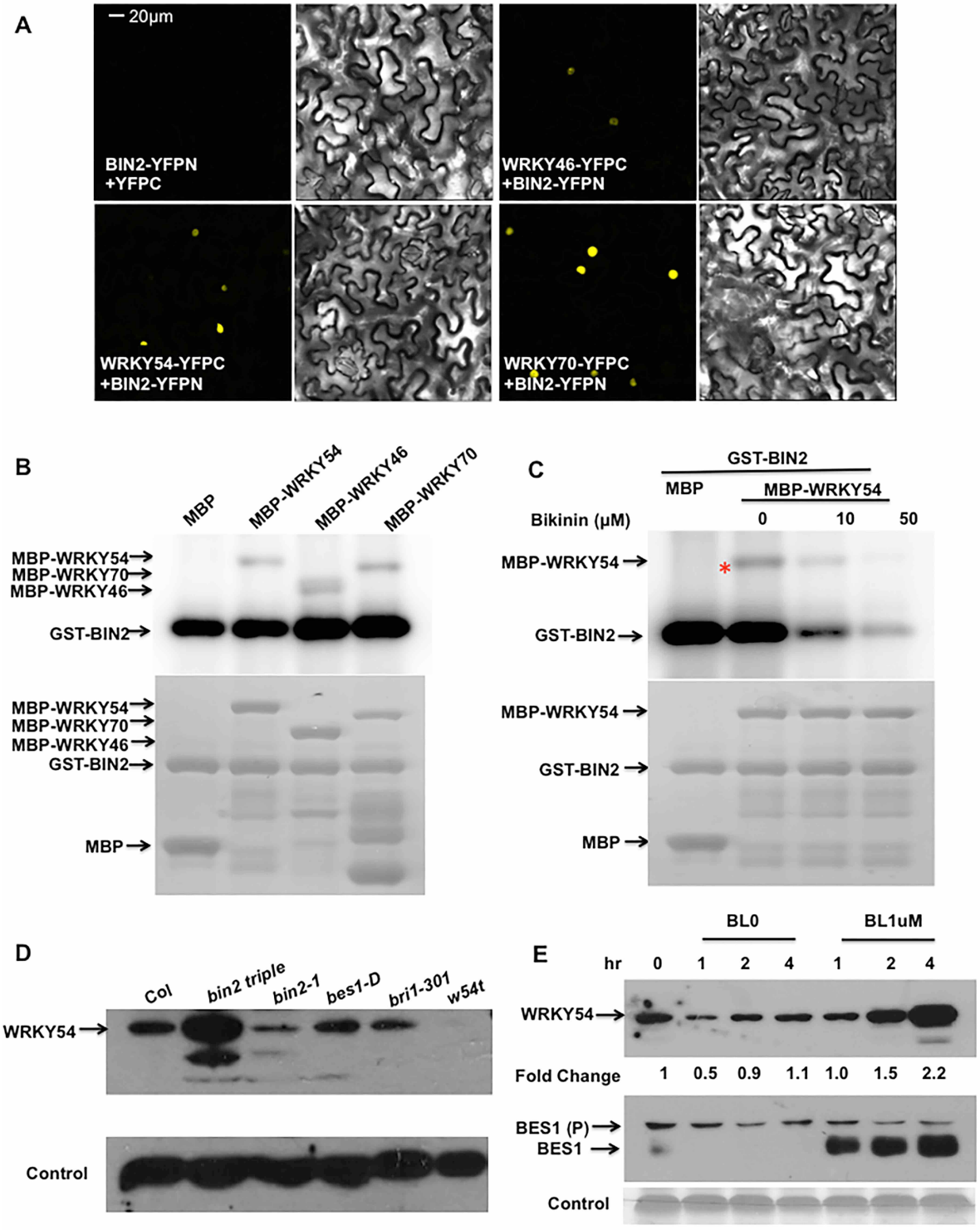

Figure 6. BIN2 kinase phosphorylates and destabilized WRKY54 protein. (A) WRKY46/54/70 interact with BIN2 by BiFC assay in vivo. Co-transformation of WRKY46/54/70-YFPC and BIN2-YFPN led to the expression of YFP signal, whereas no signal was detected when BIN2-YFPN and YFPC or WRKY46/54/70-YFPC and YFPN

were co-expressed (see Figure S7F). The experiments were performed twice with similar results. (B) *In vitro* kinase assays show BIN2 phosphorylates WRKY54/46/70 (top). The loading controls of MBP, MBP-WRKY54/46/70 and GST-BIN2 by CBB staining are shown in bottom panel. (C) The phosphorylation of WRKY54 by BIN2 was inhibited with the increasing concentrations of bikini (top). The loading controls are shown in the bottom. (D) The WRKY54 protein level was detected in indicated BR mutants and WT with WRKY54 antibody. The *w54t* mutant was used as a negative control. (E) WRKY54 protein accumulated upon BL treatment. Two-week-old WT seedlings were treated with or without 1μm BL for indicated time and used to prepare protein to detect WRKY54 (*top*), BES1 (*Middle*), and a control protein (*Bottom*).

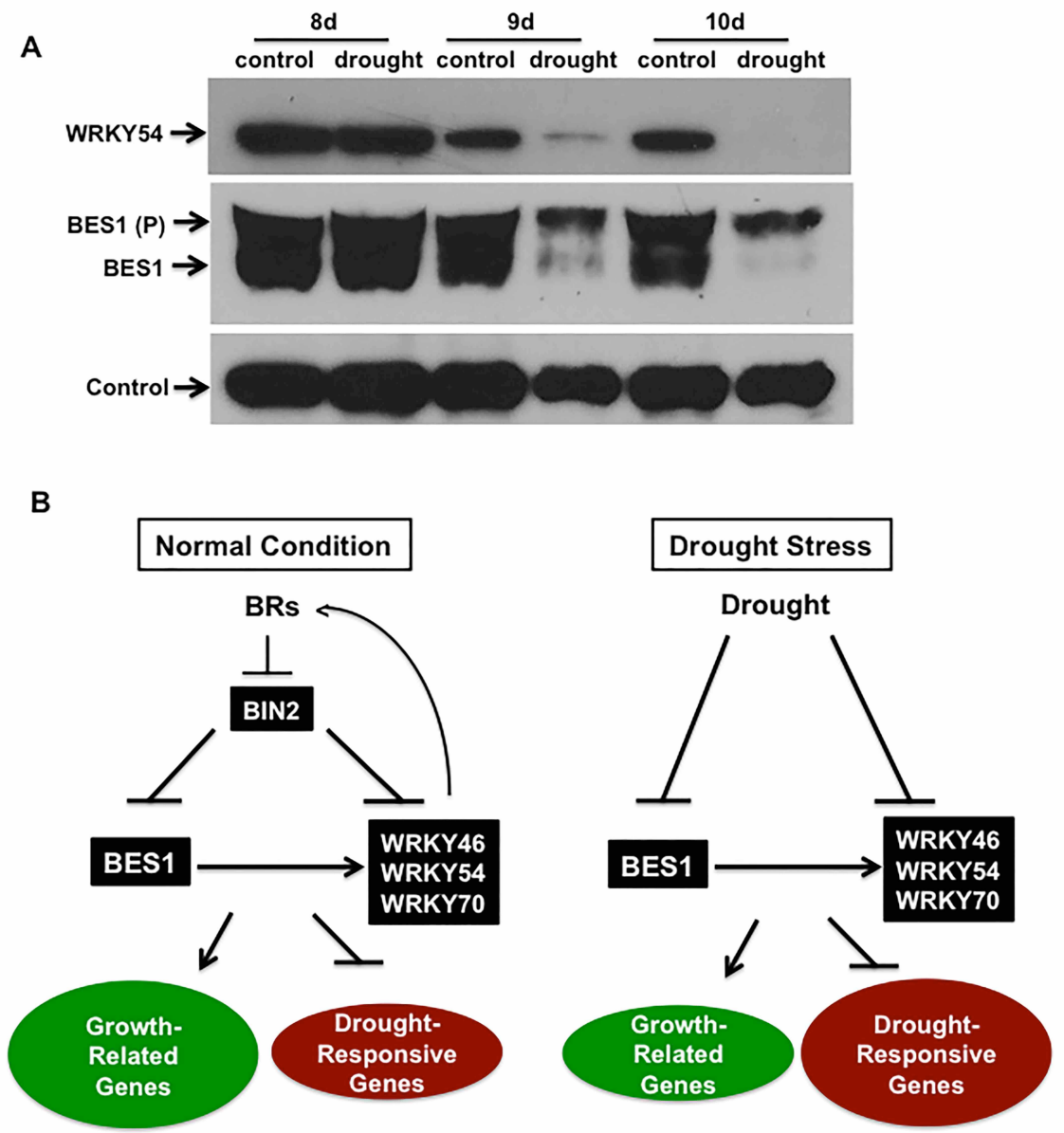

Figure 7. A working model of WRKY46/54/70 in plant growth and stress response. (A) WRKY54 and BES1 protein decreased with increasing drought treatment time. The 8d, 9d and 10d indicate days of drought treatment or controls. (B) A working model of WRKY46/54/70 in BR-regulated growth and drought stress response. WRKY46/54/70 are regulated by BR signaling through BIN2 and BES1, and cooperate with BES1 to promote plant growth and inhibit drought responses. WRKY46/54/70 also slightly promote BR biosynthesis. Under normal growth condition (Left), WRKY46/54/70 and BES1 positively co-regulate growth-related genes and negatively control the expression of drought-responsive genes to promote growth. BRs regulate WRKY46/54/70 both transcriptionally and post-transcriptionally through BES1 and BIN2, respectively. Under drought stress condition (Right), WRKY46/54/70 and BES1 protein are destabilized,

which leads to repression of growth-related genes and alleviation of WRKY46/54/70's inhibitory effect on drought-related genes, leading to reduced growth and increased drought tolerance.

Supplemental Figure 1. WRKY T-DNA insertion mutants.
Supplemental Figure 2. *wrky* mutants displayed dwarf phenotype.
Supplemental Figure 3. Group III WRKY (WRKY30/41/46/53/54/70) function redundantly and play positive role in plant growth.
Supplemental Figure 4. The *wrky* mutants have slightly reduced endogenous BR level.
Supplemental Figure 5. Different hormonal response of WT, *wrky46*, *wrky54*, *wrky70* and *w54t*.
Supplemental Figure 6. The clustering analysis of genes differentially expressed in *wrkyS*.
Supplemental Figure 7. WRKY46/54/70 interact with BES1/BIN2 and are phosphorylated by BIN2.
Supplemental Figure 8. The drought phenotype of WT, *wrky* single, double mutants and triple mutants.
Supplemental Figure 9. WRKY54 antibody test in WT, *wrky* single, triple and sextuple mutants.
Supplemental Figure 10. Gene Ontology (GO) Term analysis of 9130 genes differentially expressed in *w54t* mutant.
Supplemental Table 1: Genes up- or down-regulated in *bes1-D.*
Supplemental Table 2: Genes up- or down-regulated in *wrky46 wrky54 wrky70* triple mutant.
Supplemental Table 3: Genes up- or down-regulated by dehydration treatment in wild-type plants.
Supplemental Table 4: primers used in this study.
Supplemental Table 5: Annotation of the genes used in Fig 2C and 2D.

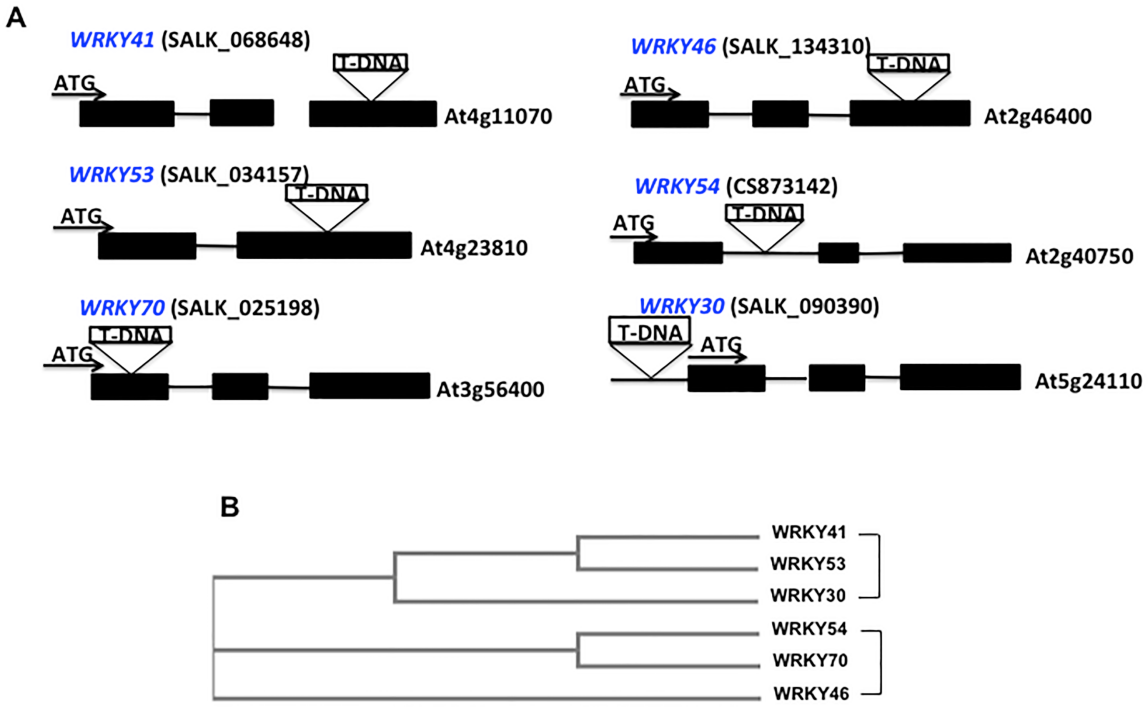

Supplemental Figure 1. WRKY T-DNA insertion mutants. (A) Schematic representation of T-DNA knockout alleles of group III *WRKY* genes. The exons (black boxes) and introns (lines) and positions of T-DNA insertions are indicated with. (B) The phylogenetic tree of the WRKY proteins from *Arabidopsis*.

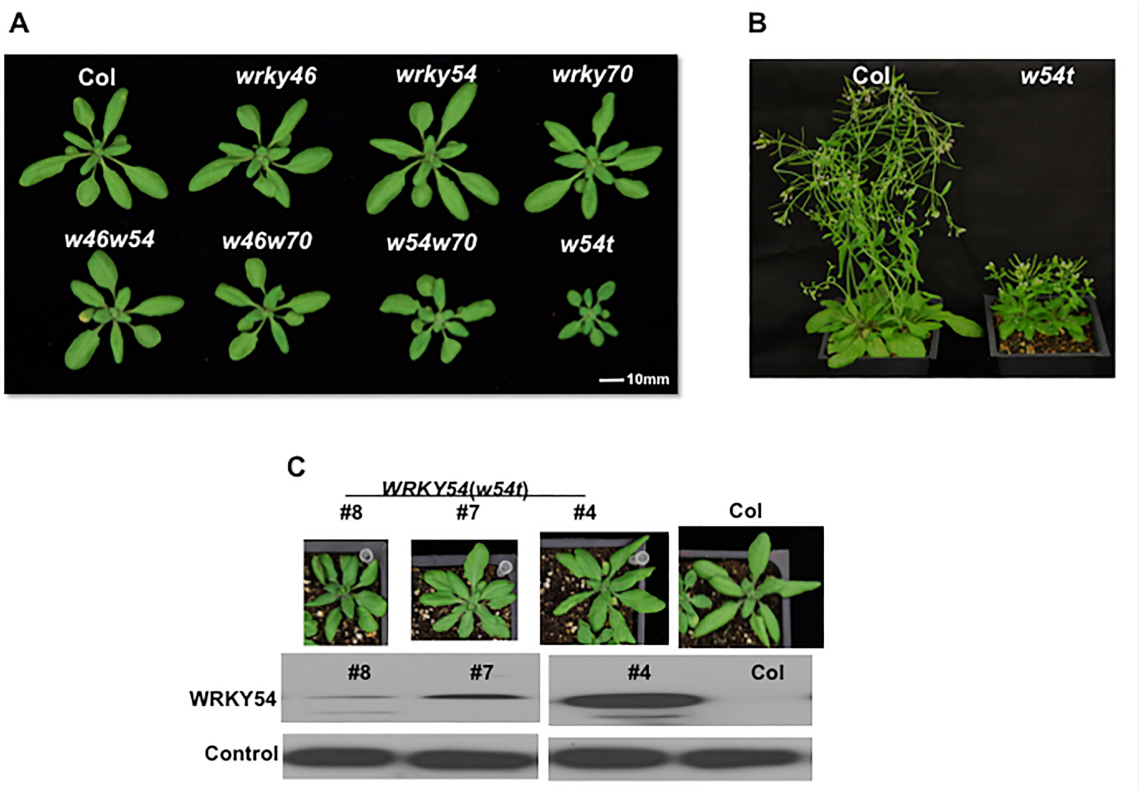

Supplemental Figure 2. The *wrky* mutants displayed dwarf phenotype. (A) The phenotype of three-week-old *wrky* single, double and triple (*wrky46 wrky54 wrky70)* mutants. (B) The phenotype of WT and *wrky46 wrky54 wrky70 (w54t)* mutant at flowering stage. (C) The phenotype of three lines of transgenic complementation is consistent with WRKY54 protein expression level and a loading control was shown at the bottom.

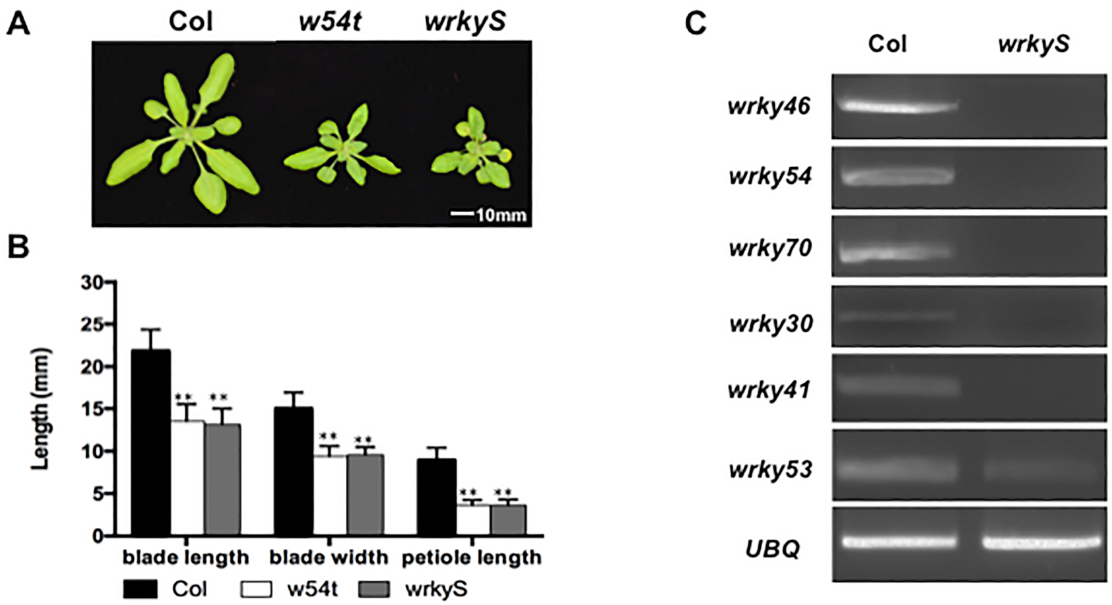

Supplemental Figure 3. Group III WRKY (WRKY30/41/46/53/54/70) function redundantly and play positive role in plant growth. (A) The growth phenotype of three-week-old WT*, wrky46 wrky54 wrky70 (w54t)* and *wrky30 wrky41 wrky46 wrky53 wrky54 wrky70 (wrkyS)*. (B) The blade lengths, blade widths and petiole lengths of the 6th leaves of WT*, w54t* and *wrkyS* were measured. (C) RT-PCR result indicated that the expression of six genes is knockout or reduced in *wrkyS* mutant.

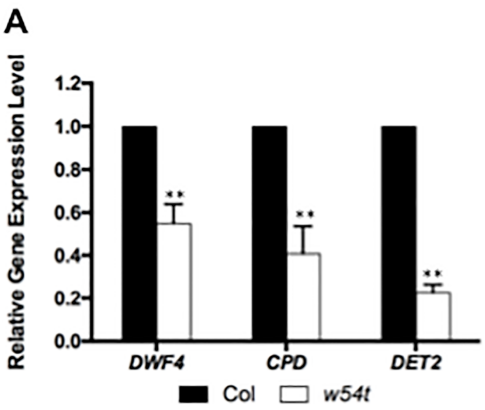

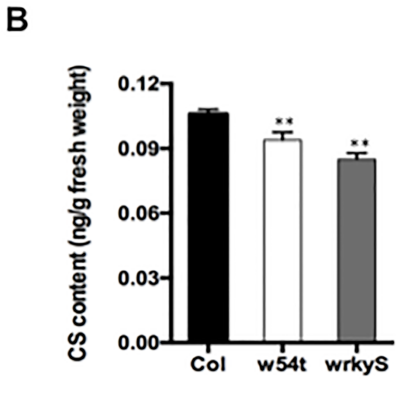

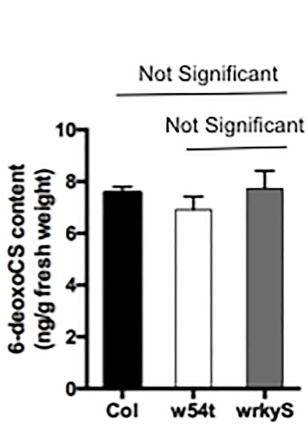

D

	content (ng/g FW)		
	CS	6-deoxoCS	BL
Col_1	0.108	7.83	NQ
Col_2	0.106	7.42	NQ
Col_3	0.104	7.45	NQ
*w54t*_1	0.092	6.97	NQ
*w54t*_2	0.091	7.38	NQ
*w54t*_3	0.098	6.37	NQ
*wrkyS*_1	0.088	7.98	NQ
*wrkyS*_2	0.083	8.25	NQ
*wrkyS*_3	0.084	6.95	NQ

Supplemental Figure 4. The *wrky* mutants have slightly reduced endogenous BR level.

(A) The expression of *DWF4*, *DET2* and *CPD* was determined in four-week-old *w54)* compared to WT by qPCR. Error bars indicate standard deviation. The significance of difference was analyzed in all studies by Student's t test (* $P < 0.05$, ** $P < 0.01$). (B) The endogenous level of CS from three-week-old WT, *w54t* and *wrkyS* plants was determined. (C) The endogenous level of 6-deoxoCS from three-week-old WT, *w54t* and *wrkyS* was determined. (D) The amount of BR precursors in WT*, w54t and wrkyS.*

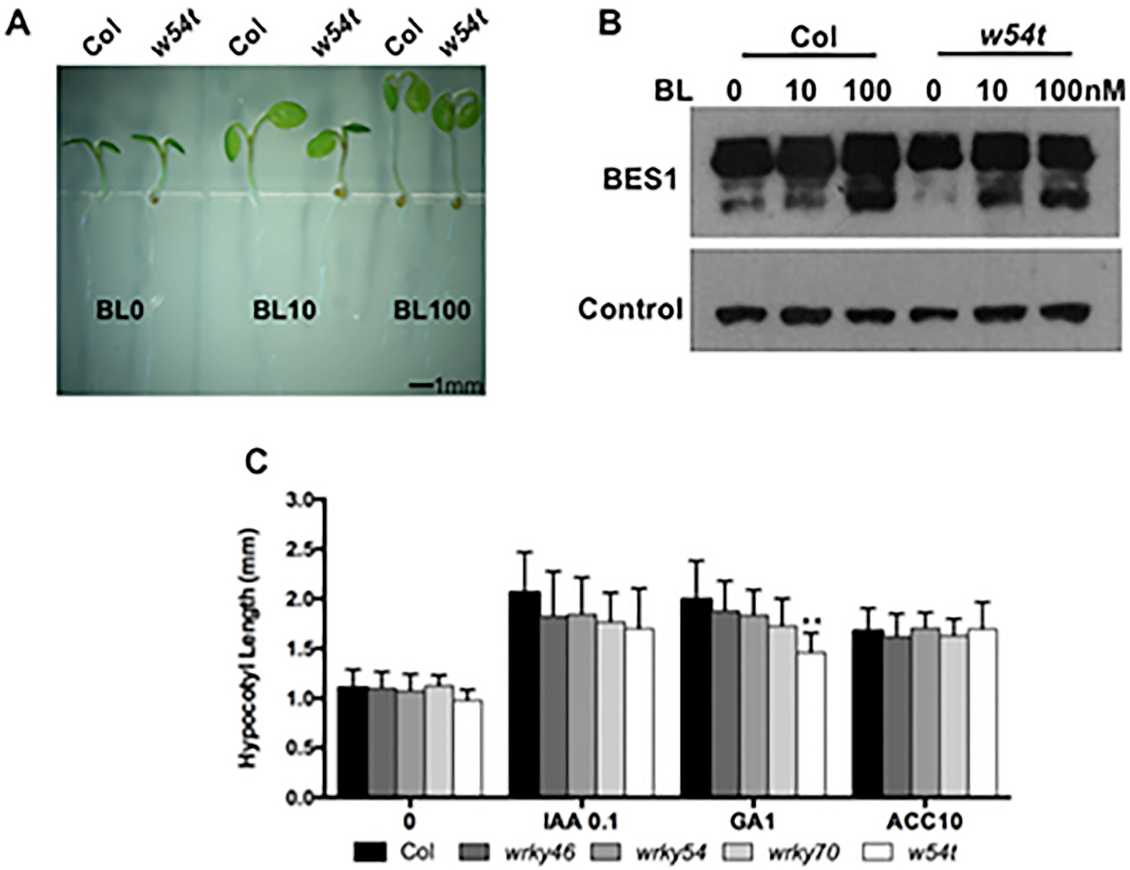

Supplemental Figure 5. Different hormonal response of WT, *wrky46*, *wrky54*, *wrky70* and *w54t*. (A) 5-day-old Col and *w54t* seedlings grown under light on 1⁄2 MS medium with 0, 10nM and 100nM BL. Scale bar, 1mm. (B) BES1 protein levels were determined by immunoblot with two-week-old WT seedlings growing on 1⁄2 MS medium with 0, 10nm and 100nm BL. The treatment and growth condition is the same as in (Figure 1F). HERK1 was used as a loading control (bottom panels). (C) Hypocotyl length of 6-day-old seedlings grown on ½ MS medium with 0.1μm IAA, 1μm GA and 10μm ACC. Relative mean was calculated and the SD was also presented.

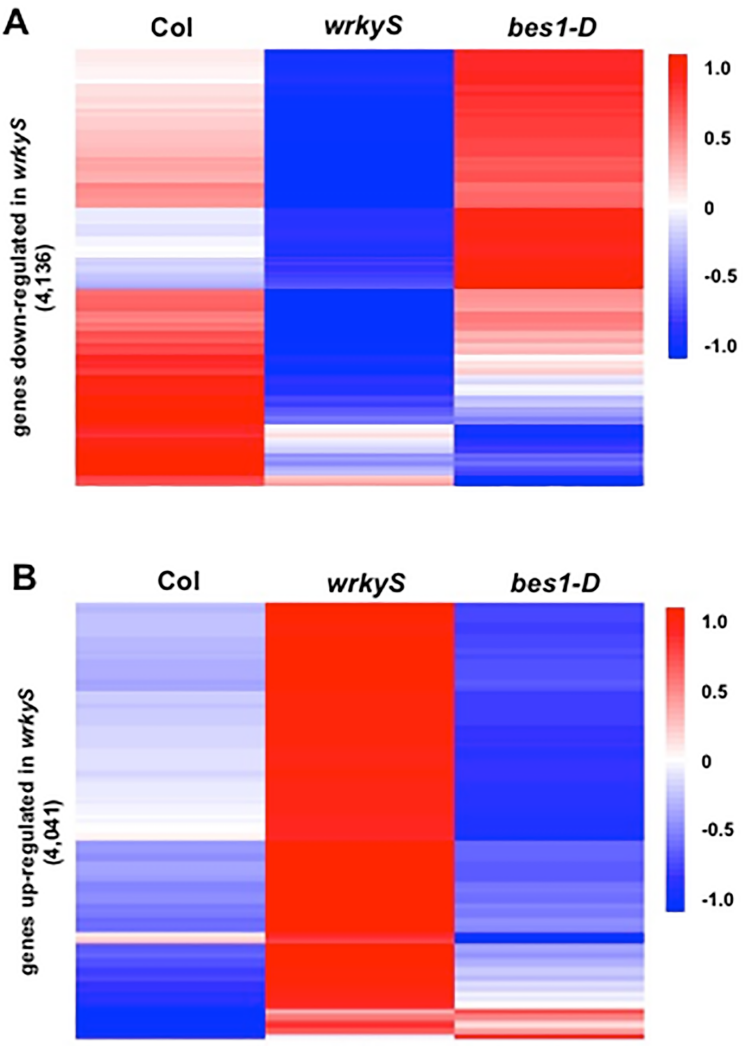

Supplemental Figure 6. The clustering analysis of genes differentially expressed in *wrkyS*.

(A) Clustering analysis of genes down-regulated in *wrkyS* in WT, *bes1-D* and *wrkyS*.

(B) Clustering analysis of genes up-regulated in *wrkyS* in WT, *bes1-D* and *wrkyS*.

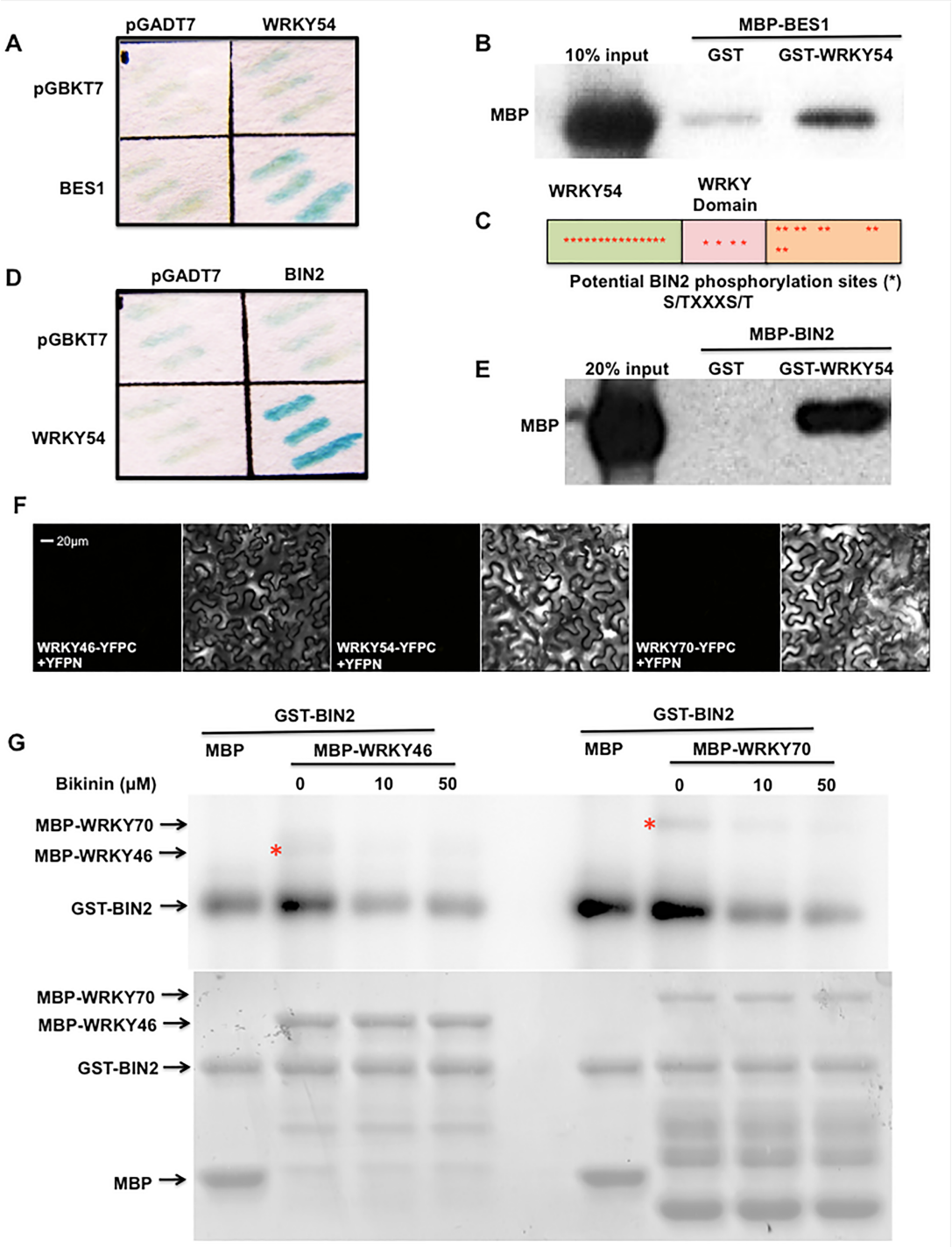

Supplemental Figure 7. WRKY46/54/70 interacts with BES1/BIN2 and are phosphorylated by BIN2. (A) – (B) WRKY54 interacts with BES1 by yeast two-hybrid assay (A), in vitro GST pull-down assay (B). (C) The domain structure of WRKY54 protein. * indicates the potential BIN2 phosphorylation sites. Totally 29 potential BIN2 phosphorylation sites are found in WRKY54 protein. (D) – (E) WRKY54 interacts with BIN2 by yeast two-hybrid (D) and GST pull-down assay (E). (F) The control co-transformation of WRKY46/54/70-YFC and YFPN. (G) The phosphorylation of WRKY46

(Left) and WRKY70 (Right) by BIN2 was inhibited with the increasing concentrations of

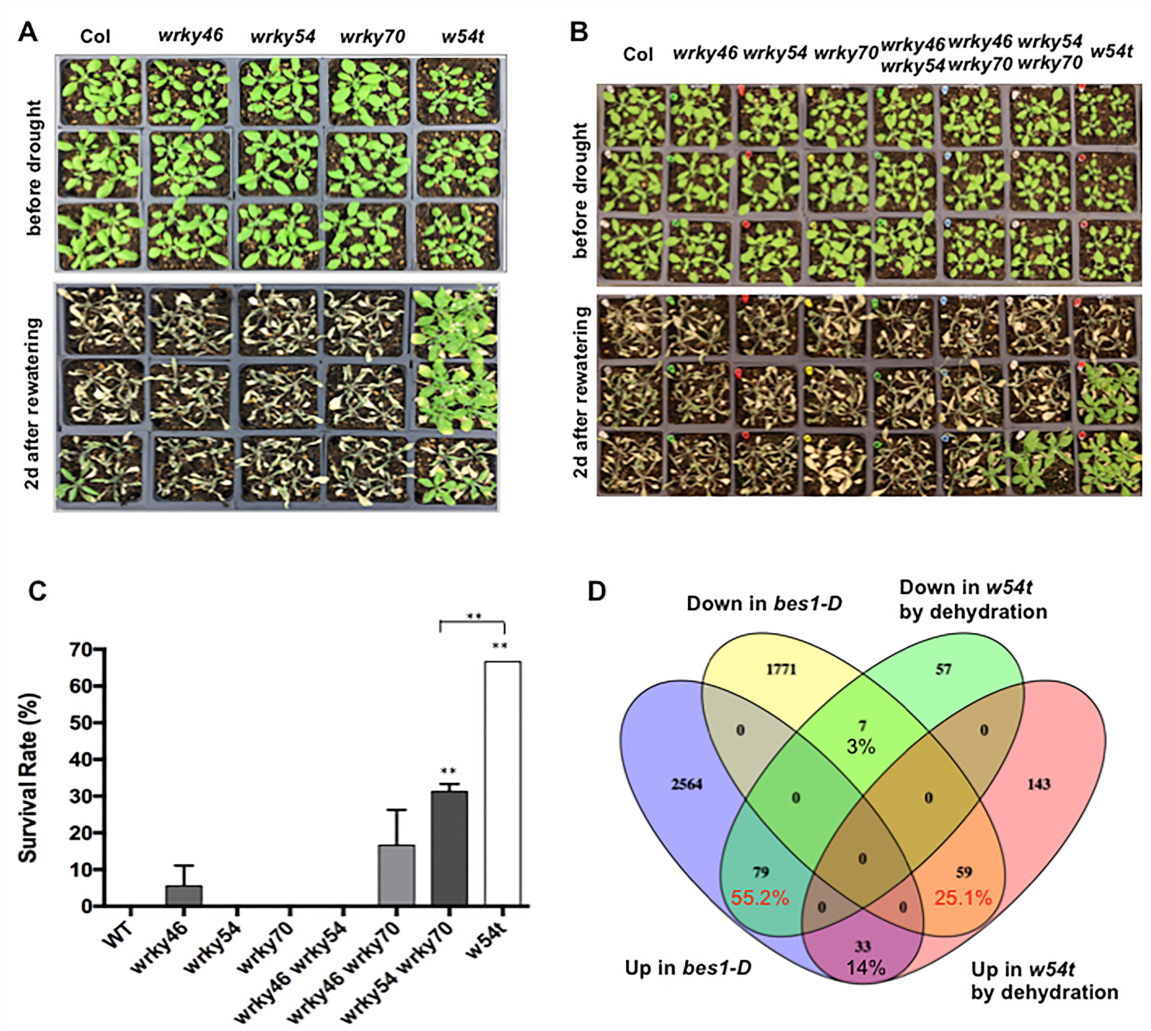

bikinin.

Supplemental Figure 8. The drought phenotype of WT, *wrky* single, double mutants and triple mutants. (A) The phenotype of 4-week-old WT, *wrky46*, *wrky54*, *wrky70* and *w54t* before drought, after drought and two days after watering in larger set of experiments. (B) The phenotype of four-week-old WT, *wrky46*, *wrky54*, *wrky70*, *wrky46 wrky54*, *wrky46 wrky70*, *wrky54 wrky70* and *w54t* before drought and two days after watering. (C) The survival rates for *wrky* mutants were determined. The average and SD were from three biological repeats. (D) Venny analysis showed overlaps among genes up- or down-regulated in *w54t* by dehydration with those differentially expressed in *bes1-D*.

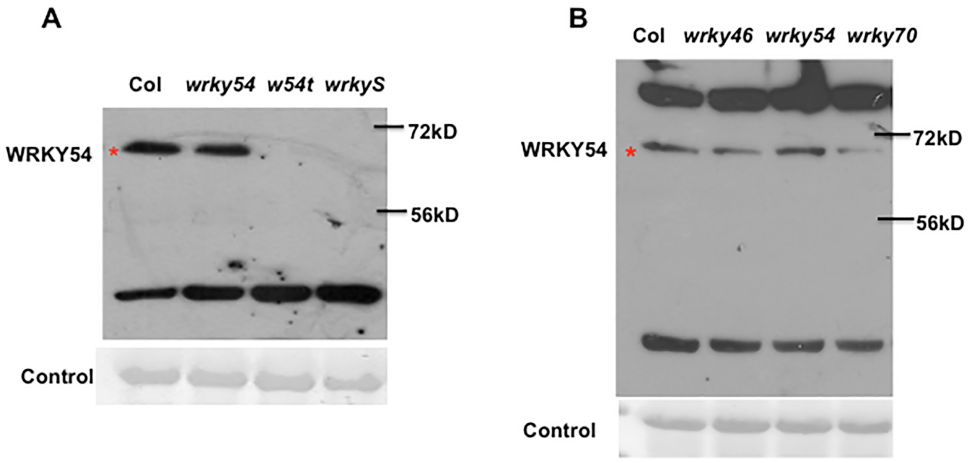

Supplemental Figure 9. WRKY54 antibody test in WT, *wrky* single, triple and sextuple mutants. (A) The test of WRKY54 antibody in WT, *wrky54*, *w54t* and *wrkyS.* The antibody recognizes a ~70 kDa band that is reduced in *wrky54* single mutant, and abolished in *w54t* and *wrkyS* mutants. The results suggest that the antibody recognize WRKY54 and its close homologs WRKY46 and WRKY70. A lower molecular weight band is a non-specific background. (B) The test of WRKY54 antibody in WT, *wrky46*, *wrky54* and *wrky70* single mutants. The results suggest that the antibody recognize WRKY70 more specifically, which could be explained that WRKY54 and WRKY70 are homologs and have a high similarity.

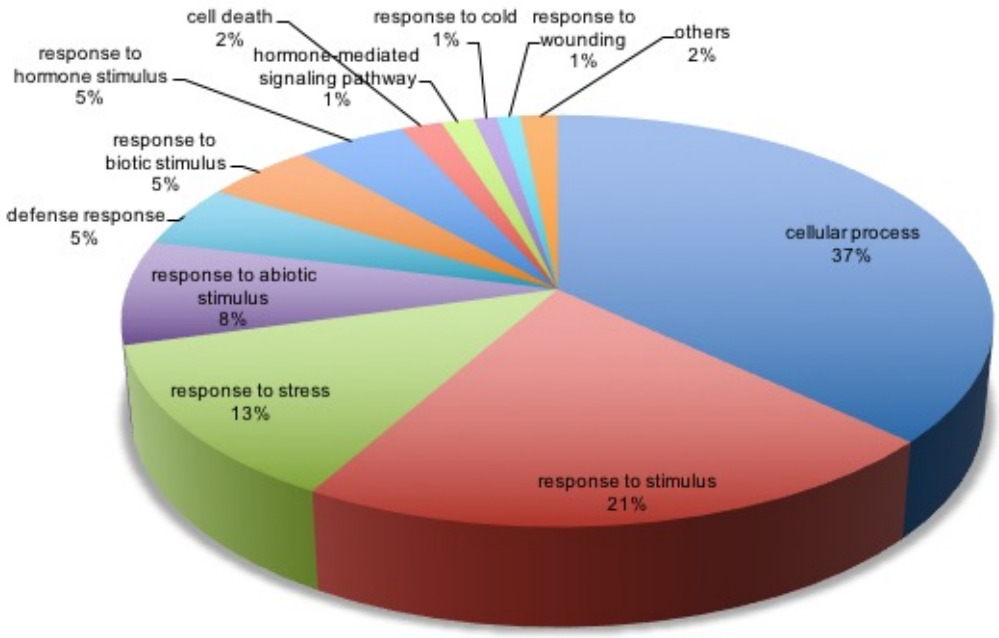

cellular process	36.90%
response to stimulus	21.30%
response to stress	12.50%
response to abiotic stimulus	8.20%
defense response	4.90%
response to biotic stimulus	4.70%
response to hormone stimulus	4.70%
cell death	1.80%
hormone-mediated signaling pathway	1.40%
response to cold	1.00%
response to wounding	1.00%

Supplemental Figure 10. Gene Ontology (GO) Term analysis of 9130 genes differentially expressed in *w54t* mutant.

Table S1: Genes up- or down-regulated in *bes1-D.*

Table S2: Genes up- or down-regulated in *wrky46 wrky54 wrky70* triple mutant.

Table S3: Genes up- or down-regulated by dehydration treatment in wild-type plants.

Table S4: primers used in this study.

Gene		Sequences
Genotyping		
wrky46	Forward	GATGATAAGCCTTGAAGATC
	Reverse	TCATGTAACTTTAGTCCTAT
wrky54	Forward	TGTCAATGCTATGGTGCAAG
	Reverse	GGTGTAAAAAGAGAAGTATA
wrky70	Forward	GTGACCATCATGATGAGATC
	Reverse	AGTACATACACTCATTAGAG
wrky30	Forward	AAAAGTCGCCGAAAAATTGAC
	Reverse	TTATTTTTGCATGGCTTCTGG
wrky41	Forward	GAAAGGTTCCAGGATCTCCAG
	Reverse	GGGGAAGCCTGTGTTAATCTC
wrky53	Forward	TCAGGCACGACTTAGAGAAGC
	Reverse	GGGAAAGTTGTGTCAATCTCG
Complementation		
WRKY54 (EcoRI/KpnI)	Forward	CGCGAATTCtctgtaatttctagagaattaataagc
	Reverse	CGCGGTACCTCTTGATCAGAAAAAAATCAAAGGAAGATGC
Yeast two hybrid		
WRKY54-pGADT7		
(BamHI/XhoII)	Forward	CGCGGATCCATATGGATTCGAATAGTAACAACACG
	Reverse	GCGCTCGAGTCACATAGCACTTGTTCTTTCATAATCAGC
WRKY54-pGBKT7		
(BamHI/PstI)	Forward	CGCGGATCCatATGGATTCGAATAGTAACAACACG
	Reverse	GCGCTGCAGTCACATAGCACTTGTTCTTTCATAATCAGC
Protein expression		
WRKY46-MBP		
(KpnI/SalI)	Forward	CGCGGTACCATGATGATGGAAGAGAAACTTGTGA
	Reverse	CGCGTCGACCGACCACAACCAATCCTGTCCGAAA
WRKY54-MBP/GST		
(BamHI/XhoI)	Forward	CGC GGATCC ATGGATTCGAATAGTAACAACACG
	Reverse	GCGCTCGAGTCACATAGCACTTGTTCTTTCATAATCAGC

WRKY70-MBP (EcoRI/BamHI)	Forward	CGCGAATTCATGGATACTAATAAAGCAAAAAAGC
	Reverse	CGCGGATCCAGATAGATTCGAACATGAACTGAAG
BiFC		
WRKY46-YFPC	Forward	CGCGGTACCATGATGATGGAAGAGAAACTTGTGA
	Reverse	CGCGTCGACCGACCACAACCAATCCTGTCCGAAA
WRKY54-YFPC	Forward	CGC GGATCC ATGGATTCGAATAGTAACAACACGA
	Reverse	CGC TCTAGA CATAGCACTTGTTCTTTCATAATCA
WRKY70-YFPC	Forward	CGCGGTACCATGGATACTAATAAAGCAAAAAAGC
	Reverse	CGCGGATCCAGATAGATTCGAACATGAACTGAAG
Luciferase assay		
At2g45210P (BamHI/HindIII)	Forward	CGCGGATCCTCATCAACGTACACAAG
	Reverse	CGCAAGCTTCTTCTTATAGCTAACTTT
At1g43910P (BamHI/HindIII)	Forward	CGC GGATCC TCTTACTTCTTAACTCGTACATGCC
	Reverse	CGC AAGCTT TTGTGCTTAAGAGAAGAAGGAAGAT
GLYI7P_WT (BamHI/HindIII)	Forward	GCG GGATCC AATACATTTTCCCACAAGTGAC
	Reverse	CGG AAGCTT TTTTTCTTTCTTACCCAGAGAGACG
GLYI7P_Wbox_mutation	Forward	see below
	Reverse	see below
GLYI7P_Gbox_mutation	Forward	see below
	Reverse	see below
GLYI7P_WGbox_mutation	Forward	see below
	Reverse	see below
Gene expression		
DWF4	Forward	ATGACCAACCTAATCTCTT
	Reverse	TACGAGAAACCCTAATAGGC
DET2	Forward	CTGGTTCGAGTTGGTAAGCT
	Reverse	CACATAACATATGATAAACTAG
CPD	Forward	CAACCTCCACGATCATGACTC
	Reverse	CATTAGAAGGGCCTGTCGTTAC
At5g26690	Forward	GCAAACATGCAATCATGGAAG
	Reverse	TGGTCCGACGCTGATTACTAC
At2g22122	Forward	GGTGTTGACGGTGAAGA
	Reverse	CTCACACTTCATAATTCAC
At5g18020	Forward	GGATTCGATCATCCAATGGGT
	Reverse	GTCTATTTCTAACTAGG
At2g45210	Forward	GCATGCTGATGAGACCATTAG

	Reverse	GCTTCTCGAAGCAGCTCACC
At1g43910	Forward	GAGCTGATGCTTCTCGTAGA
	Reverse	AGTACAATTGTCCATGAG
At1g19250	Forward	GCTATTGTTCCTGAACCTT
	Reverse	ACATTGAACGTAGCTCTG
ABI5	Forward	GAGTAGTGGATGGTCCAGTG
	Reverse	TCATCAATGTCCGCAATCTC
GLYI7	Forward	GGACATGGAATTGGGATTCATCTTCT
	Reverse	GGTCCACTTGGATGCCACCTTCTTCA
RD20	Forward	GCAAATACGCGCTAACGGTTAAAGAT
	Reverse	CCTCTCACAGCTTCTTTAGATAGGAA
WRKY30	Forward	GAGCTGGTGTTGATAGAACG
	Reverse	ctcggatatttgaatagga
WRKY41	Forward	ACCTCATGACGATATCTT
	Reverse	AGTGTGTGTTCCTCTGTA
WRKY46	Forward	AGCGAAGCCTTGAGATCGAT
	Reverse	actgccattaagagagagac
WRKY53	Forward	CACACACTTGTTCGCAGG
	Reverse	TCTTTACCATCATCAAGC
WRKY54	Forward	GATCACATACAAGGATCGTG
	Reverse	agacctagtgctgattcatc
WRKY70	Forward	GATTGGGACCCGTTAAGGGT
	Reverse	ccactctacatggcctaat

Promoter sequences used in dual luciferase assay

Yellow highlight indicates W-box or its mutant form. Blue highlight indicates G-box or its mutant form.

GLYI7_mWbox (gBlock Gene Fragments, HindIII/BamHI)

CGCAAGCTTaatacattttcccacaagtgacagagcaaacaaaattcacatatttttgtctattacactttggtgtcaga
caaaaatgttacgtagatttatggcggtggattataacattgtaactttaaatatcttttaacgtaagaaacaaaactccaaaa
ttggtgtttatttttaaaaataaaaatttgaggggcatgtatgtttgtttagttgattcacgtgttctttgtgtctgaaaattctgaattt
gatgattttgaaaaaggaaaaaaagatacgaggtatcctcaattccaaaaggatgaatgatacaactcatatatacaaga
ttatagtaaaaagaagggatgcatataaagaaacatagacatcatcgccatccatcctcagatcagttccgtagtttactgg
atcacgacacacacacatatacacgtgtacatataagccattcttatcaaaaaaaaaaccttcctcctgaattctcattcatt
atataggcgtatatttcggaattctaagttttgttgctacgatcgagccagcgttctgtttctgtacgtctctctgggtaagaaaga
aaaaGGATCCCGC

GLYI7_mGbox (gBlock Gene Fragments, HindIII/BamHI)

CGCAAGCTTaatacattttcccacaagtgacagagcaaacaaaattcacatatttttgtctattacactttggtgtcaga
ctgacttgttacgtagatttatggcggtggattataacattgtaactttaaatatcttttaacgtaagaaacaaaactccaaaatt
ggtgtttatttttaaaaataaaaatttgaggggcatgtatgtttgtttagttgattaaaaaattctttgtgtctgaaaattctgaattt
gatgattttgaaaaaggaaaaaaagatacgaggtatcctcaattccaaaaggatgaatgatacaactcatatatacaaga

ttatagtaaaaagaagggatgcatataaagaaacatagacatcatcgccatccatcctcagatcagttccgtagtttactgg
atcacgacacacacacatataaaaaaatacatataagccattcttatcaaaatgaccaccttcctcctgaattctcattcatt
atataggcgtatatttcggaattctaagttttgttgctacgatcgagccagcgttctgtttctgtacgtctctctgggtaagaaaga
aaaaGGATCCCGC

GLYI7_mWGbox (gBlock Gene Fragments, HindIII/BamHI)
CGCAAGCTTaatacattttcccacaagtgacagagcaaacaaaattcacatatttttgtctattacactttggtgtcaga
caaaaatgttacgtagatttatggcggtggattataacattgtaactttaaatatcttttaacgtaagaaacaaaactccaaaa
ttggtgtttatttttaaaaataaaaatttgaggggcatgtatgtttgtttagttgattaaaaaattctttgtgtctgaaaattctgaatt
tgatgattttgaaaaaggaaaaaaagatacgaggtatcctcaattccaaaaggatgaatgatacaactcatatatacaag
attatagtaaaaagaagggatgcatataaagaaacatagacatcatcgccatccatcctcagatcagttccgtagtttactg
gatcacgacacacacacatataaaaaaatacatataagccattcttatcaaaaaaaaaaccttcctcctgaattctcattca
ttatataggcgtatatttcggaattctaagttttgttgctacgatcgagccagcgttctgtttctgtacgtctctctgggtaagaaag
aaaaaGGATCCCGC

Table S5: Annotation of the genes used in Fig 2C and 2D.

GeneID	Col	*bes1-D*	sig	Annotation
AT5G26690	182.1	719.8	yes	Heavy metal transport/detoxification superfamily protein
AT2G22122	195.7	854.3	yes	Unknown protein
AT5G18020	559.6	1963.5	yes	SAUR-like auxin-responsive protein family
AT2G45210	334.2	211.8	no	Senescence-associated gene 201 (SAG201)
AT1G43910	144.6	29.2	yes	P-loop containing nucleoside triphosphate hydrolases superfamily protein
AT1G19250	39.4	5.2	yes	flavin-dependent monooxygenase 1